UNIVERSIDADE FEDERAL DA BAHIA

PÓS-GRADUAÇÃO EM ECOLOGIA: TEORIA, APLICAÇÃO E VALORES

DOUTORADO EM ECOLOGIA

DANIELE DE ALMEIDA MIRANDA

COMPOSTOS PER- E POLIFLUOROALQUILADOS EM AMBIENTES TROPICAIS: DEGRADAÇÃO, DISPERSÃO E BIOMAGNIFICAÇÃO

Salvador, fevereiro de 2021

DANIELE DE ALMEIDA MIRANDA

COMPOSTOS PER- E POLIFLUOROALQUILADOS EM AMBIENTES TROPICAIS: DEGRADAÇÃO, DISPERSÃO E BIOMAGNIFICAÇÃO

Tese apresentada ao Programa de Pós-Graduação em Ecologia: Teoria, Aplicação e Valores, como parte dos requisitos exigidos para obtenção do título de Doutora em Ecologia.

Orientadora: Dra. Vanessa Hatje

Coorientadora: Dra. Juliana Leonel

Salvador, fevereiro de 2021

Miranda, Daniele de Almeida.
Compostos per- e polifluoroalquilados em ambientes tropicais: degradação, dispersão e biomagnificação / Daniele de Almeida Miranda. - 2021.
178 f.: il.

Orientadora: Profa. Dra. Vanessa Hatje.
Coorientadora: Profa. Dra. Juliana Leonel.
Tese (doutorado) - Universidade Federal da Bahia, Instituto de Biologia, Salvador, 2021.

1. Ecologia marinha. 2. Toxicologia ambiental. 3. Toxicologia ambiental - Todos os Santos, Baía de (BA). 3. Produtos químicos - Aspectos ambientais. 4. Produtos químicos - Toxicologia. I. Hatje, Vanessa. II. Universidade Federal da Bahia. Instituto de Biologia. III. Título.

CDD - 577.7
CDU - 574.58

A nós (Mulheres & Pretas & Nordestinas).
Eu sou porque nós somos.
Ubuntu

Agradecimentos

Agradeço a minha orientadora, Vanessa Hatje, que aceitou embarcar nessa jornada comigo. Eu sei o quão desafiador foi a construção dessa tese, da definição do tema até a última linha do presente documento. Obrigada por estar sempre presente, direcionando a proa desse barco (muito bem governado) e remando junto comigo. A minha coorientadora, Juliana Leonel, pelas oportunidades, palavras de conforto, ouvidos e abraços de sempre. Que honra poder dizer que fui orientada por duas mulheres, mães, pesquisadoras, e tantas outras coisas. Obrigada!

Aos meus colegas do Laboratório de Oceanografia Química (LOQ) Ana, Ingrid, Laís, Manuela, Maurício, Tácila, Taiana, Vinícius. Obrigada pela ajuda nos campos, pelos cafés da tarde, pelos bolos, mas, principalmente, pelo apoio. A tradição que circula no LOQ envolve parceria, cooperação e amizade, não tem espaço para outra coisa. Agradeço especialmente a Raíza e ao Rodrigo, pelos abraços e ouvidos, por sempre poder contar com vocês para acalentar as minhas frustrações no processo de doutorado e pelas injeções de ânimo constantes (Obs.: continuo achando um absurdo o/a aniversariante pagar pelo próprio bolo. Não faz sentido!).

Many thanks to the Stockholm University and the Department of Environment Sciences (ACES) for having me for 14 months during my PhD internship. Especially for my supervisor there, Prof. Jonathan Benskin. Thanks for your unconditional support and for always have kind words, for believing in me, and for helping me to keep trusting in my ideas and in the relevance of my work. Oskar Sandblom, thanks a lot for helping me with the LC-MS/MS. I wouldn't have done so many things during my internship without your help! Thanks to Jana Johansson for supervising me during Jon's parental leave and for all your help during my internship. Thanks to everyone at ACESo for all support. Tack så mycket!

A minha imensa rede de apoio composta por família, amigas e amigos de todos os cantos desse país (e do mundo)! Tenho certeza que esse processo teria sido muito mais difícil sem vocês. Obrigada!

Agradeço à Universidade Federal da Bahia por ser referência no Nordeste, no Brasil e na América latina. Ao Instituto de Biologia e ao Programa de Pós-Graduação em Ecologia: Teoria, Aplicações e Valores. Aos Professores, Funcionários e Secretárias do PPGEcoTAV. Agradeço também a Profª Ana Cecília Rizzatti-Barbosa por participar da banca de acompanhamento da minha tese e de tantos outros momentos importantes. Agradeço a banca examinadora pelas valiosas contribuições para a construção final dessa tese.

Essa pesquisa foi financiada pela Fundação de Amparo à Pesquisa do Estado da Bahia, Brasil (FAPESB) (PET0034/2012), Conselho Nacional de Pesquisa (CNPq) (441829/2014-7; 441264/2017-4), The Rufford Foundation (n° 2991-2), FAPESB (bolsa de doutorado, nº BOL0122/2017), Coordenação de Aperfeiçoamento de Pessoal de Nível Superior (CAPES) (bolsa de doutorado sanduíche nº 88881.188589/2018-01), Programa de Pesquisa Multidisciplinar Baía de Todos os Santos, Instituto Kirimurê e Centro Interdisciplinar de Energia e Ambiente.

Agradeço também a todas as mulheres que tiveram que lutar para ter espaço, àquelas que vieram antes de mim. Àquelas que abriram e facilitaram o meu caminho, as que caminharam lado a lado comigo e as que estão por vir. Empieza el matriarcado!

Muito obrigada!

“Das verdes profundezas do Atlântico em alto-mar, muitos caminhos levam de volta à costa”

Rachel Carson em *Primavera Silenciosa*

Texto de divulgação

Compostos per- e polifluoroalquilados em ambientes tropicais: degradação, dispersão e biomagnificação

Daniele de Almeida Miranda

Os compostos per- e polifluoroalquilados (PFAS) são amplamente utilizados em uma variedade de aplicações, como revestimentos resistentes a água e a óleo, pesticidas, espuma de combate a incêndio, surfactantes, etc. A forte ligação entre os átomos de flúor e carbono presentes na estrutura química dos PFAS resulta em sua baixa degradabilidade e alta persistência. Essas características que são atrativas para a sua ampla utilização comercial, também chamam atenção pelo potencial tóxico à saúde humana e a vida selvagem. Ainda assim, estudos avaliando a presença destes compostos, bem como os impactos destes nos processos ecológicos em ambientes tropicais são escassos. Diante disso, o presente estudo investigou a ocorrência de PFAS em ambientes tropicais e os processos de degradação, dispersão e biomagnificação desses compostos. A degradação do formicida fluorado Sulfluramida foi avaliada pela primeira vez em um experimento manipulativo de campo. Esse experimento mostrou a lenta degradação que o pesticida apresenta em solos de mangue devido às condições de baixo teor de oxigênio nesse ambiente. Ainda, a distribuição espacial dos compostos PFAS foi avaliada em comparação a circulação de massas de água e processo de ressurgência para melhor entender a dispersão desses compostos no lado oeste do oceano Atlântico tropical entre 15ºN e 23ºS. Por último, a bioacumulação dos compostos PFAS em uma cadeia alimentar do estuário do rio Subaé, Bahia, foi estudada. Foi observado que os PFAS se acumulam de forma diferente entre os grupos de organismos e que alguns PFAS estão bioacumulando ao longo da cadeia alimentar. A presente tese aborda, pela primeira vez, um extensivo esforço amostral para avaliar a presença de PFAS em diferentes matrizes bióticas e abióticas em ambientes tropicais, trazendo enfoque para esse grupo de compostos que vem sendo muito estudado mundialmente, mas ainda recebe pouca atenção no Brasil.

Resumo

Compostos per- e polifluoroalquilados (PFAS) são amplamente utilizados em diversas aplicações como surfactantes, pesticidas, espuma de combate a incêndio, etc. Esses compostos são conhecidos mundialmente não somente pela sua versatilidade de usos, mas também devido às suas características de persistência, toxicidade e bioacumulação. Também por essas características, os PFAS estão presentes em diversas matrizes ambientais. Uma vez no ambiente, uma série de processos naturais (e.g., degradação, dispersão e biomagnificação) governa o destino, toxicidade e transporte desses compostos, porém, esses processos naturais ainda são pouco estudados. O principal objetivo desta tese foi estabelecer ligações entre a presença de PFAS em compartimentos bióticos e abióticos em ambientes tropicais e os processos que controlam os padrões de distribuição observados. A pesquisa foi desenvolvida em solos de manguezal (Jaguaripe-BA), em águas oceânicas (oceano Atlântico Tropical Oeste) e na cadeia trófica de um estuário (rio Subaé-BA). Inicialmente, um experimento manipulativo de degradação de um formicida a base de PFAS (i.e., Sulfluramida) foi realizado em solos de mangue. O ambiente anóxico dos solos do mangue atuou como reservatório de contaminantes, retardando a exportação dos produtos de degradação, mais tóxicos, para áreas adjacentes. No estudo seguinte, a ocorrência de PFAS ao longo de um transecto no oeste do Oceano Atlântico Tropical (TAO) (15ºN-23ºS) foi estudada para avaliar a influência da circulação na dispersão desses compostos. Diferentes perfis espaciais e verticais de PFAS foram observados ao longo da coluna d'água entre as zonas do TAO (i.e., Atlântico Norte, Equador, Atlântico Sul e águas costeiras brasileiras). Correntes superficiais, ressurgência costeira, e a origem das massas de água foram fatores importantes para explicar as concentrações de PFAS e as distribuições verticais dos compostos ao longo do transecto no TAO. Por último, no estudo de biomagnificação, PFAS foram encontrados em todas as 21 espécies estudadas, distribuídas em 3 níveis tróficos em um estuário tropical. A biomagnificação de perfluorooctano sulfônico (PFOS), *N*-Etil perfluorooctano sulfonamida (EtFOSA) e ácido perfluorononanóico (PFNA) foi observada na cadeia trófica estudada do estuário do rio Subaé. O perfil de PFAS encontrado nesse estuário indicou a presença de fontes difusas desses compostos para os organismos. Os resultados observados nos estudos mostraram que a presença e o comportamento dos PFAS estão relacionados a fatores referentes aos compostos como padrão de utilização, fontes para o

ambiente e suas propriedades, além dos processos químicos e biológicos naturais que controlam a interação dos PFAS com o ambiente.

Palavras-chave: Baía de Todos os Santos, PFAS, Biomagnificação, Biomonitoramento

Abstract

Per- and polyfluoroalkyl substances (PFAS) are widely used in several applications such as surfactants, pesticides, aqueous firefighting foam, etc. These compounds are known worldwide not only for their versatility but also due to their persistent, toxic, and bioaccumulative characteristics. PFAS have been detected in several environmental matrices. Once in the environment, a variety of natural processes (e.g., degradation, dispersion, and biomagnification) drives the pathways, toxicity, and transport of these compounds, however, these natural processes are still poorly understood in tropical environments. The main objective of this thesis was to establish links between the presence of PFAS in biotic and abiotic compartments in tropical environments and the processes that control their distribution. The study was carried out in mangrove soils (Jaguaripe-BA), in ocean waters (Western Tropical Atlantic Ocean), and in the food web of an estuary (Subaé-BA river). Initially, a manipulative degradation experiment of a PFAS-based formicide (i.e., Sulfluramid) was carried out in mangrove soils. The anoxic environment of the mangrove soils acted as a reservoir of contaminants, delaying the export of more toxic degradation products to adjacent areas. In the following study, the occurrence of PFAS along a transect in the western Tropical Atlantic Ocean (TAO) (15ºN-23ºS) was studied to assess the influence of physical oceanographic processes on the dispersion of these compounds. Different spatial and vertical PFAS profiles were observed along the water column between the TAO zones (i.e., North Atlantic, Ecuador, South Atlantic, and Brazilian coastal waters). Surface currents, coastal upwelling, and the origin of water masses were important factors in explaining the concentrations of PFAS and the vertical distributions of the compounds along the TAO transect. Finally, in the biomagnification study, PFAS were found in all 21 species studied, distributed over 3 trophic levels in the Subaé estuary. The biomagnification of sulfonic perfluorooctane (PFOS), *N*-Ethyl perfluoro-octane sulfonamide (EtFOSA), and perfluorononanoic acid (PFNA) was also observed. PFAS profiles found in the Subaé estuary indicated the presence of diffuse sources of these compounds. The results showed that the presence and behavior of PFAS in tropical environments are related to several factors including the use of these compounds, their properties and sources the environment, in addition to the chemical and biological natural processes that control the interaction of PFAS with the environment.

Keyword: Todos os Santos Bay, PFAS, Biomagnification, Biomonitoring**.**

Lista de abreviaturas e siglas

AABW – Água de Fundo da Antártica **(***Abyssal Antarctic Bottom Water*)

AAIW – Água Intermediária da Antártica (*Antarctic Intermediate Water*)

ACN – Acetonitrila (*Acetonitrile*)

AFFF – Espuma aquosa de combate a incêmdio **(***aqueous film-forming foam*)

ATSDR – Agência para o Registro de Substâncias Tóxicas e Doenças (*Agency for Toxic Substances and Disease Registry*)

BC – Corrente do Brasil **(***Brazil Current*)

BTS – Baía de Todos os Santos (*Todos os Santos Bay)*

CFC – Clorofluorcarbonetos (*Chlorofluorocarbons*)

COT – Carbono orgânico Total (*Total organic carbono*)

dw – peso seco (*dry weight*)

ESI – Ionização por electrospray (*Electrospray Ionisation*)

EtFOSA – *N*-Etil perfluorooctano sulfonamida (*N-ethyl perfluorooctane sulfonamide*)

EtFOSAA – Ácido acético *N*-Etil perfluorooctano sulfonamida (*N-Ethyl perfluorooctane sulfonamido acetic acid*)

FASAs – Perfluoroalcanossulfonamidas (*Perfluoroalkyl sulfonamide derivatives*)

FOSA – Perfluorooctano sulfonamida (*Perfluorooctanesulfonamide acid*)

FOSAA - Ácido acético perfluorooctano sulfonamida (*perfluorooctanesulfonamido acetate acid*)

FTOH – Fluorotelômeroalcool (*Fluorotelomer alcohols*)

HDPE - Polietileno de alta densidade (*high-density polyethylene*)

HRMS – *High-resolution mass spectrometry*

IAEA – Agência internacional de energia atômica (*International Atomic Energy Agency*)

IRMS - Espectrômetro de massa de razão isotópica **(***Isotope Ratio Mass Spectrometry*)

LC – Cromatografia líquida (*Liquid chromatography*)

LOD – Limite de detecção (*Limit of detection*)

LOQ – Limite de quantificação (*Limit of quantification*)

MC – Mangue controle sem raiz (*control mangrove without roots*)

MCR – Mangue controle com raiz (*control mangrove with roots*)

MeFOSA - *N*-Metil perfluorooctano sulfonamida (*N*-methylperfluoro-1-octanesulfonamide)

MeOH – Metanol

MI - Mangue contaminado sem raiz (*impacted mangrove soils without mangrove roots*)

MIR – Mangue contaminado com raiz (*impacted mangrove soils with roots*)

MMA – Ministério do Meio Ambiente

MOW - Mediterranean Overflow Water

MPS - Material particulado em suspensão

n – número de amostras

NAC – Corrente do Atlântico Norte (*North Atlantic Current*)

NACW – Água Central do Atlântico Norte (*North Atlantic Central Water*)

NADW – Água de Profunda do Atlântico Norte (*North Atlantic Deep Water*)

NBC – Corrente Norte do Brasil (*North Brazil Current*)

NEC – Corrente Norte Equatorial (*North Equatorial Current*)

NECC – Contracorrente Norte Equatorial (*North Equatorial Countercurrent*)

NI – Ionização por electrospray negativa (*Negative electrospray ionization*)

PBDEs – Éteres difenílicos polibromados

PCB – Bifenilas policloradas

PFAAs – Ácidos perfluoroalquilados (*Perfluoroalkyl Acids*)

PFAS - Compostos per- e polifluoroalquilados (*Per- and polyfluoroalkyl substances*)

PFBA – Ácido perfluorobutanóico (*Perfluorobutanoic acid*)

PFBS – Ácido perfluorobutano sulfônico (*Perfluorobutanesulfonic acid*)

PFC – Compostos perfluorados (*Perfluorinated compounds*)

PFCAs – Ácidos carboxílicos perfluoroalquilados (*Perfluoroalkyl carboxylic acids*)

PFDA - Ácido perfluorodecanóico (*Perfluorodecanoic acid*)

PFDoDA - Ácido perfluorododecanóico (*Perfluorododecanoic acid*)

PFDS - Ácido perfluorodecano sulfônico (*Perfluorodecanesulfonic acid*)

PFHpA - Ácido perfluoroheptanóico (*Perfluoroheptanoic acid*)

PFHxA – Ácido perfluorohexanóico (*Perfluorohexanoic acid*)

PFHxS – Ácido perfluorohexano sulfônico (*Perfluorohexanesulfonic acid*)

PFNA – Ácido perfluorononanóico (*Perfluorononanoic acid*)

PFOA – Ácido perfluorooctanóico (*Perfluorooctane sulfonic acid*)

PFOS – Ácido perfluorooctano sulfônico (*Perfluorooctane sulfonic acid*)

PFPeDA - Ácido perfluoropentadecanóico (*Perfluoropentadecanoate acid*)

PFSAs – Ácidos perfluoroalquilados sulfônicos (*Perfluoroalkyl sulfonic acids*)

PFTeDA – Ácido perfluorotetradecanóico **(***Perfluorotetradecanoic acid*)

PFTrDA - Ácido perfluorotridecanóico (*Perfluorotridecanoic acid*)

PFUnDA - Ácido perfluorounodecanóico (*Perfluoroundecanoic acid*)

PNUMA – Programa das Nações Unidas para o Meio Ambiente

POPs – Poluentes orgânicos persistentes

POSF – Perfluorooctano sulfonilfluorido (*Perfluorooctane-1-sulfonyl fluoride)*

PP – Polipropileno

ppq – partes-por-quadrilhão (*part-per-quadrillion*)

ppt – partes-por-trilhão (*part-per-trillion*)

PTFE – Polifluorotetrafluoroetileno

RSD - desvio padrão relativo (*relative standard deviation*)

SAC – Corrente do Atlântico Sul (*South Atlantic Current*)

SACW – Água Central do Atlântico Sul (*South Atlantic Central Water*)

SD – desvio padrão (*standard deviation*)

SEC – Corrente Sul Equatorial (*South Equatorial Current*)

SECC – Contracorrente Sul Equatorial (*South Equatorial Countercurrent*)

SI – Informação suplementar (*Supplementary information*)

SPE – Extração em fase sólida (*Solid phase extraction*)

TAO – Oceano Atlântico Tropical **(***Tropical Atlantic Ocean*)

TMF – Fator de magnificação trófica (*Trophic Magnification Factor*)

TN – Nitrogênio Total (*total nitrogen*)

TW – Águas superficiais tropicais **(***Tropical Surface Waters*)

UNEP – Programa Ambiental das Nações Unidas

wb – corpo inteiro (*whole body*)

ww – peso úmido (*wet weight*)

Lista de Figuras

Lista de Tabelas

Sumário

Estrutura da Tese

A presente tese é composta por seis capítulos, sendo três capítulos estruturais (introdução, metodologia e conclusão) e três capítulos de resultados. No **Capítulo 1 – Introdução**, os compostos per- e polifluoroalquilados (PFAS) são apresentados, além de uma visão geral dos estudos com PFAS em matrizes ambientais no Brasil. Os objetivos da tese também são apresentados nesse capítulo. No **Capítulo 2 – Metodologia** há a descrição das áreas de estudo onde os experimentos/amostragens, apresentados nos próximos capítulos, foram realizados, assim como os delineamentos amostrais para cada capítulo mensurativo/manipulativo e as análises químicas realizadas. Os capítulos 3 ao 5 apresentam os resultados de três estudos de natureza empírica, sendo o primeiro (capítulo 3) um estudo manipulativo, enquanto os capítulos 4 e 5 têm natureza mensurativa. Esses capítulos são apresentados em formato de artigo, em inglês, estruturados de acordo com as exigências das respectivas revistas científicas escolhidas para submissão, os quais foram estruturados como segue:

Capítulo 3 – Estudo manipulativo in situ de degradação da Sulfluramida em solos de manguezais (*Sulfluramid degradation in tropical mangrove soil)*

Manuscrito a ser submetido ao periódico *Marine Pollution Bulletin*

A degradação do formicida Sulfluramida foi avaliada através de um experimento manipulativo *in situ* realizado no estuário do rio Jaguaripe. Para este estudo, foi realizada a contaminação de solos de mangue com o produto supracitado e, posterior, avaliação da degradação do pesticida em condições ambientais ao longo de 192 dias.

Capítulo 4 – Avaliação de ácidos perfluoroalquilados em água oceânica (*Perfluoroalkyl Acids (PFAAs) in the Western Tropical Atlantic Ocean)*

Manuscrito a ser submetido ao periódico *Environmental Science and Technology*

A dispersão dos ácidos perfluoroalquilados (PFAAs) foi avaliada no Atlântico Tropical Oeste entre 15ºN e 23ºS para entender quais os processos que atuam no espalhamento desses compostos. Foram coletadas 16 amostras superficiais ao longo do transecto N-S e 6 perfis verticais ao longo de toda coluna d'água.

Capítulo 5 - Estudo de biomagnificação de compostos per- e polifluoroalquilados em estuário tropical (*Bioaccumulation of Per- and polyfluoroalkyl substances (PFAS) in a tropical estuarine food web)*

Artigo publicado no periódico *Science of the Total Environment*

A biomagnificação de compostos per- e polifluoroalquilados (PFAS) foi avaliada em uma cadeia alimentar do estuário tropical do rio Subaé. Foram avaliadas 21 espécies de diferentes grupos taxonômicos, distribuídas em 3 níveis tróficos para avaliar a amplificação das concentrações de PFAS nos organismos estuarinos analisados.

Por fim, o último capítulo, **Capítulo 6 – Conclusões,** apresenta as conclusões gerais da tese.

Capítulo 1: Introdução geral

A discussão sobre microcontaminantes ambientais ganhou espaço em 1962, quando no livro "Primavera Silenciosa" Rachel Carson chama atenção pela primeira vez para os efeitos prejudiciais de pesticidas no meio ambiente e na saúde humana. Neste, a autora fez um apelo para considerar as consequências não intencionais ou imprevistas de produtos químicos lançados inadvertidamente no meio ambiente. Décadas após esta publicação, a preocupação com a entrada de novos produtos químicos sintéticos no ambiente permanece presente. Calcula-se que existam atualmente mais de 350 mil substâncias sintéticas registrados em bases de dados mundiais. Acredita-se que esse número seja ainda maior, considerando que esse compilado de dados para registro de químicos sintetizados/em uso para América do Sul, África e Ásia Ocidental são inexistentes (Wang et al., 2020).

Eventualmente, grande parte dos pesticidas e de compostos químicos sintéticos de uso doméstico e industrial entram nos sistemas aquáticos e representam uma ameaça ao meio ambiente (Schwarzenbach et al., 2006). As fontes desses compostos para o ambiente podem ser difusas, quando múltiplas rotas são atribuídas como fontes do contaminante (ex. águas superficiais e subterrâneas contaminadas, poluição atmosférica etc.) ou pontuais, onde a entrada do contaminante é atribuída a uma única fonte (ex. esgoto, aterro, efluente). Uma vez que os contaminantes atingem os corpos d'água, a estrutura do habitat pode ser alterada quimicamente, dependendo das características dos contaminantes.

Uma vez no ambiente, uma série de processos físicos, químicos e biológicos vão governar o destino, transporte e toxicidade dos contaminantes. Por exemplo, a biomagnificação é um importante mecanismo biológico para aumentar a concentração de micronutrientes (ex. ômega 3) em organismos do topo da cadeia alimentar (Barclay et al., 1994). No entanto, diversos contaminantes podem ser acumulados pelo mesmo processo, e assim aumentar as suas concentrações em organismos de topo de cadeia (ex. mercúrio e poluentes orgânicos persistentes - POPs) (Le Croizier et al., 2019; Miranda et al., 2021; Power et al., 2002). A amplificação da concentração de contaminantes ao longo da cadeia trófica pode constituir um risco (eco)toxicológico potencial para organismos de diferentes níveis tróficos em uma cadeia alimentar (Lau et al., 2007). Outro processo natural

importante observado na natureza é a acumulação de sedimento e matéria orgânica em solos de mangue (Alongi, 2014; Atwood et al., 2017). Porém, esse processo também pode ser acompanhado por um acúmulo de contaminantes, transformando o ambiente de mangue em um reservatório de poluentes (Lewis et al., 2011), que eventualmente podem ser exportados para áreas adjacentes. Como último exemplo de processos naturais que podem direcionar a presença de contaminantes no meio ambiente, estão as correntes oceânicas que atuam na dispersão de contaminantes de áreas fontes para áreas pristinas (Muir et al., 2019).

Entre os diversos grupos de contaminantes que vem sendo detectados no ambiente nas últimas décadas, os POPs representam uma classe de compostos químicos sintéticos que causam grande preocupação mundial (Fernández and Grimalt, 2003). São classificados como POPs os compostos que somam as características de elevada toxicidade, resistência à degradação, potencial para bioacumulação e capacidade para serem transportados para regiões remotas (UNEP, 2009). Para abordar a preocupação global relacionada aos POPs, o Programa das Nações Unidas para o Meio Ambiente (PNUMA) propôs um tratado mundial para atuar sob os problemas relacionados a esses compostos. Neste tratado, a Convenção de Estocolmo, os países signatários concordaram em reduzir ou eliminar a produção, uso e/ou liberação de doze compostos organoclorados, apelidados em inglês como *dirty dozen*. Essa lista é atualizada à medida que novos compostos são avaliados e classificados de acordo com as características dos POPs. Por exemplo, em 2009 alguns compostos a base de flúor, denominados como per- e polifluoroalquilados (PFAS), foram incluídos na lista de compostos controlados (UNEP, 2009). Desde a implementação da Convenção de Estocolmo em 2001, esforços vêm sendo feitos pelos países signatários para reduzir as concentrações ambientais dos poluentes listados no tratado, principalmente através da eliminação e controle de fontes poluidoras (UNEP, 2019).

Compostos per- e polifluoroalquilados (PFAS)

São classificados como PFAS o grupo de substâncias alifáticas sintéticas que têm a sua estrutura básica constituída por moléculas de carbono e flúor. A sua fórmula química primária é composta por C_nF_{2n+1}-R, em que o "R" representa o grupo funcional conectado a cadeia fluoroalquil. Esta estrutura confere propriedades anfipáticas a molécula, favorecendo a sua utilização em diferentes finalidades industriais (e.g. surfactantes, impermeabilizante de roupas, carpetes, revestimento de embalagens de alimentos, etc.)

(Buck et al., 2011). A alta persistência dos PFAS se deve a ligação C-F presente nos compostos, que promove alta estabilidade e baixa degradabilidade, sendo por isso chamados de *forever chemicals* (Wang et al., 2017). Essa alta persistência e resistência estão ligadas a presença do flúor, que é o elemento com maior eletronegatividade da tabela periódica, o que o coloca no topo dos oxidantes inorgânicos em força iônica. Esses compostos atendiam pela sigla em inglês PFC (*perfluorinated compounds*) até 2011, porém eram muitas vezes confundidos com outros compostos orgânicos de propriedades diferentes, mas também com flúor em sua composição, como os clorofluorcarbonetos (CFC). Foi então que Buck *et al.* (2011) propôs a sigla PFAS como uma nova terminologia para o grupo, em substituição ao uso de PFC (Fig. 1).

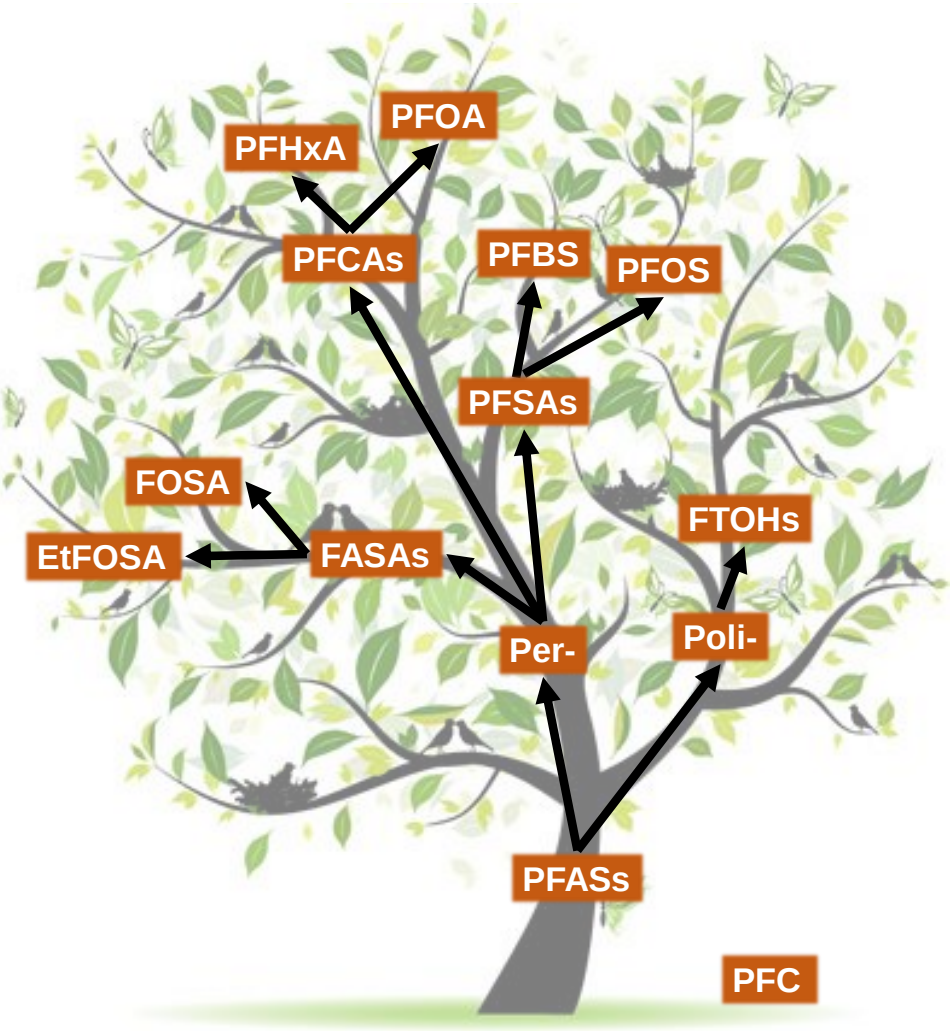

Figura 1. Árvore esquemática dos compostos per- e polifluoroalquilados (PFAS) com exemplos para alguns subgrupos. FASA: perfluoroalcanossulfonamidas; FOSA: perfluorooctano sulfonamida; EtFOSA: *N*-Etil perfluorooctano sulfonamida; PFSAs: ácidos perfluoroalquilados sulfônicos; PFBS: ácido perfluorobutanóico sulfônico; PFOS: ácido perfluooroctano sulfônico; PFCAs: ácidos carboxílicos perfluoroalquilados; PFHxA: ácido perfluorohexanóico; PFOA: ácido perfluorooctanóico; Poli-: polifluoroalquilados; e FTOHs: fluorotelômer álcool. A sigla para compostos perfluorados (PFC) foi mantida no desenho para lembrar o uso obsoleto do termo. Adaptado de *Agency for Toxic Substances and Disease Registry* (ATSDR).

A sigla PFAS compreende os compostos perfluoroalquilados (Figura 2), que apresentam todos os átomos de hidrogênio ligados a cadeia carbônica substituídos por flúor (ex. ácido perfluorooctano sulfônico, PFOS) e os polifluoroalquilados, que possuem ao menos um, mas não todos os átomos de H substituídos por flúor (ex. polifluorotetrafluoroetileno, PTFE). Junto a cadeia perfluoroalquilica que tende a ser hidrofóbica, os PFAS apresentam um radical hidrofílico que pode ser carbônico (ácidos carboxílicos perfluoroalquilados, PFCAs) ou sulfônico (ácidos sulfônicos perfluoroalquilados, PFSAs) (Fig. 1), além dos grupos fosfatados (ésteres de polifluoroalquil fosfato (PAPs)), alcóolicos (FTOHs) e outras classes. Os compostos mais frequentemente detectados no ambiente são os ácidos perfluoroalquilados (PFAAs), eles apresentam diversos usos comerciais e têm as maiores persistências dentre os PFAS.

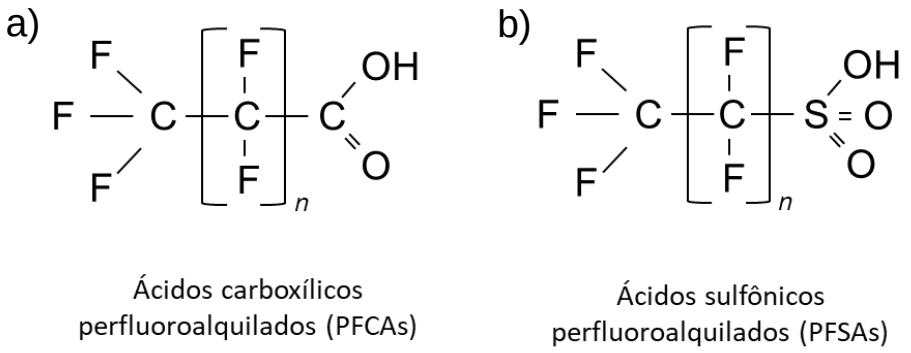

Figura 2: Exemplo de estruturas químicas de compostos perfluoroalquilados (PFAS). a) Ácidos carboxílicos perfluoroalquilados (PFCAs) e b) Ácidos sulfônicos perfluoroalquilados (PFSAs)

Os PFAAs são também subdivididos em compostos de cadeia longa ou de cadeia curta, sendo essa classificação diferente quando se trata de compostos sulfônicos e carboxilados. Os PFCAs de cadeia longa são representados por $C_n \geq 7$ e os PFSAs $C_n \geq 6$, pois os compostos sulfonados apresentaram maior toxicidade do que os carboxilados com o aumento do número de carbonos na cadeia acima de 6 (Buck et al., 2011). Em geral, os compostos de cadeia longa, tanto PFCAs quanto PFSAs, tendem a apresentar maiores toxicidades teóricas quando comparados aos compostos de cadeia curta, além de apresentarem maiores tempos de meia vida em matrizes ambientais (Zhao et al., 2016). No entanto, estudos recentes vêm demonstrando potencias tóxicos de compostos de cadeia curta semelhantes aos compostos de cadeia longa. Dois compostos de cadeia longa que vêm sendo extensivamente estudados devido à suas características tóxicas são o PFOS e o ácido perfluorooctanóico (PFOA) (Lau et al., 2007). O PFOS e seus sais entraram na lista de produtos da Convenção de Estocolmo em 2009 com comercialização,

produção e utilização restrita e o PFOA foi recentemente adicionado à lista de produtos proibidos em 2018 (UNEP, 2019). No entanto, apesar do Brasil ser signatário da Convenção de Estocolmo desde 2001, os registros de importação e exportação apontam um aumento da utilização de PFAS no país (Gilljam et al., 2016).

Os PFAS começaram a ser produzidos e comercializados na década de 50 (Buck et al., 2011) e passaram a ser amplamente utilizados em uma série de aplicações, como, por exemplo, em impermeabilizantes e revestimentos antiaderente em panelas Teflon® (e.g., PTFE) produzido pela 3M (Glüge et al., 2020; Prevedouros et al., 2006). Entre 1960 e 2000 os volumes de produção de PFAS cresceram exponencialmente, passando de dezenas para centenas de toneladas sintetizadas nas principais plantas de produção localizadas nos Estados Unidos e na Europa (Prevedouros et al., 2006). A 3M, uma das maiores indústrias produtoras de PFAS, interrompeu a utilização de alguns PFAS de cadeia longa quando a detecção desses compostos em matrizes ambientais e os seus riscos à saúde humana começaram a ser questionados (3M, 2003; Giesy and Kannan, 2001). Hoje, mundialmente, são mais de quatro mil PFAS identificados, sendo cerca de 70 com metodologia analítica bem estabelecida e 20 deles acompanhados em programas de monitoramento (Glüge et al., 2020). Desses, apenas três grupos estão atualmente sob regulamentação pela Convenção de Estocolmo (i.e., PFOA, PFOS, perfluorooctano sulfonil fluoreto (POSF-F) e seus sais).

PFAS são resistentes tanto a degradação biótica quanto abiótica, facilitando a sua dispersão e acumulação em diversas matrizes ambientais, até mesmo em zonas remotas. A toxicidade vai variar de acordo com a estrutura do PFAS, porém a maior parte dos estudos focaram em PFOA e PFOS como mais tóxicos até então (Lau et al., 2007; Salihovic et al., 2018). A grande preocupação com a toxicidade dos PFAS está relacionada a sua característica proteinofílica (Goeritz et al., 2013). Por essa propriedade afinidade a proteína os PFAS são encontrados ligados a albumina em sangue humano (Kannan et al., 2004; Papadopoulou et al., 2016), em diferentes tecidos de animais (Houde et al., 2011, 2006) e até no leite materno (Kim et al., 2011; Papadopoulou et al., 2016). Além disso, os PFAS possuem a capacidade de ultrapassar a barreira placentária, representando um risco também para o feto (Gützkow et al., 2012). Outro efeito adverso da exposição do feto a PFAS, como nascimento com baixo peso corpóreo, já foi observado (Olsen et al., 2009). Além de câncer nos rins e testículos de adultos (Vaughn

et al., 2013), disfunção da tireoide (Andersson et al., 2019), e outros implicações relacionados a desregulação endócrina (Lau et al., 2007).

Existe uma pressão para que os PFAS, assim como outros POPs (ex. bifenilas policloradas - PCBs, éteres difenílicos polibromados - PBDEs, etc.), sejam tratados como uma classe pelas agências reguladoras, pois esse grupo de compostos compartilha características similares (Kwiatkowski et al., 2020). Esses compostos podem entrar no ambiente de forma direta (Wang et al., 2014), pelo seu uso em produtos de consumo ou através de precursores como as perfluoroalquil sulfonamidas (Avendaño and Liu, 2015). Essas substâncias podem ser degradadas no meio ambiente e metabolizadas para uma forma de PFAS mais persistente, muitas vezes, mais tóxica (Zabaleta et al., 2018).

O ambiente aquático é uma via de transporte importante para esses compostos, uma vez que a maior parte dos PFAS mais persistentes apresentam baixa volatilidade como característica comum. Quando esses compostos entram em corpos d'agua, seja por fontes diretas (Gobelius et al., 2017) ou através da degradação de precursores (Benskin et al., 2013), eles podem ser transportados por longas distâncias (Yamashita et al., 2008) e se acumular por diferentes vias em solos, sedimentos e/ou na biota (Dalahmeh et al., 2018; Nascimento et al., 2018; Zhao et al., 2018). Os organismos podem assimilar os PFAS através do contato com sedimento/solo contaminado, através da água (bioconcentração) (Babut et al., 2017), e/ou dieta (bioacumulação) e ampliar essas concentrações através da biomagnificação em diferentes níveis tróficos (Miranda et al., 2021). As fontes de exposição no ambiente e as características dos compostos vão determinar as vias de entrada e acumulação desses compostos nas diferentes matrizes ambientais. Esses compostos podem também se espalhar no ambiente marinho através das correntes oceânicas (Yamashita et al., 2008) e até mesmo por spray marinho (Johansson et al., 2019).

A preocupação com PFAS no ambiente ganhou espaço em 2001, quando um estudo global avaliando a contaminação por PFAS na vida selvagem foi reportado pela primeira vez (Giesy and Kannan, 2001). Posteriormente, um estudo avaliando testemunhos de solo mostrou que a contaminação ambiental por PFAS data a década de 50, quando análises mostraram concentrações de PFOS em 1952, além de outros PFAS como por exemplo a perfluorooctano sulfonamida (FOSA) em 1970 (Yeung et al., 2013). Desde então, diversos estudos vêm sendo conduzidos tanto em áreas próximas as plantas

de produção e uso de PFAS, para avaliar a exposição que esses pontos críticos representam para a população local, meio ambiente e vida selvagem (Munoz et al., 2017; Mussabek et al., 2020; Song et al., 2018), quanto em áreas remotas, no intuito de estimar o alcance desses compostos em áreas pristinas (Cai et al., 2012; MacInnis et al., 2019; Spaan et al., 2020). Porém, ainda assim, estudos avaliando a presença de PFAS em ambientes tropicais ainda são escassos.

PFAS no Brasil

Ainda que a problemática relacionada a persistência e toxicidade dos PFAS para o ambiente e saúde humana seja amplamente abordada mundialmente, poucos estudos avaliaram esses compostos no Brasil. O primeiro estudo publicado com PFAS no Brasil avaliou a presença de PFAS em sangue humano (Kannan et al., 2004). Os resultados mostraram que PFOS foi o principal PFAS encontrado nas amostras de sangue entre os quatro compostos estudados e em concentrações relativamente menores em comparação aos outros países estudados. Após esse estudo inicial, três estudos foram publicados analisando PFAS na biota das regiões sul e sudeste do Brasil. Os estudos analisaram tecido hepático de boto cinza (*Sotalia guianensis*) no Rio de Janeiro (Dorneles et al., 2008; Quinete et al., 2009) e toninhas (*Pontoporia blainvillei*) e lobos marinhos (*Arctocephalus tropicalis*), na costa do Rio Grande (Leonel et al., 2008). Bivalves (*Perna perna*), fígado e músculo de peixes (*Lepidopus caudatus, Micropogonias furnieri, Mugil liza, Tilapia rendalli, Geophagus brasiliensis*) também foram avaliados em um dos estudos do Rio de Janeiro (Quinete et al., 2009). PFAS foram observados em folhas, no sul da Bahia, em uma área de cultivo de eucalipto manejada com Sulfluramida, um formicida a base de PFAS (Nascimento et al., 2018). Devido à natureza das matrizes analisadas e fontes de compostos para as áreas de estudo, as concentrações e perfil de PFAS variou significativamente (Tabela 1), porém a presença de PFOS e PFOA foi observada na maior parte dos organismos analisados. Em resumo, foram publicados apenas 4 estudos investigando PFAS na biota brasileira antes da presente tese e um em sangue humano, mostrando a incipiência de estudo investigando PFAS na região.

Tabela 1. Estudos realizados no Brasil com matrizes ambientais avaliando perfluorooctano sulfônico (PFOS) e ácido perfluorooctanóico (PFOA). Num. de PFAS se refere ao número de compostos analisados por estudo.

Referência	Matriz	Local	PFOS	PFOA	Num. de PFAS
Dorneles et al. (2008)	Golfinho Tecido hepático	Baía de Guanabara	43,0 - 2431 ng g^{-1}	< 7,3 ng g^{-1}	4
Leonel et al. (2008)	Lobos marinhos - Tecido hepático	Rio Grande do Sul	< 0,10 - 21,6 ng g^{-1}	< 0,20 ng g^{-1}	10
	Golfinhos - Tecido hepático	Rio Grande do Sul	3,60 - 42,0 ng g^{-1}	< 0,20 ng g^{-1}	10
Quinete et al. (2009)	Ostra	Baía de Guanabara - RJ	< 0,95 - 4,46 ng g^{-1}	< 0,84 - 6,02 ng g^{-1}	10
	Peixes - Tecido hepático	Baía de Guanabara/rio Paraíba do Sul - RJ	< 0,62 - 28,9 ng g^{-1}	< 0,46 - 1,42 ng g^{-1}	10
	Golfinho - Tecido hepático	Rio Paraíba do Sul- RJ	25,9 - 149 ng g^{-1}	0,70 - 1,86 ng g^{-1}	10
Nascimento et al. (2018)	Folha de eucalipto	Sul da Bahia	226 - 322 pg g^{-1}	< 26,0 pg g^{-1}	19
Quinete et al. (2009)	Água marinha costeira	Baía de Guanabara - RJ	0,40 - 0,92 ng L^{-1}	0,77 - 3,25 ng L^{-1}	10
	Água marinha costeira	Foz do rio Paraíba do Sul - RJ	< 0,10 - 0,69 ng L^{-1}	< 0,09 -1,22 ng L^{-1}	10
Gilljam et al. (2016)	Água estuarina	Baía de Todos os Santos - BA	63,0 - 1061 ng L^{-1}	92,0 - 298 ng L^{-1}	21
Nascimento et al. (2018)	Água marinha costeira	Sul da Bahia	186 - 2850 pg g^{-1}	141 - 3310 pg g^{-1}	19
	Solo	Sul da Bahia	297 - 3770 pg g^{-1}	< 26,0 pg g^{-1}	19
	Sedimento	Sul da Bahia	7,00 - 37,0 pg g^{-1}	14,0 - 58,0 pg g^{-1}	19

PFOS e PFOA também foram encontrados frequentemente em amostras de água engarrafada e água de torneira (Quinete et al., 2009; Schwanz et al., 2016) no sul do país, em ambientes marinhos no Rio de Janeiro (Quinete et al., 2009) e na Bahia, dentro (Gilljam et al., 2016) e fora da Baía de Todos os Santos (BTS) (Nascimento et al., 2018). No entanto, enquanto o ácido perfluorohexano sulfônico (PFHxS) esteve entre os mais detectados no Rio de Janeiro, FOSA foi o PFAS mais encontrado na BTS. O padrão de distribuição de PFAS na BTS sugere o uso da Sulfluramida (*N*-Etil perfluorooctano sulfonamida, EtFOSA), um formicida fluorado largamente utilizado para combater formigas de corte (*Atta* ssp. e *Acromyrmex* ssp.) principalmente em plantações de *Eucaliptus* sp. e *Pinus* sp., como uma das principais fontes de PFAS para os principais estuários da BTS (Paraguaçu e Subaé) (Gilljam et al., 2016).

A Sulfluramida passou a ser utilizada no Brasil como uma substituição menos tóxica e persistente ao pesticida organoclorado Mirex em 1993, quando o seu potencial como precursor do PFOS ainda não era discutido. Apesar da tendência mundial em reduzir a produção e utilização de PFAS de cadeia longa, alguns desses compostos (i.e., EtFOSA, POSF e PFOS) ainda são amplamente utilizados no Brasil (Gilljam et al., 2016; Nascimento et al., 2018), sob exceção prevista na Convenção de Estocolmo (MMA, 2015). O uso maciço da Sulfluramida no Brasil, produto que já foi banido em diversos lugares do mundo, pode representar um risco para o meio ambiente e para a população humana através do consumo de água e organismos contaminados pelos produtos de degradação do formicida.

Recentemente, estudos têm mostrado que a presença de PFOS em regiões costeiras e oceânicas (e.g., Atlântico Sul) (Benskin et al., 2012; González-Gaya et al.,

2014; Nascimento et al., 2018) pode estar associada a utilização do formicida, além de outras fontes. O Brasil está entre os maiores importadores de Sulfluramida no mundo e a Bahia está entre os cinco estados que mais a comercializam no país (MMA, 2015). Os estudos realizados até o momento avaliando a degradação da Sulfluramida e/ou ao princípio ativo do formicida (i.e., EtFOSA) são escassos e limitados a experimentos laboratoriais (Avendaño and Liu, 2015; Zabaleta et al., 2018), onde não é possível avaliar a sinergia das variáveis ambientais no processo de metabolização do formicida. Outras fontes de PFAS para o meio ambiente também devem ser consideradas, visto que existe permissão pelo Plano de Implementação da Convenção de Estocolmo no Brasil para uso de PFOS em espuma de combate a incêndio, galvanoplastia e outros produtos de consumo (MMA, 2015). Somado ao uso de PFAS como formicida, os resíduos industriais e domésticos perfazem grande parte das fontes desses compostos para o ambiente no Brasil.

Diante do exposto é possível observar que estudos avaliando a presença de PFAS em ambientes tropicais é ainda incipiente e que estudos avaliando os mecanismos naturais que influenciam a ocorrência desses compostos nesses ambientes são inexistentes. Sendo assim, a presente tese visa avaliar como a degradação desses compostos em ambientes de mangue acontece (Capítulo 3), como a dispersão desses compostos ocorre no oeste do oceano Atlântico Tropical (Capítulo 4) e, por último, avaliar a ocorrência de bioacumulação de PFAS através da cadeia de um estuário tropical (Capitulo 5).

Objetivo Geral

Avaliar a distribuição de compostos per- e polifluoroalquilados nas águas do Atlântico tropical (23°S-15°N) e em estuários da Baía de Todos os Santos, visando a identificação de fontes, processos de dispersão, degradação e biomagnificação.

Objetivos específicos

1. Avaliar se o processo de degradação da Sulfluramida em solos de mangues contaminados é uma fonte indireta de PFOS para o meio ambiente;

2. Avaliar se os padrões de circulação, *phase-out* de alguns PFAS e o uso intensivo de formicidas no Brasil determinam o padrão de ocorrência destes compostos no Oceano Atlântico Tropical;

3. Verificar se os PFAS biomagnificam ao longo da cadeia trófica do estuário do rio Subaé, Baía de Todos os Santos, Bahia.

Capítulo 2: Metodologia Geral

Área de estudo

Cada um dos capítulos da presente tese foi desenvolvido em uma área de estudo diferente na zona tropical, sendo os capítulos 3 e 5 executados na Baía de Todos os Santos (BTS) (12°35′30″-13°07′30″S e 038°29′00″-038°48′00″W) e o capítulo 4 em águas oceânicas (Fig. 3).

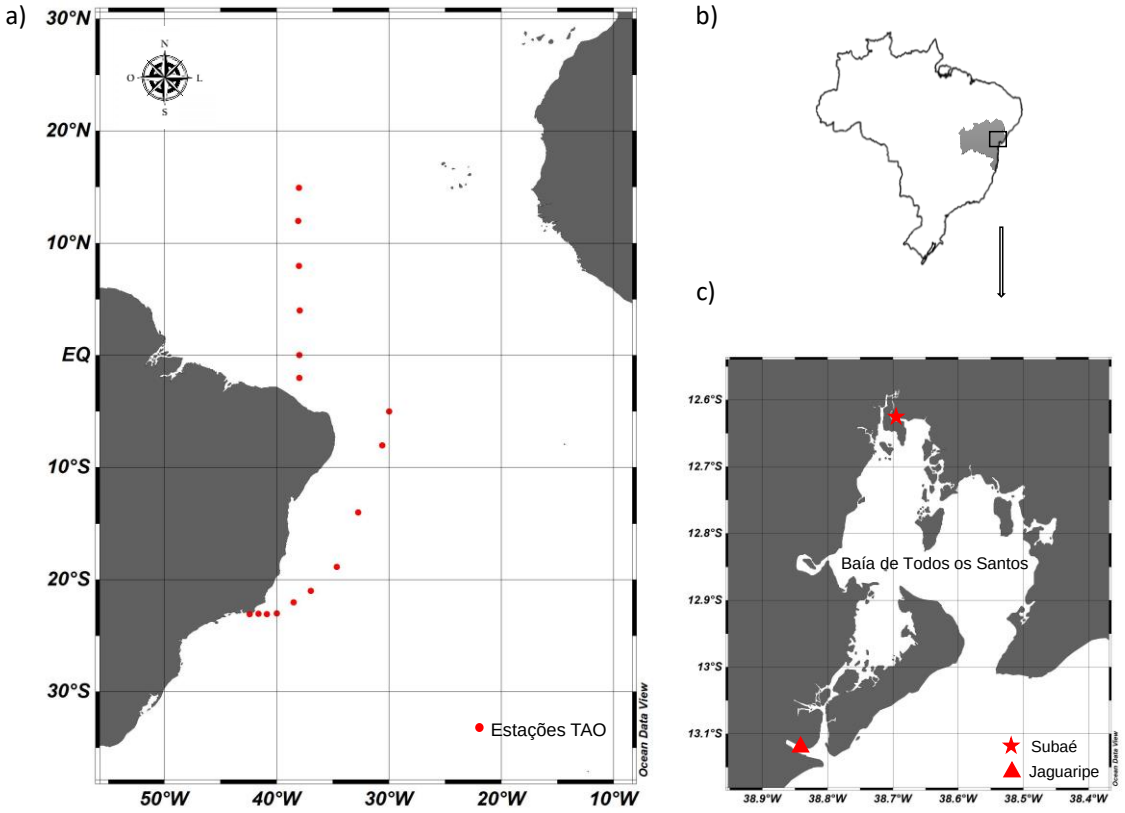

Figura 3. Pontos de estudo para a presente tese. a) Estações TAO (oceano Atlântico Tropical) (capítulo 4); b) Mapa do Brasil destacando o estado da Bahia. O quadrado preto representa a Baía de Todos os Santos (BTS); c) Estuários Jaguaripe e Subaé na BTS, onde os capítulos 3 e 5 foram desenvolvidos.

A BTS é caracterizada por um clima tropical úmido, com temperatura média anual em torno de 25 °C e precipitação de 2100 mm, com marés mesotidais semidiurnas que controlam as correntes no interior da baía (Cirano and Lessa, 2007). A baía tem três grandes afluentes: Rio Paraguaçu (56.300 km^2), Rio Jaguaripe (2.200 km^2) e Rio Subaé (600 km^2). Embora Subaé seja o menor dos três rios, e tenha uma vazão média mensal baixa (9 m^3 s^{-1}), é conhecido por ser um *hotspot* de contaminação, devido ao seu histórico de contaminação por elementos traços (Hatje et al., 2006; Krull et al., 2014). O rio Jaguaripe é o mais preservado dos três tributários que deságuam na BTS (Egres et al., 2019; Hatje and Barros, 2012; Krull et al., 2014). O capítulo 4 foi desenvolvido em uma

área de maior abrangência, entre as latitudes de 15ºN a 23ºS no Oceano Atlântico Tropical e na plataforma continental do Rio de Janeiro (23°S). As áreas de estudo serão descritas em maior detalhamento nos capítulos da tese que se seguem.

Desenho amostral

A seguir serão descritos os desenhos amostrais de cada um dos capítulos de dados (i.e., capítulos 3, 4 e 5) com informações sobre data de coleta, número de amostras e procedimentos de amostragem.

Capítulo 3: Estudo manipulativo in situ de degradação da Sulfluramida em solos de manguezais

Entre abril e outubro de 2017 foi realizado o experimento manipulativo no estuário do Rio Jaguaripe, Bahia, para avaliar a degradação da Sulfluramida em solos de mangue. O experimento foi realizado em 10 pontos, sendo 6 áreas impactadas, contaminadas com o formicida Sulfluramida (autorização para atividade com finalidade científica emitida pelo SISBIO: n° 57866-1) e 4 áreas controles (número de amostras total = 84). Os tratamentos consistiam de tubos de PVC de 20 centímetros de profundidade e 15 cm de diâmetro. No campo, dois quilos de solos de mangue foram retirados de cada área delimitada pelo tubo de PVC, pesados, homogeneizados com 500 g de isca formicida Sulfluramida (Grão Forte®, 0,3% EtFOSA) e devolvidos ao tubo de PVC (Fig. 4) onde permaneceram durante todo o experimento. O desenho experimental empregado para cada tratamento (Fig. 4), incluiu áreas com e sem pneumatóforos tanto para os tratamentos controle, como para os tratamentos que foram contaminados por Sulfluramida.

Figura 4. Exemplo do tratamento do experimento no mangue

O experimento ocorreu ao longo de 192 dias. Este período foi estipulado considerando o processo de degradação da Sulfluramida visto em experimentos de laboratório (Avendaño and Liu, 2015; Zabaleta et al., 2018), assumindo o tempo médio de meia vida dos compostos intermediários, até o seu produto final de degradação (PFOS) nos solos. Após a adição da Sulfluramida, cada tratamento foi amostrado em 9 momentos (T) entre o primeiro e último dia do experimento (192 dias), sendo eles: T1: tempo zero; T1': tempo zero após a adição da Sulfluramida; T2: 2 d; T3: 15 d; T4: 30 d; T5: 60 d; T6: 90 d; T7: 156 d; T8: 192 d (Fig. 5). Foram coletadas amostras de solos em cada um dos tempos (T1-T8), conforme ilustrado abaixo:

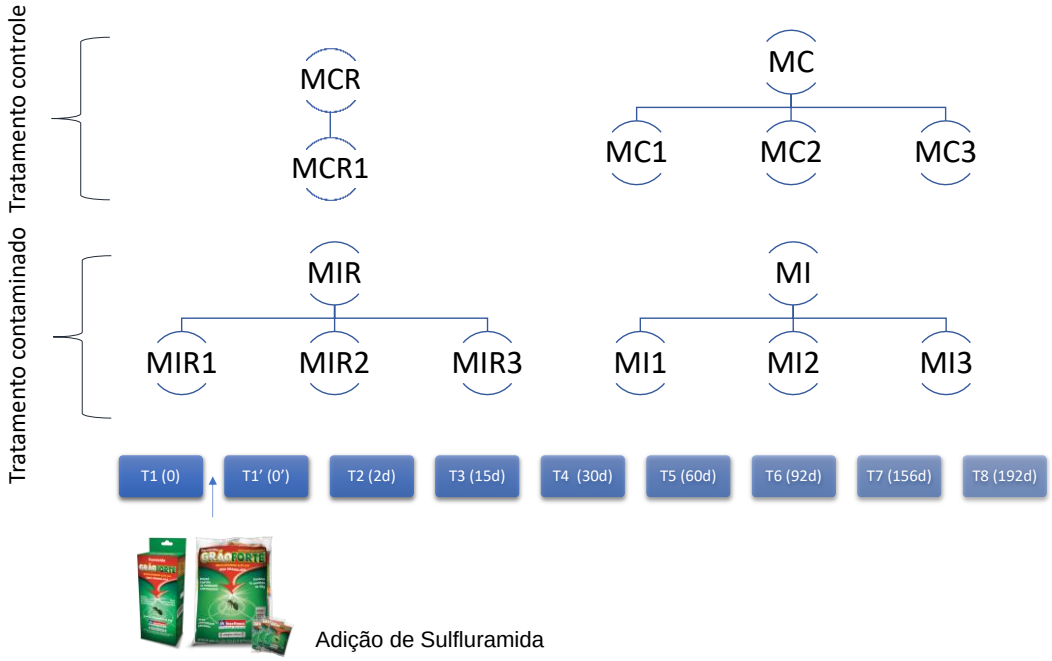

Figura 5. Esquema mostrando o delineamento amostral do experimento manipulativo in situ da degradação da Sulfluramida em solos de mangue. Onde MI: Mangue contaminado sem raiz; MIR: Mangue contaminado com raiz; MC: Mangue controle sem raiz; MCR: Mangue controle com raiz.

Capítulo 4: Avaliação de PFAAs em água oceânica

Amostras de água foram coletadas ao longo do oceano Atlântico Tropical Oeste entre 13 de novembro de 2017 e 14 de janeiro de 2018 a bordo do navio Oceanográfico Vital de Oliveira, durante os cruzeiros PIRATA XVII/ GEOTRACES GApr10 (http://pirata.ccst.inpe.br/en/home). Para avaliar a dispersão de PFAAs ao longo do transecto entre 15ºN e 23ºS do oceano Atlântico (Fig. 3), foram coletadas 51 amostras de água do mar, sendo elas divididas em 16 amostras superficiais e 6 perfis verticais, onde foram amostradas entre 4 e 9 profundidades entre 5 a 5845 m. As amostras foram coletadas com garrafas NISKIN e refrigeradas logo após a coleta. Dados de salinidade,

temperatura e oxigênio foram registrados com o auxílio de uma sonda multiparâmetros acoplada ao amostrador tipo *Rosette*, simultaneamente a coleta das amostras.

Capítulo 5: Estudo de biomagnificação em estuário tropical

As amostras do estudo de bioacumulação foram coletadas entre março e abril de 2016. Foram coletadas 21 espécies de organismos estuarinos, incluindo ostra de mangue (*Crassostrea rhizophorae*, n = 14), sururu (*Mytella guyanensis*, n = 63), siri azul (*Callinectes sapidus*, n = 4), chumbinho (*Anomalocardia brasiliana*, n = 5), poliqueta (amostra composta), ostra de mangue (*Crassostrea brasiliana*, n = 5), moapen (*Tagelus plebeius*, n = 60), caranguejo (*Ucides cordatus*, n = 6), camarão (*Litopenaeus* sp., n = 18), aratu (*Goniopsis cruentata*, n = 12), tainha (*Mugil* sp., n = 3), choupa (*Genyatremus luteus*, n = 3), Carapeba (*Diapterus* sp., n = 9), carapeba prateada (*Eucinostomus* sp., n = 1), bagre (*Cathorops spixii*, n = 5), robalo-peva (*Centropomus parallelus*, n = 3), mirucaia (*Stellifer* sp., n = 6), cabeçudo (*Caranx* sp., n = 5), bagre amarelo (*Aspistor luniscutis*, n = 3), robalo-comum (*Centropomus undecimalis*, n = 3) e cangauá (*Ctenosciaena gracilicirrhus*, n = 1). Amostras compostas de folhas de árvores de mangue (*Rhizophora mangle*, *Laguncularia racemosa* e *Avicenia* sp.), Biofilme (amostra composta) e sedimentos (n = 4) foram coletados com uma colher limpa no mesmo local que os organismos bentônicos durante a maré baixa, quando o sedimento foi exposto. O material particulado em suspensão (MPS) foi amostrado durante a maré de cheia em três pontos (n = 3) entre a localização dos locais de amostragem de sedimento. Estas amostras foram refrigeradas em campo. No laboratório, as amostras foram identificadas, os tecidos de interesse foram retirados, secos e armazenadas em dessecador até o momento da análise.

Análises químicas

Os procedimentos de preparo de material e coleta foram específicos de cada estudo e são apresentados em detalhe em cada capítulo. Abaixo será apresentada uma síntese dos procedimentos analíticos aplicados.

Extração de PFAS

Para as amostras de sedimentos, solos e biota foi utilizado um método descrito previamente (Zabaleta et al., 2018). As amostras foram pesadas em um tubo de polipropileno de 50 mL (0,5 g) e, em seguida, foram adicionados 2 ng de padrão interno e 8 mL de acetonitrila (ACN). Esta mistura foi sonicada em banho de ultrassom por 20 min. Posteriormente, os tubos foram agitados durante 40 minutos em mesa agitadora e

centrifugados à 2900 rpm durante 20 minutos. O sobrenadante foi removido e 8 mL de ACN com NaOH 25mM (7,2 mL ACN + 0,6 mL água deionizada + 0,2 mL NaOH 1M) foi adicionado e a sonicação e centrifugação foram repetidas. Os sobrenadantes das duas etapas foram combinados e reduzidos a secura em fluxo suave de nitrogênio (grau analítico, 5,0). O extrato foi ressuspendido em 400 µL de metanol (MeOH): água Milli-Q (1: 1, v / v) com ácido fórmico 20 mM e formiato de amônio 20 mM. O procedimento para extração de PFAS no MPS seguiu a mesma metodologia, porém o solvente utilizado para extração foi metanol puro. Os extratos foram transferidos para ampolas e mantidos fechados até o momento das análises.

As amostras de água do mar foram extraídas em fase sólida (SPE, sigla em inglês para *Solid Phase Extraction*) com cartuchos de fraca troca iônica (Waters Oasis® *Weak-anion exchange* WAX SPE (6 cm^3, 150 mg, 30 µm)). Os cartuchos foram previamente condicionados com 15 mL de 0,3% de NH_4OH em MeOH seguido por 4,5 mL de ácido fórmico 0,1 M em água Milli-Q ultrapura. Após o condicionamento dos cartuchos, as amostras de água do mar (500 mL cada) foram extraídas. Em seguida, os cartuchos foram lavados com 5 mL de MeOH a 20% em ácido fórmico 0,1 M e 2 mL de NH_4OH a 0,3% em água Milli-Q. As amostras foram eluidas com 3 mL de NH_4OH a 0,3% em MeOH. Os extratos foram então evaporados sob um fluxo suave de nitrogênio até um volume final de 100 µL e transferidos para *vials* de polietileno de alta densidade (HDPE) e, então, armazenados em geladeira até o momento da análise.

Identificação e Quantificação de PFAS

A análise de identificação e quantificação de 22 PFAS (Tabela 2) foi realizada por cromatografia líquida (LC) acoplada a duplo espectrômetro de massas triplo quadrupolo (MS/MS) (Waters Acquity UPLC; Waters Xevo TQ-S). As alíquotas das amostras injetadas no equipamento variaram de 5 µL para amostras de sedimento, biota e MPS a 20 µL para amostras de água do mar. As alíquotas foram cromatografadas em coluna analítica BEH C18 (2,1 × 50 mm, tamanho de partícula de 1,7 µm, Waters) operada a uma taxa de fluxo de 0,4 mL min^{-1}, usando uma composição de fase móvel de 90% água/10 % de acetonitrila contendo 2 mM de acetato de amônio (solvente A) e 100% de acetonitrila contendo 2 mM de acetato de amônio (solvente B). O MS/MS foi operado em ionização por eletrospray negativo, modo de monitoramento de reação múltipla. A identificação dos analitos foi baseada em seus respectivos tempos de retenção a partir de padrões analíticos e íons de transição (2 para cada analito). A quantificação dos analitos

nas amostras foi determinada através da diluição de isótopos ou uma abordagem de padrão interno. Quando presentes, os isômeros ramificados (i.e., br-) foram determinados semiquantitativamente usando a curva de calibração para o isômero linear (i.e., L-). Brancos, réplicas e experimentos de fortificação e recuperação foram analisados em cada lote analítico (máximo de 10 amostras reais) a fim de avaliar contaminação, precisão e exatidão das análises. Os resultados dos controles de qualidade serão apresentados nos capítulos de dados a seguir. Essas análises foram realizadas na Universidade de Estocolmo, Departamento de Ciências Ambientais (ACES), durante o período de doutorado sanduíche no exterior.

Tabela 2. Compostos perfluoroalquilados (PFAS) analisados na presente tese.

Acronimo	Nomenclatura	Fórmula	CAS#
	Ácidos carboxílicos perfluoroalquilados (PFCAs)		
PFBA	Ácido perfluorobutanóico	C_3F_7COOH	375-22-4
PFPeA	Ácido perfluoropentanóico	C_4F_9COOH	2706-90-3
PFHxA	Ácido perfluorohexanóico	C_5F_7COOH	307-24-4
PFHpA	Ácido perfluoroheptanóico	$C_6F_{13}COOH$	375-85-9
PFOA	Ácido perfluorooctanóico	$C_7F_{15}COOH$	335-67-1
PFNA	Ácido perfluorononanóico	$C_8F_{17}COOH$	375-95-1
PFDA	Ácido perfluorodecanóico	$C_9F_{19}COOH$	335-76-2
PFUnDA	Ácido perfluorounodecanóico	$C_{10}F_{21}COOH$	2058-94-8
PFDoDA	Ácido perfluorododecanóico	$C_{11}F_{23}COOH$	307-55-1
PFTrDA	Ácido perfluorotridecanóico	$C_{12}F_{25}COOH$	72629-94-8
PFTeDA	Ácido perfluorotetradecanóico	$C_{13}F_{27}COOH$	376-06-7
PFPeDA	Ácido perfluoropentadecanóico	$C_{14}F_{29}COOH$	1214264-29-5
	Ácidos perfluoroalquilados sulfônicos (PFSAs)		
PFBS	Ácido perfluorobutano sulfônico	$C_4F_9SO_3H$	375-73-5
PFHxS	Ácido perfluorohexano sulfônico	$C_6F_{13}SO_3H$	355-46-4
PFOS	Ácido perfluorooctano sulfônico	$C_8F_{17}SO_3H$	1763-23-1
PFDS	Ácido perfluorodecano sulfônico	$C_{10}F_{21}SO_3H$	355-77-3
	Derivados acéticos de Perfluoroalcanos sulfonamidas (FASAAs)		
FOSAA	Ácido acético perfluorooctano sulfonamida	$C_8F_{17}SO_2NHCH_2COOH$	2806-24-8
MeFOSAA	Ácido acético *N*-Metil perfluorooctano sulfonamida	$C_{11}H_3D_3F_{17}NO_4S$	1400690-70-1
EtFOSAA	Ácido acético *N*-Etilperfluorooctano sulfonamida	$C_8F_{17}SO_2NH(C_2H_5)CH_2COOH$	2991-50-6
	Perfluoroalcanos sulfonamidas (FASAs)		
MeFOSA	*N*-Metil perfluorooctano sulfonamida	$C_{11}H_8F_{17}NO_3S$	24448-09-7
FOSA	Perfluorooctano sulfonamida	$C_8F_{17}SO_2NH_2$	754-91-6
EtFOSA	*N*-Etil perfluorooctano sulfonamida	$C_8F_{17}SO_2NH(C_2H_5)$	4151-50-2

Carbono Nitrogênio e seus isótopos estáveis ($\delta^{13}C$ e $\delta^{15}N$)

As determinações de Carbono orgânico total (COT), nitrogênio total (NT) e a composição isotópica de N e C ($\delta^{15}N$ e $\delta^{13}C$) em solos de manguezais foram determinadas usando um espectrômetro de massa de razão isotópica Delta V (Thermo Fisher, EUA). A precisão do método foi determinada usando materiais de referência certificados (USGS-

40 e USGS-41). As amostras para o estudo de degradação foram analisadas no Laboratório de Física Nuclear Aplicada na Universidade Federal da Bahia.

COT, NT e isótopos estáveis de N e C ($\delta^{15}N$ e $\delta^{13}C$) também foram analisados em sedimentos, músculos de peixes e crustáceos, corpo inteiro de poliquetas e tecidos moles de bivalves para o estudo de biomagnificação. Assim como para os solos de manguezais, as amostras foram tratadas com 0,1 M HCl para remoção de carbonatos antes da análise de COT e $\delta^{13}C$. As razões dos isótopos estáveis foram medidas usando um espectrômetro de massa de razão isotópica (IsoPrime100, Isoprime, Cheadle, UK) acoplado em fluxo contínuo a um analisador elementar (MICRO, Elementar Analysensysteme GmbH, Hanau, Alemanha). Materiais de referência certificados da *International Atomic Energy Agency* (IAEA, Viena, Áustria) foram utilizados como padrões primários e sulfato de amônio e ácido sulfanílico como padrão analítico secundário. As amostras para o estudo de biomagnificação foram analisadas na Universidade de Liége, Bélgica.

Referências bibliográficas

3M, C., 2003. The Science of Organic Fluorochemistry. Washington, D.C.

Alongi, D.M., 2014. Carbon Cycling and Storage in Mangrove Forests. Ann. Rev. Mar. Sci. 6, 195–219. https://doi.org/10.1146/annurev-marine-010213-135020

Andersson, E.M., Scott, K., Xu, Y., Li, Y., Olsson, D.S., Fletcher, T., Jakobsson, K., 2019. High exposure to perfluorinated compounds in drinking water and thyroid disease. A cohort study from Ronneby, Sweden. Environ. Res. 176, 108540. https://doi.org/https://doi.org/10.1016/j.envres.2019.108540

Atwood, T.B., Connolly, R.M., Almahasheer, H., Carnell, P.E., Duarte, C.M., Ewers Lewis, C.J., Irigoien, X., Kelleway, J.J., Lavery, P.S., Macreadie, P.I., Serrano, O., Sanders, C.J., Santos, I., Steven, A.D.L., Lovelock, C.E., 2017. Global patterns in mangrove soil carbon stocks and losses. Nat. Clim. Chang. 7, 523–528. https://doi.org/10.1038/nclimate3326

Avendaño, S., Liu, J., 2015. Production of PFOS from aerobic soil biotransformation of two perfluoroalkyl sulfonamide derivatives. Chemosphere 119, 1084–1090. https://doi.org/10.1016/j.chemosphere.2014.09.059

Babut, M., Labadie, P., Simonnet-Laprade, C., Munoz, G., Roger, M.-C., Ferrari, B.J.D., Budzinski, H., Sivade, E., 2017. Per- and poly-fluoroalkyl compounds in freshwater fish from the Rhône River: Influence of fish size, diet, prey contamination and biotransformation. Sci. Total Environ. 605–606, 38–47. https://doi.org/https://doi.org/10.1016/j.scitotenv.2017.06.111

Barclay, W.R., Meager, K.M., Abril, J.R., 1994. Heterotrophic production of long chain omega-3 fatty acids utilizing algae and algae-like microorganisms. J. Appl. Phycol. 6, 123–129. https://doi.org/10.1007/BF02186066

Benskin, J.P., Ikonomou, M.G., Gobas, F.A.P.C., Begley, T.H., Woudneh, M.B., Cosgrove, J.R., 2013. Biodegradation of N-Ethyl Perfluorooctane Sulfonamido Ethanol (EtFOSE) and EtFOSE-Based Phosphate Diester (SAmPAP Diester) in Marine Sediments. Environ. Sci. Technol. 47, 1381–1389. https://doi.org/10.1021/es304336r

Benskin, J.P., Muir, D.C.G., Scott, B.F., Spencer, C., De Silva, A.O., Kylin, H., Martin,

J.W., Morris, A., Lohmann, R., Tomy, G., Rosenberg, B., Taniyasu, S., Yamashita, N., 2012. Perfluoroalkyl Acids in the Atlantic and Canadian Arctic Oceans. Environ. Sci. Technol. 46, 5815–5823. https://doi.org/10.1021/es300578x

Buck, R.C., Franklin, J., Berger, U., Conder, J.M., Cousins, I.T., de Voogt, P., Jensen, A.A., Kannan, K., Mabury, S.A., van Leeuwen, S.P.J., 2011. Perfluoroalkyl and Polyfluoroalkyl Substances in the Environment: Terminology, Classification, and Origins. Integr. Environ. Assess. Manag. 7, 513–541. https://doi.org/10.1002/ieam.258

Cai, M., Yang, H., Xie, Z., Zhao, Z., Wang, F., Lu, Z., Sturm, R., Ebinghaus, R., 2012. Per- and polyfluoroalkyl substances in snow, lake, surface runoff water and coastal seawater in Fildes Peninsula, King George Island, Antarctica. J. Hazard. Mater. 209–210, 335–342. https://doi.org/https://doi.org/10.1016/j.jhazmat.2012.01.030

Cirano, M., Lessa, G.C., 2007. Oceanographic characteristics of BaÃ\-a de Todos os Santos, Brazil. Rev. Bras. GeofÃ\-sica 25, 363–387.

Dalahmeh, S., Tirgani, S., Komakech, A.J., Niwagaba, C.B., Ahrens, L., 2018. Per- and polyfluoroalkyl substances (PFASs) in water, soil and plants in wetlands and agricultural areas in Kampala, Uganda. Sci. Total Environ. 631–632, 660–667. https://doi.org/10.1016/j.scitotenv.2018.03.024

Dorneles, P.R., Lailson-Brito, J., Azevedo, A.F., Meyer, J., Vidal, L.G., Fragoso, A.B., Torres, J.P., Malm, O., Blust, R., Das, K., 2008. High accumulation of perfluorooctane sulfonate (PFOS) in marine tucuxi dolphins (Sotalia guianensis) from the Brazilian coast. Environ. Sci. Technol. 42, 5368–5373. https://doi.org/10.1021/es800702k

Egres, A.G., Hatje, V., Miranda, D.A., Gallucci, F., Barros, F., 2019. Functional response of tropical estuarine benthic assemblages to perturbation by Polycyclic Aromatic Hydrocarbons. Ecol. Indic. 96, 229–240. https://doi.org/https://doi.org/10.1016/j.ecolind.2018.08.062

Fernández, P., Grimalt, J.O., 2003. n the Global Distribution of Persistent Organic Pollutants. Chim. Int. J. Chem. 57, 514–521. https://doi.org/10.2533/000942903777679000

Giesy, J.P., Kannan, K., 2001. Global distribution of perfluorooctane sulfonate in

wildlife. Environ. Sci. Technol. 35, 1339–1342. https://doi.org/10.1021/es001834k

Gilljam, J.L., Leonel, J., Cousins, I.T., Benskin, J.P., 2016. Is Ongoing Sulfluramid Use in South America a Significant Source of Perfluorooctanesulfonate (PFOS)? Production Inventories, Environmental Fate, and Local Occurrence. Environ. Sci. Technol. 50, 653–659. https://doi.org/10.1021/acs.est5b04544

Glüge, J., Scheringer, M., Cousins, I.T., DeWitt, J.C., Goldenman, G., Herzke, D., Lohmann, R., Ng, C.A., Trier, X., Wang, Z., 2020. An overview of the uses of per- and polyfluoroalkyl substances (PFAS). Environ. Sci. Process. Impacts. https://doi.org/10.1039/D0EM00291G

Gobelius, L., Lewis, J., Ahrens, L., 2017. Plant Uptake of Per- and Polyfluoroalkyl Substances at a Contaminated Fire Training Facility to Evaluate the Phytoremediation Potential of Various Plant Species. Environ. Sci. Technol. 51, 12602–12610. https://doi.org/10.1021/acs.est.7b02926

Goeritz, I., Falk, S., Stahl, T., Schaefers, C., Schlechtriem, C., 2013. Biomagnification and tissue distribution of perfluoroalkyl substances (PFASs) in market-size rainbow trout (Oncorhynchus mykiss). Environ. Toxicol. Chem. 32, 2078–2088. https://doi.org/10.1002/etc.2279

González-Gaya, B., Dachs, J., Roscales, J.L., Caballero, G., Jiménez, B., 2014. Perfluoroalkylated Substances in the Global Tropical and Subtropical Surface Oceans. Environ. Sci. Technol. 48, 13076–13084. https://doi.org/10.1021/es503490z

Gützkow, K.B., Haug, L.S., Thomsen, C., Sabaredzovic, A., Becher, G., Brunborg, G., 2012. Placental transfer of perfluorinated compounds is selective – A Norwegian Mother and Child sub-cohort study. Int. J. Hyg. Environ. Health 215, 216–219. https://doi.org/https://doi.org/10.1016/j.ijheh.2011.08.011

Hatje, V., Barros, F., 2012. Overview of the 20th century impact of trace metal contamination in the estuaries of Todos os Santos Bay: Past, present and future scenarios. Mar. Pollut. Bull. 64, 2603–2614. https://doi.org/https://doi.org/10.1016/j.marpolbul.2012.07.009

Hatje, V., Barros, F., Figueiredo, D.G., Santos, V.L.C.S., Peso-Aguiar, M.C., 2006. Trace metal contamination and benthic assemblages in Subaé estuarine system, Brazil.

Mar. Pollut. Bull. 52, 982–987. https://doi.org/https://doi.org/10.1016/j.marpolbul.2006.04.016

Houde, M., De Silva, A.O., Muir, D.C.G., Letcher, R.J., 2011. Monitoring of Perfluorinated Compounds in Aquatic Biota: An Updated Review PFCs in Aquatic Biota. Environ. Sci. Technol. 45, 7962–7973. https://doi.org/10.1021/es104326w

Houde, M., Martin, J.W., Letcher, R.J., Solomon, K.R., Muir, D.C.G., 2006. Biological monitoring of polyfluoroalkyl substances: A review. Environ. Sci. Technol. 40, 3463–3473. https://doi.org/10.1021/es052580b

Johansson, J.H., Salter, M.E., Acosta Navarro, J.C., Leck, C., Nilsson, E.D., Cousins, I.T., 2019. Global transport of perfluoroalkyl acids via sea spray aerosol. Environ. Sci. Process. Impacts 21, 635–649. https://doi.org/10.1039/C8EM00525G

Kannan, K., Corsolini, S., Falandysz, J., Fillmann, G., Kumar, K.S., Loganathan, B.G., Mohd, M.A., Olivero, J., Van Wouwe, N., Yang, J.H., Aldous, K.M., 2004. Perfluorooctanesulfonate and related fluorochemicals in human blood from several countries. Environ. Sci. Technol. 38, 4489–4495. https://doi.org/10.1021/es0493446

Kim, S.-K., Lee, K.T., Kang, C.S., Tao, L., Kannan, K., Kim, K.-R., Kim, C.-K., Lee, J.S., Park, P.S., Yoo, Y.W., Ha, J.Y., Shin, Y.-S., Lee, J.-H., 2011. Distribution of perfluorochemicals between sera and milk from the same mothers and implications for prenatal and postnatal exposures. Environ. Pollut. 159, 169–174. https://doi.org/https://doi.org/10.1016/j.envpol.2010.09.008

Krull, M., Abessa, D.M.S., Hatje, V., Barros, F., 2014. Integrated assessment of metal contamination in sediments from two tropical estuaries. Ecotoxicol. Environ. Saf. 106, 195–203. https://doi.org/https://doi.org/10.1016/j.ecoenv.2014.04.038

Kwiatkowski, C.F., Andrews, D.Q., Birnbaum, L.S., Bruton, T.A., DeWitt, J.C., Knappe, D.R.U., Maffini, M. V, Miller, M.F., Pelch, K.E., Reade, A., Soehl, A., Trier, X., Venier, M., Wagner, C.C., Wang, Z., Blum, A., 2020. Scientific Basis for Managing PFAS as a Chemical Class. Environ. Sci. Technol. Lett. 7, 532–543. https://doi.org/10.1021/acs.estlett.0c00255

Lau, C., Anitole, K., Hodes, C., Lai, D., Pfahles-Hutchens, A., Seed, J., 2007. Perfluoroalkyl Acids: A Review of Monitoring and Toxicological Findings. Toxicol. Sci. 99, 366–394.

Le Croizier, G., Schaal, G., Point, D., Le Loc'h, F., Machu, E., Fall, M., Munaron, J.M., Boyé, A., Walter, P., Laë, R., Tito De Morais, L., 2019. Stable isotope analyses revealed the influence of foraging habitat on mercury accumulation in tropical coastal marine fish. Sci. Total Environ. 650, 2129–2140. https://doi.org/10.1016/j.scitotenv.2018.09.330

Leonel, J., Kannan, K., Tao, L., Fillmann, G., Montone, R.C., 2008. A baseline study of perfluorochemicals in Franciscana dolphin and Subantarctic fur seal from coastal waters of Southern Brazil. Mar. Pollut. Bull. 56, 778–781. https://doi.org/10.1016/j.marpolbul.2008.01.012

Lewis, M., Pryor, R., Wilking, L., 2011. Fate and effects of anthropogenic chemicals in mangrove ecosystems: A review. Environ. Pollut. 159, 2328–2346. https://doi.org/https://doi.org/10.1016/j.envpol.2011.04.027

MacInnis, J.J., Lehnherr, I., Muir, D.C.G., Quinlan, R., De Silva, A.O., 2019. Characterization of perfluoroalkyl substances in sediment cores from High and Low Arctic lakes in Canada. Sci. Total Environ. 666, 414–422. https://doi.org/https://doi.org/10.1016/j.scitotenv.2019.02.210

Miranda, D.A., Benskin, J.P., Awad, R., Lepoint, G., Leonel, J., Hatje, V., 2021. Bioaccumulation of Per- and polyfluoroalkyl substances (PFASs) in a tropical estuarine food web. Sci. Total Environ. 754, 142146. https://doi.org/https://doi.org/10.1016/j.scitotenv.2020.142146

MMA, (Ministério do Meio Ambiente), 2015. Plano Nacional de Implementação da Convenção de Estocolmo no Brasil.

Muir, D., Bossi, R., Carlsson, P., Evans, M., De Silva, A., Halsall, C., Rauert, C., Herzke, D., Hung, H., Letcher, R., Rigét, F., Roos, A., 2019. Levels and trends of poly- and perfluoroalkyl substances in the Arctic environment – An update. Emerg. Contam. 5, 240–271. https://doi.org/https://doi.org/10.1016/j.emcon.2019.06.002

Munoz, G., Labadie, P., Botta, F., Lestremau, F., Lopez, B., Geneste, E., Pardon, P., Dévier, M.-H., Budzinski, H., 2017. Occurrence survey and spatial distribution of perfluoroalkyl and polyfluoroalkyl surfactants in groundwater, surface water, and sediments from tropical environments. Sci. Total Environ. 607–608, 243–252. https://doi.org/https://doi.org/10.1016/j.scitotenv.2017.06.146

Mussabek, D., Persson, K.M., Berndtsson, R., Ahrens, L., Nakagawa, K., Imura, T., 2020. Impact of the Sediment Organic vs. Mineral Content on Distribution of the Per- and Polyfluoroalkyl Substances (PFAS) in Lake Sediment. Int. J. Environ. Res. Public Health 17. https://doi.org/10.3390/ijerph17165642

Nascimento, R.A., Nunoo, D.B.O., Bizkarguenaga, E., Schultes, L., Zabaleta, I., Benskin, J.P., Spanó, S., Leonel, J., 2018. Sulfluramid use in Brazilian agriculture: A source of per- and polyfluoroalkyl substances (PFASs) to the environment. Environ. Pollut. 242, 1436–1443. https://doi.org/10.1016/J.ENVPOL.2018.07.122

Olsen, G.W., Butenhoff, J.L., Zobel, L.R., 2009. Perfluoroalkyl chemicals and human fetal development: An epidemiologic review with clinical and toxicological perspectives. Reprod. Toxicol. 27, 212–230. https://doi.org/https://doi.org/10.1016/j.reprotox.2009.02.001

Papadopoulou, E., Sabaredzovic, A., Namork, E., Nygaard, U.C., Granum, B., Haug, L.S., 2016. Exposure of Norwegian toddlers to perfluoroalkyl substances (PFAS): The association with breastfeeding and maternal PFAS concentrations. Environ. Int. 94, 687–694. https://doi.org/https://doi.org/10.1016/j.envint.2016.07.006

Power, M., Klein, G.M., Guiguer, K.R.R.A., Kwan, M.K.H., 2002. Mercury accumulation in the fish community of a sub-Arctic lake in relation to trophic position and carbon sources. J. Appl. Ecol. 39, 819–830. https://doi.org/https://doi.org/10.1046/j.1365-2664.2002.00758.x

Prevedouros, K., Cousins, I.T., Buck, R.C., Korzeniowski, S.H., 2006. Sources, Fate and Transport of Perfluorocarboxylates. Environ. Sci. Technol. 40, 32–44. https://doi.org/10.1021/es0512475

Quinete, N., Wu, Q., Zhang, T., Yun, S.H., Moreira, I., Kannan, K., 2009. Specific profiles of perfluorinated compounds in surface and drinking waters and accumulation in mussels, fish, and dolphins from southeastern Brazil. Chemosphere 77, 863–869. https://doi.org/https://doi.org/10.1016/j.chemosphere.2009.07.079

Salihovic, S., Stubleski, J., Kärrman, A., Larsson, A., Fall, T., Lind, L., Lind, P.M., 2018. Changes in markers of liver function in relation to changes in perfluoroalkyl substances - A longitudinal study. Environ. Int. 117, 196–203. https://doi.org/10.1016/j.envint.2018.04.052

Schwanz, T.G., Llorca, M., Farré, M., Barceló, D., 2016. Perfluoroalkyl substances assessment in drinking waters from Brazil, France and Spain. Sci. Total Environ. 539, 143–152. https://doi.org/10.1016/j.scitotenv.2015.08.034

Schwarzenbach, R.P., Escher, B.I., Fenner, K., Hofstetter, T.B., Johnson, C.A., von Gunten, U., Wehrli, B., 2006. The Challenge of Micropollutants in Aquatic Systems. Science (80-.). 313, 1072 LP – 1077. https://doi.org/10.1126/science.1127291

Song, X., Vestergren, R., Shi, Y., Huang, J., Cai, Y., 2018. Emissions, Transport, and Fate of Emerging Per- and Polyfluoroalkyl Substances from One of the Major Fluoropolymer Manufacturing Facilities in China. Environ. Sci. Technol. https://doi.org/10.1021/acs.est.7b06657

Spaan, K.M., van Noordenburg, C., Plassmann, M.M., Schultes, L., Shaw, S., Berger, M., Heide-Jørgensen, M.P., Rosing-Asvid, A., Granquist, S.M., Dietz, R., Sonne, C., Rigét, F., Roos, A., Benskin, J.P., 2020. Fluorine Mass Balance and Suspect Screening in Marine Mammals from the Northern Hemisphere. Environ. Sci. Technol. 54, 4046–4058. https://doi.org/10.1021/acs.est.9b06773

UNEP, 2019. Conference of the Parties to the Stockholm Convention on Persistent Organic Pollutants Ninth meeting [WWW Document]. URL http://chm.pops.int/TheConvention/ConferenceoftheParties/Meetings/COP9/tabid/7521/Default.aspx (accessed 1.20.21).

UNEP, 2009. The Stockholm Convention [WWW Document]. URL http://chm.pops.int/Convention/ThePOPs/%0AListingofPOPs/tabid/2509/Default.aspx (accessed 3.15.20).

Vaughn, B., Andrea, W., Kyle, S., 2013. Perfluorooctanoic Acid (PFOA) Exposures and Incident Cancers among Adults Living Near a Chemical Plant. Environ. Health Perspect. 121, 1313–1318. https://doi.org/10.1289/ehp.1306615

Wang, Z., Cousins, I.T., Scheringer, M., Buck, R.C., Hungerbühler, K., 2014. Global emission inventories for C4–C14 perfluoroalkyl carboxylic acid (PFCA) homologues from 1951 to 2030, part II: The remaining pieces of the puzzle. Environ. Int. 69, 166–176. https://doi.org/https://doi.org/10.1016/j.envint.2014.04.006

Wang, Z., Dewitt, J.C., Higgins, C.P., Cousins, I.T., 2017. A Never-Ending Story of Per- and Polyfluoroalkyl Substances (PFASs)? Environ. Sci. Technol. 51, 2508–2518.

https://doi.org/10.1021/acs.est.6b04806

Wang, Z., Walker, G.W., Muir, D.C.G., Nagatani-Yoshida, K., 2020. Toward a Global Understanding of Chemical Pollution: A First Comprehensive Analysis of National and Regional Chemical Inventories. Environ. Sci. Technol. 54, 2575–2584. https://doi.org/10.1021/acs.est.9b06379

Yamashita, N., Taniyasu, S., Petrick, G., Wei, S., Gamo, T., Lam, P.K.S., Kannan, K., 2008. Perfluorinated acids as novel chemical tracers of global circulation of ocean waters. Chemosphere 70, 1247–1255. https://doi.org/https://doi.org/10.1016/j.chemosphere.2007.07.079

Yeung, L.W.Y., De Silva, A.O., Loi, E.I.H., Marvin, C.H., Taniyasu, S., Yamashita, N., Mabury, S.A., Muir, D.C.G., Lam, P.K.S., 2013. Perfluoroalkyl substances and extractable organic fluorine in surface sediments and cores from Lake Ontario. Environ. Int. 59, 389–397. https://doi.org/https://doi.org/10.1016/j.envint.2013.06.026

Zabaleta, I., Bizkarguenaga, E., Nunoo, D.B.O., Schultes, L., Leonel, J., Prieto, A., Zuloaga, O., Benskin, J.P., 2018. Biodegradation and Uptake of the Pesticide Sulfluramid in a Soil-Carrot Mesocosm. Environ. Sci. Technol. 52, 2603–2611. https://doi.org/10.1021/acs.est.7b03876

Zhao, P., Xia, X., Dong, J., Xia, N., Jiang, X., Li, Y., Zhu, Y., 2016. Short- and long-chain perfluoroalkyl substances in the water, suspended particulate matter, and surface sediment of a turbid river. Sci. Total Environ. 568, 57–65. https://doi.org/https://doi.org/10.1016/j.scitotenv.2016.05.221

Zhao, S., Wang, B., Zhu, L., Liang, T., Chen, M., Yang, L., Lv, J., Liu, L., 2018. Uptake, elimination and biotransformation of N-ethyl perfluorooctane sulfonamide (N-EtFOSA) by the earthworms (Eisenia fetida) after in vivo and in vitro exposure. Environ. Pollut. 241, 19–25. https://doi.org/https://doi.org/10.1016/j.envpol.2018.05.046

Capítulo 3: *Sulfluramid degradation in tropical mangrove soil*

Manuscrito a ser submetido ao periódico *Marine Pollution Bulletin*

Sulfluramid degradation in tropical mangrove soils

Daniele de A. Miranda[a,*], Juliana Leonel[b], Vanessa Hatje[a]

[a] CIEnAm - Centro Interdisciplinar de Energia e Ambiente, Universidade Federal da Bahia, 41170-115, Salvador, BA, Brazil;

[b]Coordenação de Oceanografia, Universidade Federal de Santa Catarina.

*Corresponding autor

Daniele Miranda (danielealmeida@ufba.br)

Universidade Federal da Bahia

CIEnAm, Campus Ondina

Salvador, Bahia, Brazil, 41170-115

Abstract

Sulfluramid is a perfluoroalkylated-based formicide extensively used in Brazil, which has the perfluorooctane sulfonic acid (PFOS) precursor *N*-ethyl perfluorooctane sulfonamide (EtFOSA) as active ingredient. Here, we described the degradation of Sulfluramid in mangrove soils along 192 days in a in situ manipulative experiment to assess whether the use of this formicide in forestry nearby mangroves could be an important source of perfluorooctane sulfonic acid (PFOS) for the environment. Between 22 to 52 % depletion of EtFOSA, depending on the mangrove soil conditions (i.e. with or without roots) was observed at the end of the experiment. The slow EtFOSA degradation was explained by the mangrove soil properties, including anoxic conditions and the predominance of fine grain soils, that seems to slow down the degradation rate. Perfluorooctanesulfonamide acid (FOSA) was the major degradation product of EtFOSA, although in low rates than previously reported. Although EtFOSA was not observed here as an important source of PFOS to the environment, the slow EtFOSA degradation in mangrove soil must be closely observed, as mangrove soils are important reservoir of contaminants that may slowly release PFOS as its degradation product into surrounded areas.

Key words: EtFOSA, biodegradation, PFOS, mangrove soils, POPs

1. Introduction

Per- and polyfluoroalkyl substances (PFAS) are a class of synthetic substances that share remarkable properties (e.g., high surface activity, water- and oil-repellency, and thermal and chemical stability) due to their strong electronegativity associated with the C-F bound (Buck et al., 2011). This group of compounds have been used since the 1950s, being applied in a range of industrial applications, consumer products, and also pesticides (Glüge et al., 2020). Among them, perfluorooctane sulfonic acid (PFOS) receives special attention since it can bioaccumulate through the food web (Houde et al., 2011; Miranda et al., 2021; Munoz et al., 2017) and due to its toxicity for animals and humans (Lau et al., 2007). PFOS has already been found in human blood (Kannan et al., 2004; Wang et al., 2018) and in the wildlife (Leonel et al., 2008; Quinete et al., 2009; Routti et al., 2017). Its presence in environmental matrices is associated to direct sources, by its use from industrial activities (Wang et al., 2017, 2014), and indirect sources due to biotic and abiotic degradation of its precursors in the environment (Gebbink et al., 2015; Sedlak et al., 2017). It has been suggested that biodegradation processes of *N*-ethyl perfluorooctane sulfonamide (EtFOSA) represents an important route for PFOS exposure to humans and wildlife especially after the implementation of the Stockholm Convention restrictions (UNEP, 2009; Zabaleta et al., 2018).

EtFOSA is the active ingredient of Sulfluramid, a PFAS-based formicide extensively used to combat leaf cutting ants (*Atta* sp. and *Acromyrmex* spp.) in eucalyptus and pine plantations (Gilljam et al., 2016; Nagamoto et al., 2004). This formicide was first used in Brazil in 1993, as a replacement for the organochlorine pesticide Mirex (UNEP, 2009). The Sulfluramid active ingredient EtFOSA is a synthetic compound obtained from perfluorooctane-1-sulfonyl fluoride (POSF) by electrochemical fluorination (Buck et al., 2011), which can lead to a final product with other PFAS as impurities. In 2009

Sulfluramid precursors POSF and PFOS, and their salts, were added to the restriction list of the Stockholm Convention on Persistent Organic Pollutants (POPs) (UNEP, 2009). Currently, Brazil is one of the few countries allowed by the Stockholm Convention to produce Sulfluramid (MMA, 2015). Brazil imports ~ 30 tons y^{-1} of POSF since 2007 (MDIC, 2019). The manufacture and use of Sulfluramid in Brazil from 2004 to 2015 was expected to generate between ~170 and 600 tons of PFOS due to the biodegradation of the formicide (Gilljam et al., 2016). Combined, Sulfluramid and POSF may represent a significant source of PFOS to the aquatic environment.

Laboratory experiments evaluated the degradation of Sulfluramid bait and its technical product and indicated the EtFOSA as a PFOS precursor (PreFOS) in soils with and without crops (Avendaño and Liu, 2015; Zabaleta et al., 2018). Also recent studies, that analyzed the *N*-EtFOSA degradation during hydroponically plant growth under laboratory conditions, found that perfluorooctanesulfonamide acetate acid (FOSAA), perfluorooctanesulfonamide acid (FOSA), and PFOS are the main final products of EtFOSA degradation in a microcosms experiment (Yin et al., 2018). These three laboratory studies showed how live/active soils play an important role in the EtFOSA degradation. Nonetheless, no study has been made in the field to evaluate the degradation of Sulfluramid, where environmental conditions are complex, naturally variable, and dynamic due to the heterogeneity of the soil physical-chemical properties (e.g., organic matter, salinity, grain size), local hydrodynamics, pluviometry regime and so on.

Here, we performed a manipulative experiment to test if the degradation of the Sulfluramid baits in pristine tropical mangrove soils could act as a diffuse source of PFOS to the environment. To the best of our knowledge, no manipulative experiment has yet been performed to evaluate Sulfluramid degradation in situ, let alone in mangrove soils.

2. Methodology

2.1. Study area

Todos os Santos Bay (BTS) is the second largest bay in Brazil (13°7'0.22"S 38°53'7.41"W), characterized by a mesotidal semidiurnal tides with a tropical climate (Cirano and Lessa, 2007). Jaguaripe river is the second largest tributary of the BTS (2200m²) and the least impacted among the BTS estuaries (Egres et al., 2019; Krull et al., 2014). The mean temperature at Jaguaripe river is among 25ºC and the precipitation of 2100 mm annually. The estuary is surrounded by mangroves (Costa et al., 2015), and at the lower estuary, where this study was realized, it is dominated by *Rhizophora mangle* (Hatje et al., 2020).

2.2. Experimental design and mangrove soil contamination

The manipulative experiment was carried out in April 2017 and was composed by four treatments: i. 3 control mangrove without roots (MC), ii. 1 control mangrove with A*vicennia sp.* pneumatophores (MCR), iii. 3 mangrove soils with A*vicennia sp.* pneumatophores that were impacted with commercial Sulfluramid baits (MIR); and iv. 3 mangrove soils without mangrove roots that were impacted with commercial Sulfluramid baits (MI). Each experiment was performed in demarcated areas using PVC tubes (15 cm diameter x 20 cm depth). For the contamination of the soils (i.e., MI and MIR), 2 kg of soils were removed from each studied demarcated area and mixed with 500 g of Grão Forte® Sulfuramid baits (license of experiment SISBIO: n° 57866-1). The contaminated soils were then relocated to their original demarcated areas. At the end of the experiment, the contaminated soils were removed and sent to a specialized waste treatment plant.

2.3. Sampling

All labware used on sampling and extraction procedures was previously rinsed with 1% NH_4OH in methanol. Soils were sampled at 9 times over the course of the experiment

that lasted 6 months (Table S1). Soils from each site (i.e. MC, MCR, MI, and MIR) were sampled on day zero (0; right before the contamination of the soils by the baits), 0' (immediately after the addition of Sulfluramid baits), then after 2, 15, 30, 60, 92, 156, and 192 days of contamination of the soils. The sampling intervals were determined by what has been seen in the L-EtFOSA degradation laboratory experiments in previous studies (Avendaño and Liu, 2015; Zabaleta et al., 2018). After sampling, soils were frozen, freeze-dried, and stored in desiccators in room temperature prior to further processing. The experiment was carried out in an area that was not subjected to the tide inundation, i.e., the soils were air-exposed during the entire experiment.

2.4. Granulometry

Grain size distribution was determined by soil separation using sieves ranging from -1.5 to 4.0 phi. After sieving, the fractions were weighed and the results were classified using the SysGRan software version 3.0 (Camargo, 2006).

2.5. Total organic carbon (TOC), total nitrogen (TN) and their stable isotope analysis

Before total organic carbon (TOC) and $\delta^{13}C_{org}$ analysis, samples were acidified with 1 M HCl to remove carbonates. TOC and TN and its isotopes were determined using a Delta V Isotope Ratio Mass Spectrometer (Thermo Fisher, USA). Precision was determined using USGS-40 and USGS-41 certified material were 0.30 ‰ for $\delta^{13}C$ and 0.25 ‰ for $\delta^{15}N$.

2.6. Extraction

The list of PFAS analyzed in our study is summarized in Table S2. Soil samples were extracted according to Zabaleta et al. (2018). In summary, 0.5 g of samples with 2 ng of internal standard was sonicated for 20 minutes with 8 mL of Acetonitrile (ACN), homogenized in an orbital shaker for 40 minutes and centrifugated during 20 minutes at 2900 rpm. The procedure was then repeated, after adding 8 mL of ACN with 25mM

NaOH. The extracts were then combined and dried under low nitrogen flow. Details of these procedures can be found in the Supporting Information (SI).

2.7. Instrumental analysis

Instrumental analysis was carried out by ultra-performance liquid chromatography-tandem mass spectrometry (UPLC-MS/MS) using a Waters Acquity UPLC coupled to a Waters Xevo TQ-S triple quadrupole mass spectrometer (Waters) as described by Miranda et al. (2021). Five µL of extracts were injected onto an BEH C18 analytical column (2.1×50mm, 1.7 µm particle size, Waters) operated at a flow rate of 0.4 mL/min, using a mobile phase composition of 90% water/10% acetonitrile containing 2 mM ammonium acetate (solvent A) and 100% acetonitrile containing 2 mM ammonium acetate (solvent B). The gradient profile started at 90 % A (hold time 0.3 min), followed by a linear decrease to 20 % by 4.5 min, then to 0 % by 4.6 min (hold time 3 min). The mobile phase composition was returned to initial conditions by 9.5 min. Analysis was made with the instrument operating in negative electrospray ionization and selected reaction monitoring mode with 2 to 4 transitions per analyte (see Table S3). Individual isomers were determined using isomer-specific calibration curves prepared from characterized technical standards. Branched isomers (i.e. br-) were quantified separately from the linear isomer using their specific linear isomer calibration curve. Therefore, concentration of branched isomers should be considered semi-quantitative giving the differences in response factors between branched and linear isomers. All PFASs concentrations are reported in dry weight (dw).

2.8. Quality Control

Each batch of 16 samples was processed with laboratory blanks (reagents only, n = 2) and spiked samples with native standards (n = 3, 2 ng). Limits of detection (LOD) were estimated as the concentration obtained by a signal-to-noise ratio of 3 (Table S4).

Concentrations of PFASs in laboratory blanks were low or non-detected for all compounds, except for EtFOSA values (Table S4). Results of spike/recovery experiments presented good accuracy and precision for most targets (86 ± 19%, average ± RSD) (Table S4). Perfluoroheptanoic acid (PFHpA), Perfluorotetradecanoic acid (PFTeDA), and EtFOSA showed either low (i.e. PFHpA and PFTeDA) or high recoveries (i.e. EtFOSA). For these compounds, results are semi-qualitative, and only the distribution pattern observed during the compound degradation should be considered, rather than the absolute values. Results are showed as average ± standard deviation (SD).

3. Results and Discussion

3.1. Soil characteristics

Soils were predominantly composed of fine-grained particles (silt + clay = 46.9 ± 11.1 % + 53.1 ± 11.1 %) (Table S5). TOC and TN contents in soils were 2.40 ± 0.80 % and 0.15 ± 0.06 %, respectively, in control treatments, within the range previously observed for the area (Hatje et al., 2020). Contents of TOC and TN were higher in impacted treatments, i.e., 5.90 ± 2.60 % and 0.30 ± 0.08 %, respectively. Differences in control and impacted sites organic matter contents (Table S6), are associated with the presence of the Sulfluramid baits in the impacted treatments, which is composed of more than 99% of orange pulp, according to the Grão Forte® product label (Insetimax, 2016). The C/N ratio was 16.2 ± 4.19 in control sites and 19.8 ± 5.10 in impacted areas, similar to those in the surrounded mangrove showing the predominance of organic matter from terrigenous sources (Hatje et al., 2020). This was confirmed by the values of $\delta^{13}C$ (-25.1 ± 2.21 ‰) for control areas that indicates the mangrove as the main source. Values for $\delta^{15}N$ in control areas was 2.80 ± 0.86 ‰ (Table S6), in agreement with environments that receive low contribution of anthropogenic organic matter. $\delta^{13}C$ and $\delta^{15}N$ for impacted area were -26.2 ± 2.20 ‰ and 3.94 ± 0.67 ‰, respectively, in higher range compared to control

200 areas probably also due to the formicide baits in the impacted treatment, but no value of
201 $\delta^{15}N$ for Sulfluramid was found for comparison.

202 *3.2. EtFOSA in the Sulfluramid bait and other target compounds*

203 *3.2.1. Control treatments*

204 Most of the target compounds were either absent or in low concentrations in control
205 treatments (i.e., MC and MCR) through the experiment (Table S7-S8), except for
206 ∑EtFOSA (i.e., sum of linear and branched compounds) and L-FOSA that were
207 constantly observed in both MC and MCR. Perfluorohexanoic acid (L-PFHxA) and L-
208 FOSAA were detected in one case each in MC in low concentrations (MCT7: 0.15 ± 0.18
209 and; MCT8: 0.17 ± 0.14 ng g^{-1}, respectively). A few compounds were detected below
210 0.50 ng g^{-1} in MCR (i.e., *N*-Ethyl perfluorooctane sulfonamido acetic acid [L-EtFOSAA],
211 L-FOSAA, *N*-methylperfluoro-1-octanesulfonamide [L-MeFOSA], and L-PFOS). L-
212 EtFOSA was present in control treatments from T2 to T8 in MC and from T1 to T8 in
213 MCR, in concentrations that ranged from 0.41 ± 0.56 to 45.1 ± 14.3 ng g^{-1} and from 1.97
214 to 20.4 ng g^{-1}, respectively (Figure S2). L-FOSA was detected (T2, T5, T7, and T8) in
215 concentrations from 0.07 to 0.20 ng g^{-1} in MC and in concentrations between 0.06 to 10.1
216 ng g^{-1} in MCR (Table S8, Figure S2). The presence of those compounds in the control
217 treatments could be a result of cross-contamination either between the control and
218 impacted treatments or in the analytical procedures (e.g., carryover in the LC
219 chromatography column), lab contamination should also be considered. Along the
220 experiment, there were periods of rain that could have eroded soils and promoted the
221 transport of contaminated soil. Nonetheless, the values observed here were consistently
222 low and did not compromised the patterns observed for the degradation experiment.

223

3.2.2. Impacted treatments

The ∑EtFOSA observed here on the day of the spike (i.e. MIT1'; 8254 ± 1168 ng g^{-1} and MIT1R': 6573 ± 381 ng g^{-1}), was higher than those reported by Zabaleta et al. (2018) for the same Sulfluramid bait brand (i.e. 0.0024 % of ∑EtFOSA, 4800 ng g^{-1}). The dissimilarity in concentrations can reflect either a poor homogenization of the Sulfluramid baits with soils during the addition of the spike or a result of an overestimation during quantification for this specific compound.

The L-EtFOSA degradation was different for the MI and MIR treatments. While in MI the L-EtFOSA concentrations varied from 6098 ± 874 to 6792 ± 2495 ng g^{-1} from day 0' to day 192, it varied between 4645 ± 366 and 2239 ± 908 ng g^{-1} in MIR (Figure 1). As such, a depletion of 52 % was observed in MIR by the day 192 and of 22 % from day 0 to day 156 in MI, followed by an increase of L-EtFOSA concentration on the last day of the experiment. The presence of pneumatophores in mangrove soils promotes higher oxygenation in the soils (Kitaya et al., 2002), which could be favoring the EtFOSA biodegradation, increasing its depletion rate in the MIR treatment. The MI treatment was located in uneven terrain, while MIR was in a flat area. This might reflect the important control that roots exercise on the accumulation pattern of particles in mangrove soils and, potentially, degradation of target compounds. The irregular terrain and the absence of roots that helps to stabilize the soil could have facilitated the leaching during the rainy season. It must be promoting the removal of surface contaminated soils from the experiment sites and, consequently, exposing deep soil layers with more preserved Sulfluramid baits, and enabling the transport of contaminated soils among different sites. Also, due to the peculiarities of in situ experiments subjected to the natural environmental processes, such as leaching and/or volatilization of PFASs, a mole balance of the input and output of compounds could not be performed. In addition, the plant uptake was not

249 considered here due to the low growth rate of mangrove trees (i.e. 1.2 to 3.3 mm y^{-1}
250 (Menezes et al., 2003)) and the duration of the experiment (192 days). Thus, the
251 accumulation of compounds in mangroves was assumed to be irrelevant, even though the
252 plant uptake can be an important pathway of PFAS removal from soils (Zabaleta et al.,
253 2018; Zhao et al., 2018).

254 Studies evaluating the degradation of Sulfluramid baits or active ingredient are scarce and
255 were conducted in different soils (i.e., forest soil) under controlled laboratory conditions.
256 Zabaleta et al. (2018) estimated a 50 % depletion (or half-life) over 11 days for L-
257 EtFOSA. Other degradation laboratory experiments performed with the L-EtFOSA active
258 ingredient showed half-lives varying from ~14 to ~40 days (Avendaño and Liu, 2015;
259 Zabaleta et al., 2018), depending on the microbial activity in soils (i.e., activated/live or
260 inactivated/sterile soil) (Table 1). The slow L-EtFOSA breakdown observed here was
261 only seen before when the L-EtFOSA was tested in a laboratory experiment with
262 inactivated/sterile soil (Avendaño and Liu, 2015). Our results for Sulfluramid baits
263 degradation in mangrove soil together with the degradation of the Sulfluramid active
264 ingredient in previous studies suggest that aerobic microbial activity is a major factor
265 controlling the Sulfluramid breakdown rate. Thus, the microbial activity in the anoxic soil
266 environment studied here is not as effective in L-EtFOSA biodegradation as previously
267 mentioned for the aerobic degradation observed in coarser forest soils (Table 1)
268 (Avendaño and Liu, 2015; Zabaleta et al., 2018).

269 Mangrove soils are well-known to be long-term sinks for organic matter due to their soil
270 properties, which includes the anoxic conditions and cohesive fine sediment that provides
271 physical-chemical protection to organic matter that can be preserved over millennium
272 timescales (Alongi, 2014; Atwood et al., 2017). In addition, the richness of mangrove soil
273 in tannins and other phenolic compounds from mangrove leaves favors the inhibition of

microbial activity and growth (Alongi, 1994). Therefore, the process of organic matter decomposition is slower in this environment, which improves its conservation in the mangrove soil (Maie et al., 2008), and similarly the biodegradation of organic contaminants in this environment. These conditions force the organic matter (and possibly L-EtFOSA) to be degraded by alternatives pathways, such as by the use of sulfur instead of oxygen (Raven et al., 2019). In this anoxic soils, the anaerobic microorganisms use sulfate in replacement of oxygen to degrade the organic matter, which is very abundant in marine soil due to the absence of oxygen in the free form (Jørgensen et al., 2019). Also, the high salinity in these environments affects microbial soil communities by reducing their speed of enzymatic synthesis and metabolic rates (Yan et al., 2015), then contributing to L-EtFOSA preservation. Thus, the Sulfluramid, as the organic matter in mangrove soils, degrades in slow rates. Considering that EtFOSA has already been detected in estuarine organisms and sediments in a tropical mangrove area nearby (Miranda et al., 2021), the mangroves might be acting as an environmental filter, storing EtFOSA leached from forestry that employs the Sulfluramid and gradually releasing it to the surrounding estuaries and eventually accumulating in the biota (Miranda et al., 2021).

Together with the anoxic conditions and grain size of soils, TOC content was previous considered as an important driver explaining the PFAS biotransformation in sterile soil (Zabaleta et al., 2018). However, the initial TOC content in mangrove soils (T1) was 2.40 ± 0.80 %, which is substantially lower than the values of previous studies (i.e., 5.90 to 53.0 %) (Avendaño and Liu, 2015; Zabaleta et al., 2018). As such, it is not expected that the organic matter content, specially under anoxic and saline conditions would be a major variable controlling the degradation rate of EtFOSA. These hypotheses, nevertheless, are yet to be tested.

Besides the active ingredient of the formicide (i.e., EtFOSA), many other PFAS compounds (i.e., perfluorobutanoic acid [PFBA], PFHxA, PFHpA, perfluorooctanoic acid [PFOA], PFOS, FOSA, MeFOSA, and EtFOSAA) were present in the contaminated treatments MI and MIR in the range of 1.15 to 12.2 ng g^{-1} (Table S9-S10). The rare detection and/or absence of these compounds in control treatments, in contrast with the high and constant detection of those PFASs through the experiment in the impacted treatments confirm that these compounds are impurities in the Sulfluramid baits. Some compounds such as PFOA, PFOS, FOSA, and FOSAA were previously detected in a laboratory experiment using the same Sulfluramid baits brand (Zabaleta et al., 2018). Nevertheless, the content of impurities observed here and in the previous studies was low and does not represent a relevant source to the environment.

FOSA was the major degradation product of L-EtFOSA. For the MI and MIR treatments, L-FOSA was found in concentrations ranging from 12.2 ± 1.20 (T1') to 24.6 ± 6.86 (T8) ng g^{-1} and from 9.60 ± 0.51 (T1') to 68.3 ± 11.9 (T8) ng g^{-1}, respectively. Besides the different range in concentrations, L-FOSA degradation kinetic was also different. The exponential growth constant (k) was 0.00208 and 0.00998 for MI and MIR, respectively, which represents L-FOSA formation five times slower in MI than in MIR (Table S11, Figure 2). The already mentioned better oxygenation in MIR might have favored this faster FOSA production due to EtFOSA dealkylation promoted by the aerobic biodegradation (Liu and Mejia Avendaño, 2013). Also, it was observed a faster FOSA formation in the first 15 days for MI compared to MIR (Figure 1), followed by a slow increase in its concentration until the end of the experiment. In the MIR treatment, L-FOSA showed a slow formation until day 92 followed by a sharp increase in the interval of day 92 to 156, which was in alignment with the depletion of L-EtFOSA (Figure 1b), suggesting that the Sulfluramid degradation main activity occurred after 90 days of the

start of this experiment. This pattern was not observed in the MI treatment (Figure 1a) probably due to the higher leaching and soil mobilization.

L-PFOS was observed in higher concentrations as Sulfluramid baits impurity (MIT1': 11.4 ± 1.82; and MIRT1': 10.9 ± 0.43 ng g^{-1}) than as a EtFOSA degradation product in the course of the experiment. These values dropped in both treatments until day ~156, from where a small increase of L-PFOS concentrations was observed, which might be associated to L-PFOS formation from L-FOSA degradation. The aerobic biotransformation pathway described by Avendaño and Liu (2015) suggested that EtFOSA is rapidly biotransformed to FOSA and then to PFOS, different from the low PFOS formation seen here in anoxic soils. The biotransformation activity of EtFOSA to FOSA and from FOSA to PFOS detected in the present experiment (Figure 1), differs from previous experiments using Sulfluramid baits and its active ingredient (Avendaño and Liu, 2015; Zabaleta et al., 2018). We hypothesize that the difference among studies is driven by the degradation pathway, that in the case of mangrove soils is realized through anaerobic degradation due to the anoxic conditions of mangrove soils. An alternative pathway in the EtFOSA degradation would be FOSA to FOSAA degradation and, then, PFOS (Liu and Mejia Avendaño, 2013). However, this process does not seem to be important in mangrove soils, since FOSAA formation was only observed in one treatment (MIR) after 90 days and in a low concentration (Figure 1b, Table S10). The potentially higher oxygenation in MIR compared to MI might have favored its formation.

4. Environmental implications and perspectives

Sulfluramid is not directly used in mangrove soil, but this ecosystem represents an important transition environment that receives and stores a large number of contaminants, including this formicide. To understand this formicide breakdown under anaerobic

conditions brings new insights when compared to previous studies specially for tropical areas that uses it in forestry, potentially impacting a series of ecosystems along the continuum continent-ocean. The slow EtFOSA degradation observed here warrants caution since the mangrove can be acting as a reservoir of this contaminant, which eventually can be released, and gradually contaminate biota, estuaries, and ocean waters. Mangrove is a transition area from forests to the ocean and shows high environmental importance due to the relevant ecosystem services that they provide.

Acknowledgments

This work was supported by Fundação de Amparo à Pesquisa do Estado da Bahia, Brazil (FAPESB) (PET0034/2012), Conselho Nacional de Desenvolvimento Científico (CNPq) (441829/2014-7), and the Rufford Foundation (nº 2992-1). The authors were supported by FAPESB (D. Miranda, nº BOL0122/2017), and CNPq (V. Hatje - 304823/2018-0; J. Leonel - 401443/2016-7 and 310786/2018-5). Thanks to Vinicius Patire for the collaboration with the Isotope Data.

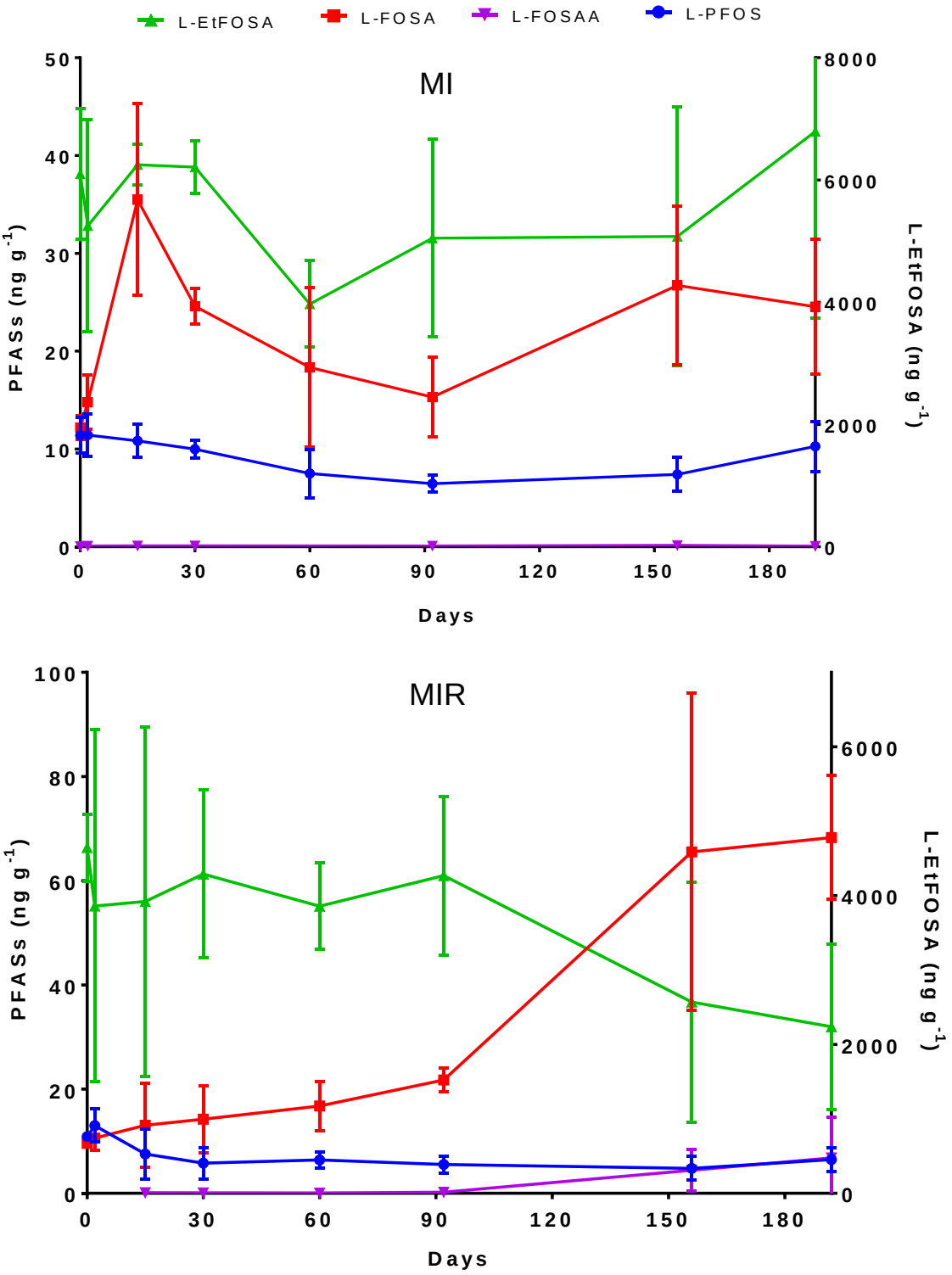

Figure 1: Concentrations of EtFOSA and its degradation products over time in mangrove soils after the addition of Sulfluramid baits. Left axis (PFAS ng g^{-1}) represents the concentrations for L-FOSA, L-FOSAA, L-EtFOSAA, and L-PFOS, whereas right axis shows L-EtFOSA (ng g^{-1}). MI: Mangrove impacted without roots and MIR: Mangrove impacted with roots.

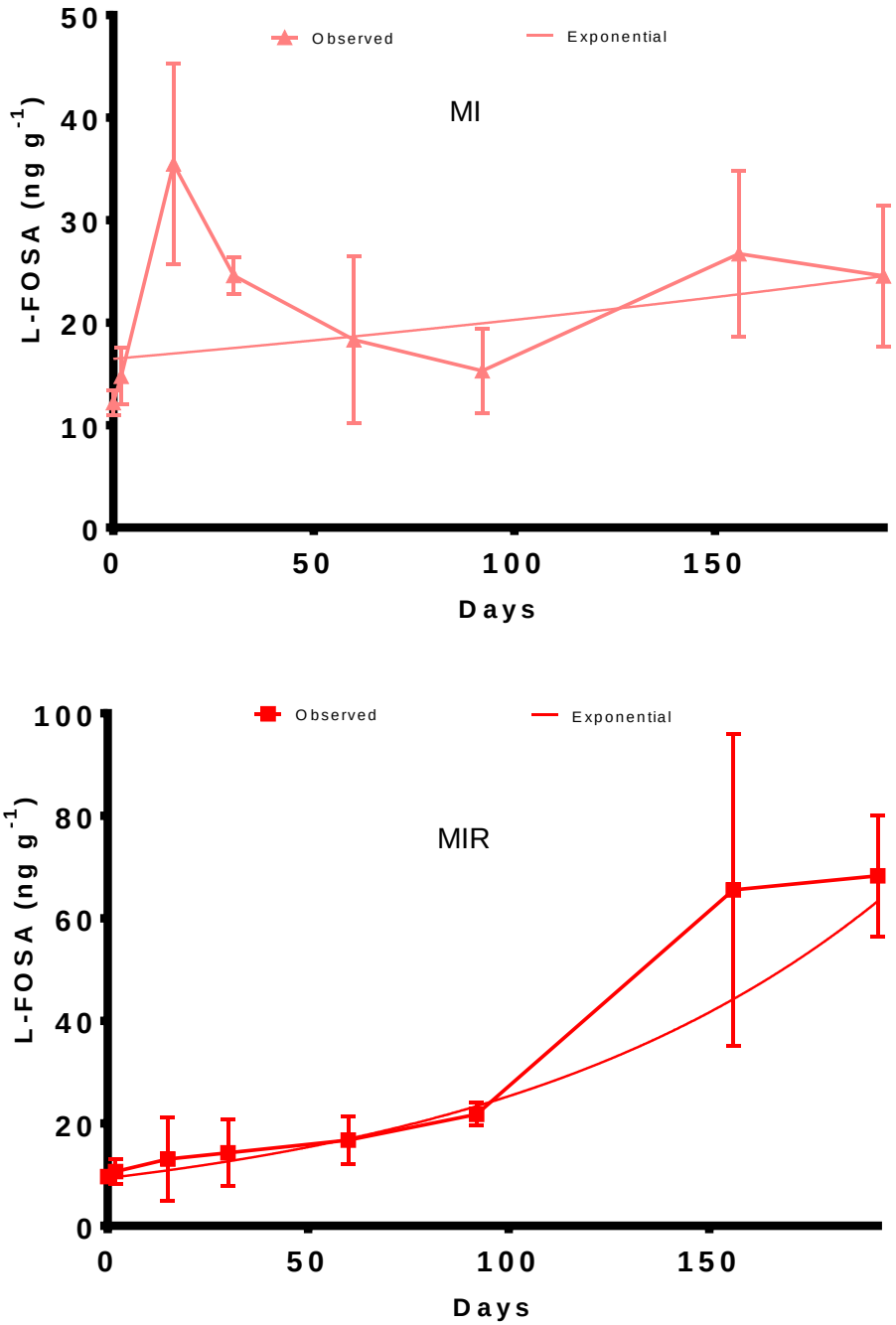

367

368 **Figure 2:** Exponential growth of L-FOSA in MI (Mangrove impacted without roots) and MIR
369 (Mangrove impacted with roots) treatments in mangrove soil.

370 **Table 1:** Comparison of studies in which EtFOSA degradation that was evaluated both as active
371 ingredient (technical EtFOSA) form and as Sulfluramid baits. The result showed for TOC of the
372 present study represents the average ± standard deviation of day 1 before contamination for all
373 analyzed treatments (MC, MCR, MI and MIR).

EtFOSA	pH	Half-life (days)	Soil type	Crop Presence	TOC (%)	Reference
Active ingredient	7.4	13.9±2.1	activated sandy loam	no	5.9	Avendaño et al. (2015)
Active ingredient	7.4	**	inactivated sandy loam	no	5.9	Avendaño et al. (2015)
Active ingredient	5.7	33.6±9.0	activated sandy loam	no	53	Zabaleta et al. (2018)
Active ingredient	5.7	40.0±7.8	inactivated sandy loam	no	53	Zabaleta et al. (2018)
Active ingredient	5.7	35.8±3.7	activated sandy loam	yes	53	Zabaleta et al. (2018)
Sulfluramid bait	5.7	11.5±2.1	activated sandy loam	yes	53	Zabaleta et al. (2018)
Sulfluramid bait	*	>192	activated silt-clay	yes	2.4 ± 0.8	this study

374 *pH was not measured for the present study
375 **no EtFOSA degradation was observed
376

377 5. References

378 Alongi, D.M., 2014. Carbon Cycling and Storage in Mangrove Forests. Ann. Rev. Mar.
379 Sci. 6, 195–219. https://doi.org/10.1146/annurev-marine-010213-135020

380 Alongi, D.M., 1994. The role of bacteria in nutrient recycling in tropical mangrove and
381 other coastal benthic ecosystems. Hydrobiologia 285, 19–32.
382 https://doi.org/10.1007/BF00005650

383 Atwood, T.B., Connolly, R.M., Almahasheer, H., Carnell, P.E., Duarte, C.M., Ewers
384 Lewis, C.J., Irigoien, X., Kelleway, J.J., Lavery, P.S., Macreadie, P.I., Serrano, O.,
385 Sanders, C.J., Santos, I., Steven, A.D.L., Lovelock, C.E., 2017. Global patterns in
386 mangrove soil carbon stocks and losses. Nat. Clim. Chang. 7, 523–528.
387 https://doi.org/10.1038/nclimate3326

388 Avendaño, S., Liu, J., 2015. Production of PFOS from aerobic soil biotransformation of
389 two perfluoroalkyl sulfonamide derivatives. Chemosphere 119, 1084–1090.
390 https://doi.org/10.1016/j.chemosphere.2014.09.059

391 Buck, R.C., Franklin, J., Berger, U., Conder, J.M., Cousins, I.T., de Voogt, P., Jensen,
392 A.A., Kannan, K., Mabury, S.A., van Leeuwen, S.P.J., 2011. Perfluoroalkyl and
393 Polyfluoroalkyl Substances in the Environment: Terminology, Classification, and
394 Origins. Integr. Environ. Assess. Manag. 7, 513–541.
395 https://doi.org/10.1002/ieam.258

396 Camargo, M.., 2006. SYSGRAN: um sistema de código aberto para análises
397 granulométricas do sedimento. Rev. Bras. Geociências 36, 371–378.

398 Cirano, M., Lessa, G.C., 2007. Oceanographic characteristics of BaÃ\-a de Todos os
399 Santos, Brazil. Rev. Bras. GeofÃ\-sica 25, 363–387.

400 Costa, P., Dórea, A., Mariano-Neto, E., Barros, F., 2015. Are there general spatial patterns
401 of mangrove structure and composition along estuarine salinity gradients in Todos
402 os Santos Bay? Estuar. Coast. Shelf Sci. 166, 83–91.
403 https://doi.org/https://doi.org/10.1016/j.ecss.2015.08.014

404 Egres, A.G., Hatje, V., Miranda, D.A., Gallucci, F., Barros, F., 2019. Functional response

405 of tropical estuarine benthic assemblages to perturbation by Polycyclic Aromatic
406 Hydrocarbons. Ecol. Indic. 96, 229–240.
407 https://doi.org/https://doi.org/10.1016/j.ecolind.2018.08.062

408 Gebbink, W.A., Berger, U., Cousins, I.T., 2015. Estimating human exposure to PFOS
409 isomers and PFCA homologues: The relative importance of direct and indirect
410 (precursor) exposure. Environ. Int. 74, 160–169.
411 https://doi.org/10.1016/j.envint.2014.10.013

412 Gilljam, J.L., Leonel, J., Cousins, I.T., Benskin, J.P., 2016. Is Ongoing Sulfluramid Use
413 in South America a Significant Source of Perfluorooctanesulfonate (PFOS)?
414 Production Inventories, Environmental Fate, and Local Occurrence. Environ. Sci.
415 Technol. 50, 653–659. https://doi.org/10.1021/acs.est5b04544

416 Glüge, J., Scheringer, M., Cousins, I.T., DeWitt, J.C., Goldenman, G., Herzke, D.,
417 Lohmann, R., Ng, C.A., Trier, X., Wang, Z., 2020. An overview of the uses of per-
418 and polyfluoroalkyl substances (PFAS). Environ. Sci. Process. Impacts.
419 https://doi.org/10.1039/D0EM00291G

420 Hatje, V., Masqué, P., Patire, V.F., Dórea, A., Barros, F., 2020. Blue carbon stocks,
421 accumulation rates, and associated spatial variability in Brazilian mangroves.
422 Limnol. Oceanogr. n/a. https://doi.org/https://doi.org/10.1002/lno.11607

423 Houde, M., De Silva, A.O., Muir, D.C.G., Letcher, R.J., 2011. Monitoring of
424 Perfluorinated Compounds in Aquatic Biota: An Updated Review PFCs in Aquatic
425 Biota. Environ. Sci. Technol. 45, 7962–7973. https://doi.org/10.1021/es104326w

426 Insetimax, 2016. FISPQ - Ficha de Informação de Segurança de Produtos Químicos (Grão
427 Forte).

428 Jørgensen, B.B., Findlay, A.J., Pellerin, A., 2019. The Biogeochemical Sulfur Cycle of
429 Marine Sediments. Front. Microbiol. 10, 849.
430 https://doi.org/10.3389/fmicb.2019.00849

431 Kannan, K., Corsolini, S., Falandysz, J., Fillmann, G., Kumar, K.S., Loganathan, B.G.,
432 Mohd, M.A., Olivero, J., Van Wouwe, N., Yang, J.H., Aldous, K.M., 2004.
433 Perfluorooctanesulfonate and related fluorochemicals in human blood from several

countries. Environ. Sci. Technol. 38, 4489–4495. https://doi.org/10.1021/es0493446

Kitaya, Y., Yabuki, K., Kiyota, M., Tani, A., Hirano, T., Aiga, I., 2002. Gas exchange and oxygen concentration in pneumatophores and prop roots of four mangrove species. Trees 16, 155–158. https://doi.org/10.1007/s00468-002-0167-5

Krull, M., Abessa, D.M.S., Hatje, V., Barros, F., 2014. Integrated assessment of metal contamination in sediments from two tropical estuaries. Ecotoxicol. Environ. Saf. 106, 195–203. https://doi.org/https://doi.org/10.1016/j.ecoenv.2014.04.038

Lau, C., Anitole, K., Hodes, C., Lai, D., Pfahles-Hutchens, A., Seed, J., 2007. Perfluoroalkyl Acids: A Review of Monitoring and Toxicological Findings. Toxicol. Sci. 99, 366–394.

Leonel, J., Kannan, K., Tao, L., Fillmann, G., Montone, R.C., 2008. A baseline study of perfluorochemicals in Franciscana dolphin and Subantarctic fur seal from coastal waters of Southern Brazil. Mar. Pollut. Bull. 56, 778–781. https://doi.org/10.1016/j.marpolbul.2008.01.012

Liu, J., Mejia Avendaño, S., 2013. Microbial degradation of polyfluoroalkyl chemicals in the environment: A review. Environ. Int. 61, 98–114. https://doi.org/https://doi.org/10.1016/j.envint.2013.08.022

Maie, N., Pisani, O., JaffÉ, R., 2008. Mangrove tannins in aquatic ecosystems: Their fate and possible influence on dissolved organic carbon and nitrogen cycling. Limnol. Oceanogr. 53, 160–171. https://doi.org/https://doi.org/10.4319/lo.2008.53.1.0160

MDIC, 2019. Bureau of Foreign Trade [WWW Document]. URL http://comexstat.mdic.gov.br/pt/geral

Menezes, M., Berger, U., Worbes, M., 2003. Annual growth rings and long-term growth patterns of mangrove trees from the Bragança peninsula, North Brazil. Wetl. Ecol. Manag. 11, 233–242. https://doi.org/10.1023/A:1025059315146

Miranda, D.A., Benskin, J.P., Awad, R., Lepoint, G., Leonel, J., Hatje, V., 2021. Bioaccumulation of Per- and polyfluoroalkyl substances (PFASs) in a tropical estuarine food web. Sci. Total Environ. 754, 142146.

https://doi.org/https://doi.org/10.1016/j.scitotenv.2020.142146

MMA, (Ministério do Meio Ambiente), 2015. Plano Nacional de Implementação da Convenção de Estocolmo no Brasil.

Munoz, G., Labadie, P., Botta, F., Lestremau, F., Lopez, B., Geneste, E., Pardon, P., Dévier, M.-H., Budzinski, H., 2017. Occurrence survey and spatial distribution of perfluoroalkyl and polyfluoroalkyl surfactants in groundwater, surface water, and sediments from tropical environments. Sci. Total Environ. 607–608, 243–252. https://doi.org/https://doi.org/10.1016/j.scitotenv.2017.06.146

Nagamoto, N.S., Forti, L.C., Andrade, A.P.P., Boaretto, M.A.C., Wilcken, C.F., 2004. Method for the evaluation of insecticidal activity over time in Atta sexdens rubropilosa workers (Hymenoptera : Formicidae). SOCIOBIOLOGY 44, 413–431.

Quinete, N., Wu, Q., Zhang, T., Yun, S.H., Moreira, I., Kannan, K., 2009. Specific profiles of perfluorinated compounds in surface and drinking waters and accumulation in mussels, fish, and dolphins from southeastern Brazil. Chemosphere 77, 863–869. https://doi.org/https://doi.org/10.1016/j.chemosphere.2009.07.079

Raven, M.R., Fike, D.A., Gomes, M.L., Webb, S.M., 2019. Chemical and Isotopic Evidence for Organic Matter Sulfurization in Redox Gradients Around Mangrove Roots . Front. Earth Sci. .

Routti, H., Aars, J., Fuglei, E., Hanssen, L., Lone, K., Polder, A., Pedersen, Å.O., Tartu, S., Welker, J.M., Yoccoz, N.G., 2017. Emission Changes Dwarf the Influence of Feeding Habits on Temporal Trends of Per- and Polyfluoroalkyl Substances in Two Arctic Top Predators. Environ. Sci. Technol. 51, 11996–12006. https://doi.org/10.1021/acs.est.7b03585

Sedlak, M.D., Benskin, J.P., Wong, A., Grace, R., Greig, D.J., 2017. Per- and polyfluoroalkyl substances (PFASs) in San Francisco Bay wildlife: Temporal trends, exposure pathways, and notable presence of precursor compounds. Chemosphere 185, 1217–1226. https://doi.org/10.1016/j.chemosphere.2017.04.096

UNEP, 2009. The Stockholm Convention [WWW Document]. URL http://chm.pops.int/Convention/ThePOPs/%0AListingofPOPs/tabid/2509/Default.a

spx (accessed 3.15.20).

Wang, Y., Zhong, Y., Li, J., Zhang, J., Lyu, B., Zhao, Y., Wu, Y., 2018. Occurrence of perfluoroalkyl substances in matched human serum, urine, hair and nail. J. Environ. Sci. 67, 191–197. https://doi.org/https://doi.org/10.1016/j.jes.2017.08.017

Wang, Z., Boucher, J.M., Scheringer, M., Cousins, I.T., Hungerbühler, K., 2017. Toward a Comprehensive Global Emission Inventory of C4-C10Perfluoroalkanesulfonic Acids (PFSAs) and Related Precursors: Focus on the Life Cycle of C8-Based Products and Ongoing Industrial Transition. Environ. Sci. Technol. 51, 4482–4493. https://doi.org/10.1021/acs.est.6b06191

Wang, Z., Cousins, I.T., Scheringer, M., Buck, R.C., Hungerbühler, K., 2014. Global emission inventories for C4–C14 perfluoroalkyl carboxylic acid (PFCA) homologues from 1951 to 2030, part II: The remaining pieces of the puzzle. Environ. Int. 69, 166–176. https://doi.org/10.1016/j.envint.2014.04.006

Yan, N., Marschner, P., Cao, W., Zuo, C., Qin, W., 2015. Influence of salinity and water content on soil microorganisms. Int. Soil Water Conserv. Res. 3, 316–323. https://doi.org/https://doi.org/10.1016/j.iswcr.2015.11.003

Yin, T., Te, S.H., Reinhard, M., Yang, Y., Chen, H., He, Y., Gin, K.Y.-H., 2018. Biotransformation of Sulfluramid (N-ethyl perfluorooctane sulfonamide) and dynamics of associated rhizospheric microbial community in microcosms of wetland plants. Chemosphere 211, 379–389. https://doi.org/https://doi.org/10.1016/j.chemosphere.2018.07.157

Zabaleta, I., Bizkarguenaga, E., Nunoo, D.B.O., Schultes, L., Leonel, J., Prieto, A., Zuloaga, O., Benskin, J.P., 2018. Biodegradation and Uptake of the Pesticide Sulfluramid in a Soil-Carrot Mesocosm. Environ. Sci. Technol. 52, 2603–2611. https://doi.org/10.1021/acs.est.7b03876

Zhao, S., Zhou, T., Zhu, L., Wang, B., Li, Z., Yang, L., Liu, L., 2018. Uptake, translocation and biotransformation of N-ethyl perfluorooctanesulfonamide (N-EtFOSA) by hydroponically grown plants. Environ. Pollut. 235, 404–410. https://doi.org/https://doi.org/10.1016/j.envpol.2017.12.053

Supporting Information

Sulfluramid degradation in tropical mangrove soils

Daniele de A. Miranda[a,*], Juliana Leonel[b], Vanessa Hatje[a]

[a] CIEnAm - Centro Interdisciplinar de Energia e Ambiente, Universidade Federal da Bahia, 41170-115, Salvador, BA, Brazil;

[b]*Coordenação de Oceanografia, Universidade Federal de Santa Catarina.*

*Corresponding autor

Daniele Miranda (danielealmeida@ufba.br)

Universidade Federal da Bahia

CIEnAm I, Campus Ondina

Salvador, Bahia, Brazil. CEP: 41170-115

Standards and reagents

Methanol MeOH (HPLC grade) was purchased from J.T. Baker (Atlantic Labo, France). Acetonitrile was purchased from Honeywell (Steinheim, Germany). Formic acid and acetic acid were purchased from Merck (Darmstadt, Germany). Ammonium formate salts was purchased from FLUKA analytical (Buchs, Switzerland). Ammonium hydroxide salts was purchased from Mallinckrodt chemicals (Dublin, Ireland). All standards were purchased from Wellington Laboratories (Guelph, ON, Canada). Lastly, water was purified with a Millipore water purification system (Millipore, Bedford, MA, USA and had a resistance of 18,2 MΩ cm^{-1}.

Grão Forte®, a commercial Sulfluramid formulation (0.3 % *N*-ethyl perfluorooctane sulfonamide [EtFOSA]), was obtained from Insetimax Industrial Chemicals (Brazil). Authentic standards of 3 (*N*-alkyl substituted) perfluorooctane sulfonamides (I-methylperfluoro-1-octanesulfonamide [MeFOSA], EtFOSA, and FOSA), 3 perfluoroctane sulfonamidoacetates (I-methylperfluoro-1-octanesulfonamidoacetic acid [MeFOSAA], FOSAA, and I-ethylperfluoro-1-octanesulfonamidoacetic acid [EtFOSAA]), 9 perfluoroalkyl carboxylates (C_5-C_{14}PFCAs: perfluoropentanoic acid [PFPeA], perfluoroheptanoic acid [PFHpA], perfluorooctanoic acid [PFOA], perfluorononanoic acid [PFNA], perfluorodecanoic acid [PFDA], perfluoroundecanoic acid [PFUnDA], perfluorododecanoic acid [PFDoDA], perfluorotridecanoic acid [PFTrDA], perfluorotetradecanoic acid [PFTeDA]), and 4 perfluoroalkyl sulfonates (PFSAs; perfluorobutanesulfonic [PFBS], perfluorohexanesulfonic [PFHxS], PFOS, and perfluorodecanesulfonic [PFDS]), as well as the isotopically-labelled standards $^{13}C_4$-PFHpA, $^{13}C_4$-PFOA, $^{13}C_5$-PFNA, $^{13}C_2$-PFDA, $^{13}C_2$-PFUnDA, $^{13}C_2$-PFDoDA, $^{18}O_2$-PFHxS, $^{13}C_4$-PFOS, $^{13}C_8$-FOSA, D_5-EtFOSA, D_3-MeFOSAA, D_5-EtFOSAA, and the recovery standards used to monitor internal standards performance $^{13}C_8$- PFOA and $^{13}C_8$-PFOS were purchased from Wellington Laboratories (Guelph, ON, Canada).

Cleaning materials

Polypropylene bottles, tubes and spoons were used to handle sediment samples. These materials were kept in an Extran® bath (10%) for at least 24 h and then washed with water and rinsed with Milli-Q® water. The materials were dried at environment temperature and then cleaned three times with 1% of NaOH in methanol. Glass materials were calcined at 450° C for 4 hours and rinsed three times with 1% of NaOH in methanol.

Carbon and Nitrogen isotopic analysis

Prior to the TOC analysis, the sediment was decarbonated by chemical attack with HCl (10 %). Approximately 0.03 g of decarbonated sediment was weighed in tin capsules. The C and N isotopes were determined with an Isotope Ratio Mass Spectrometry (IRMS, Thermo Scientific, Delta V Advantage). The equipment was stabilized with 10 blanks runs prior to the sample analysis.

Extraction of sediments

Sediment samples were extract at Federal University of Bahia (Brazil), using previously published method by Zabaleta et al. (2018). First of all, 500 mg of sediment were weighted in a 50 mL polypropylene tube, and then 2 ng of isotopically-labelled standards and 8 mL of acetonitrile (ACN) were added. The mixture was sonicated for 20 min. The tubes were shaken for 40 minutes and then centrifuged by 2900 rpm for 20 minutes. The supernatant was removed and an 8 mL of ACN with 25mM NaOH (7.2 mL ACN + 0.6 mL deionized water + 0.2 mL NaOH 1M) was added and the procedure (ultrasonic, shaken and centrifuged) were repeated. The supernatant was put together with another one. The final extract was dried until dryness by a gently nitrogen (analytical grade, 5.0) flux. The extract was in 400 μL of methanol (MeOH):Milli-Q water (1:1, v/v) with 20 mM formic acid and 20 mM ammonium formate. Extracts were transferred to an ampoule and sealed.

84 **Table S1:** Description of the temporal sampling design of the Sulfluramid
85 degradation field experiment.

ID	Period
T1 (day zero)	Initial time
T1' (day zero)	Sulfluramid bait spike in impacted areas
T2	2 days after spike
T3	15 days after spike
T4	30 days after spike
T5	60 days after spike
T6	92 days after spike
T7	156 days after spike
T8	192 days after spike

86

87

Table S1: Perfluoroalkyl substances (PFASs) analyzed in the present study.

Acronym	Name	Formula	CAS#
	Perfluoroalkyl carboxylic acids (PFCAs)		
PFBA	Perfluorobutanoic acid	C_3F_7COOH	375-22-4
PFPeA	Perfluoropentanoic acid	C_4F_9COOH	2706-90-3
PFHxA*	Perfluorohexanoic acid	$C_5F_{11}COOH$	307-24-4
PFHpA	Perfluoroheptanoic acid	$C_6F_{13}COOH$	375-85-9
PFOA*	Perfluorooctanoic acid	$C_7F_{15}COOH$	335-67-1
PFNA	Perfluorononanoic acid	$C_8F_{17}COOH$	375-95-1
PFDA	Perfluorodecanoic acid	$C_9F_{19}COOH$	335-76-2
PFUnDA	Perfluoroundecanoic acid	$C_{10}F_{21}COOH$	2058-94-8
PFDoDA	Perfluorododecanoic acid	$C_{11}F_{23}COOH$	307-55-1
PFTriDA	Perfluorotridecanoic acid	$C_{12}F_{25}COOH$	72629-94-8
PFTeDA	Perfluorotetradecanoic acid	$C_{13}F_{27}COOH$	376-06-7
PFPeDA	Perfluoropentadecanoate	$C_{14}F_{29}COO^-$	1214264-29-5
	Perfluoroalkyl sulfonic acids (PFSAs)		
PFBS	Perfluorobutanesulfonic acid	$C_4F_9SO_3H$	375-73-5
PFHxS*	Perfluorohexanesulfonic acid	$C_6F_{13}SO_3H$	355-46-4
PFOS*	Perfluorooctanesulfonic acid	$C_8F_{17}SO_3H$	1763-23-1
PFDS*	Perfluorodecanesulfonic acid	$C_{10}F_{21}SO_3H$	355-77-3
	Perfluoroalkyl sulfonamido acetic derivatives (FASAAs)		
FOSAA*	Perfluorooctanesulfonamido acetic acid	$C_8F_{17}SO_2NHCH_2COOH$	2806-24-8
MeFOSAA*	*N*-methylperfluoro-1-octanesulfonamidoacetic acid	$C_{11}H_3D_3F_{17}NO_4S$	1400690-70-1
EtFOSAA*	*N*-Ethyl perfluorooctane sulfonamido acetic acid	$C_8F_{17}SO_2NH(C_2H_5)CH_2COOH$	2991-50-6
	Perfluoroalkyl sulfonamide derivatives (FASAs)		
MeFOSA	N-methylperfluoro-1-octanesulfonamide	$C_{11}H_8F_{17}NO_3S$	24448-09-7
FOSA*	Perfluorooctanesulfonamide	$C_8F_{17}SO_2NH_2$	754-91-6
EtFOSA*	*N*-Ethyl perfluorooctanesulfonamide	$C_8F_{17}SO_2NH(C_2H_5)$	4151-50-2

*Compounds analyzed for both linear (L-) and branched (Br-) isomers.

Table S2: List of retention times, monitored ions, and internal standards for each compound analyzed in the present study.

Target	Retention Time (min)	Quant. Ion (m/z)	Qual Ion (m/z)	Standard	Internal Standard	IS Ion	Data quality
PFBA	0.54	213/169	213/149	L-PFBA	^{13}C-PFBA	217/172	Quantitative
L-PFPeA	0.99	263/219	263/169	L-PFPeA	^{13}C-PFPeA	266/222	Quantitative
L-PFHpA	2.18	363/319	363/169	L-PFHpA	^{13}C-PFHpA	367/322	Quantitative
L-PFOA	2.49	413/369	413/169	L-PFOA	^{13}C-PFOA	417/372	Quantitative
Br-PFOA	~2.49	413/369	413/169	L-PFOA	^{13}C-PFOA	417/372	Semi-quantitative
L-PFNA	2.76	463/419	463/219	L-PFNA	^{13}C-PFNA	468/423	Quantitative
L-PFDA	3.02	513/469	513/269	L-PFDA	^{13}C-PFDA	515/470	Quantitative
L-PFUnDA	3.27	563/519	563/269	L-PFUnDA	^{13}C-PFUnDA	565/520	Quantitative
L-PFDoDA	3.52	613/569	613/169	L-PFDoDA	^{13}C-PFDoA	615/570	Quantitative
L-PFTrDA	3.74	663/619	663/169	L-PFTrDA	^{13}C-PFDoA	615/570	Quantitative
L-PFTeDA	3.97	713/669	713/169	L-PFTeDA	^{13}C-PFDoA	615/570	Quantitative
L-PFPeDA	4.20	763/719	763/169	L-PFTeDA	^{13}C-PFDoA	615/570	Qualitative
L-PFBS	1.69	298.9/80	298.9/99	L-PFBS	^{18}O-PFHxS	403/84	Quantitative
L-PFHxS	2.92	399/80	399/99	L-PFHxS	^{18}O-PFHxS	403/84	Quantitative
Br-PFHxS	2.50	399/80	399/99	L-PFHxS	^{18}O-PFHxS	403/84	Semi-quantitative
L-PFOS	3.07	498.9/80	498.9/99	L-PFOS	^{13}C-PFOS	503/80	Quantitative
Br-PFOS	~2.95	498.9/80	498.9/99	L-PFOS	^{13}C--PFOS	503/80	Semi-quantitative
L-PFDS	3.57	598.9/80	599/99	L-PFDS	^{13}C-PFOS	503/80	Quantitative
Br-PFDS	~3.47	599/80	599/99	L-PFDS	^{13}C-PFOS	503/80	Semi-quantitative
L-FOSA	4.17	498/78	498/169	L-FOSA	^{13}C-FOSA	506/78	Quantitative
Br-FOSA	4.05	498/78	498/169	L-FOSA	^{13}C-FOSA	506/78	Semi-quantitative
L-MeFOSA	3.07	512/169	512/219	L-CH_3FOSA	D^3-MeFOSAA	515/169	Quantitative
Br- MeFOSA	~3.07	512/169	512/219	L-CH_3FOSA	D^3-MeFOSAA	515/169	Semi-quantitative
L-EtFOSA	4.91	526/169	526/219	L-EtFOSA	D_5-EtFOSA	531/219	Quantitative
Br-EtFOSA	~4.91	526/169	526/219	L-EtFOSA	D^5-EtFOSA	531/219	Semi-quantitative
L-FOSAA	3.07	556/419	556/483	L-MeFOSAA	D^3-MeFOSAA	573/419	Quantitative
Br-EtFOSA	~3.07	556/419	556/483	L-MeFOSAA	D^3-MeFOSAA	573/419	Semi-quantitative
L-MeFOSAA	3.10	570/419	570/483	L- MeFOSAA	D^3- CH3FOSAA	573/419	Quantitative
Br- MeFOSAA	3.00	570/419	570/483	L- MeFOSAA	D^3- CH3FOSAA	573/419	Semi-quantitative
L-EtFOSAA	3.23	584/419	584/526	L-EtFOSAA	D^5-EtFOSAA	589/419	Quantitative
Br-EtFOSAA	3.13	584/419	584/526	L-EtFOSAA	D^5-EtFOSAA	589/419	Semi-quantitative

Recovery standards

Target	Retention Time (min)	Quant. Ion (m/z)
$^{13}C_8$-PFOA	2.49	421/376
$^{13}C_8$-PFOS	3.07	506.9/80

Table S3: Individual limits of detection (LD), blank, and spike recovery used in the analyses.

		Blank		Spike/Recovery	
Compound	**LD (ng g^{-1})**	**Average (ng g^{-1})**	**RSD (%)**	**Average (ng g^{-1})**	**RSD (%)**
PFBA	2.00	< LD		87	10
PFPeA	0.20	< LD		89	36
L-PFHxA	0.11	< LD		87	3
L-PFHxA	0.10	< LD		-	-
PFHpA	0.09	< LD		59	12
L-PFOA	0.70	< LD		85	5
Br-PFOA	0.05	< LD		-	-
PFNA	1.15	< LD		88	4
PFDA	0.05	< LD		87	4
PFUnDA	0.28	< LD		93	4
PFDoDA	0.05	< LD		89	4
PFTriDA	0.07	< LD		56	13
PFTeDA	0.07	< LD		27	6
PFPeDA*	0.05	< LD		-	-
PFBS	0.05	< LD		77	11
L-PFHxS	0.05	< LD		88	3
Br-PFHxS	0.05	< LD		-	-
L-PFOS	0.20	< LD		78	13
Br-PFOS	0.05	< LD		-	-
L-PFDS	0.05	< LD		73	10
Br-PFDS	0.10	< LD		-	-
L-FOSA	0.05	< LD		84	20
Br-FOSA	0.05	< LD		-	-
L-MeFOSA	0.05	< LD		78	11
Br-MeFOSA	0.11	< LD		-	-
L-EtFOSA**	0.05	96.9	202	20639	8083612
Br-EtFOSA**	0.05	20.5	8.7	-	-
L-FOSAA	0.05	< LD		99	19
Br-FOSAA	0.05	< LD		-	-
L-MeFOSAA	0.05	< LD		102	9
Br-MeFOSAA	0.05	< LD		-	-
L-EtFOSAA	0.05	< LD		82	5
Br-EtFOSAA	0.05	< LD		-	-

*There was no data for PFPeDA recovery since there is an absence of native standard. In this case, the data quality was semi-quantitative based on another long-chain carboxilated compounds.

**EtFOSA recoveries showed high contamination by the Sulfluramid baits

Table S5: Overview soil characteristics background day 0 (T1). N = 10 (average ± SD).

Particle classification	Value (%)
Sand	-
Clay	53.1 ± 11.1
Silt	46.9 ± 11.1

106 **Table S6:** Individual values of Carbon, Nitrogen, their Isotopes and C/N ratios for soil samples.

Time	Treatment	%C	%N	$\delta^{13}C$ ‰	$\delta^{15}N$ ‰	C/N
T1	CIT1	2.86	0.27	-22.5	3.79	10.8
	CIRT1	1.60	0.15	-22.2	2.41	11.0
	MIT1	2.53	0.21	-23.1	2.82	12.1
	MIRT1	4.34	0.36	-22.0	4.03	11.9
T2	CIT2	2.00	0.18	-22.1	2.86	11.4
	CIRT2	1.95	0.16	-22.1	2.71	12.0
	MIT2	5.95	0.34	-22.8	4.34	17.7
	MIRT2	3.54	0.20	-23.0	3.64	17.5
T3	CIT3	2.21	0.20	-22.0	3.33	11.2
	CIRT3	1.60	0.14	-22.2	2.86	11.1
	MIT3	6.80	0.40	-23.0	5.00	16.3
	MIRT3	7.60	0.30	-26.4	4.90	25.8
T4	CIT4	3.20	0.20	-26.7	3.50	18.8
	CIRT4	2.10	0.10	-26.7	2.80	17.5
	MIT4	8.27	0.30	-27.6	4.54	27.5
	MIRT4	5.91	0.23	-27.6	3.98	25.6
T5	CIT5	3.15	0.17	-26.7	3.47	18.8
	CIRT5	3.30	0.20	-26.6	3.60	18.6
	MIT5	7.00	0.30	-27.6	4.50	25.0
	MIRT5	4.30	0.20	-27.9	3.80	21.5
T6	CIT6	2.82	0.16	-26.8	2.88	17.7
	CIRT6	0.84	0.07	-26.9	0.96	12.4
	MIT6	6.59	0.31	-27.6	4.37	21.0
	MIRT6	4.00	0.24	-28.7	3.73	17.1
T7	CIT7	2.49	0.13	-26.7	2.58	19.0
	CIRT7	1.57	0.08	-26.8	1.68	20.4
	MIT7	3.72	0.21	-23.7	2.64	16.3
	MIRT7	5.21	0.31	-22.3	3.24	15.0
T8	CIT8	1.94	0.09	-26.8	1.56	22.2
	CIRT8	1.27	0.06	-26.7	1.02	22.1
	MIT8	10.03	0.50	-27.3	4.25	20.3
	MIRT8	4.88	0.31	-27.0	3.32	15.8
Control average± SD		2.40 ± 0.80	0.15 ± 0.06	-25.1±.2.21	2.80 ± 0.86	16.2 ± 4.19
Impacted average±SD		5.90 ± 2.60	0.30 ± 0.08	-26.2 ± 2.20	3.94 ± 0.67	19.8 ± 5.10

107

108

Table S7: Concentration (ng g^{-1}) of detected isomers ± standard deviation (n=3) in sediment control without roots (MC).

Compound	MCT1	MCT2	MCT3	MCT4	MCT5	MCT6	MCT7	MCT8
PFBA	< 2.00	< 2.00	< 2.00	< 2.00	< 2.00	< 2.00	< 2.00	< 2.00
PFPeA	< 0.20	< 0.20	< 0.20	< 0.20	< 0.20	< 0.20	< 0.20	< 0.20
L-PFHxA	< 0.11	< 0.11	< 0.11	< 0.11	< 0.11	< 0.11	< 0.11	0.15±0.18
Br-PFHxA	< 0.11	< 0.11	< 0.11	< 0.11	< 0.11	< 0.11	< 0.11	< 0.11
PFHpA	< 0.09	< 0.09	< 0.09	< 0.09	< 0.09	< 0.09	< 0.09	< 0.09
L-PFOA	< 0.70	< 0.70	< 0.70	< 0.70	< 0.70	< 0.70	< 0.70	< 0.70
Br-PFOA	< 0.70	< 0.70	< 0.70	< 0.70	< 0.70	< 0.70	< 0.70	< 0.70
PFNA	< 1.15	< 1.15	< 1.15	< 1.15	< 1.15	< 1.15	< 1.15	< 1.15
PFDA	< 0.05	< 0.05	< 0.05	< 0.05	< 0.05	< 0.05	< 0.05	< 0.05
PFUnDA	< 0.28	< 0.28	< 0.28	< 0.28	< 0.28	< 0.28	< 0.28	< 0.28
PFDoDA	< 0.05	< 0.05	< 0.05	< 0.05	< 0.05	< 0.05	< 0.05	< 0.05
PFTriDA	< 0.07	< 0.07	< 0.07	< 0.07	< 0.07	< 0.07	< 0.07	< 0.07
PFTeDA	< 0.07	< 0.07	< 0.07	< 0.07	< 0.07	< 0.07	< 0.07	< 0.07
PFPeDA	< 0.05	< 0.05	< 0.05	< 0.05	< 0.05	< 0.05	< 0.05	< 0.05
PFBS	< 0.05	< 0.05	< 0.05	< 0.05	< 0.05	< 0.05	< 0.05	< 0.05
L-PFHxS	< 0.05	< 0.05	< 0.05	< 0.05	< 0.05	< 0.05	< 0.05	< 0.05
Br-PFHxS	< 0.05	< 0.05	< 0.05	< 0.05	< 0.05	< 0.05	< 0.05	< 0.05
L-PFOS	< 0.20	< 0.20	< 0.20	< 0.20	< 0.20	< 0.20	< 0.20	< 0.20
Br-PFOS	< 0.20	< 0.20	< 0.20	< 0.20	< 0.20	< 0.20	< 0.20	< 0.20
L-PFDS	< 0.05	< 0.05	< 0.05	< 0.05	< 0.05	< 0.05	< 0.05	< 0.05
Br-PFDS	< 0.05	< 0.05	< 0.05	< 0.05	< 0.05	< 0.05	< 0.05	< 0.05
L-FOSA	< 0.05	0.20±0.08	< 0.05	< 0.05	0.07±0.04	< 0.05	0.07±0.03	0.17±0.17
Br-FOSA	< 0.05	< 0.05	< 0.05	< 0.05	< 0.05	< 0.05	< 0.05	< 0.05
L-CH_3FOSA	< 0.05	< 0.05	< 0.05	< 0.05	< 0.05	< 0.05	< 0.05	< 0.05
Br-CH_3FOSA	< 0.05	< 0.05	< 0.05	< 0.05	< 0.05	< 0.05	< 0.05	< 0.05
L-EtFOSA	< 0.05	29.4±16.2	6.59±3.74	0.41±0.56	3.11±2.88	9.43±7.51	8.57±4.05	45.1±14.3
Br-EtFOSA	< 0.05	11.3±6.80	1.38±0.59	0.28±0.38	0.60±0.58	2.51±2.21	2.80±0.59	12.3±3.91
L-FOSAA	< 0.05	< 0.05	< 0.05	< 0.05	< 0.05	< 0.05	0.17±0.14	< 0.05
Br-FOSAA	< 0.05	< 0.05	< 0.05	< 0.05	< 0.05	< 0.05	< 0.05	< 0.05
L-CH_3FOSAA	< 0.05	< 0.05	< 0.05	< 0.05	< 0.05	< 0.05	< 0.05	< 0.05
Br-CH_3FOSAA	< 0.05	< 0.05	< 0.05	< 0.05	< 0.05	< 0.05	< 0.05	< 0.05
L-EtFOSAA	< 0.05	< 0.05	< 0.05	< 0.05	< 0.05	< 0.05	< 0.05	< 0.05
Br-EtFOSAA	< 0.05	< 0.05	< 0.05	< 0.05	< 0.05	< 0.05	< 0.05	< 0.05

111 **Table S8:** Concentration (ng g^{-1}) of detected isomers ± standard deviation (n=1) in sediment control with roots (MCR).

Compound	MCR4T1	MCR4T2	MCR4T3	MCR4T4	MCR4T5	MCR4T6	MCR4T7	MCR4T8
PFBA	< 2.00	< 2.00	< 2.00	< 2.00	< 2.00	< 2.00	< 2.00	< 2.00
PFPeA	< 0.20	< 0.20	< 0.20	< 0.20	< 0.20	< 0.20	< 0.20	< 0.20
L-PFHxA	< 0.11	< 0.11	< 0.11	< 0.11	< 0.11	< 0.11	< 0.11	< 0.11
Br-PFHxA	< 0.11	< 0.11	< 0.11	< 0.11	< 0.11	< 0.11	< 0.11	< 0.11
PFHpA	< 0.09	< 0.09	< 0.09	< 0.09	< 0.09	< 0.09	< 0.09	< 0.09
L-PFOA	< 0.70	< 0.70	< 0.70	< 0.70	< 0.70	< 0.70	< 0.70	< 0.70
Br-PFOA	< 0.70	< 0.70	< 0.70	< 0.70	< 0.70	< 0.70	< 0.70	< 0.70
PFNA	< 1.15	< 1.15	< 1.15	< 1.15	< 1.15	< 1.15	< 1.15	< 1.15
PFDA	< 0.05	< 0.05	< 0.05	< 0.05	< 0.05	< 0.05	< 0.05	< 0.05
PFUnDA	< 0.28	< 0.28	< 0.28	< 0.28	< 0.28	< 0.28	< 0.28	< 0.28
PFDoDA	< 0.05	< 0.05	< 0.05	< 0.05	< 0.05	< 0.05	< 0.05	< 0.05
PFTriDA	< 0.07	< 0.07	< 0.07	< 0.07	< 0.07	< 0.07	< 0.07	< 0.07
PFTeDA	< 0.07	< 0.07	< 0.07	< 0.07	< 0.07	< 0.07	< 0.07	< 0.07
PFPeDA	< 0.05	< 0.05	< 0.05	< 0.05	< 0.05	< 0.05	< 0.05	< 0.05
PFBS	< 0.05	< 0.05	< 0.05	< 0.05	< 0.05	< 0.05	< 0.05	< 0.05
L-PFHxS	< 0.05	< 0.05	< 0.05	< 0.05	< 0.05	< 0.05	< 0.05	< 0.05
Br-PFHxS	< 0.05	< 0.05	< 0.05	< 0.05	< 0.05	< 0.05	< 0.05	< 0.05
L-PFOS	< 0.20	< 0.20	< 0.20	< 0.20	0.26	< 0.20	< 0.20	< 0.20
Br-PFOS	< 0.20	< 0.20	< 0.20	< 0.20	< 0.20	< 0.20	< 0.20	< 0.20
L-PFDS	< 0.05	< 0.05	< 0.05	< 0.05	< 0.05	< 0.05	< 0.05	< 0.05
Br-PFDS	< 0.05	< 0.05	< 0.05	< 0.05	< 0.05	< 0.05	< 0.05	< 0.05
L-FOSA	< 0.05	0.06	< 0.05	0.29	10.1	0.06	0.05	< 0.05
Br-FOSA	< 0.05	< 0.05	< 0.05	< 0.05	0.63	< 0.05	< 0.05	< 0.05
L-CH_3FOSA	< 0.05	< 0.05	< 0.05	< 0.05	0.42	< 0.05	< 0.05	< 0.05
Br-CH_3FOSA	< 0.05	< 0.05	< 0.05	< 0.05	0.08	< 0.05	< 0.05	< 0.05
L-EtFOSA	5.26	9.68	1.97	3.98	n.r.	12.4	10.8	20.4
Br-EtFOSA	1.05	2.36	1.62	0.87	n.r.	4.20	2.82	5.80
L-FOSAA	< 0.05	< 0.05	< 0.05	< 0.05	< 0.05	< 0.05	0.21	< 0.05
Br-FOSAA	< 0.05	< 0.05	< 0.05	< 0.05	< 0.05	< 0.05	< 0.05	< 0.05
L-CH_3FOSAA	< 0.05	< 0.05	< 0.05	< 0.05	< 0.05	< 0.05	< 0.05	< 0.05
Br-CH_3FOSAA	< 0.05	< 0.05	< 0.05	< 0.05	< 0.05	< 0.05	< 0.05	< 0.05
L-EtFOSAA	< 0.05	< 0.05	< 0.05	< 0.05	0.34	< 0.05	< 0.05	< 0.05
Br-EtFOSAA	< 0.05	< 0.05	< 0.05	< 0.05	< 0.05	< 0.05	< 0.05	< 0.05

112 n.r.: non reported
113

Table S9: Concentration (ng g^{-1}) of detected isomers ± standard deviation (n=3) in sediment impact without roots (MI).

Compound	MIT1	MIT1'	MIT2	MIT3	MIT4	MIT5	MIT6	MIT7	MIT8
PFBA	< 2.00	35.5±37.0	21.3±4.69	0.27±0.36	< 2.00	< 2.00	< 2.00	< 2.00	< 2.00
PFPeA	< 0.20	< 0.20	< 0.20	< 0.20	< 0.20	< 0.20	< 0.20	< 0.20	< 0.20
L-PFHxA	< 0.11	1.15±0.16	1.19±0.16	0.70±0.04	0.63±0.09	0.36±0.05	0.31±0.06	0.23±0.03	0.45±0.13
Br-PFHxA	< 0.11	0.18±0.05	0.16±0.04	0.23±0.08	0.30±0.04	1.19±0.46	2.92±1.03	2.18±1.20	3.39±1.80
PFHpA	< 0.09	< 0.09	0.82±0.12	0.57±0.24	0.71±0.24	0.17±0.12	0.33±0.07	0.38±0.10	0.43±0.12
L-PFOA	< 0.70	3.97±0.81	4.09±0.85	3.90±0.58	3.29±0.35	2.42±0.54	1.86±0.41	2.38±0.64	2.76±0.52
Br-PFOA	< 0.70	< 0.70	< 0.70	< 0.70	< 0.70	< 0.70	< 0.70	< 0.70	< 0.70
PFNA	< 1.15	< 1.15	< 1.15	< 1.15	< 1.15	< 1.15	< 1.15	< 1.15	< 1.15
PFDA	< 0.05	< 0.05	< 0.05	< 0.05	< 0.05	< 0.05	< 0.05	< 0.05	< 0.05
PFUnDA	< 0.28	< 0.28	0.30±0.25	< 0.28	< 0.28	< 0.28	< 0.28	< 0.28	< 0.28
PFDoDA	< 0.05	< 0.05	< 0.05	< 0.05	< 0.05	< 0.05	< 0.05	< 0.05	< 0.05
PFTriDA	< 0.07	< 0.07	< 0.07	< 0.07	< 0.07	< 0.07	< 0.07	< 0.07	< 0.07
PFTeDA	< 0.07	< 0.07	< 0.07	< 0.07	< 0.07	< 0.07	< 0.07	< 0.07	< 0.07
PFPeDA	< 0.05	< 0.05	< 0.05	< 0.05	< 0.05	< 0.05	< 0.05	< 0.05	< 0.05
PFBS	< 0.05	< 0.05	< 0.05	< 0.05	< 0.05	< 0.05	< 0.05	< 0.05	< 0.05
L-PFHxS	< 0.05	< 0.05	< 0.05	< 0.05	< 0.05	< 0.05	< 0.05	< 0.05	< 0.05
Br-PFHxS	< 0.05	< 0.05	< 0.05	< 0.05	< 0.05	< 0.05	< 0.05	< 0.05	< 0.05
L-PFOS	< 0.20	11.4±1.82	11.4±2.15	10.8±1.71	9.99±0.93	7.50±2.48	6.45±0.87	7.40±1.72	10.3±2.56
Br-PFOS	< 0.20	5.04±0.58	5.28±1.04	5.04±0.75	4.86±0.40	3.42±1.04	2.64±0.39	3.29±0.58	4.52±1.46
L-PFDS	< 0.05	< 0.05	< 0.05	< 0.05	< 0.05	< 0.05	< 0.05	< 0.05	< 0.05
Br-PFDS	< 0.05	< 0.05	< 0.05	< 0.05	< 0.05	< 0.05	< 0.05	< 0.05	< 0.05
L-FOSA	< 0.05	12.2±1.20	14.8±2.77	35.5±9.81	24.6±1.81	12.2±12.0	15.3±4.10	26.7±8.08	24.6±6.86
Br-FOSA	< 0.05	1.09±0.15	1.39±0.40	3.07±0.82	2.49±0.27	1.14	1.23±0.20	2.18±0.81	2.06
L-CH_3FOSA	< 0.05	0.51±0.07	0.45±0.29	0.29±0.23	0.49±0.18	0.29	0.16±0.13	0.29±0.22	0.73±0.11
Br-CH_3FOSA	< 0.05	< 0.05	< 0.05	0.05±0.07	< 0.05	< 0.05	< 0.05	< 0.05	< 0.05
L-EtFOSA	< 0.05	6098±874.1	5251±1413	6249±235.6	6210±347.9	3971±501.5	5049±1317	5076±1727	6792±2495
Br-EtFOSA	< 0.05	2156±297	2062±649	7010±6509	2473±151	1494±201	1818±477	1904±638	2482±937
L-FOSAA	< 0.05	< 0.05	< 0.05	0.11±0.04	0.10±0.04	< 0.05	0.08±0.04	0.15±0.09	0.06±0.04
Br-FOSAA	< 0.05	< 0.05	< 0.05	< 0.05	< 0.05	< 0.05	< 0.05	< 0.05	< 0.05
L-CH_3FOSAA	< 0.05	< 0.05	< 0.05	< 0.05	< 0.05	< 0.05	< 0.05	< 0.05	< 0.05
Br-CH_3FOSAA	< 0.05	< 0.05	< 0.05	< 0.05	< 0.05	< 0.05	< 0.05	< 0.05	< 0.05
L-EtFOSAA	< 0.05	0.65±0.17	0.72±0.18	0.58±0.12	0.53±0.05	0.32±0.31	0.41±0.08	0.40±0.12	0.48±0.08
Br-EtFOSAA	< 0.05	< 0.05	< 0.05	< 0.05	< 0.05	< 0.05	< 0.05	< 0.05	< 0.05

Table S10: Concentration (ng g^{-1}) of detected isomers ± standard deviation (n=3) in sediment impact with roots (MIR).

Compound	MIRT1	MIRT1'	MIRT2	MIRT3	MIRT4	MIRT5	MIRT6	MIRT7	MIRT8
PFBA	< 2.00	8.88±11.5	18.7±16.6	19.9±16.5	< 2.00	< 2.00	< 2.00	< 2.00	< 2.00
PFPeA	< 0.20	< 0.20	< 0.20	< 0.20	< 0.20	< 0.20	< 0.20	< 0.20	< 0.20
L-PFHxA	< 0.11	1.04±0.05	1.19±0.25	0.47±0.30	0.30±0.19	0.18±0.08	0.13±0.06	0.13±0.04	0.20±0.08
Br-PFHxA	< 0.11	< 0.11	0.14±0.01	< 0.11	0.44±0.13	0.73±0.47	1.45±0.64	0.20±0.24	0.33±0.35
PFHpA	< 0.09	0.70±0.04	0.76±0.26	0.24±0.20	0.30±0.20	< 0.09	0.26±0.04	0.54±0.13	0.58±0.12
L-PFOA	< 0.70	3.49±0.18	4.10±0.73	2.79±1.59	1.93±0.96	1.73±0.50	1.66±0.40	2.69±0.91	2.72±0.49
Br-PFOA	< 0.70	< 0.70	0.46±0.18	< 0.70	< 0.70	< 0.70	< 0.70	< 0.70	< 0.70
PFNA	< 1.15	< 1.15	< 1.15	< 1.15	< 1.15	< 1.15	< 1.15	< 1.15	< 1.15
PFDA	< 0.05	< 0.05	< 0.05	< 0.05	< 0.05	< 0.05	< 0.05	< 0.05	< 0.05
PFUnDA	< 0.28	< 0.28	< 0.28	< 0.28	< 0.28	< 0.28	< 0.28	< 0.28	< 0.28
PFDoDA	< 0.05	< 0.05	< 0.05	< 0.05	< 0.05	< 0.05	< 0.05	< 0.05	< 0.05
PFTriDA	< 0.07	< 0.07	< 0.07	< 0.07	< 0.07	< 0.07	< 0.07	< 0.07	< 0.07
PFTeDA	< 0.07	< 0.07	< 0.07	< 0.07	< 0.07	< 0.07	< 0.07	< 0.07	< 0.07
PFPeDA	< 0.05	< 0.05	< 0.05	< 0.05	< 0.05	< 0.05	< 0.05	< 0.05	< 0.05
PFBS	< 0.05	< 0.05	< 0.05	< 0.05	< 0.05	< 0.05	< 0.05	< 0.05	< 0.05
L-PFHxS	< 0.05	< 0.05	0.11±0.12	< 0.05	< 0.05	< 0.05	< 0.05	0.05±0.04	0.06±0.01
Br-PFHxS	< 0.05	< 0.05	< 0.05	< 0.05	< 0.05	0.05±0.04	0.06±0.03	< 0.05	0.05±0.02
L-PFOS	< 0.20	10.9±0.43	13.0±3.20	7.56±4.83	5.78±3.02	6.41±1.61	5.52±1.63	4.79±2.30	6.46±2.28
Br-PFOS	< 0.20	4.89±0.21	5.66±0.11	3.65±2.43	2.47±1.30	2.90±0.86	2.26±0.90	1.13±0.37	1.49±0.86
L-PFDS	< 0.05	< 0.05	< 0.05	< 0.05	< 0.05	< 0.05	< 0.05	< 0.05	< 0.05
Br-PFDS	< 0.05	< 0.05	< 0.05	< 0.05	< 0.05	< 0.05	< 0.05	< 0.05	< 0.05
L-FOSA	< 0.05	9.60±0.51	10.6±2.39	13.1±8.08	14.2±6.45	16.8±4.68	21.8±2.24	65.5±30.5	68.3±11.9
Br-FOSA	< 0.05	0.82±0.14	0.71±0.15	1.04±0.59	1.19±0.51	1.33±0.22	1.34±0.16	3.85±1.40	3.64±0.23
L-CH_3FOSA	< 0.05	0.33±0.20	0.22±0.12	0.34±0.20	0.14±0.20	0.39±0.06	0.27±0.26	0.42±0.31	0.30±0.04
Br-CH_3FOSA	< 0.05	< 0.05	< 0.05	< 0.05	< 0.05	0.06±0.05	< 0.05	< 0.05	< 0.05
L-EtFOSA	8.49	4645±366	3860±1932	3920±1659	4289±922	3857±473	4269±870	2571±1318	2239±908
Br-EtFOSA	3.22	1928±97.1	1413±743	1566±604	1746±400	1628±307	1468±250	1015±679	861±371
L-FOSAA	< 0.05	< 0.05	< 0.05	0.09±0.10	0.07±0.92	0.07±0.02	0.20±0.13	4.41±4.05	6.81±7.73
Br-FOSAA	< 0.05	< 0.05	< 0.05	< 0.05	< 0.05	< 0.05	< 0.05	< 0.05	< 0.05
L-CH_3FOSAA	< 0.05	< 0.05	< 0.05	< 0.05	< 0.05	< 0.05	< 0.05	< 0.05	< 0.05
Br-CH_3FOSAA	< 0.05	< 0.05	< 0.05	< 0.05	< 0.05	< 0.05	< 0.05	< 0.05	< 0.05
L-EtFOSAA	< 0.05	0.55±0.11	0.71±0.19	0.36±0.23	0.31±0.10	0.37±0.09	0.45±0.06	0.16±0.01	0.30±0.12
Br-EtFOSAA	< 0.05	< 0.05	< 0.05	< 0.05	< 0.05	< 0.05	< 0.05	< 0.05	< 0.05

Table S11: Outputs of Exponential growth for L-FOSA formation in MI and MIR treatments in the present study. Exponential growth decay was adjusted by Y=Y0*exp(k*X) equation.

Exponential growth equation	**MI**	**MIR**
Best-fit values		
Y0	16.47	9.328
k	0.00208	0.00998
Tau	481.5	100.2
Doubling Time	333.7	69.48
Goodness of Fit		
Robust Sum of Squares	13.33	18.64
RSDR	7.568	5.782
Number of points		
n	23	24

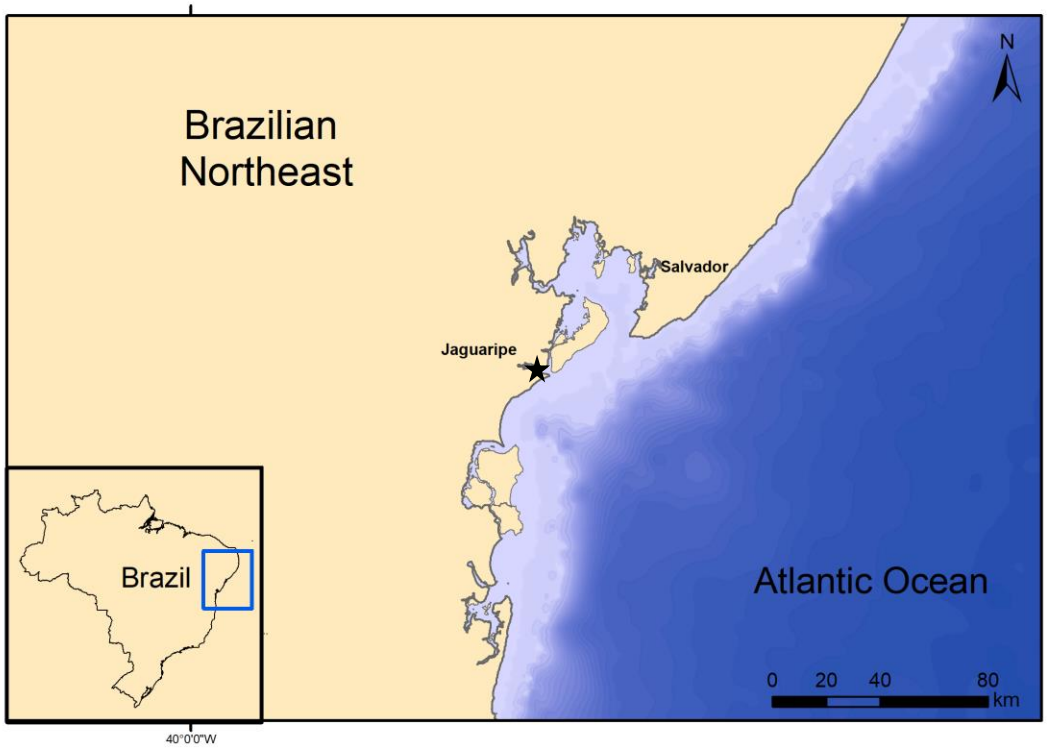

Figure S1: Estuarine area were the in-situ experiment from the present study were carried out.

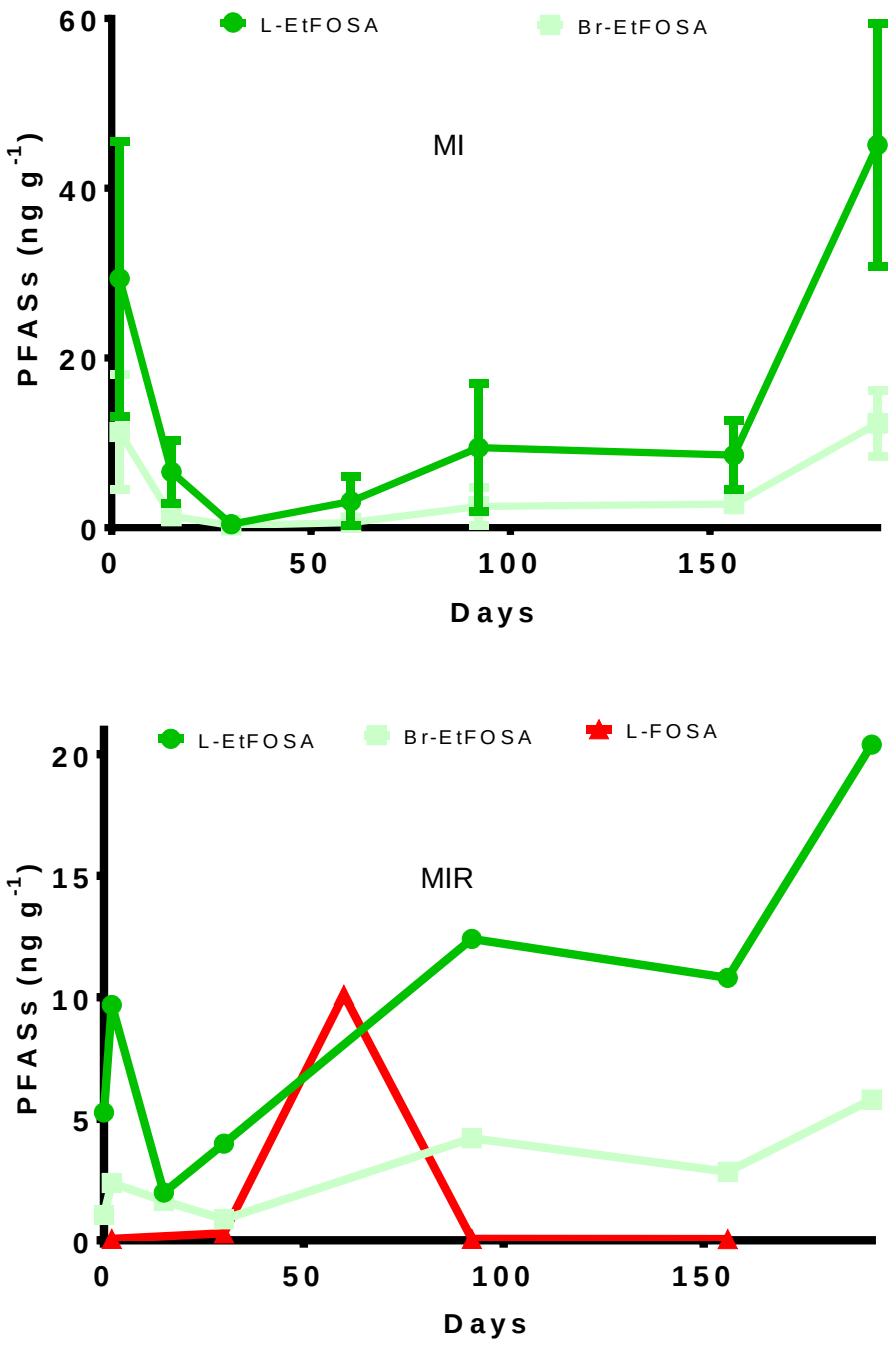

Figure S2: Concentrations of PFASs found in the Control treatments, where a) shows mangrove controls without roots (MC) and b) shows mangrove control with roots (MCR) detected compounds

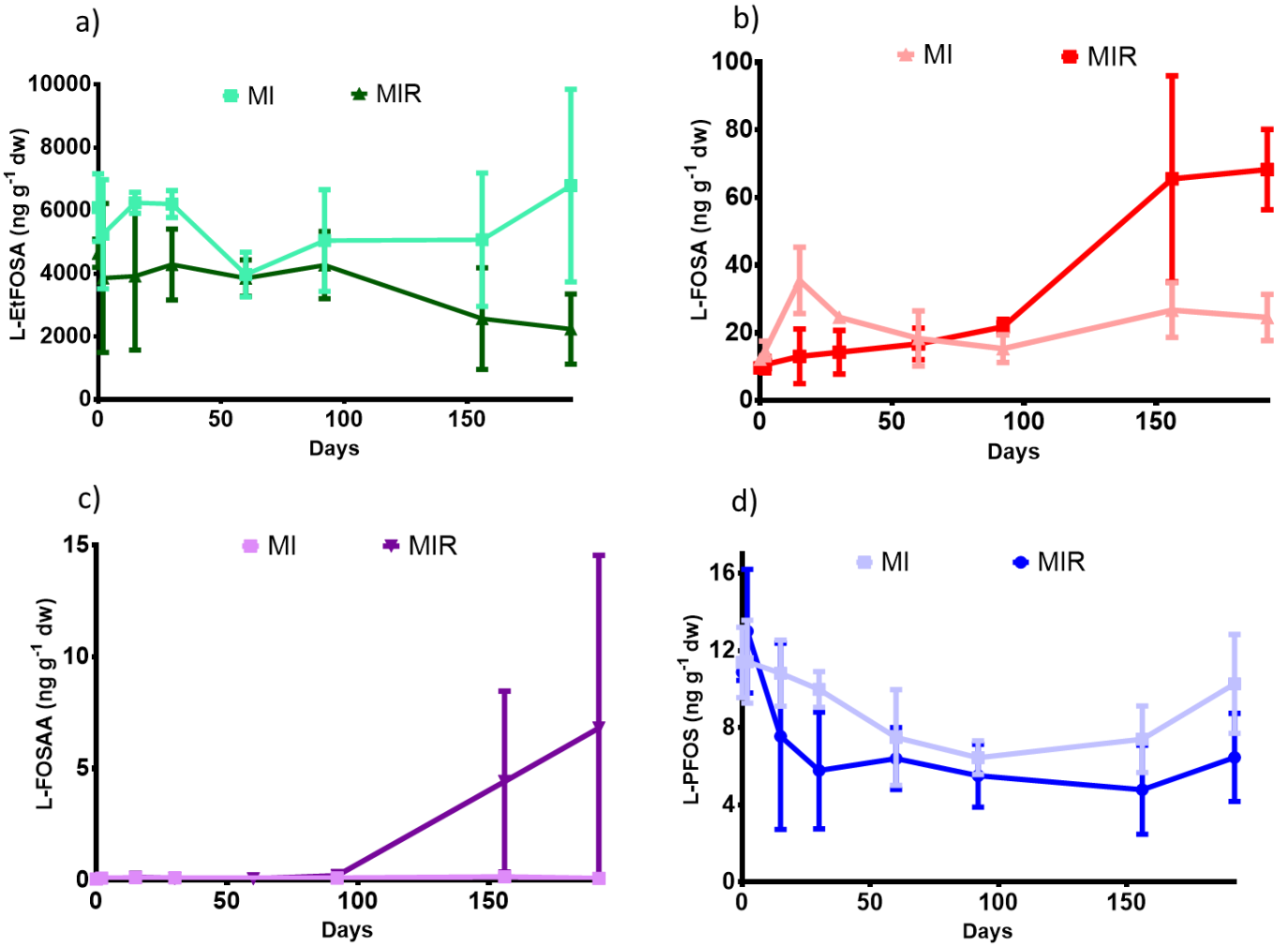

Figure S3: Main PFAS compounds found in the experiment in both treatments (MI and MIR). a) Sulfluramid active ingredient (L-EtFOSA) and its degradation products b) L-FOSA, c) L-FOSAA and d) L-PFOS.

Reference

Zabaleta, I., Bizkarguenaga, E., Nunoo, D.B.O., Schultes, L., Leonel, J., Prieto, A., Zuloaga, O., Benskin, J.P., 2018. Biodegradation and Uptake of the Pesticide Sulfluramid in a Soil-Carrot Mesocosm. Environ. Sci. Technol. 52, 2603–2611. https://doi.org/10.1021/acs.est.7b03876

Capítulo 4: *Perfluoroalkyl Acids (PFAAs) in the Western Tropical Atlantic Ocean*

Perfluoroalkyl Acids (PFAAs) in the Western Tropical Atlantic Ocean

Daniele de A. Miranda[a,b]*, Juliana Leonel[c], Jonathan P. Benskin[b], Jana Johansson[b], Vanessa Hatje[a]

[a]Centro Interdisciplinar de Energia e Ambiente (CIEnAm) and Inst. de Química, Universidade Federal da Bahia, 41170-115, Salvador, BA, Brazil;

[b]Department of Environmental Science, Stockholm University, Stockholm, Sweden.

[c]Coordenação de Oceanografia, Universidade Federal de Santa Catarina, Florianópolis, SC, Brazil.

*Corresponding author

Daniele Miranda (danielealmeida@ufba.br / Daniele.Miranda@aces.su.se)

Universidade Federal da Bahia

CIEnAm I, Campus Ondina

Salvador, Bahia, Brazil. CEP: 41170-115

Abstract

The dispersion of perfluoroalkyl acids (PFAAs) in surface and deep-water profiles was evaluated through the Western Tropical Atlantic Ocean (TAO) between 15°N and 23°S. Sum PFAA concentrations (∑PFAAs) in surface waters ranged from 13 to 74 pg L^{-1}, which is lower than previously reported in the same area and also in higher latitudes. Perfluoroalkyl carboxylates (PFCAs) were the predominant PFAAs present in the Western TAO. The sixteen surface samples showed different PFAA distributions, with the predominance of L-PFOA along the transect (67%; 11 ± 8 pg L^{-1}), and detection of perfluoroalkyl sulfonic acids (PFSAs) only in the Southern TAO. Perfluoroheptanoic acid (PFHpA) was often detected in the vertical profiles, being associated with indirect input as impurity of other compounds and degradation processes. Vertical profiles showed different PFAA distribution patterns (i.e., profiles and concentrations) in the TAO latitudinal sectors (North, Equator, South Atlantic, and in the Brazilian coastal zone), with coastal samples displaying increasing PFAA concentrations from bottom to surface and the offshore profiles displaying higher PFAA detection frequencies in the intermediate water masses. Together with the surface currents and coastal upwelling, the origin of the water masses were important factors in explaining PFAA concentrations and profile distributions in the TAO.

Key words: POPs; PFAAs; PFHxA; GEOTRACES; Tropical Atlantic Ocean.

Introduction

Perfluoroalkyl acids (PFAAs) are fully fluorinated organic compounds that have been used since the 1950s (Buck et al., 2011), but only emerged as a new class of global pollutants in the early 2000s (3M, 2003). Their unique physical-chemical properties (including stability, amphipathicity, and high surface activity), have made them attractive for use in a wide range of products (Glüge et al., 2020). However, these properties also contribute to their persistence in the environment and accumulation in biota (Lau et al., 2007). As a result PFAAs have been detected globally in water, sediments, humans, and biota (Houde et al., 2011), and their occurrence in those matrices is of great concern due to their toxicity to wildlife and humans (Lau et al., 2007; Wang et al., 2019). Furthermore, some PFAAs and their precursors are known to bioaccumulate through marine and estuarine food chains (Houde et al., 2006; Loi et al., 2011; Miranda et al., 2021; Simonnet-Laprade et al., 2019).

PFAAs may be released into the environment from either direct use or via transformation of PFAA-precursors (Buck et al., 2011). Long range transport may occur via the atmosphere (gas and/or on particles) (Dreyer et al., 2015; Gawor et al., 2014; Jahnke et al., 2007; Wang et al., 2017) and by oceanic currents (Benskin et al., 2012b; González-Gaya et al., 2014; Yamashita et al., 2008; Zhao et al., 2012). Furthermore, PFAAs present in the oceans can be transported to the atmosphere via sea spray aerosol (Johansson et al., 2019). Previous studies reported high PFAA concentrations in the North Atlantic Ocean (Muir et al., 2019; Yamashita et al., 2005) associated with production and usage of PFAAs in the USA and Europe. PFAAs have also been detected in the Equatorial and Southern Atlantic waters (Ahrens et al., 2009; Benskin et al., 2012b; González-Gaya et al., 2014, 2019; Yamashita et al., 2005, 2008; Zhao et al., 2012). Long-range oceanic transport is an important source of PFAAs to the Southern Atlantic ocean (Yamashita et al., 2008; Zhang et al., 2017), considering the relatively small regional inputs observed there (Munoz et al., 2018; Nascimento et al., 2018; Quinete et al., 2009). Moreover, previous studies highlighted the role of PFAAs to trace ocean circulation, similarly to other

contaminants such as tritium, chlorofluorocarbons (CFCs), and lead (Bowman et al., 2020; Bridgestock et al., 2018; Doney et al., 1997; Hatje et al., 2018; Kieke et al., 2006).

The production and use of PFAAs has changed over the past decades. Regulatory measures restricted the use of perfluorooctane sulfonic acid (PFOS) in 2009 and prohibited the use and production of perfluorooctanoic acid (PFOA) in 2018 (UNEP, 2019); the latter being the most widespread PFAA in seawater (Muir et al., 2019; Shan et al., 2021; Yamashita et al., 2008, 2005). The phase-out of these compounds is expected to result in a decrease in their concentrations in surface seawater.

Although some studies have been carried out in the Tropical Atlantic Ocean (TAO), most were limited to surface waters and/or the first few hundred meters of the water column (Ahrens et al., 2009, 2010; Benskin et al., 2012b; González-Gaya et al., 2014, 2019; Yamashita et al., 2005; Zhao et al., 2012). Studies found contrasting results for surface seawater in the western TAO (Benskin et al., 2012b; González-Gaya et al., 2014). For example, Benskin et al. (2012b) found ∑PFAAs in the order of part-per-quadrillion (ppq), while González-Gaya et al. (2014) measured the same compounds (i.e. PFOS and other sulfonic compounds) in part-per-trillion (ppt). The difference between studies remains unclear, besides the time difference between the sampling years, it may be reflecting analytical and/or environmental conditions or a punctual discharge of PFAAs after the first study.

The present work studied the occurrence of PFAAs in coastal and oceanic waters of the Western Tropical Atlantic Ocean (15°N to 23°S) to identify sources, distribution patterns, transport routes, and fate of PFAAs. To the best of our knowledge, this is the first study that investigated a range of PFAAs (i.e. 14 compounds) in deep offshore ocean waters. To date, only one study investigated a few compounds (i.e. PFOA, perfluorobutane sulfonate [PFBS], and PFOS) in deep water profiles (i.e. below 4000 m) (Yamashita et al., 2008), and it was in the North Atlantic. We used the measured data to better understand: (1) the importance of surface currents in the spread of legacy and new PFAAs in the ocean and (2) the processes

affecting the vertical distribution of PFAAs in water column, and (3) the use of some long-chain compounds as tracers of global circulation.

Materials and Methods

Oceanographic setting

Surface circulation

Equatorial and Tropical Western Atlantic. The sampled area (i.e., surface samples from #1.1 to #6.1 and #14.1, Figure 1) is mostly influenced by Equatorial westward currents (Figure 1), being limited by the Equatorial flanks of the northern and southern subtropical gyres. While the North Equatorial Current (NEC) is fed by the Canary Current System and totally belongs to the Northern Hemisphere, the South Equatorial Current (SEC) is formed by 3 branches (South SEC, Central SEC and North SEC), with the first two branches crossing the South Atlantic at different latitudes under the influence of the Angola and the Benguela Current System. At the surface, the NEC and SEC are separated by the eastward flows of the North Equatorial Countercurrent (NECC) and the South Equatorial Countercurrent (SECC).

South Tropical Western Atlantic. The SEC reaches the Brazilian margin at 10° - 15°S (i.e. surface samples #14.1 and from #7.1 to #13.1, Figure 1), forming the northward North Brazil Current (NBC) and the southward Brazil Current (BC). BC is the Western Boundary Current that closes the South Atlantic subtropical gyre. This subtropical gyre is also composed of the eastward South Atlantic Current (SAC), followed by the Benguela Current and Agulhas waters flux intrusion and finally the SEC.

Water masses. The thermohaline structure of the sampled transect is characterized vertically by different water masses (Figure S1) that was seen here along the depths in stations #1, #5, #7, and #9. Tropical Surface Waters (TW) are present in the mixed layer (top ~100 m), which are characterized by warm and high salinity waters. Intermediate waters are represented by the North Atlantic Central Water (NACW), and South Atlantic Central Water (SACW) both

presented between ~ 200 to ~ 600 m (Stramma and England, 1999; Talley and Raymer, 1982; Tsuchiya et al., 1994). NACW is formed at the south flank of the Gulf Stream (Talley and Raymer, 1982), while SACW is formed by the confluence of Brazil and Malvinas currents at 35°S and by different modal waters, including the Southern Tropical Indian Modal Water (STIMW) and flows within the SAC until it merges into SEC at 10°S (Azar et al., 2020; Talley, 2013). Below the SACW, the Antarctic Intermediate Water (AAIW) extends from ~600 m to more than 1200 m depth. In the Atlantic, it is formed near the Drake Passage, but the region also receives AAIW from the Indian Ocean through the Agulhas Current leakage; it is transported by the South Atlantic subtropical gyre (Stramma and England, 1999). The North Atlantic Deep Water (NADW) is the following water mass occupying the depth of ~1200 - 3500 m (Ferreira and Kerr, 2017). This water mass is formed by the confluence of deep water in the Nordic and Labrador Seas and is then transported equatorward. Lastly, the Abyssal Antarctic Bottom Water (AABW) is originated in the Southern Ocean south of the Antarctic Circumpolar Current by brine rejection in the Weddell Sea (Talley, 2013). A summary of those water masses physicochemical characteristics can be seen in the Table S1 in Supplementary Information (SI).

Cabo Frio, Rio de Janeiro Upwelling. At 23°S (stations #15 and #16), due to northeast strong winds, there is a modification in the coastal current direction from north-south to east-west that promotes the seasonal upwelling of the SACW to the photic zone of the continental shelf, being intensified during the summer (Lessa et al., 2014; Valentin, 2001).

Sampling campaign

Sixteen surface water sites and 6 full depth water profiles (Figure 1, Table S2) were sampled between November 2017 and January 2018 in the Tropical Atlantic Ocean (15°N to 23°S) on board of the R/V Vital de Oliveira, during the PIRATA XVII/GEOTRACES GApr10 cruise. Samples were collected to cover the most important water masses and oceanographic features

of the region. Samples were grouped in 4 zones: Northern TAO (samples #1 to #4), Equator (#5), Southern TAO (#6, #14, and #7 to #12), and coastal samples (#13, 15, and #16). Seawater samples were collected using NISKIN bottles and were stored in 0.5 L polypropylene (PP) bottles. All sample bottles had been pre-cleaned by rinsing 3 times with 1 % ammonium hydroxide in methanol in a clean laboratory and then washing 3 times with seawater immediately prior to sampling. All samples were kept at 4 ºC until analysis.

Standards and reagents

A total of 13 PFAAs were investigated in this work, including 1 perfluorooctane sulfonamide, 9 PFCAs, and 4 PFSAs (Table S3). Authentic standards of perfluooctane sulfonamide (FOSA), perfluorohexanoic acid (PFHxA), perfluoroheptanoic acid (PFHpA), perfluorooctanoic acid (PFOA), perfluorononanoic acid (PFNA), perfluorodecanoic acid (PFDA), perfluoroundecanoic acid (PFUnDA), perfluorododecanoic acid (PFDoDA), perfluorotridecanoic acid (PFTriDA), perfluorotetradecanoic acid (PFTeDA)), perfluorobutanesulfonic acid (PFBS), perfluorohexanesulfonic acid (PFHxS), PFOS, and perfluorodecanesulfonic acid (PFDS) as well as the internal standards $^{13}C_2$-PFHxA, $^{13}C_4$-PFHpA, $^{13}C_4$-PFOA, $^{13}C_5$-PFNA, $^{13}C_2$-PFDA, $^{13}C_2$-PFUnDA, $^{13}C_2$-PFDoDA, $^{18}O_2$-PFHxS, $^{13}C_4$-PFOS, and $^{13}C_8$-FOSA were purchased from Wellington Laboratories (Guelph, ON, Canada).

Sample treatment

Samples (n = 51) were extracted using a method previously described in Gilljam et al. (2016). Briefly, isotopically labeled internal standards (100 pg) were added to each sample at least 24 hours prior to extraction. Samples were extracted by solid phase extraction (SPE) with Waters Oasis® Weak-anion exchange WAX SPE cartridges (6 cm^3, 150 mg, 30 µm). WAX SPE cartridges were conditioned with 15 mL of 0.3 % of NH_4OH in Methanol (MeOH) followed by 4.5 mL of 0.1 M formic acid in ultrapure Milli-Q water, and then loaded with unfiltered (whole sample) seawater samples (0.5 L). After loading, the WAX SPE cartridges were washed

with 5 mL of 20% MeOH in 0.1 M formic acid and 2 mL of 0.3% NH_4OH in Milli-Q water. Samples were eluted with 3 mL of 0.3 % NH_4OH in MeOH. Extracts were evaporated under a gentle flow of nitrogen to a final volume of 100 µL and transferred to a high-density polyethylene (HDPE) vials and then stored in fridge until analysis. No buffer or recovery standard was used to reduce the risk of adding PFAAs which may occur as impurities.

Instrumental analysis

Instrumental analysis was carried out by ultra-performance liquid chromatography-tandem mass spectrometry using a Waters Acquity UPLC coupled to a Waters Xevo TQ-S triple quadrupole mass spectrometer operated in negative electrospray ionization, multiple reaction monitoring mode. Twenty microliter aliquots of each sample were chromatographed on a BEH C18 analytical column (2.1×50 mm, 1.7 µm particle size, Waters) operated at a flow rate of 0.4 mL min^{-1}, using a mobile phase composition of 90 % water/10 % acetonitrile containing 2 mM ammonium acetate (solvent A) and 99 % acetonitrile and 1% water containing 2 mM ammonium acetate (solvent B). The mobile phase gradient profile is shown in Table S4. A total of two precursor/product ion transitions were monitored per analyte (Table S5); one for quantification and the other for qualification. Quantitative determination of target compounds was carried out either by isotope dilution or an internal standard approach using a linear calibration curve with 1/x weighting. Branched isomers were determined semi-quantitatively using the calibration curve for the linear isomer. The data throughout the manuscript is presented as average ± SD.

Quality assurance/Quality control

Laboratory, bottle, and field blanks were routinely analyzed. Field blanks were composed of PP clean water bottles filled up with 1 mL of C18 SPE-extracted ultrapure water in Brazil (Universidade Federal da Bahia), transported to the field, and uncapped during sampling collection. Bottle blanks were transported empty and kept sealed during the entire sampling collection and filed up at the moment of real sample analysis with 500 mL of polished ultra-

pure water (i.e. ultra-pure water that was passed through a conditioned WAX SPE cartridge) in Stockholm University, Sweden. Laboratory blanks (1 mL) were running together with the real samples with polished ultra-pure water, spiked with isotopically labeled internal standards (100 pg), and analyzed for every 12 samples. More details on PFAAs-extraction method optimization can be found in SI.

Percent recoveries (Table S6) from spike experiments consisting of addition of 50 pg of individual native standards (500 mL; n = 8) ranged between 70 and 92% for most substances, except for PFTeDA, PFTriDA that showed low recovery (27 ± 8 %, 40 ± 12 %, respectively), and higher recovery for PFBS (124 ± 64 %) (Table S6). Recoveries using a higher fortification level (500 pg of individual PFAS into 500 mL; n=8) were mostly between 60 and 110%, except for PFTeDA (34 ± 11%), PFBS (136 ± 124%), and FOSA (132 ± 84%). Method detection limits (MDL) and method quantification limits (MQLs; Table S6) were calculated as the concentration of each compound producing a signal-to-noise ratio > 3 and >10, respectively. MDL ranged from 0.50 (L-PFOA) to 6.88 pg L^{-1} (PFTriDA), where MQL were in between 1.67 (PFDA/PFTeDA) to 22.9 pg L^{-1} (PFTriDA). Concentrations below MDL were not included in any PFAA sum. Individual PFAA concentrations for laboratory blanks were always <1 pg L^{-1}. PFAA contamination in field blanks was also very low (<5 pg L^{-1}), but slightly higher than lab blanks, possibly due to contamination introduced when preparing the field blanks (Table S7). Overall, blank contamination was very low and consistent, therefore blank corrections were not applied (see Table S7). PFHpA, PFOA (linear and branched), and PFHxS could not be reported for profile #1 (15°N) due to contamination of the reagents used for this batch of samples (SI, Table S7). These reagents were removed when processing subsequent batches and did not affect any other samples.

Results and discussion

PFAAs in surface samples

227 Nine of the 13 PFAAs investigated here (i.e., PFHxA, PFHpA, PFOA, PFNA, PFDA,
228 PFDoDA, PFBS, PFOS, and FOSA) were detected in most of the surface water samples above
229 MDL (Table S8), with ΣPFAA concentrations ranging from 13 to 74 pg L^{-1} (Figure 2, Table
230 S8). Concentrations in samples #5.1 (0°), #10.1 (21°S) and #13.1 (23°S) were below the MDL.
231 There was observed a latitudinal trend in the surface PFAA concentrations and compounds
232 profile, being associated with different surface currents directions passing through the region
233 (Figure 1). For example, L-PFHxA was frequently detected over the entire transect (40 %
234 detection frequency [df]; 13 ± 4 pg L^{-1}; average of the sampling points ± SD), which was also
235 observed in a previous study for the same latitude (i.e. 12°N to 22°S) collected 10 years earlier
236 (11 ± 10 pg L^{-1}, n = 12 sampling points) (Benskin et al., 2012b). The detection of this compound
237 was mainly associated with surface currents from African systems (i.e #2.1 and #3.1: Guinea
238 Dome; #7.1 and #14.1: Angola Basin) and South Equatorial Current (#8.1). PFHxA was
239 previously observed as the main compound in the eastern TAO sampled 7 years earlier (13 ±
240 2 pg L^{-1}) (Zhao et al., 2012), which must be the source of this compound for the sampled area
241 in the present study. There was observed a peak of compounds in the sample #7.1 (8°S, Figure
242 2), within the sum of PFHxA (9 pg L^{-1}), PFOA (Linear + Branched = 31 pg L^{-1}), and FOSA
243 (10 pg L^{-1}) being associated to the previously mentioned contribution of Angola Basin. This
244 peak of compounds in TAO at 8°S was previously observed 10 years before this study (Benskin
245 et al., 2012b), although in a higher number of compounds (11 PFAAs) and in higher
246 concentrations ($\sum_{11}$PFAA= 250 pg L^{-1}).
247 PFOA was the most frequently detected PFAA over the entire transect (67 % detection
248 frequency [df]; 11 ± 8 pg L^{-1}; average of the sampling points ± SD), corroborating previous
249 results for the same latitude (i.e. 12°N to 25°S) collected 10 years earlier (21 ± 11 pg L^{-1}, n =
250 12 sampling points) (Benskin et al., 2012b). Nonetheless, PFOA concentrations from 2008 and
251 2009 reported by Ahrens et al. (2009) and (2010), respectively, were in much higher
252 concentrations in the eastern TAO (11° to 8°N, n = 3, 78 ± 9 pg L^{-1}; and 15°N to 23°S, n = 7,

253 54 ± 10 pg L^{-1}, respectively), while concentrations below MDL (< 4 and < 12 pg L^{-1}) were
254 found in the southern Equator in 2008 (Ahrens et al., 2009) and 2010 (Zhao et al., 2012) (Table
255 S2), suggesting different sources for those regions in eastern TAO.
256 $\sum_7$PFAA concentrations observed through the TAO (13 – 74 pg L^{-1}) are lower than those in
257 roughly corresponding latitudes reported by Benskin et al. (2012b) ($\sum_7$PFAA: 49 to 162 pg L^{-1})
258 and Ahrens et al. (2009) ($\sum_7$PFAA: 27 to 187 pg L^{-1}) for the same compounds, and orders of
259 magnitude lower than concentrations in high latitudes of the Northern Hemisphere (Yamashita
260 et al., 2005; Yeung et al., 2017; Zhao et al., 2012). The lower PFAA concentrations detected
261 in the TAO was expected considering (1) the distance to the main PFAA sources (e.g., USA
262 and Europe); (2) the progressive phase-out and voluntary changes in PFAAs uses along the
263 years; (3) and the predominant direction of currents that takes much of the surface water from
264 the hotspots northward to the Arctic, by the prolongation of the Gulf Stream current, the North
265 Atlantic Current (NAC) (Stendardo et al., 2020; Zhang et al., 2017). Consequently, the southern
266 surface branch of the NAC, driven towards the equator, carries lower amounts of PFAAs than
267 the northern branch (Ahrens et al., 2009). The southern branch of the NAC feeds the Canary
268 Current system and, in turn, the North Equatorial system. The Canary Current spreads PFAAs
269 from Europe to Equatorial waters (Ahrens et al., 2009; Zhao et al., 2012), and the source of
270 compounds to this current system may include contaminants from the English Channel
271 (McLachlan et al., 2007), North sea (Joerss et al., 2019), and Bay of Biscay (Zhao et al., 2012).
272 These sources were previously reported as important contaminant contributors to the Canary
273 Current system, showing similar PFAA profiles with a high contribution of PFCAs.
274 Sample #1.1 (15°N) showed the highest ΣPFAA concentrations among the surface samples in
275 the Northern TAO (15°N; 38 pg L^{-1}). The other samples from the northern TAO (#2.1 - #6.1)
276 are less influenced by the North Equatorial current and more influenced by the east-west
277 Equatorial Currents, which seem to decrease PFAAs concentrations in the region (Ahrens et
278 al., 2009), resulting in lower ∑PFAA concentration (14 to 32 pg L^{-1}). PFAA sources for the

east-west Equatorial Currents are unclear but may include atmospheric deposition, in particular considering the elevated precipitation rate in this area (Camara et al., 2015) and the lack of large input of PFAA reported for the western Africa coast (Ahrens et al., 2009). The atmospheric deposition of PFCAs and PFSA-precursors (i.e., FASA, fluorotelomer alcohols [FTOHs], and others) was previously reported for the eastern Atlantic, showing a gradual concentration decrease southward (from ~53°N to ~33°S) (Dreyer et al., 2009; Jahnke et al., 2007).

PFSAs and perfluoroalkyl sulfonamides (PFBS: 6 ± 2 pg L^{-1}; PFOS: 1 ± 0.1 pg L^{-1}; and FOSA: 6 ± 3 pg L^{-1}) were only present in the southern TAO, in coastal waters (#15.1 and #16.1; 23°S), and in two samples offshore (#7.1 and #11.1; 8° and 22°S). In comparison, Benskin et al. (2012b) observed higher detection frequency of these substances for the western TAO (Figure S2; PFOS, 18 – 52 pg L^{-1}, FOSA 1 – 3 pg L^{-1}), although FOSA concentrations were lower. While PFOS was rarely observed in surface sample here, previous studies carried out in a similar area to this one suggested the ongoing use of the PFOS-precursor (PreFOS) formicide Sulfluramid (*N*-ethyl perfluorooctane sulfonamide; EtFOSA) in South America may contribute to the increase of the ∑PFSAs in the Atlantic (Benskin et al., 2012b; González-Gaya et al., 2014). To date, occurrence of PFAAs in marine and estuaries waters of South America remains associated with multiple sources including Sulfluramid use in Brazilian forestry (Gilljam et al., 2016; Nascimento et al., 2018) due to the environmental transformation (either biotic or abiotic) of this formicide to FOSA and PFOS (Avendaño and Liu, 2015).

The transect in the continental shelf of the Rio de Janeiro (#13.1, #15.1, and #16.1; 23ºS) showed different ∑PFAA concentrations and profiles towards the coast (Figure 2). While site #15.1 (Fig. 2) showed the highest concentration of PFAAs (74 pg L^{-1}) and the highest concentration of L-PFOA (30 pg L^{-1}) in the whole transect, the sample #16.1 showed the second lowest ∑PFAA (15 pg L^{-1}). The concentrations and PFAA profiles observed here were lower

than previous studies carried out near urban areas in the North Atlantic (Zhang et al., 2019) and Pacific (Kwok et al., 2015), and different from other TAO zones in this study. Although the presence of PFAAs in the TAO have been associated with riverine inputs (Munoz et al., 2017; Nascimento et al., 2018), the lower PFAA concentration in #16.1 compared to #15.1 suggests an additional source of contaminants other than direct continental input to the former samples. Nevertheless, PFOA detected here was previously observed in the main bay and river around the sampled area (Quinete et al., 2009). Although atmospheric deposition can be an important contaminant source, carrying continental solids and gas particulates with fluorinated precursors (Dreyer et al., 2009; Jahnke et al., 2007; Simcik and Dorweiler, 2006), the distinct PFAAs profile and levels in the region reinforce the influence of other sources. According to NOAA meteorological back air trajectories data (Figures S3 and S4), the study sites (i.e., #13.1, #15.1 and #16.1) are under the influence of the same wind field, carrying continental air masses to the sampled area. In case the atmospheric deposition was an important source for the region, it would be expected for a more homogenous PFAA distribution over the coastal samples. As such, continental inputs and the different hydrographic processes acting in the water column (i.e., upwelling) should be considered to explain the observed distribution patterns. More details on how the hydrographic processes can be acting to spread these compounds through the water column is given in the next section.

PFAAs in deep water samples

Eleven of 13 analyzed PFAAs were detected in deep profiles (Figures 3 and 4, Table S8). The vertical PFAA patterns were different across TAO zones, except for the remarkable predominance of long-chain PFCAs compared to PFSAs. Most compounds were detected in the mixed layer (TW) and intermediate central waters (both NACW and SACW, between ~135 and ~525 m deep) and, occasionally, in the bottom water (AABW) (Figure 3; individual PFAA

329 profiles: Figures S5 and S6). The profile at station #9 (18°S) showed different distribution of
330 compounds with the highest ∑PFAAs in the NADW (84 and 92 pg L^{-1} at 1399 and 2500 m
331 deep, respectively). The higher concentrations in intermediate waters are associated with the
332 area of formation of these water masses and their trajectory in both hemispheres in the ocean
333 surface (Peña-Izquierdo et al., 2015; Stramma and England, 1999); being exposed to PFAA
334 inputs by both atmospheric deposition and from rivers. NACW (15°N) showed a different
335 profile from SACW, with PFHpA, PFNA, PFOS representing the dominant PFASs, at
336 concentrations of 35 ± 18, 7 ± 7, 8 ± 4 pg L^{-1} (average of samples in the same water mass ±
337 SD), respectively (Figure 3, Table S8). The frequent occurrence of PFHpA has been previously
338 observed in the Atlantic, Mediterranean, and Arctic surface waters (Benskin et al., 2012b;
339 Brumovský et al., 2016; Joerss et al., 2020), and its detection was suggested as an impurity in
340 consumer products and degradation of Fluorotelomer Alcohols (FTOHs) (Simcik and
341 Dorweiler, 2006), whereas PFNA and PFOS were associated with direct releases into the
342 environment (Wang et al., 2014). The intensive historical use of PFAA-based products in the
343 Northern Hemisphere, explains the occurrence of PFHpA and PFNA in the NACW, whereas
344 the rare detection and low concentrations of PFOS may reflect its progressive phase-out, which
345 started in the early 2000s (3M, 2003).

346 In the Southern TAO, at 8°S (#7) and 18°S (#9), the SACW displayed a larger number of
347 compounds and higher concentrations than in the same water mass at the Equator (#5) (Figure
348 3, Table S8). Whereas PFOA was detected in the SACW and in similar concentrations among
349 profiles (30, 13 ± 5, and 22 pg L^{-1}; #5, #7, and #9, respectively), FOSA showed an increasing
350 trend from 18°S northwards to the Equator (59 ± 47, 30 ± 26, and 6 ± 2 pg L^{-1}, in samples #5,
351 #7, and #9, respectively). The reason for these findings is unclear, but are likely associated with
352 different inputs to the individual sampling stations. PFHpA was observed in both stations in
353 the southern hemisphere at SACW (#7 = 48 ± 32; and #9 = 37 pg L^{-1}) and in the NACW (#1:

354 35 ± 18 pg L^{-1}). High PFAA concentrations in one of the seawater current sources for SACW
355 (i.e. Malvinas current) had been previously associated with the inputs of Sulfluramid and other
356 industrial and consumer products carried by the Plata River to the ocean (Benskin et al., 2012b).
357 PFOA and PFOS were measured in surface waters by Benskin et al. (2012b) in higher
358 concentrations than observed here, where PFHpA and FOSA were rarely detected,
359 nevertheless, they were detected here in both deep profiles in the southern TAO. The SACW
360 also receives input from the Indian Ocean via the Agulhas leakage, which is an important
361 feature to the transference of heat and salts to the Atlantic Ocean (Laxenaire et al., 2020), and
362 should be considered as a potential source of PFAAs.

363 PFAAs were detected in AAIW in 3 of the 4 profiles along the TAO transect. The AAIW,
364 formed in the Subantarctic Front between 50-60°S, crosses the Atlantic northward, transporting
365 less saline water from the Southern to Northern Hemisphere (Sørensen et al., 2001). During its
366 transport northward, AAIW follows the SAC, and similar to the SACW, AAIW also receives
367 inputs from the Agulhas leakage (Azar et al., 2020). There are no previous studies analyzing
368 vertical profiles in the Indian Ocean, but González-Gaya et al. (2014) observed similar PFAAs
369 in surface samples (i.e. PFHpA, PFOA, PFNA, PFOS, PFDA) to what was observed here. Also,
370 FOSA was not observed in the previous study in surface waters (González-Gaya et al., 2014),
371 suggesting an additional source of this compound for both SACW and AAIW not elucidated
372 here. It is interesting to notice the detection of PFHpA in AAIW at 18°S (#9, 20 pg L^{-1}), its
373 absence at 8°S and in the Equator, and its highest concentration at 15°N (#1, 50 pg L^{-1}).
374 Whereas the presence of this compound in the Southern Hemisphere can be associated with the
375 Agulhas leakage, in the Northern Hemisphere its source is unclear, but could be related with
376 the Mediterranean Overflow Water (MOW). Even though MOW did not reach this region of
377 the Northern Atlantic, anticyclonic eddies of nearly pure Mediterranean water, called Meddies,
378 propagate southwestward distributing their properties, including contaminants (I

379 Bashmachnikov et al., 2015). The Mediterranean Sea displayed high levels of PFHpA due to
380 continental inputs (Brumovský et al., 2016) and, hence, may represent an important source of
381 this compound to the mAAIW at 15°N (#1).

382 Below the AAIW, the deep layer is occupied by the NADW. This water mass is formed by the
383 sink of surface waters in the Labrador Sea, in a hotspot for PFAAs compounds (Benskin et al.,
384 2012b; Yamashita et al., 2008; Zhang et al., 2017). The mechanism of water formation in this
385 region is well-known as an important pathway to remove PFAAs from the ocean surface
386 (Lohmann et al., 2013). This water mass is part of the overturning circulation and moves
387 southward until it gets to the Antarctic at 60°S (Brix and Gerdes, 2003), being remarkable in
388 the transport of cold water from North to South Hemisphere and for the spread of PFAAs
389 compound in the same direction (Zhang et al., 2017). The only study reporting PFAAs in deep
390 Atlantic waters, carried out in 2002, showed slightly higher concentrations of PFOA and PFOS
391 than measured here (~50 pg L^{-1} and ~10 pg L^{-1}, respectively), but in the same order of
392 magnitude for stations in the Labrador Sea and Middle Atlantic Ocean (25°N) (Yamashita et
393 al., 2008). It was calculated that CFC present in the NADW formation area (i.e. Labrador Sea,
394 47°N) reaches 20°S after ~40 years (Rhein et al., 2015) by the spreading of this water mass
395 southwards. Considering that the production peak of PFAAs such as PFOA and PFOS occurred
396 in ~1970s (Prevedouros et al., 2006), the NADW formation area could be the source of PFHpA,
397 (L- and Br-) PFOA, FOSA, PFOS and other PFAAs found at latitude 18°S (#9). The high
398 concentrations associated with peak PFAA production appears to be moving southward (Figure
399 3).
400 The bottom water mass in the Atlantic is occupied by the AABW that showed only L-PFOA,
401 PFOS, and FOSA above the MDL, in Equator (#5). Both L-PFOA and PFOS were already
402 observed in deep waters (~5000 m) but at higher latitudes (25°N) and in low concentrations
403 (Yamashita et al., 2008). This water mass is formed by the abrupt sink of high saline and cold

404 water in the Antarctic. Although PFAAs have been measured in Antarctic snow in high
405 concentrations (Cai et al., 2012; Xie et al., 2020; Zhao et al., 2012), the detection of these
406 compounds (i.e. L-PFOA, PFOS and FOSA) at the interface between the NADW and AABW
407 (i.e. 4500 m) is likely a combined signature of the former water mass. A possible explanation
408 for this is mainly because there was not enough time for the contaminated waters in the
409 Antarctic region to reach the sampling point at the Equator.

410 *Cabo Frio, Rio de Janeiro Upwelling*

411 The two vertical profiles sampled at the Brazilian continental shelf (stations #15 and #16, 23°S)
412 displayed a PFAA distribution which was opposite to that observed in offshore areas, with high
413 concentrations in the bottom samples (in particular in sample #15, 75 m but also #16, 68 m)
414 and low concentrations in the surface (Figure 4). This result was unexpected due to the
415 proximity to a highly industrialized and urbanized area, which was previously associated with
416 high PFAA concentrations in surface waters (Kwok et al., 2015).

417 Despite their close proximity, the two profiles presented distinct concentrations, with PFAA
418 concentrations in #15 varying from 2 pg L^{-1} (PFOS) to 123 pg L^{-1} (PFHpA) while in #16,
419 concentrations varied from 18 pg L^{-1} (L-PFOA) to 173 pg L^{-1} (PFHpA). This inconsistency
420 could be due to physical processes occurring in the area. This region is known for the
421 occurrence of upwelling intensified during the austral spring and summer (September to
422 March), when the SACW is conducted from a depth of ~300 m to the surface (Valentin, 2001).
423 Moreover, salinity, temperature, and oxygen profiles (Figures S7 and S8, Table S2) recorded
424 the occurrence of recent upwelling events in #16 where SACW was outcropped, but the same
425 was not observed in #15. SACW upwelling is induced when the NE trade winds push TW
426 offshore explaining the lower concentrations in the station near the cost (#16) and higher
427 concentrations in #15.

Previous data from river waters surrounding the upwelling stations showed L-PFOA, PFHpA, and PFOS among the most often detected compounds, with individual concentrations ranging from 150 to 3250 pg L^{-1}, 111 to 1970 pg L^{-1}, and 170 to 920 pg L^{-1}, respectively (Quinete et al., 2009). Together, the direct input by coastal water systems and the resuspension of contaminated particulate/sediments forced by the upwelling may be impacting PFAA distribution patterns observed in the deepest sampling points. Once in the seawater, these compounds will partition in different proportions to the particulate material according to their chemical structure, with long-chain compounds in greater affinity with the solid phase. A previous study showed the sediment signature of carbon-nitrogen ratio and their isotopes (i.e. C/N ratio and $\delta^{13}C$ and $\delta^{15}N$) associated with organic matter inflow from Paraiba do Sul River and lower degree from Guanabara Bay to the continental shelf of Rio de Janeiro for the same area studied here (Albuquerque et al., 2014). However, more data would be necessary to confirm this hypothesis, together with the direct input by the upwelling of SACW. Thus, those forces must be investigated separately to better understand the influence of each forcing in more detail in the future.

The complex myriad of water sources (i.e., coastal inputs, upwelling, and open waters) and also atmospheric deposition, might explain the latitudinal variation found in PFAA concentrations in the western TAO. Surface and vertical profile samples showed differences in the composition of PFAAs, although PFCAs were the dominant group in surface and deep waters. The effects of the phase-out of PFOS are already observable in ocean waters, which showed decreased concentration with increasing distance from emission sources in the North Hemisphere. The composition of PFAAs in the current investigation varied with depth, highlighting the contribution of different water masses in the stratification of these contaminants, although those results must be interpreted cautiously due to the low concentrations of the compounds. The present results showed that the detection of PFAAs in

intermediate layers reinforce the oceanic transport as an important pathway to distribute these contaminants, and its importance as ocean tracers.

Acknowledgments

This work was supported by Fundação de Amparo à Pesquisa do Estado da Bahia, Brazil (FAPESB) (PET0034/2012), Conselho Nacional de Desenvolvimento Científico (CNPq) (441829/2014-7), and the Rufford Foundation (nº 2992-1). The authors were supported by FAPESB (D. Miranda, nº BOL0122/2017), Coordenação de Aperfeiçoamento de Pessoal de Nível Superior, Brazil (Ph.D. Sandwich, D. Miranda, nº 88881.188589/2018-01), and CNPq (V. Hatje - 304823/2018-0). J. Leonel were sponsored by CNPq (401443/2016-7 and 310786/2018-5).

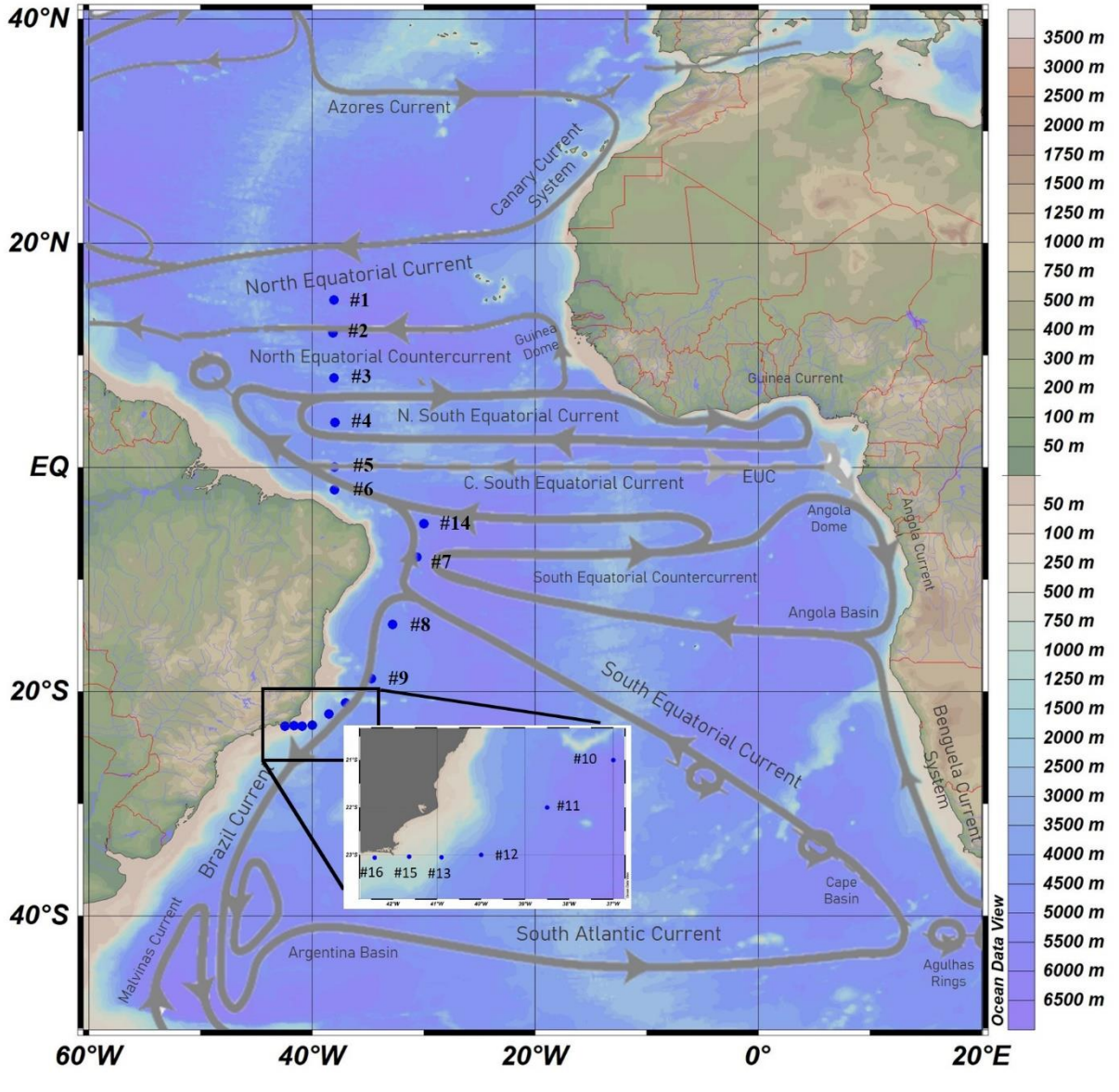

Figure 1: Location of sampling sites (#1 - #16) along the Western Tropical Atlantic Ocean. Deep water profiles were collected at #1, #5, #7, #9, #15, and #16. Grey arrows represent the main surface currents in the region (adapted from Talley (2013)).

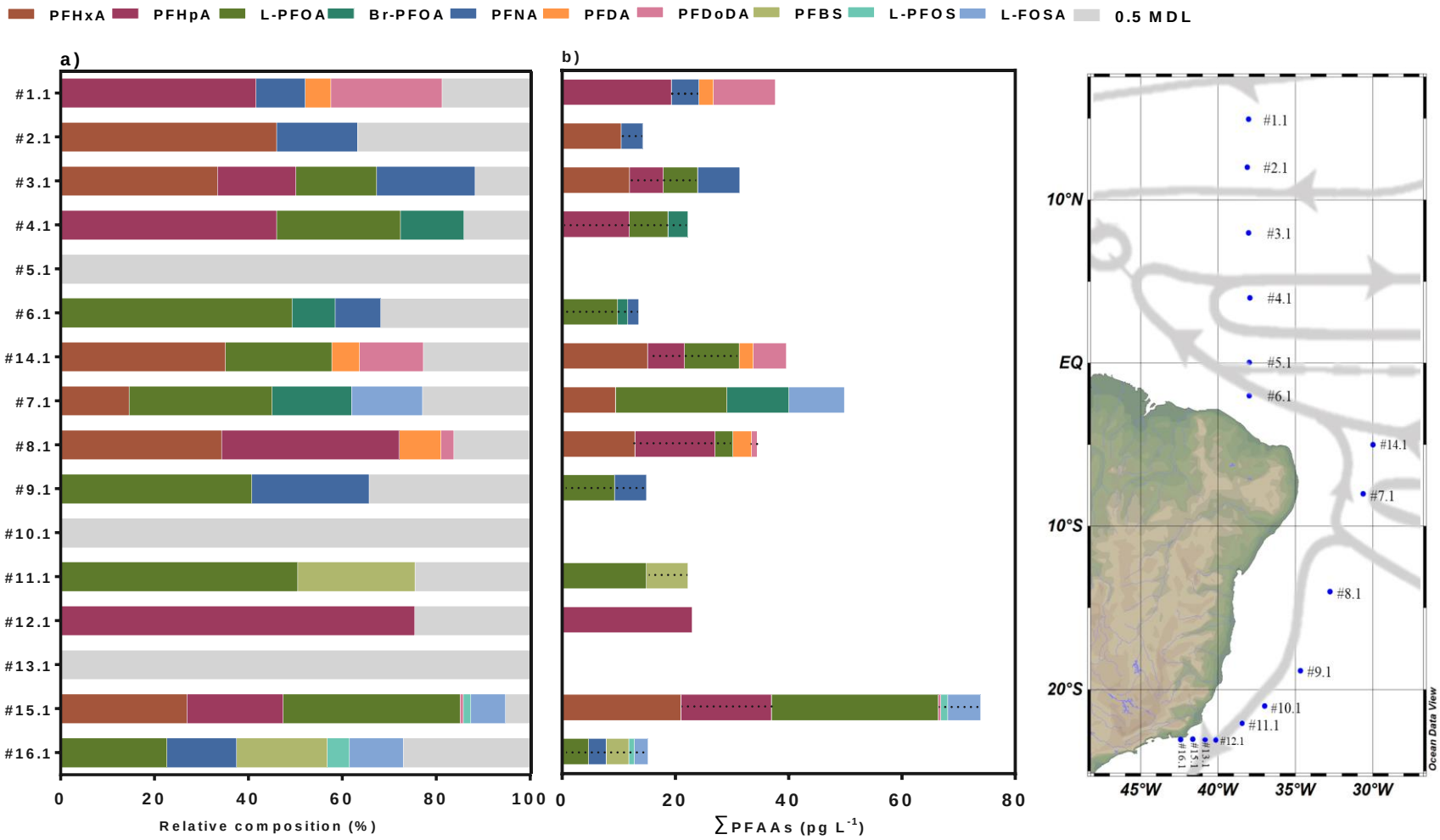

Figure 2: Relative composition (a) and the sum (∑) of PFAAs in surface waters (b) of the Western Tropical Atlantic Ocean (c). Samples #5.1, #10.1, and #13.1 presented concentrations below detection limits for all compounds, hence are not included in panels (a) and (b). Concentrations below Method Detection Limit (MDL) were not computed in the PFAA sum. PFHxA and PFOA (L- and Br-) were not reported for #1.1 due to analytical issues. Grey bars in (a) represent sum of half values of the MDL. Values above MDL and below method quantification limit are showed with a dashed line in (b). Grey arrows in (c) show the surface current directions.

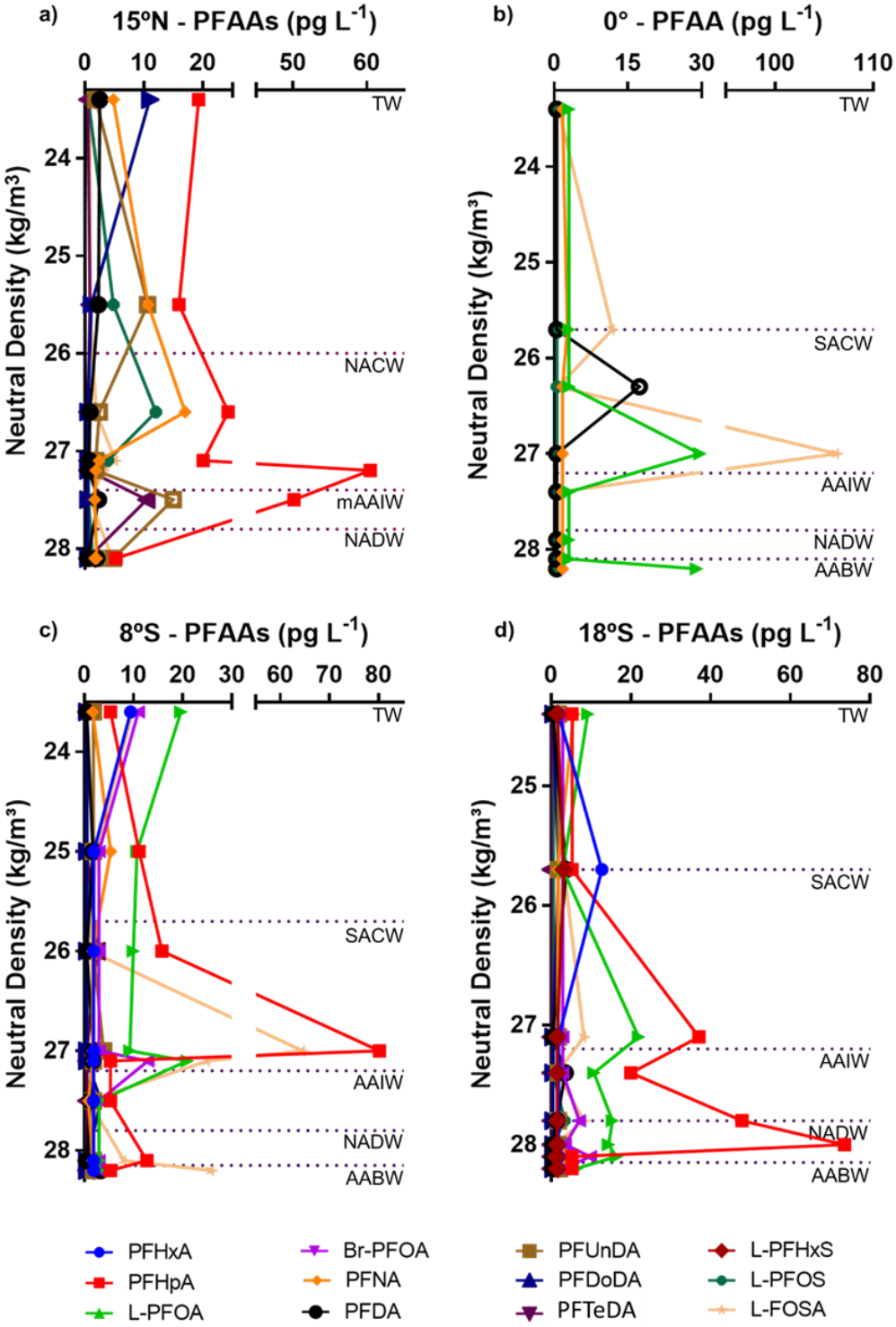

Figure 3: Vertical profiles of PFAAs (pg L^{-1}) in ocean water columns above method detection limits (MDL) from Tropical Atlantic Ocean ((a)15°N [#1]; (b) 0° [#5]; (c) 8°S [#7]; and (d) 18°S [#9]) together with Neutral Density (kg/m³). PFHxA and PFOA (L- and Br-) were not reported for 15°N due to analytical issues. Dotted lines represent the water masses (TW: Tropical Water; NACW: North Atlantic Central Water; SACW: South Atlantic Central Water; AAIW: Antarctic Intermediate Water; mAAIW: modified AAIW; NADW: North Atlantic Deep Water; AABW: Antarctic Bottom Water).

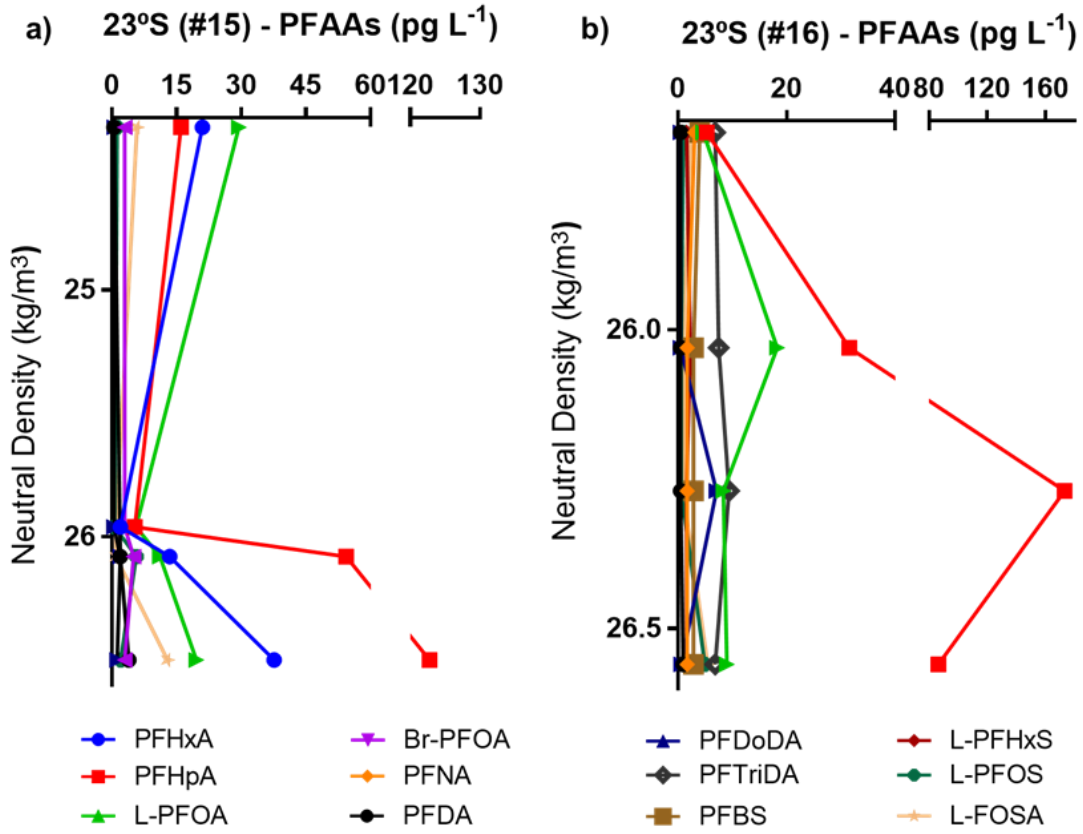

481
482 **Figure 4:** Vertical profiles of PFAAs (pg L^{-1}) in ocean water columns from Rio de Janeiro
483 upwelling at 23°S ((a) #15 and (b) #16) together with Neutral Density (kg/m³).
484

References

3M, C., 2003. The Science of Organic Fluorochemistry. Washington, D.C.

Ahrens, L., Barber, J.L., Xie, Z., Ebinghaus, R., 2009. Longitudinal and Latitudinal Distribution of Perfluoroalkyl Compounds in the Surface Water of the Atlantic Ocean. Environ. Sci. Technol. 43, 3122–3127. https://doi.org/10.1021/es803507p

Ahrens, L., Xie, Z., Ebinghaus, R., 2010. Distribution of perfluoroalkyl compounds in seawater from Northern Europe, Atlantic Ocean, and Southern Ocean. Chemosphere 78, 1011–1016. https://doi.org/https://doi.org/10.1016/j.chemosphere.2009.11.038

Albuquerque, A.L.S., Belém, A.L., Zuluaga, F.J.B., Cordeiro, L.G.M., Mendonza, U., Knoppers, B.A., GurgelL, M.H.C., MEYERS, P.A., CAPILLA, R., 2014. Particle Fluxes and Bulk Geochemical Characterization of the Cabo Frio Upwelling System in Southeastern Brazil: Sediment Trap Experiments between Spring 2010 and Summer 2012. An. Acad. Bras. Cienc.

Avendaño, S., Liu, J., 2015. Production of PFOS from aerobic soil biotransformation of two perfluoroalkyl sulfonamide derivatives. Chemosphere 119, 1084–1090. https://doi.org/10.1016/j.chemosphere.2014.09.059

Azar, E., Piñango, A., Wallner-Kersanach, M., Kerr, R., 2020. Source waters contribution to the tropical Atlantic central layer: New insights on the Indo-Atlantic exchanges. Deep Sea Res. Part I Oceanogr. Res. Pap. 103450. https://doi.org/https://doi.org/10.1016/j.dsr.2020.103450

Bashmachnikov, I., Nascimento, Â., Neves, F., Menezes, T., Koldunov, N. V., 2015. Distribution of intermediate water masses in the subtropical northeast Atlantic. Ocean Sci. 11, 803–827.

Bashmachnikov, I, Neves, F., Calheiros, T., Carton, X., 2015. Properties and pathways of Mediterranean water eddies in the Atlantic. Prog. Oceanogr. 137, 149–172. https://doi.org/https://doi.org/10.1016/j.pocean.2015.06.001

Benskin, J.P., Li, B., Ikonomou, M.G., Grace, J.R., Li, L.Y., 2012a. Per- and Poly fl uoroalkyl Substances in Land fi ll Leachate: Patterns, Time Trends, and Sources. Environ. Sci. Technol. 46, 11532–11540.

Benskin, J.P., Muir, D.C.G., Scott, B.F., Spencer, C., De Silva, A.O., Kylin, H., Martin, J.W., Morris, A., Lohmann, R., Tomy, G., Rosenberg, B., Taniyasu, S., Yamashita, N., 2012b. Perfluoroalkyl Acids in the Atlantic and Canadian Arctic Oceans. Environ. Sci. Technol. 46, 5815–5823. https://doi.org/10.1021/es300578x

Bowman, K.L., Lamborg, C.H., Agather, A.M., 2020. A global perspective on mercury cycling in the ocean. Sci. Total Environ. 710, 136166. https://doi.org/https://doi.org/10.1016/j.scitotenv.2019.136166

Bridgestock, L., Rehkämper, M., van de Flierdt, T., Paul, M., Milne, A., Lohan, M.C., Achterberg, E.P., 2018. The distribution of lead concentrations and isotope compositions in the eastern Tropical Atlantic Ocean. Geochim. Cosmochim. Acta 225, 36–51. https://doi.org/https://doi.org/10.1016/j.gca.2018.01.018

Brix, H., Gerdes, R., 2003. North Atlantic Deep Water and Antarctic Bottom Water: Their interaction and influence on the variability of the global ocean circulation. J. Geophys. Res. Ocean. 108. https://doi.org/10.1029/2002JC001335

Brumovský, M., Karásková, P., Borghini, M., Nizzetto, L., 2016. Per- and polyfluoroalkyl substances in the Western Mediterranean Sea waters. Chemosphere 159, 308–316. https://doi.org/https://doi.org/10.1016/j.chemosphere.2016.06.015

Buck, R.C., Franklin, J., Berger, U., Conder, J.M., Cousins, I.T., de Voogt, P., Jensen, A.A.,

Kannan, K., Mabury, S.A., van Leeuwen, S.P.J., 2011. Perfluoroalkyl and Polyfluoroalkyl Substances in the Environment: Terminology, Classification, and Origins. Integr. Environ. Assess. Manag. 7, 513–541. https://doi.org/10.1002/ieam.258

Cai, M., Yang, H., Xie, Z., Zhao, Z., Wang, F., Lu, Z., Sturm, R., Ebinghaus, R., 2012. Per- and polyfluoroalkyl substances in snow, lake, surface runoff water and coastal seawater in Fildes Peninsula, King George Island, Antarctica. J. Hazard. Mater. 209–210, 335–342. https://doi.org/https://doi.org/10.1016/j.jhazmat.2012.01.030

Camara, I., Kolodziejczyk, N., Mignot, J., Lazar, A., Gaye, A.T., 2015. On the seasonal variations of salinity of the tropical Atlantic mixed layer. J. Geophys. Res. Ocean. 120, 4441–4462. https://doi.org/10.1002/2015JC010865

Doney, S.C., Jenkins, W.J., Bullister, J.L., 1997. A comparison of ocean tracer dating techniques on a meridional section in the eastern North Atlantic. Deep Sea Res. Part I Oceanogr. Res. Pap. 44, 603–626. https://doi.org/https://doi.org/10.1016/S0967-0637(96)00105-7

Dreyer, A., Kirchgeorg, T., Weinberg, I., Matthias, V., 2015. Particle-size distribution of airborne poly- and perfluorinated alkyl substances. Chemosphere 129, 142–149. https://doi.org/10.1016/j.chemosphere.2014.06.069

Dreyer, A., Weinberg, I., Temme, C., Ebinghaus, R., 2009. Polyfluorinated Compounds in the Atmosphere of the Atlantic and Southern Oceans: Evidence for a Global Distribution. Environ. Sci. Technol. 43, 6507–6514. https://doi.org/10.1021/es9010465

Emílsson, I., 1961. The shelf and coastal waters off southern Brazil . Bol. do Inst. Ocean. .

Ferreira, M.L. de C., Kerr, R., 2017. Source water distribution and quantification of North Atlantic Deep Water and Antarctic Bottom Water in the Atlantic Ocean. Prog. Oceanogr. 153, 66–83. https://doi.org/https://doi.org/10.1016/j.pocean.2017.04.003

Gawor, A., Shunthirasingham, C., Hayward, S.J., Lei, Y.D., Gouin, T., Mmereki, B.T., Masamba, W., Ruepert, C., Castillo, L.E., Shoeib, M., Lee, S.C., Harner, T., Wania, F., 2014. Neutral polyfluoroalkyl substances in the global Atmosphere. Environ. Sci. Process. Impacts 16, 404–413. https://doi.org/10.1039/C3EM00499F

Gilljam, J.L., Leonel, J., Cousins, I.T., Benskin, J.P., 2016. Is Ongoing Sulfluramid Use in South America a Significant Source of Perfluorooctanesulfonate (PFOS)? Production Inventories, Environmental Fate, and Local Occurrence. Environ. Sci. Technol. 50, 653–659. https://doi.org/10.1021/acs.est5b04544

Glüge, J., Scheringer, M., Cousins, I.T., DeWitt, J.C., Goldenman, G., Herzke, D., Lohmann, R., Ng, C.A., Trier, X., Wang, Z., 2020. An overview of the uses of per- and polyfluoroalkyl substances (PFAS). Environ. Sci. Process. Impacts. https://doi.org/10.1039/D0EM00291G

González-Gaya, B., Casal, P., Jurado, E., Dachs, J., Jiménez, B., 2019. Vertical transport and sinks of perfluoroalkyl substances in the global open ocean. Environ. Sci. Process. Impacts 21, 1957–1969. https://doi.org/10.1039/C9EM00266A

González-Gaya, B., Dachs, J., Roscales, J.L., Caballero, G., Jiménez, B., 2014. Perfluoroalkylated Substances in the Global Tropical and Subtropical Surface Oceans. Environ. Sci. Technol. 48, 13076–13084. https://doi.org/10.1021/es503490z

Hatje, V., Lamborg, C.H., Boyle, E.A., 2018. Trace-Metal Contaminants: Human Footprint on the Ocean. Elements 14, 403–408. https://doi.org/10.2138/gselements.14.6.403

Houde, M., De Silva, A.O., Muir, D.C.G., Letcher, R.J., 2011. Monitoring of Perfluorinated Compounds in Aquatic Biota: An Updated Review PFCs in Aquatic Biota. Environ. Sci. Technol. 45, 7962–7973. https://doi.org/10.1021/es104326w

574 Houde, M., Martin, J.W., Letcher, R.J., Solomon, K.R., Muir, D.C.G., 2006. Biological
575 monitoring of polyfluoroalkyl substances: A review. Environ. Sci. Technol. 40, 3463–3473.
576 https://doi.org/10.1021/es052580b

577 Jahnke, A., Berger, U., Ebinghaus, R., Temme, C., 2007. Latitudinal Gradient of Airborne
578 Polyfluorinated Alkyl Substances in the Marine Atmosphere between Germany and South
579 Africa (53° N−33° S). Environ. Sci. Technol. 41, 3055–3061.
580 https://doi.org/10.1021/es062389h

581 Joerss, H., Apel, C., Ebinghaus, R., 2019. Emerging per- and polyfluoroalkyl substances (PFASs)
582 in surface water and sediment of the North and Baltic Seas. Sci. Total Environ. 686, 360–
583 369. https://doi.org/https://doi.org/10.1016/j.scitotenv.2019.05.363

584 Joerss, H., Xie, Z., Wagner, C.C., von Appen, W.-J., Sunderland, E.M., Ebinghaus, R., 2020.
585 Transport of Legacy Perfluoroalkyl Substances and the Replacement Compound HFPO-DA
586 through the Atlantic Gateway to the Arctic Ocean—Is the Arctic a Sink or a Source? Environ.
587 Sci. Technol. 54, 9958–9967. https://doi.org/10.1021/acs.est.0c00228

588 Johansson, J.H., Salter, M.E., Acosta Navarro, J.C., Leck, C., Nilsson, E.D., Cousins, I.T., 2019.
589 Global transport of perfluoroalkyl acids via sea spray aerosol. Environ. Sci. Process. Impacts
590 21, 635–649. https://doi.org/10.1039/C8EM00525G

591 Kieke, D., Rhein, M., Stramma, L., Smethie, W.M., LeBel, D.A., Zenk, W., 2006. Changes in the
592 CFC Inventories and Formation Rates of Upper Labrador Sea Water, 1997–2001. J. Phys.
593 Oceanogr. 36, 64–86. https://doi.org/10.1175/JPO2814.1

594 Kwok, K.Y., Wang, X.-H., Ya, M., Li, Y., Zhang, X.-H., Yamashita, N., Lam, J.C.W., Lam,
595 P.K.S., 2015. Occurrence and distribution of conventional and new classes of per- and
596 polyfluoroalkyl substances (PFASs) in the South China Sea. J. Hazard. Mater. 285, 389–397.
597 https://doi.org/10.1016/j.jhazmat.2014.10.065

598 Lau, C., Anitole, K., Hodes, C., Lai, D., Pfahles-Hutchens, A., Seed, J., 2007. Perfluoroalkyl
599 Acids: A Review of Monitoring and Toxicological Findings. Toxicol. Sci. 99, 366–394.

600 Laxenaire, R., Speich, S., Stegner, A., 2020. Agulhas Ring Heat Content and Transport in the
601 South Atlantic Estimated by Combining Satellite Altimetry and Argo Profiling Floats Data.
602 J. Geophys. Res. Ocean. 125, e2019JC015511. https://doi.org/10.1029/2019JC015511

603 Lessa, D. V, Ramos, R.P., Barbosa, C.F., Silva, A.R., Belem, A., Turcq, B., Albuquerque, A.L.,
604 2014. Planktonic foraminifera in the sediment of a western boundary upwelling system off
605 Cabo Frio, Brazil. Mar. Micropaleontol. 106, 55–68.
606 https://doi.org/https://doi.org/10.1016/j.marmicro.2013.12.003

607 Liu, M., Tanhua, T., 2019. Characteristics of Water Masses in the Atlantic Ocean based on
608 GLODAPv2 data. Ocean Sci. Discuss. 2019, 1–43. https://doi.org/10.5194/os-2018-139

609 Lohmann, R., Jurado, E., Dijkstra, H.A., Dachs, J., 2013. Vertical eddy diffusion as a key
610 mechanism for removing perfluorooctanoic acid (PFOA) from the global surface oceans.
611 Environ. Pollut. 179, 88–94. https://doi.org/https://doi.org/10.1016/j.envpol.2013.04.006

612 Loi, E., Zhao, S., Wang, B., Zhu, L., Liang, T., Chen, M., Yang, L., Lv, J., Liu, L., 2011. Trophic
613 magnification of poly- and perfluorinated compounds in a subtropical food web. Environ.
614 Sci. Technol. 45, 598–678. https://doi.org/10.1080/10643389.2011.627016

615 McLachlan, M.S., Holmström, K.E., Reth, M., Berger, U., 2007. Riverine Discharge of
616 Perfluorinated Carboxylates from the European Continent. Environ. Sci. Technol. 41, 7260–
617 7265. https://doi.org/10.1021/es071471p

618 Miranda, D.A., Benskin, J.P., Awad, R., Lepoint, G., Leonel, J., Hatje, V., 2021. Bioaccumulation

of Per- and polyfluoroalkyl substances (PFASs) in a tropical estuarine food web. Sci. Total Environ. 754, 142146. https://doi.org/https://doi.org/10.1016/j.scitotenv.2020.142146

Miranda, L.B. de, 1985. Forma da correlação T-S de massas de água das regiões costeira e oceânica entre o Cabo de São Tomé (RJ) e a Ilha de São Sebastião (SP), Brasil . Bol. do Inst. Ocean. .

Muir, D., Bossi, R., Carlsson, P., Evans, M., De Silva, A., Halsall, C., Rauert, C., Herzke, D., Hung, H., Letcher, R., Rigét, F., Roos, A., 2019. Levels and trends of poly- and perfluoroalkyl substances in the Arctic environment – An update. Emerg. Contam. 5, 240–271. https://doi.org/https://doi.org/10.1016/j.emcon.2019.06.002

Munoz, G., Fechner, L.C., Geneste, E., Pardon, P., Budzinski, H., Labadie, P., 2018. Spatio-temporal dynamics of per and polyfluoroalkyl substances (PFASs) and transfer to periphytic biofilm in an urban river: case-study on the River Seine. Environ. Sci. Pollut. Res. 25, 23574–23582. https://doi.org/10.1007/s11356-016-8051-9

Munoz, G., Labadie, P., Botta, F., Lestremau, F., Lopez, B., Geneste, E., Pardon, P., Dévier, M.-H., Budzinski, H., 2017. Occurrence survey and spatial distribution of perfluoroalkyl and polyfluoroalkyl surfactants in groundwater, surface water, and sediments from tropical environments. Sci. Total Environ. 607–608, 243–252. https://doi.org/https://doi.org/10.1016/j.scitotenv.2017.06.146

Nascimento, R.A., Nunoo, D.B.O., Bizkarguenaga, E., Schultes, L., Zabaleta, I., Benskin, J.P., Spanó, S., Leonel, J., 2018. Sulfluramid use in Brazilian agriculture: A source of per- and polyfluoroalkyl substances (PFASs) to the environment. Environ. Pollut. 242, 1436–1443. https://doi.org/10.1016/J.ENVPOL.2018.07.122

Peña-Izquierdo, J., van Sebille, E., Pelegrí, J.L., Sprintall, J., Mason, E., Llanillo, P.J., Machín, F., 2015. Water mass pathways to the North Atlantic oxygen minimum zone. J. Geophys. Res. Ocean. 120, 3350–3372. https://doi.org/10.1002/2014JC010557

Prevedouros, K., Cousins, I.T., Buck, R.C., Korzeniowski, S.H., 2006. Sources, Fate and Transport of Perfluorocarboxylates. Environ. Sci. Technol. 40, 32–44. https://doi.org/10.1021/es0512475

Quinete, N., Wu, Q., Zhang, T., Yun, S.H., Moreira, I., Kannan, K., 2009. Specific profiles of perfluorinated compounds in surface and drinking waters and accumulation in mussels, fish, and dolphins from southeastern Brazil. Chemosphere 77, 863–869. https://doi.org/https://doi.org/10.1016/j.chemosphere.2009.07.079

Rhein, M., Kieke, D., Steinfeldt, R., 2015. Advection of North Atlantic Deep Water from the Labrador Sea to the southern hemisphere. J. Geophys. Res. Ocean. 120, 2471–2487. https://doi.org/10.1002/2014JC010605

Shan, G., Qian, X., Chen, X., Feng, X., Cai, M., Yang, L., Chen, M., Zhu, L., Zhang, S., 2021. Legacy and emerging per- and poly-fluoroalkyl substances in surface seawater from northwestern Pacific to Southern Ocean: Evidences of current and historical release. J. Hazard. Mater. 411, 125049. https://doi.org/https://doi.org/10.1016/j.jhazmat.2021.125049

Silveira, I.C.A. da, Schmidt, A.C.K., Campos, E.J.D., Godoi, S.S. de, Ikeda, Y., 2000. A corrente do Brasil ao largo da costa leste brasileira . Rev. Bras. Oceanogr. .

Simcik, M.F., Dorweiler, K.J., 2006. Ratio of Perfluorochemical Concentrations as a Tracer of Atmospheric Deposition to Surface Waters. Environ. Sci. Technol. 40, 410. https://doi.org/10.1021/es052244v

Simonnet-Laprade, C., Budzinski, H., Maciejewski, K., Le Menach, K., Santos, R., Alliot, F.,

Goutte, A., Labadie, P., 2019. Biomagnification of perfluoroalkyl acids (PFAAs) in the food web of an urban river: assessment of the trophic transfer of targeted and unknown precursors and implications. Environ. Sci. Process. Impacts. https://doi.org/10.1039/C9EM00322C

Sørensen, J.V.T., Ribbe, J., Shaffer, G., 2001. Antarctic Intermediate Water Mass Formation in Ocean General Circulation Models. J. Phys. Oceanogr. 31, 3295–3311. https://doi.org/10.1175/1520-0485(2001)031<3295:AIWMFI>2.0.CO;2

Stendardo, I., Rhein, M., Steinfeldt, R., 2020. The North Atlantic Current and its Volume and Freshwater Transports in the Subpolar North Atlantic, Time Period 1993–2016. J. Geophys. Res. Ocean. 125, e2020JC016065. https://doi.org/10.1029/2020JC016065

Stramma, L., England, M., 1999. On the water masses and mean circulation of the South Atlantic Ocean. J. Geophys. Res. 104, 863–883.

Sverdup, H, U., Fleming, M.W., H., J., Richard, 1944. The Oceans: Their Physics, Chemistry, and General Biology. Q. J. R. Meteorol. Soc. 70, 159–160. https://doi.org/10.1002/qj.49707030418

Talley, L.D., 2013. Closure of the global overturning circulation through the Indian, Pacific, and Southern Oceans: Schematics and transports. Oceanography 26, 80–97.

Talley, L.D., Raymer, M.E., 1982. Eighteen degree water variability. J. Mar. Res. 40, 757–775.

Tsuchiya, M., Talkey, L.D., McCartney, M.S., 1994. Water-mass distributions in the western South Atlantic; a section from South Georgia Island (54S) northward across the equator. J. Mar. Res. 52, 55–81.

Valentin, J.L., 2001. The Cabo Frio Upwelling System, Brazil BT - Coastal Marine Ecosystems of Latin America, in: Seeliger, U., Kjerfve, B. (Eds.), . Springer Berlin Heidelberg, Berlin, Heidelberg, pp. 97–105. https://doi.org/10.1007/978-3-662-04482-7_8

Wang, Y., Wang, L., Chang, W., Zhang, Yinfeng, Zhang, Yuan, Liu, W., 2019. Neurotoxic effects of perfluoroalkyl acids: Neurobehavioral deficit and its molecular mechanism. Toxicol. Lett. 305, 65–72. https://doi.org/https://doi.org/10.1016/j.toxlet.2019.01.012

Wang, Z., Boucher, J.M., Scheringer, M., Cousins, I.T., Hungerbühler, K., 2017. Toward a Comprehensive Global Emission Inventory of C4-C10Perfluoroalkanesulfonic Acids (PFSAs) and Related Precursors: Focus on the Life Cycle of C8-Based Products and Ongoing Industrial Transition. Environ. Sci. Technol. 51, 4482–4493. https://doi.org/10.1021/acs.est.6b06191

Wang, Z., Cousins, I.T., Scheringer, M., Buck, R.C., Hungerbühler, K., 2014. Global emission inventories for C4–C14 perfluoroalkyl carboxylic acid (PFCA) homologues from 1951 to 2030, part II: The remaining pieces of the puzzle. Environ. Int. 69, 166–176. https://doi.org/10.1016/j.envint.2014.04.006

Wei, S., Chen, L.Q., Taniyasu, S., So, M.K., Murphy, M.B., Yamashita, N., Yeung, L.W.Y., Lam, P.K.S., 2007. Distribution of perfluorinated compounds in surface seawaters between Asia and Antarctica. Mar. Pollut. Bull. 54, 1813–1818. https://doi.org/https://doi.org/10.1016/j.marpolbul.2007.08.002

Xie, Z., Wang, Z., Magand, O., Thollot, A., Ebinghaus, R., Mi, W., Dommergue, A., 2020. Occurrence of legacy and emerging organic contaminants in snow at Dome C in the Antarctic. Sci. Total Environ. 741, 140200. https://doi.org/https://doi.org/10.1016/j.scitotenv.2020.140200

Yamashita, N., Kannan, K., Taniyasu, S., Horii, Y., Petrick, G., Gamo, T., 2005. A global survey of perfluorinated acids in oceans. Mar. Pollut. Bull. 51, 658–668.

https://doi.org/https://doi.org/10.1016/j.marpolbul.2005.04.026

Yamashita, N., Taniyasu, S., Petrick, G., Wei, S., Gamo, T., Lam, P.K.S., Kannan, K., 2008. Perfluorinated acids as novel chemical tracers of global circulation of ocean waters. Chemosphere 70, 1247–1255. https://doi.org/https://doi.org/10.1016/j.chemosphere.2007.07.079

Yeung, L.W.Y., Dassuncao, C., Mabury, S., Sunderland, E.M., Zhang, X., Lohmann, R., 2017. Vertical Profiles, Sources, and Transport of PFASs in the Arctic Ocean. Environ. Sci. Technol. 51, 6735–6744. https://doi.org/10.1021/acs.est.7b00788

Zhang, X., Lohmann, R., Sunderland, E.M., 2019. Poly- and Perfluoroalkyl Substances in Seawater and Plankton from the Northwestern Atlantic Margin. Environ. Sci. Technol. 53, 12348–12356. https://doi.org/10.1021/acs.est.9b03230

Zhang, X., Zhang, Y., Dassuncao, C., Lohmann, R., Sunderland, E.M., 2017. North Atlantic Deep Water formation inhibits high Arctic contamination by continental perfluorooctane sulfonate discharges. Global Biogeochem. Cycles 31, 1332–1343. https://doi.org/10.1002/2017GB005624

Zhao, Z., Xie, Z., Möller, A., Sturm, R., Tang, J., Zhang, G., Ebinghaus, R., 2012. Distribution and long-range transport of polyfluoroalkyl substances in the Arctic, Atlantic Ocean and Antarctic coast. Environ. Pollut. 170, 71–77. https://doi.org/https://doi.org/10.1016/j.envpol.2012.06.004

Supplementary Information

Perfluoroalkyl Acids (PFAAs) in the Western Tropical Atlantic Ocean

Daniele de A. Miranda[a,b]*, Juliana Leonel[c], Jonathan P. Benskin[b] , Jana Johansson[b] , Vanessa Hatje[a]

[a]Centro Interdisciplinar de Energia e Ambiente (CIEnAm) and Inst. de Química, Universidade Federal da Bahia, 41170-115, Salvador, BA, Brazil;

[b]Department of Environmental Science, Stockholm University, Stockholm, Sweden.

[c]Coordenação de Oceanografia, Universidade Federal de Santa Catarina, Florianópolis, SC, Brazil.

*Corresponding author

Daniele Miranda (danielealmeida@ufba.br / Daniele.Miranda@aces.su.se)

Universidade Federal da Bahia

CIEnAm, Campus Ondina

Salvador, Bahia, Brazil. 41170-115

Standard and reagent brands

Methanol MeOH (HPLC grade) was purchased from J.T. Baker (Atlantic Labo, France) and Merck (Darmstadt, Germany). Acetonitrile was purchased from Honeywell (Steinheim, Germany). Formic acid was purchased from Merck (Darmstadt, Germany). Ammonium hydroxide salts was purchased from Mallinckrodt chemicals (Dublin, Ireland). All standards were purchased from Wellington Laboratories (Guelph, ON, Canada). Waters Oasis® Weak-anion exchange SPE cartridges (6 cm^3, 150 mg, 30 μm) (Massachusetts, USA). SPE C18 cartridges were purchased from Phenomenex (California, USA). Lastly, water was purified with a Millipore water purification system (MilliQ, Massachusetts, USA) and had a resistance of 18.2 MΩ cm^{-1} for both Brazilian and Swedish laboratories.

PFAAs-extraction method optimization

Prior to real samples analysis, PFAAs were investigated in all WAX SPE cartridge batches, ultrapure water, reagents, and glassware in order to track contamination. There was only observed a systematic PFOA background in ultrapure water (~20 pg L^{-1}), which was associated with the Swedish tap water, as was seen before (Nascimento et al., 2018), besides other compounds in lower concentrations. To minimize the PFOA input in real samples, all ultrapure water was extracted following the same steps as this for real samples. However, PFHxA, PFOA, and PFBS were still been detected in the procedure blank tests at concentrations of 16;17±4; 18 pg L^{-1} (n = 3) after extraction, respectively. Then, the last step to eliminate possible contamination sources was the replacement of an in-use formic acid to a new lot of this reagent (sealed) resulting in laboratory blanks with PFAAs concentrations lower than 1 pg L^{-1} (Table S7).

Table S1: Water masses characteristics. Where = TW: Tropical Water; NACW: North Atlantic Central Water; SACW: South Atlantic Central Water; AAIW: Antarctic Intermediate Water; mAAIW: Mediterranean AAIW; NADW: North Atlantic Deep Water; AABW: Abyssal Antarctic Bottom Water.

Water masses	Depth (m)	Temperature (°C)	Salinity	Neutral Density (Kg/m³)
TW	0 – 116[a]	> 20[c]	> 36[c]	< 25.7[d]
NACW	100 – 700[a]	6-18[b]	34.5 – 36[b]	26 – 27.2[b]
SACW	116 – 657[a]	6 – 20[d]	34.3 – 36[a]	25.7 – 27.2 [a]
AAIW	657 – 1234[i]	3 - -6[e]	34.2 - 34.6[e]	27.4 - 27.8[a]
mAAIW	657 – 1234[g]	5.6 -6.5[g]	34.7 – 34.9[g]	27.4 – 27.8[g]
NADW	1234 – 3472[h]	3 - -4[f]	34.6 – 35[f]	27.8 – 28.2[h]
AABW	> 3472[i]	-1.9[h]	34.6[h]	< 28.2[h]

Based on: [a]Stramma and England (1999); [b]Liu & Tanhua (2019); [c]Emilsson (1961); [d]Miranda et al. (1985); [e]Sverdrup et al. (1944); [f]Silveira (2000); [g]Bashmachnikov et al. (2015); [h]Ferreira & Kerr (2017); [i]Talley (2013).

Table S2: Sample location, depth, temperature, salinity, oxygen and date of sampling. Temp.: Temperature; Sal.: Salinity; Oxyg.: Oxygen; TW: Tropical Water; SACW: South Atlantic Central Water; AAIW: Antarctic Intermediate Water; mAAIW: modified AAIW; NADW: North Atlantic Deep Water; AABW: Antarctic Bottom Water.

Sample	Cruise Station	Latitude	Longitude	Depth (m)	Station Maximun Depth (m)	Pont. Temp. (°C)	Salinity	Oxyg (µmol/kg)	Neutral Density (kg/m^3)	Water masses	Date
1.1	PIRA_004	14°56'26.40"N	38° 2'44.40"W	8	5897	26.9	36.2	192	23.4	TW	2017-Nov
1.2		14°56'26.40"N	38° 2'44.40"W	82		22.4	36.8	189	25.5	TW	2017-Nov
1.3		14°56'26.40"N	38° 2'44.40"W	132		16.9	36.3	123	26.6	NACW	2017-Nov
1.4		14°56'26.40"N	38° 2'44.40"W	420		9.9	35.1	85	27.1	NACW	2017-Nov
1.5		14°56'26.40"N	38° 2'44.40"W	525		9.02	35.0	82	27.2	NACW	2017-Nov
1.6		14°56'26.40"N	38° 2'44.40"W	900		6.17	34.8	113	27.5	mAAIW	2017-Nov
1.7		14°56'26.40"N	38° 2'44.40"W	4501		1.93	34.9	233	28.1	NADW	2017-Nov
1.8		14°56'26.40"N	38° 2'44.40"W	5845		1.75	34.9	237	28.1	NADW	2017-Nov
2.1	PIRA_007	11°59'53.40"N	38° 6'49.80"W	5	4754	28.0	34.7	192	22.2	Surface	2017-Nov
3.1	PIRA_011	7°59'13.80"N	38° 1'44.40"W	7	4221	27.9	35.9	191	23.1	Surface	2017-Nov
4.1	PIRA_015	3°59'44.88"N	37°57'42.54"W	14	4236	28.1	36.0	190	23.1	Surface	2017-Nov
5.1	PIRA_019	0° 2'41.76"N	38° 0'5.64"W	7	4448	27.2	36.2	191	23.4	TW	2017-Nov
5.2		0° 2'41.76"N	38° 0'5.64"W	135		20.7	36.5	179	25.7	SACW	2017-Nov
5.3		0° 2'41.76"N	38° 0'5.64"W	148		16.2	35.7	160	26.3	SACW	2017-Nov
5.4		0° 2'41.76"N	38° 0'5.64"W	376		9.39	34.8	138	27.0	SACW	2017-Nov
5.5		0° 2'41.76"N	38° 0'5.64"W	721		5.31	34.5	140	27.4	AAIW	2017-Nov
5.6		0° 2'41.76"N	38° 0'5.64"W	1780		3.78	35.0	234	27.9	NADW	2017-Nov
5.7		0° 2'41.76"N	38° 0'5.64"W	2901		2.55	34.9	245	28.1	NADW	2017-Nov
5.8		0° 2'41.76"N	38° 0'5.64"W	3844		1.96	34.9	249	28.1	NADW	2017-Nov
5.9		0° 2'41.76"N	38° 0'5.64"W	4431		0.75	34.7	217	28.2	AABW	2017-Nov
6.1	PIRA_021	1°59'17.28"S	38° 0'15.00"W	7	3166	27.2	36.3	192	23.7	Surface	2017-Nov
14.1	PIRA_032	4°59'56.46"S	30° 0'1.86"W	6	5011	27.3	36.4	191	23.7	TW	2017-Dec
7.1	PIRA_035	8° 0'38.16"S	30°37'36.72"W	6	5402	27.3	36.5	190	23.6	TW	2017-Dec
7.2		8° 0'38.16"S	30°37'36.72"W	113		23.8	36.7	184	25.0	TW	2017-Dec
7.3		8° 0'38.16"S	30°37'36.72"W	152		18.5	36.1	133	26.0	SACW	2017-Dec
7.4		8° 0'38.16"S	30°37'36.72"W	375		9.11	34.8	103	27.0	SACW	2017-Dec
7.5		8° 0'38.16"S	30°37'36.72"W	473		7.98	34.7	83	27.1	SACW	2017-Dec
7.6		8° 0'38.16"S	30°37'36.72"W	833		4.54	34.5	150	27.5	AAIW	2017-Dec
7.7		8° 0'38.16"S	30°37'36.72"W	3579		2.11	34.9	242	28.1	NADW	2017-Dec
7.8		8° 0'38.16"S	30°37'36.72"W	5384		0.21	34.7	210	28.2	AABW	2017-Dec

Continuation of Table S2:

Sample	Cruise Station	Latitude	Longitude	Depth (m)	Station Maximun Depth (m)	Temperature (°C)	Salinity	Oxygen (µmol/kg)	Neutral Density (kg/m)	Water masses	Date
8.1	PIRA_053	13°59'18.60" S	32°46'13.80" W	7	4593	27.6	37.0	191	24.0	Surface	2017-Dec
9.1	PIRA_058	18°50'54.84" S	34°40'40.80" W	6	4208	26.8	37.2	196	24.4	TW	2018-Jan
9.2		18°50'54.84" S	34°40'40.80" W	150		22.3	37.0	204	25.7	SACW	2018-Jan
9.3		18°50'54.84" S	34°40'40.80" W	551		7.79	34.6	167	27.1	SACW	2018-Jan
9.4		18°50'54.84" S	34°40'40.80" W	755		4.55	34.4	186	27.4	AAIW	2018-Jan
9.5		18°50'54.84" S	34°40'40.80" W	1400		4.07	34.9	204	27.8	NADW	2018-Jan
9.6		18°50'54.84" S	34°40'40.80" W	2501		2.90	34.9	240	28.0	NADW	2018-Jan
9.7		18°50'54.84" S	34°40'40.80" W	3800		1.54	34.8	231	28.1	NADW	2018-Jan
9.8		18°50'54.84" S	34°40'40.80" W	4194		0.50	34.7	214	28.2	AABW	2018-Jan
10.1	PIRA_060	21° 0'5.34" S	36°59'50.88" W	6	3996	27.3	37.2	196	24.3	Surface	2018-Jan
11.1	PIRA_061	22° 0'2.76" S	38°30'1.68" W	6	3360	26.9	37.0	195	24.3	Surface	2018-Jan
12.1	PIRA_062	22°59'57.00" S	39°59'54.00" W	7	2706	26.9	37.2	195	24.4	Surface	2018-Jan
13.1	PIRA_063	23° 3'1.80" S	40°53'58.80" W	5	2691	25.5	36.9	199	24.6	Surface	2018-Jan
15.1	PIRA_064	23° 2'11.40" S	41°38'4.20" W	7	83	23.8	36.0	211	24.4	TW	2018-Jan
15.2		23° 2'11.40" S	41°38'4.20" W	49		19.6	36.4	191	25.9	SACW	2018-Jan
15.3		23° 2'11.40" S	41°38'4.20" W	65		18.0	36.0	177	26.0	SACW	2018-Jan
15.4		23° 2'11.40" S	41°38'4.20" W	75		14.7	35.5	170	26.5	SACW	2018-Jan
16.1	PIRA_065	23° 3'23.40" S	42°25'9.60" W	7	75	20.0	36.1	209	25.7	SACW	2018-Jan
16.2		23° 3'23.40" S	42°25'9.60" W	21		18.1	36.0	225	26.0	SACW	2018-Jan
16.3		23° 3'23.40" S	42°25'9.60" W	32		16.5	35.8	183	26.3	SACW	2018-Jan
16.4		23° 3'23.40" S	42°25'9.60" W	68		13.7	35.3	191	26.6	SACW	2018-Jan

68 **Table S3:** Perfluoroalkyl substances (PFAS) analyzed in the present study.

Acronym	Name	Formula	CAS#
	Perfluoroalkyl carboxylic acids (PFCAs)		
PFHxA	Perfluorohexanoic acid	$C_5F_{11}COOH$	307-24-4
PFHpA	Perfluoroheptanoic acid	$C_6F_{13}COOH$	375-85-9
PFOA*	Perfluorooctanoic acid	$C_7F_{15}COOH$	335-67-1
PFNA	Perfluorononanoic acid	$C_8F_{17}COOH$	375-95-1
PFDA	Perfluorodecanoic acid	$C_9F_{19}COOH$	335-76-2
PFUnDA	Perfluoroundecanoic acid	$C_{10}F_{21}COOH$	2058-94-8
PFDoDA	Perfluorododecanoic acid	$C_{11}F_{23}COOH$	307-55-1
PFTriDA	Perfluorotridecanoic acid	$C_{12}F_{25}COOH$	72629-94-8
PFTeDA	Perfluorotetradecanoic acid	$C_{13}F_{27}COOH$	376-06-7
	Perfluoroalkyl sulfonic acids (PFSAs)		
PFBS	Perfluorobutanesulfonic acid	$C_4F_9SO_3H$	375-73-5
PFHxS*	Perfluorohexanesulfonic acid	$C_6F_{13}SO_3H$	355-46-4
PFOS*	Perfluorooctanesulfonic acid	$C_8F_{17}SO_3H$	1763-23-1
PFDS*	Perfluorodecanesulfonic acid	$C_{10}F_{21}SO_3H$	355-77-3
	Perfluoroalkyl sulfonamide derivatives (FASAs)		
FOSA*	Perfluorooctanesulfonamide	$C_8F_{17}SO_2NH_2$	754-91-6

69 *Compounds analysed for both linear (L-) and branched (Br-) isomers.

70

Table S4: Mobile phase gradient profile used in LC-MS/MS.

	LC Gradient Program		**LC Flow Rate**
Time (min)	Mobile phase A (%)[1]	Mobile Phase B (%)[2]	(mL/min)
0.0	90	10	0.40
0.3	90	10	0.40
4.5	20	80	0.40
4.6	0	100	0.40
7.5	0	100	0.55
9.5	90	10	0.40

[1] Mobile phase A: 90 % water and 10 % acetonitrile containing 2 mM ammonium acetate.

[2] Mobile phase B: 99 % acetonitrile and 1% water containing 2 mM ammonium acetate.

77 **Table S5:** List of retention times, and monitored qualitative and quantitative ions for each compound
78 analyzed in the present study.

Target	Retention Time (min)	Quant. Ion (m/z)	Qual Ion (m/z)	Standard	Internal Standard	IS Ion	Data quality
L-PFHxA	2.49	313/269	313/119	L-PFHxA	^{13}C-PFHxA	315/270	Quantitative
L-PFHpA	2.86	363/319	363/169	L-PFHpA	^{13}C-PFHpA	367/322	Quantitative
L-PFOA	3.19	413/369	413/169	L-PFOA	^{13}C-PFOA	417/372	Quantitative
Br-PFOA	3.15	413/369	413/169	L-PFOA	^{13}C-PFOA	417/372	Semi-quantitative
L-PFNA	3.43	463/419	463/219	L-PFNA	^{13}C-PFNA	468/423	Quantitative
L-PFDA	3.22	513/469	513/269	L-PFDA	^{13}C-PFDA	515/470	Quantitative
L-PFUnDA	3.97	563/519	563/269	L-PFUnDA	^{13}C-PFUnDA	565/520	Quantitative
L-PFDoDA	4.23	613/569	613/169	L-PFDoDA	^{13}C-PFDoA	615/570	Quantitative
L-PFTrDA	4.51	663/619	663/169	L-PFTrDA	^{13}C-PFDoA	615/570	Quantitative
L-PFTeDA	3.97	713/669	713/169	L-PFTeDA	^{13}C-PFDoA	615/570	Quantitative
L-PFBS	2.45	298.9/80	298.9/99	L-PFBS	^{18}O-PFHxS	403/84	Quantitative
L-PFHxS	3.25	399/80	399/99	L-PFHxS	^{18}O-PFHxS	403/84	Quantitative
Br-PFHxS	~3.22	399/80	399/99	L-PFHxS	^{18}O-PFHxS	403/84	Semi-quantitative
L-PFOS	3.84	498.9/80	498.9/99	L-PFOS	^{13}C-PFOS	503/80	Quantitative
Br-PFOS	~3.81	498.9/80	498.9/99	L-PFOS	^{13}C--PFOS	503/80	Semi-quantitative
L-PFDS	4.34	598.9/80	599/99	L-PFDS	^{13}C-PFOS	503/80	Quantitative
Br-PFDS	~4.31	599/80	599/99	L-PFDS	^{13}C-PFOS	503/80	Semi-quantitative
L-FOSA	4.87	498/78	498/169	L-FOSA	^{13}C-FOSA	506/78	Quantitative
Br-FOSA	~4.84	498/78	498/169	L-FOSA	^{13}C-FOSA	506/78	Semi-quantitative

79

80 **Table S6:** Values for method limit detection (MDL) and spike recovery used in the analytical
81 analyses (n = 8, each). It is based on 500 mL extractions. Branched isomers MDL are the same as
82 their linear isomers.

	MDL	**MQL**	**Spike/recovery experiments**			
			50 pg		**500 pg**	
	pg L^{-1}	pg L^{-1}	Average (%)	RSD (%)	Average (%)	RSD (%)
PFHxA	1.92	6.40	78	9	100	6
PFHpA	5.30	17.7	76	18	98	11
L-PFOA	2.98	9.92	78	14	103	12
PFNA	1.71	5.69	78	14	100	9
PFDA	0.50	1.67	75	11	100	10
PFUnDA	1.85	6.18	87	23	90	17
PFDoDA	0.50	1.67	83	15	90	32
PFTriDA	6.88	22.9	40	12	61	21
PFTeDA	0.50	1.67	27	8	34	11
PFBS	2.88	9.60	124	64	136	124
L-PFHxS	1.59	5.30	70	18	88	10
L-PFOS	0.59	1.98	92	23	110	47
L-PFDS	3.93	13.1	51	22	65	22
L-FOSA	0.89	2.97	81	27	132	84

83

84

Table S7: Values for field (n = 3, 1 mL), lab (n = 7, 1 mL) bottle (n = 2, 500 mL) used in the analytical analyses. Blank volume of 500 mL was assumed in the calculations.

	Brazil			Sweden			Bottle		
Compound	**Avg (pg L^{-1})**	**SD**	**Con. in 1 mL**	**Avg (pg L^{-1})**	**SD**	**Con. in 1 mL**	**Avg (pg L^{-1})**	**SD**	**Con. in 1 mL**
PFHxA	5.97	5.3	< 0.0060	< 1.92		< 0.0019	< 1.92		< 0.0019
PFHpA	< 5.30		< 0.0053	< 5.30		< 0.0053	< 5.30		< 0.0053
L-PFOA	<2.98		< 0.0030	<2.98		< 0.0030	<2.98		< 0.0030
Br-PFOA	<2.98		< 0.0030	<2.98		< 0.0030	<2.98		< 0.0030
PFNA	< 1.71		< 0.0017	< 1.71		< 0.0017	< 1.71		< 0.0017
PFDA	1.12	1.6	< 0.0011	0.70	1.5	< 0.0007	< 0.50		< 0.0005
PFUnDA	< 1.85		< 0.0019	< 1.85		< 0.0019	< 1.85		< 0.0019
PFDoDA	< 0.50		< 0.0005	< 0.50		< 0.0005	0.66	0.7	< 0.0007
PFTriDA	< 6.88		< 0.0069	< 6.88		< 0.0069	< 6.88		< 0.0069
PFTeDA	< 0.50		< 0.0005	< 0.50		< 0.0005	< 0.50		< 0.0005
PFBS	< 2.88	0.1	< 0.0029	< 2.88	0.0	< 0.0029	< 2.88		< 0.0029
L-PFHxS	< 1.59		< 0.0016	< 1.59		< 0.0016	< 1.59		< 0.0016
Br-PFHxS	< 1.59		< 0.0016	< 1.59		< 0.0016	< 1.59		< 0.0016
L-PFOS	4.55	6.4	< 0.0045	< 0.59		< 0.0006	< 0.59		< 0.0006
Br-PFOS	< 0.59		< 0.0006	< 0.59		< 0.0006	< 0.59		< 0.0006
L-PFDS	< 3.93		< 0.0039	< 3.93		< 0.0039	< 3.93		< 0.0039
Br-PFDS	< 3.93		< 0.0039	< 3.93		< 0.0039	< 3.93		< 0.0039
L-FOSA	< 0.89		< 0.0009	< 0.89		< 0.0009	< 0.89		< 0.0009
Br-FOSA	< 0.89		< 0.0009	< 0.89		< 0.0009	< 0.89		< 0.0009

[1]Lab blanks of PFHxA, L-PFOA, and PFHxS n = 7 due to the first batch with contamination of reagents for these compounds (5.18, 68.5 and 23.0 pg L^{-1}, respectively).

Table S8: Concentration (pg L^{-1}) of detected isomers in seawater samples. ∑PFAA consider all compounds above method detection limit (MDL). PFDS was always <MDL.

Sample n.	L-PFHxA	Br-PFHxA	PFHpA	L-PFOA	Br-PFOA	PFNA	PFDA	PFUnDA	PFDoDA	PFTriDA	PFTeDA	PFBS	L-PFHxS	L-PFOS	Br-PFOS	L-FOSA	Br-FOSA	∑ PFAA
1.1	n.r.	n.r.	19.3	n.r.	n.r.	(4.86)	2.55	(1.85)	11.0	< 6.88	< 0.50	< 2.88	n.r.	< 0.59	< 0.59	< 0.89	< 0.89	39.6
1.2	n.r.	n.r.	(16.0)	n.r.	n.r.	(10.8)	2.33	10.7	(1.10)	< 6.88	(0.86)	< 2.88	n.r.	4.83	< 0.59	< 0.89	< 0.89	46.5
1.3	n.r.	n.r.	24.3	n.r.	n.r.	(17.0)	(0.86)	(2.47)	< 0.50	< 6.88	< 0.50	< 2.88	n.r.	12.0	< 0.59	(1.91)	< 0.89	58.6
1.4	n.r.	n.r.	20.0	n.r.	n.r.	(2.39)	(0.76)	< 1.85	< 0.50	< 6.88	< 0.50	< 2.88	n.r.	3.88	< 0.59	5.20	< 0.89	32.3
1.5	n.r.	n.r.	60.5	n.r.	n.r.	(1.86)	(0.69)	< 1.85	< 0.50	< 6.88	< 0.50	< 2.88	n.r.	< 0.59	< 0.59	3.19	< 0.89	66.2
1.6	n.r.	n.r.	50.1	n.r.	n.r.	< 1.71	2.33	15.0	< 0.50	< 6.88	10.5	< 2.88	n.r.	< 0.59	< 0.59	< 0.89	< 0.89	77.9
1.7	n.r.	n.r.	< 5.30	n.r.	n.r.	(2.02)	< 0.50	4.86	< 0.50	< 6.88	< 0.50	< 2.88	n.r.	(1.31)	< 0.59	4.66	< 0.89	12.90
1.8	n.r.	n.r.	< 5.30	n.r.	n.r.	< 1.71	1.99	< 1.85	< 0.50	< 6.88	< 0.50	< 2.88	n.r.	(1.91)	< 0.59	< 0.89	< 0.89	3.91
2.1	10.43	< 1.92	< 5.30	< 2.98	< 2.99	(3.91)	< 0.50	< 1.85	< 0.50	< 6.88	< 0.50	< 2.88	< 1.59	< 0.59	< 0.59	< 0.89	< 0.89	14.3
3.1	11.9	< 1.92	(6.00)	(6.11)	< 2.98	7.47	< 0.50	< 1.85	< 0.50	< 6.88	< 0.50	< 2.88	< 1.59	< 0.59	< 0.59	< 0.89	< 0.89	31.4
4.1	< 1.92	< 1.92	(11.9)	(6.81)	(3.48)	< 1.71	< 0.50	< 1.85	< 0.50	< 6.88	< 0.50	< 2.88	< 1.59	< 0.59	< 0.59	< 0.89	< 0.89	22.2
5.1	< 1.92	< 1.92	< 5.30	< 2.98	< 2.98	< 1.71	< 0.50	< 1.85	< 0.50	< 6.88	< 0.50	< 2.88	< 1.59	< 0.59	< 0.59	< 0.89	< 0.89	n.d.
5.2	< 1.92	< 1.92	< 5.30	< 2.98	< 2.98	(2.67)	< 0.50	< 1.85	< 0.50	< 6.88	< 0.50	< 2.88	< 1.59	< 0.59	< 0.59	11.8	< 0.89	14.5
5.3	< 1.92	< 1.92	< 5.30	< 2.98	< 2.98	< 1.71	17.33	< 1.85	< 0.50	< 6.88	< 0.50	< 2.88	< 1.59	< 0.59	< 0.59	< 0.89	< 0.89	17.3
5.4	< 1.92	< 1.92	< 5.30	29.6	< 2.98	< 1.71	< 0.50	< 1.85	< 0.50	< 6.88	< 0.50	< 2.88	< 1.59	< 0.59	< 0.59	106	< 0.89	136
5.5	< 1.92	< 1.92	< 5.30	< 2.98	< 2.98	< 1.71	< 0.50	< 1.85	< 0.50	< 6.88	< 0.50	< 2.88	< 1.59	< 0.59	< 0.59	< 0.89	< 0.89	n.d.
5.6	< 1.92	< 1.92	< 5.30	< 2.98	< 2.98	< 1.71	< 0.50	< 1.85	< 0.50	< 6.88	< 0.50	< 2.88	< 1.59	< 0.59	< 0.59	< 0.89	< 0.89	n.d.
5.7	< 1.92	< 1.92	< 5.30	< 2.98	< 2.98	< 1.71	< 0.50	< 1.85	< 0.50	< 6.88	< 0.50	< 2.88	< 1.59	< 0.59	< 0.59	< 0.89	< 0.89	n.d.
5.8	< 1.92	< 1.92	< 5.30	(3.03)	< 2.98	< 1.71	< 0.50	< 1.85	< 0.50	< 6.88	< 0.50	< 2.88	< 1.59	< 0.59	< 0.59	< 0.89	< 0.89	3.03
5.9	< 1.92	< 1.92	< 5.30	28.9	< 2.98	< 1.71	< 0.50	< 1.85	< 0.50	< 6.88	< 0.50	< 2.88	< 1.59	(0.75)	< 0.59	< 0.89	< 0.89	29.7
6.1	< 1.92	< 1.92	< 5.30	(9.78)	(1.82)	(1.93)	< 0.50	< 1.85	< 0.50	< 6.88	< 0.50	< 2.88	< 1.59	< 0.59	< 0.59	< 0.89	< 0.89	13.5
14.1	15.08	< 1.92	(6.50)	(9.74)	< 2.98	< 1.71	2.55	< 1.85	5.85	< 6.88	< 0.50	< 2.88	< 1.59	< 0.59	< 0.59	< 0.89	< 0.89	39.7
7.1	9.418	< 1.92	< 5.30	19.7	11.0	< 1.71	< 0.50	< 1.85	< 0.50	< 6.88	< 0.50	< 2.88	< 1.59	< 0.59	< 0.59	9.82	< 0.89	49.9
7.2	< 1.92	< 1.92	(11.2)	10.7	< 2.98	(5.40)	1.75	< 1.85	< 0.50	< 6.88	< 0.50	< 2.88	< 1.59	< 0.59	< 0.59	(2.42)	< 0.89	31.5
7.3	< 1.92	< 1.92	(15.8)	9.98	< 2.98	< 1.71	< 0.50	< 1.85	< 0.50	< 6.88	2.60	< 2.88	< 1.59	< 0.59	< 0.59	(1.23)	< 0.89	29.6
7.4	< 1.92	< 1.92	80.2	(9.29)	< 2.98	< 1.71	1.84	(3.93)	< 0.50	< 6.88	0.50	< 2.88	< 1.59	< 0.59	< 0.59	64.5	< 0.89	160
7.5	< 1.92	< 1.92	< 5.30	20.9	13.0	< 1.71	1.72	< 1.85	< 0.50	< 6.88	< 0.50	< 2.88	< 1.59	< 0.59	< 0.59	25.1	< 0.89	60.7
7.6	< 1.92	< 1.92	< 5.30	< 2.98	< 2.98	< 1.71	(1.29)	< 1.85	3.40	< 6.88	< 0.50	< 2.88	< 1.59	< 0.59	< 0.59	< 0.89	< 0.89	4.69
7.7	< 1.92	< 1.92	(12.7)	< 2.98	< 2.98	< 1.71	< 0.50	< 1.85	< 0.50	< 6.88	< 0.50	< 2.88	< 1.59	< 0.59	< 0.59	8.07	< 0.89	20.80
7.8	< 1.92	< 1.92	< 5.30	< 2.98	< 2.98	< 1.71	3.40	< 1.85	< 0.50	< 6.88	< 0.50	< 2.88	< 1.59	(0.83)	< 0.59	25.9	< 0.89	30.1

n.r. = values non reported due to analytical issues.

Numbers in brackets are above method detection limit (MDL) but below the respective MQL. <x: below the respective MDL

94 *Continue…*

Sample n.	L-PFHxA	Br-PFHxA	PFHpA	L-PFOA	Br-PFOA	PFNA	PFDA	PFUnDA	PFDoDA	PFTriDA	PFTeDA	PFBS	L-PFHxS	L-PFOS	Br-PFOS	L-FOSA	Br-FOSA	∑PFAA
8.1	12.85	< 1.92	(14.1)	(3.16)	< 2.98	< 1.71	3.36	< 1.85	(1.06)	< 6.88	< 0.50	< 2.88	< 1.59	< 0.59	< 0.59	< 0.89	< 0.89	34.6
9.1	< 1.92	< 1.92	< 5.30	(9.25)	< 2.98	(5.68)	< 0.50	< 1.85	< 0.50	< 6.88	< 0.50	< 2.88	< 1.59	< 0.59	< 0.59	< 0.89	< 0.89	14.9
9.2	12.79	< 1.92	< 5.30	< 2.98	< 2.98	< 1.71	3.77	< 1.85	(1.92)	< 6.88	< 0.50	< 2.88	(3.24)	< 0.59	< 0.59	3.29	< 0.89	25.0
9.3	< 1.92	< 1.92	37.1	22.0	< 2.98	< 1.71	< 0.50	< 1.85	< 0.50	< 6.88	< 0.50	< 2.88	< 1.59	< 0.59	< 0.59	8.26	< 0.89	67.4
9.4	< 1.92	< 1.92	20.0	10.8	< 2.98	< 1.71	3.55	< 1.85	< 0.50	< 6.88	< 0.50	< 2.88	< 1.59	< 0.59	< 0.59	(1.49)	< 0.89	35.8
9.5	< 1.92	< 1.92	47.9	15.4	(7.07)	< 1.71	(1.47)	< 1.85	< 0.50	< 6.88	< 0.50	< 2.88	< 1.59	3.35	< 0.59	8.27	< 0.89	83.5
9.6	< 1.92	< 1.92	73.6	14.4	(3.59)	< 1.71	< 0.50	< 1.85	< 0.50	< 6.88	< 0.50	< 2.88	< 1.59	< 0.59	< 0.59	< 0.89	< 0.89	91.6
9.7	< 1.92	< 1.92	< 5.30	16.5	(9.91)	(5.04)	< 0.50	< 1.85	< 0.50	< 6.88	< 0.50	< 2.88	< 1.59	< 0.59	< 0.59	< 0.89	< 0.89	31.4
9.8	< 1.92	< 1.92	< 5.30	(6.39)	< 2.98	< 1.71	< 0.50	(2.08)	< 0.50	< 6.88	< 0.50	< 2.88	< 1.59	< 0.59	< 0.59	< 0.89	< 0.89	8.47
10.1	< 1.92	< 1.92	< 5.30	< 2.98	< 2.98	< 1.71	< 0.50	< 1.85	< 0.50	< 6.88	< 0.50	< 2.88	< 1.59	< 0.59	< 0.59	< 0.89	< 0.89	n.d.
11.1	< 1.92	< 1.92	< 5.30	14.9	< 2.98	< 1.71	< 0.50	< 1.85	< 0.50	< 6.88	< 0.50	(7.35)	< 1.59	< 0.59	< 0.59	< 0.89	< 0.89	22.2
12.1	< 1.92	< 1.92	22.9	< 2.98	< 2.98	< 1.71	< 0.50	< 1.85	< 0.50	< 6.88	< 0.50	< 2.88	< 1.59	< 0.59	< 0.59	< 0.89	< 0.89	22.9
13.1	< 1.92	< 1.92	< 5.30	< 2.98	< 2.98	< 1.71	< 0.50	< 1.85	< 0.50	< 6.88	< 0.50	< 2.88	< 1.59	< 0.59	< 0.59	< 0.89	< 0.89	n.d.
15.1	20.97	< 1.92	(16.0)	29.5	< 2.98	< 1.71	< 0.50	< 1.85	(0.54)	< 6.88	< 0.50	< 2.88	< 1.59	(1.24)	< 0.59	5.78	< 0.89	74.0
15.2	< 1.92	< 1.92	< 5.30	(5.62)	< 2.98	< 1.71	1.89	< 1.85	< 0.50	< 6.88	< 0.50	< 2.88	< 1.59	< 0.59	< 0.59	< 0.89	< 0.89	7.51
15.3	13.41	< 1.92	54.3	11.1	4.995	< 1.71	1.95	< 1.85	1.96	< 6.88	< 0.50	< 2.88	< 1.59	5.66	< 0.59	< 0.89	< 0.89	93.4
15.4	37.6	< 1.92	123	19.6	< 2.98	< 1.71	3.92	< 1.85	1.223	< 6.88	< 0.50	< 2.88	< 1.59	2.01	< 0.59	12.9	< 0.89	200
16.1	< 1.92	< 1.92	< 5.30	(4.69)	< 2.98	(3.10)	< 0.50	< 1.85	< 0.50	< 6.88	< 0.50	(4.02)	< 1.59	(0.99)	< 0.59	2.39	< 0.89	15.2
16.2	< 1.92	< 1.92	31.5	(18.3)	< 2.98	< 1.71	< 0.50	< 1.85	< 0.50	(7.52)	< 0.50	< 2.88	(2.30)	< 0.59	< 0.59	< 0.89	< 0.89	59.7
16.3	< 1.92	< 1.92	173	(8.36)	< 2.98	< 1.71	< 0.50	< 1.85	7.16	(9.40)	< 0.50	< 2.88	< 1.59	< 0.59	< 0.59	0.95	< 0.89	199
16.4	< 1.92	< 1.92	86.5	(9.00)	< 2.98	< 1.71	(0.94)	< 1.85	(0.58)	< 6.88	< 0.50	< 2.88	< 1.59	4.97	< 0.59	5.50	< 0.89	107

95

Table S9: Comparative of seawater concentrations in different studies worldwide. <x: below the respective MDL.

Reference	Sampling Year	Position	PFHxA	PFHpA	L-PFOA	PFNA	PFDA	PFDoDA	PFBS	L-PFHxS	L-PFOS	L-FOSA
Atlantic												
this study	2017	15°N-23°S	< 6.40 - 21.0	< 17.7 - 22.9	< 9.92 - 29.4	< 5.69 - 7.47	< 1.67 - 3.36	< 1.67 - 11.0	nd	nd	nd	< 2.97 - 9.82
González-Gaya et al. (2014)	2011	15°N-24°S	nd - 39	3.12 - 54	18.4 - 81.4	4.24 - 384	nd - 110	na	14.1 - 480	14.6 - 77.4	190 - 1100	nd - 6.00
Zhao et al. (2012)	2010	61°N-70°S	< 5.9 - 85	na	< 13 - 160	< 12 - 39	< 21	< 25	< 51 - 65	< 6.5 - 45	< 20 - 25	< 83
Benskin et al. (2012)	2005	11°N-21°S	14 -75	7 - 51	17 - 32	5.5 - 19	3.3 - 9.3	nd	nr	1.4 - 4.9	13 - 32	2 - 19
	2007	12°N-25°S	nd - 41	nd - 18	5.2 - 41	2.4 - 15	2.9 - 9.2	1.3 - 55	nd - 50	nd - 8.0	18 - 52	nd -2.7
Ahrens et al. (2009)	2008	15°N-26°S	< 5.7	< 5.9 - 9.7	< 4.0 - 87	< 5.1 - 35	na	na	< 1.6	nd	< 10 - 60	< 17 - 60
Ahrens et al. (2010)	2009	52°N-69°S	<3.0-117	<3.0-28	<5.2-223	<3.0-39	<5.5-37	<5.9-48	<4.4-50	<4.1-53	<11-232	<3.067
Yamashita et al. (2005)	2004	0°N-10°N	na	na	100 - 439	na	na	na	na	2.6 - 12	37 - 73	na
Pacific												
González-Gaya et al. (2014)	2011	35-0º N	nd	nd - 296	9 - 138	13 - 94	nd - 243	na	nd - 115	nd - 161	4 - 476	2 - 9
	2011	0 - 40°S	nd	nd - 143	3 - 164	16 - 35	nd - 87	na	nd - 110	nd - 71	2 - 13	nd - 6.00
Indian												
González-Gaya et al. (2014)	2011	0-40º S	nd	nd - 51	5 - 45	11 - 60	9 - 120	na	7 - 124	nd - 7	5 - 53	nd - 3
Wei et al. (2007)	2007	*	nd	nd	nd - 11.9	nd - 11	nd - 5.4	nd - 1.4	nd - 2.9	nd	nd - 23.9	na
Arctic		70°N	<1.0 - 31	<1.0 - 30	9.0 - 48.5	9 - 29.0	<1.0 - 9	<1.0 - 8	<1.0 - 18	<1.0 - 15	<1.0 - 41	na
Yeung et al. (2017)	2012	71°N	< 1.6 - 45									
Zhao et al. (2012)	2009	Greenland sea	< 5.9 - 38	na	< 13 - 160	< 12 - 16	< 21	< 25	< 51 - 65	< 6.5 - 45	< 20 - 25	< 83
Antarctic												
Cai et al. (2012)	2011	62°S	56.6 - 361	< 5.6 - 28.1	81.1 - 15,096	nd	nd	< 4.3 - 35.8	< 8.3 - 11.3	nd	nd	< 40.3 - 46.4
Wei et al. (2007)	2007	*	56.6 - 360	< 5.6 - 28.1	< 5.0	< 5.0	< 5.0	na	< 1.0 - 2.9	< 1.0	na	< 40.3 - 46.4
Zhao et al. (2012)	2010	63°S - 66°S	< 5.9	na	<13 - 15	< 12	< 21	< 25	< 51	< 6.5	< 20 - 46	< 83

* The coordinates of the sampling were not described by the author (Ahrens et al., 2010, 2009; Benskin et al., 2012a; Cai et al., 2012; González-Gaya et al., 2014; Wei et al., 2007; Yamashita et al., 2008; Yeung et al., 2017; Zhao et al., 2012)

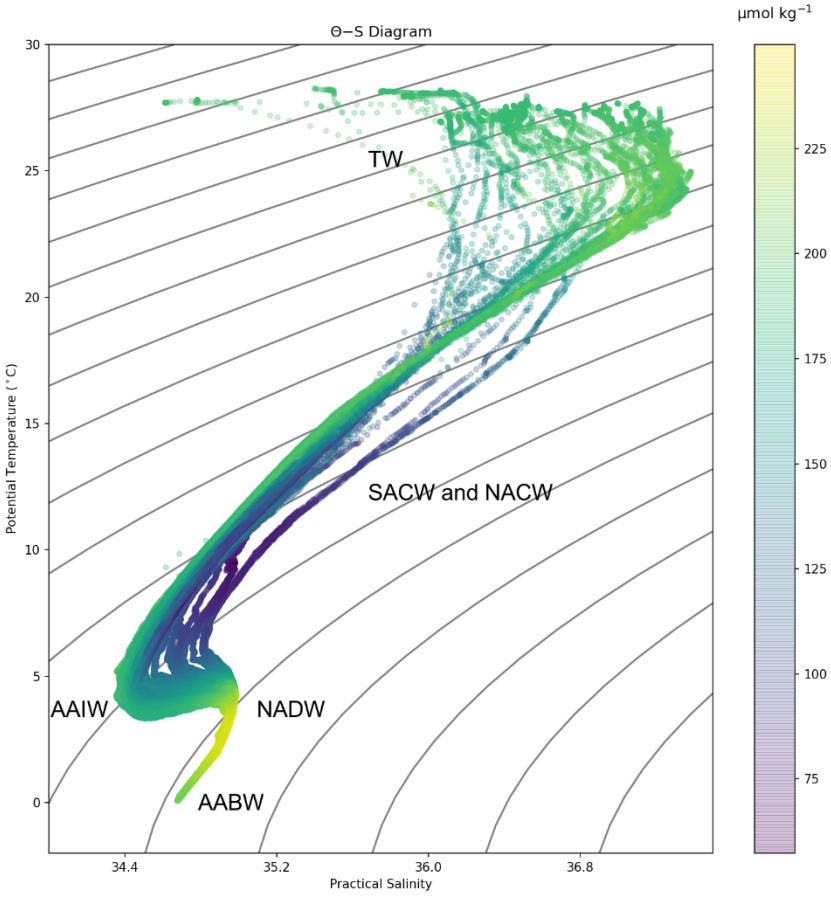

Figure S1: Temperature-salinity (T-S) diagram of the sampled transect from 15ºN to 23ºS. The colors indicate oxygen concentration in μmol kg^{-1} (scale at right). Density isopleths appears as grey line.

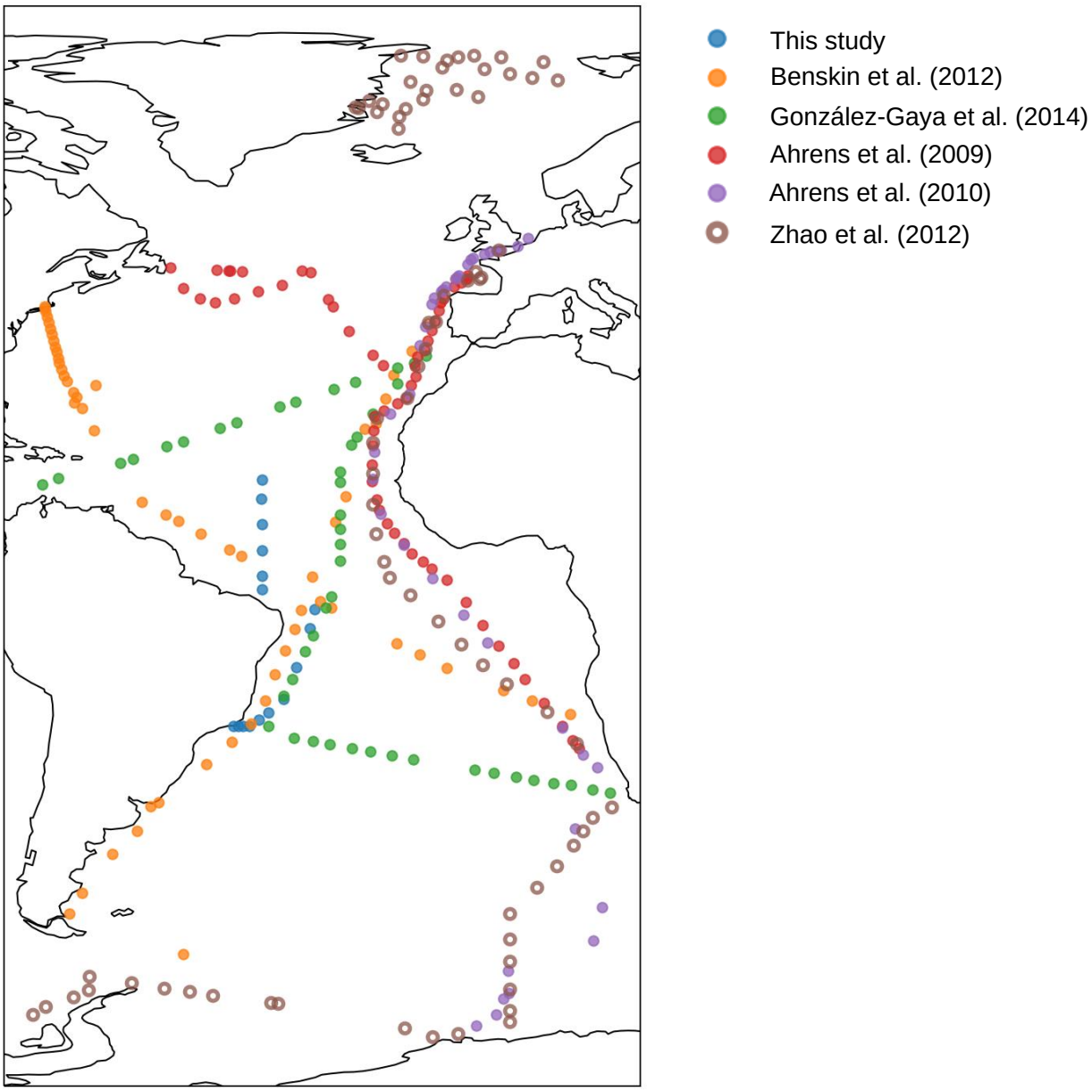

104

105 **Figure S2:** Sampling points from six different studies: present study, Benskin et al.
106 (2012b), González-Gaya et al. (2014), Ahrens et al. (2009), Ahrens et al. (2010), and Zhao
107 et al. (2012).

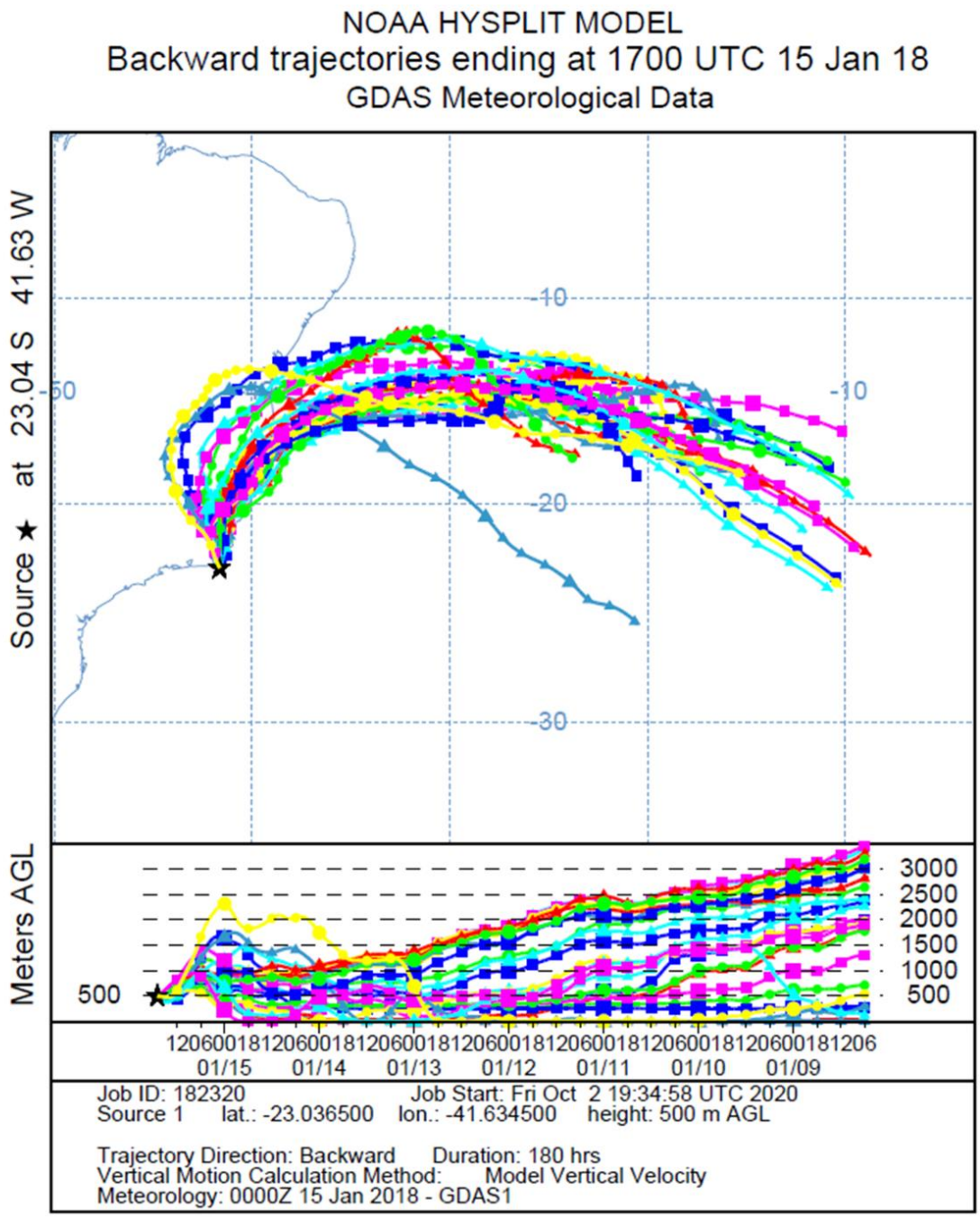

Figure S3: Backward air trajectories (72 hour) computed for sampling point #15.1 using NOAA's HYSPLIT Model.

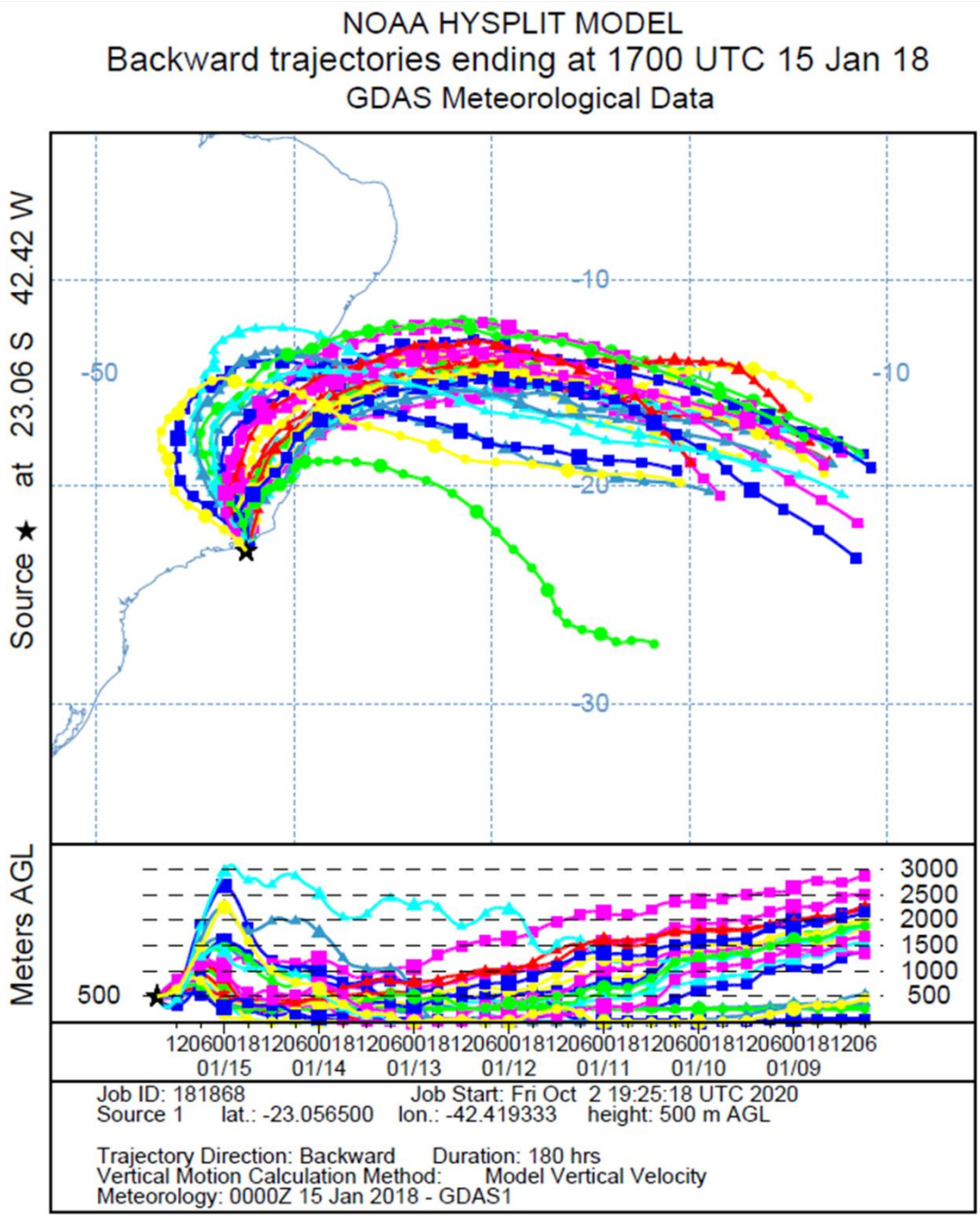

Figure S4: Backward air trajectories (72 hour) computed for sampling point #16.1 using NOAA's HYSPLIT Model.

115

a) Long: -38.1°; Lat: 14.9° (#1)

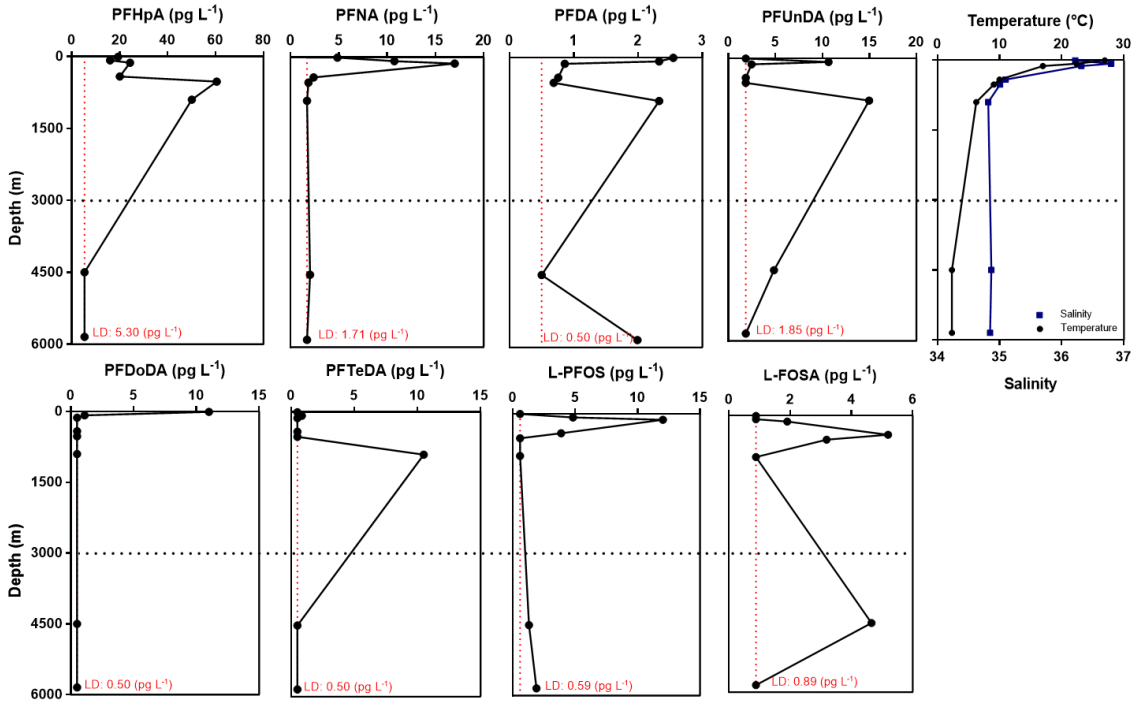

b) Long: -38.0°; Lat: 0.05° (#5)

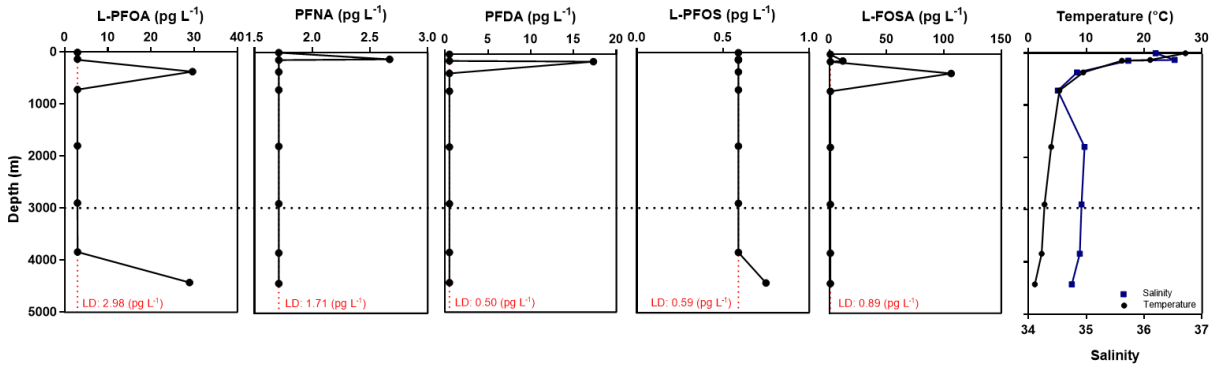

116

117 **Figure S5:** Vertical profiles of PFAAs (pg L^{-1}) detected above MDL in ocean water
118 columns from Tropical Atlantic Ocean (#1 (a) and #5 (b)) together with Salinity and
119 Temperature (°C).

120

a) Long: -30.3°; Lat: -8° (#7)

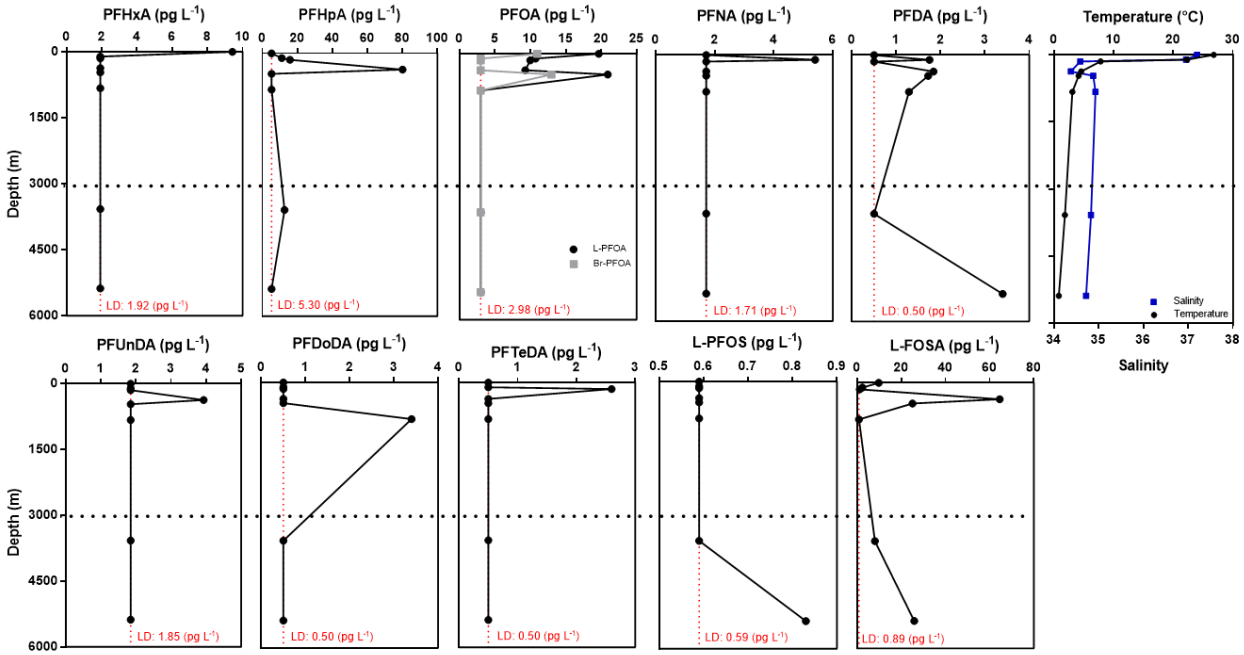

b) Long: -34.4°; Lat: -18.5° (#9)

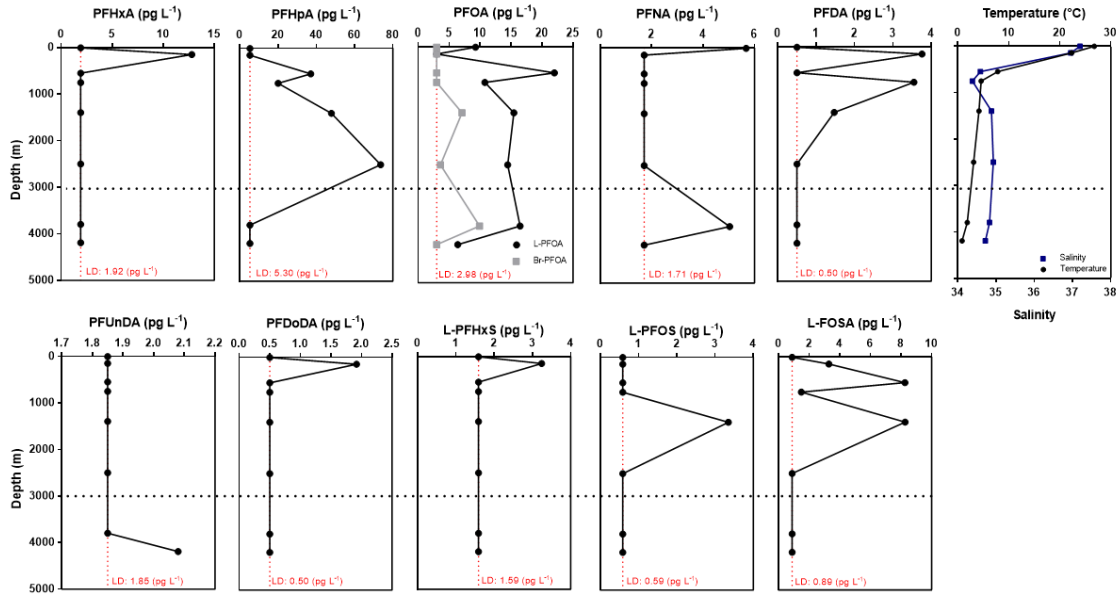

121

122 **Figure S6:** Vertical profiles of PFAAs (pg L^{-1}) detected above MDL in ocean water
123 columns from Tropical Atlantic Ocean (#7 (a) and #9 (b)) together with Salinity and
124 Temperature (°C).

125

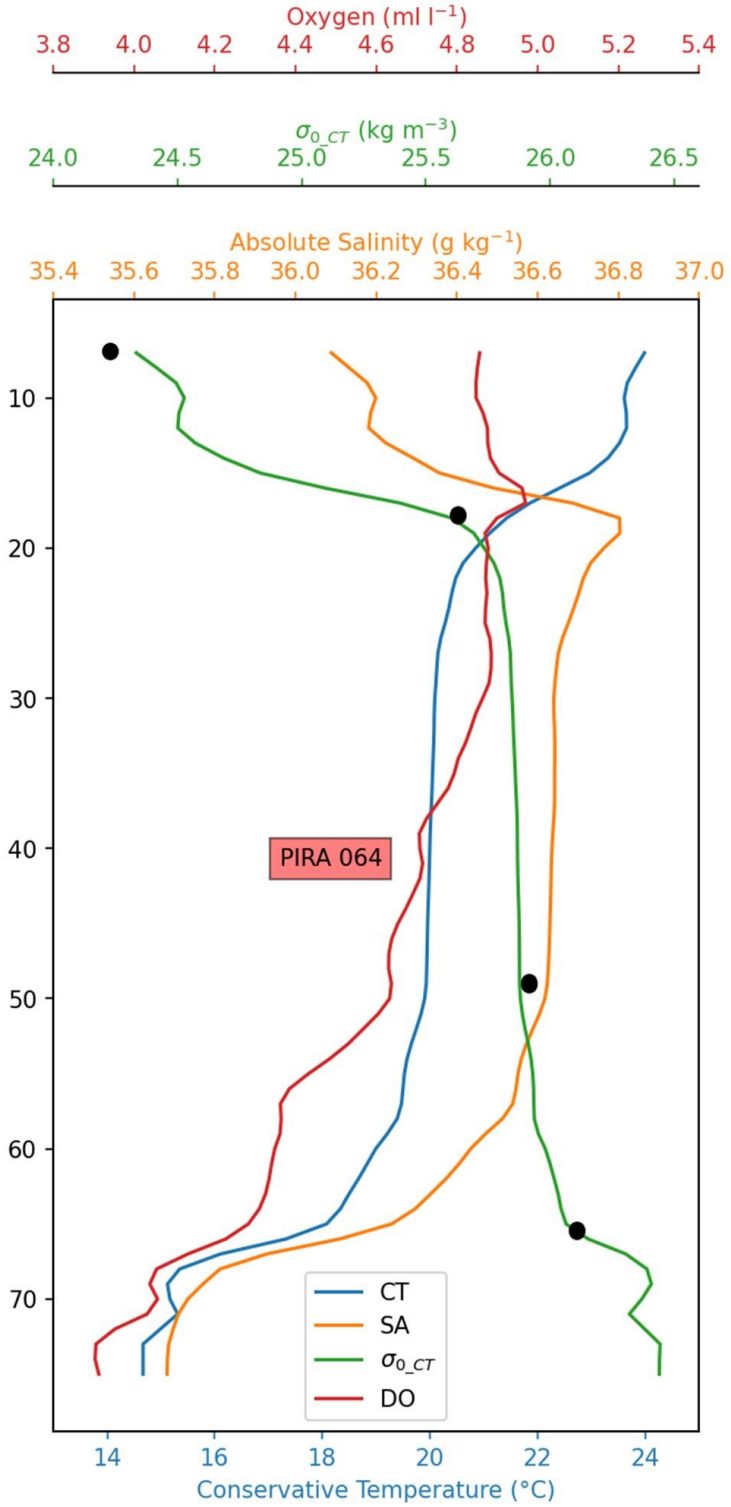

Figure S7: Vertical profile for conservative temperature, absolute salinity, oxygen, and dissolved oxygen for the sampled profile at 23ºS (#15). Black dots represent the depths where seawater samples were collected.

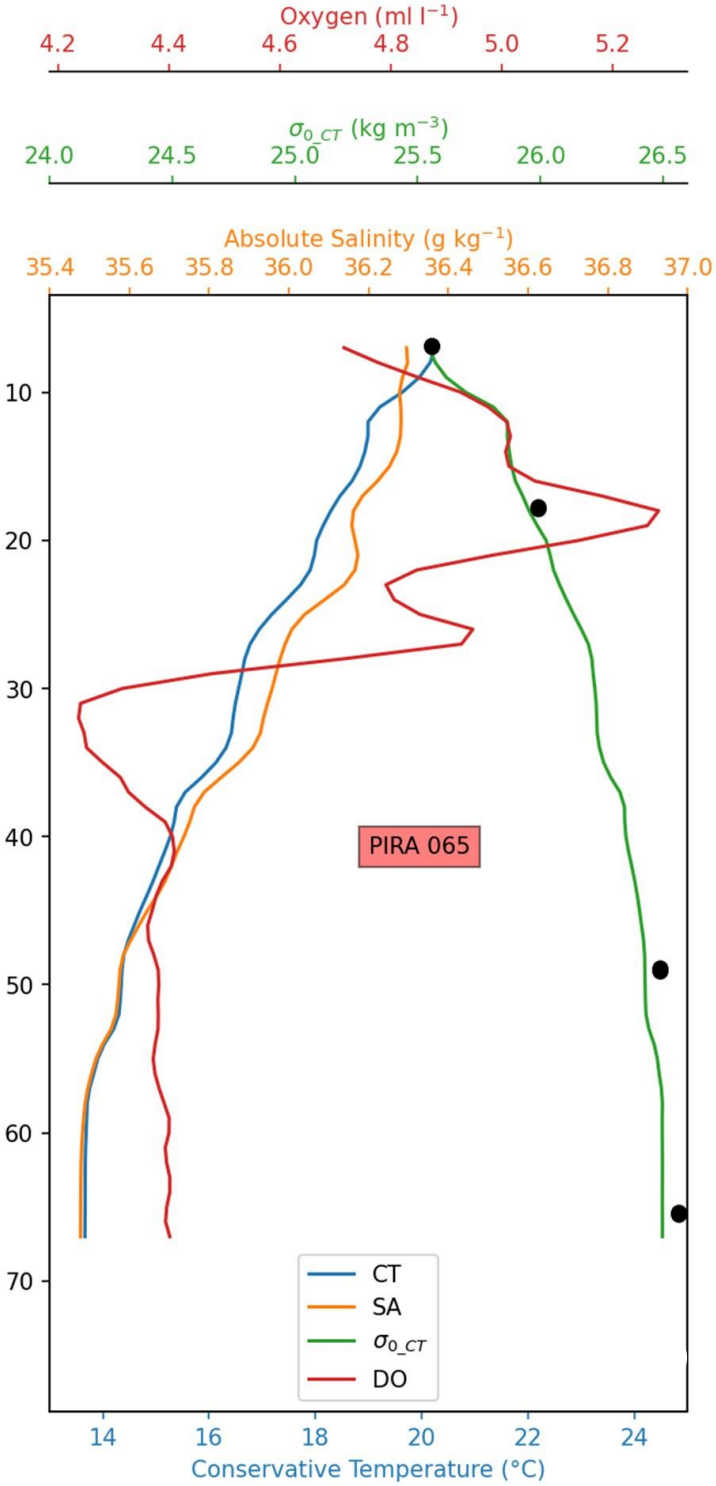

Figure S8: Vertical profile for conservative temperature, absolute salinity, oxygen, and dissolved oxygen for the sampled profile at 23ºS (#16). Black dots represent the depths where seawater samples were collected.

a) Long: -41.6°; Lat: -23.0° (#15)

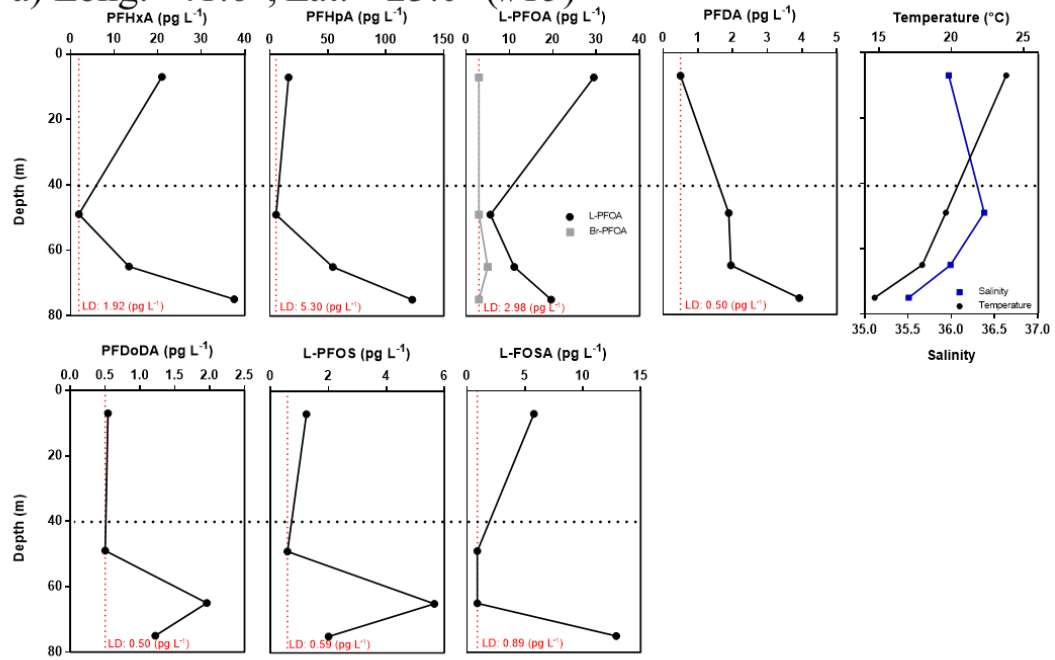

b) Long: -42.4°; Lat: -23.1° (#16)

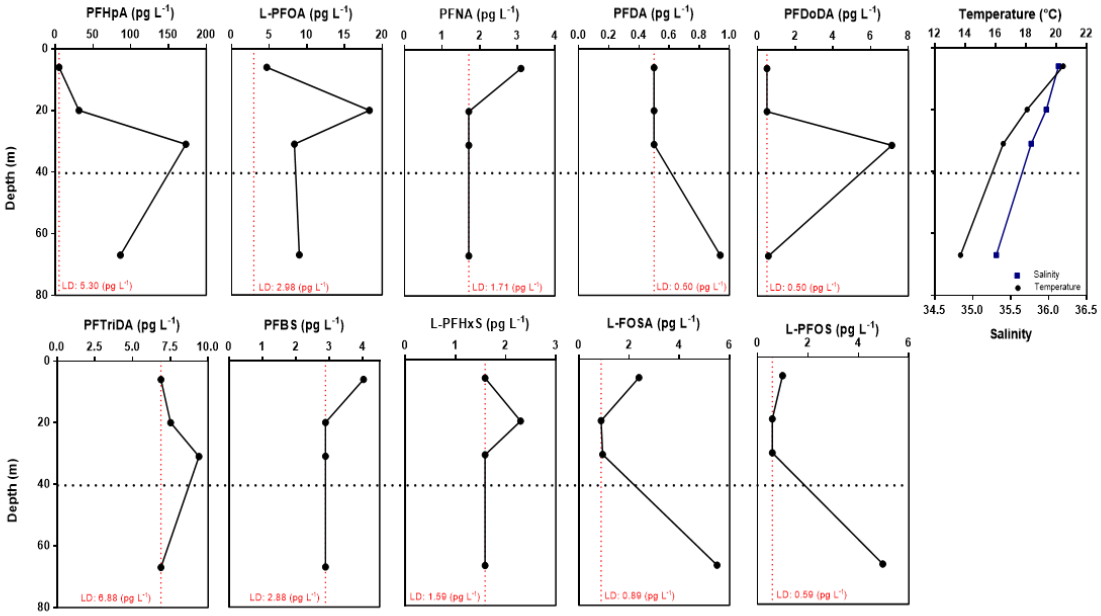

Figure S6: Vertical profiles of PFAAs (pg L^{-1}) detected above MDL in ocean water columns from Rio de Janeiro upwelling (#15 (a) and #16 (b)) together with Salinity and Temperature (°C).

Reference

Ahrens, L., Barber, J. L., Xie, Z., & Ebinghaus, R. (2009). Longitudinal and Latitudinal Distribution of Perfluoroalkyl Compounds in the Surface Water of the Atlantic Ocean. *Environmental Science & Technology*, *43*(9), 3122–3127. https://doi.org/10.1021/es803507p

Ahrens, L., Xie, Z., & Ebinghaus, R. (2010). Distribution of perfluoroalkyl compounds in seawater from Northern Europe, Atlantic Ocean, and Southern Ocean. *Chemosphere*, *78*(8), 1011–1016. https://doi.org/https://doi.org/10.1016/j.chemosphere.2009.11.038

Bashmachnikov, I., Nascimento, Â., Neves, F., Menezes, T., & Koldunov, N. V. (2015). Distribution of intermediate water masses in the subtropical northeast Atlantic. *Ocean Science*, *11*, 803–827.

Benskin, J. P., Li, B., Ikonomou, M. G., Grace, J. R., & Li, L. Y. (2012). Per- and Poly fl uoroalkyl Substances in Land fi ll Leachate: Patterns, Time Trends, and Sources. *Environ. Sci. Technol.*, *46*, 11532–11540.

Benskin, J. P., Muir, D. C. G., Scott, B. F., Spencer, C., De Silva, A. O., Kylin, H., Martin, J. W., Morris, A., Lohmann, R., Tomy, G., Rosenberg, B., Taniyasu, S., & Yamashita, N. (2012). Perfluoroalkyl Acids in the Atlantic and Canadian Arctic Oceans. *Environmental Science & Technology*, *46*(11), 5815–5823. https://doi.org/10.1021/es300578x

Cai, M., Yang, H., Xie, Z., Zhao, Z., Wang, F., Lu, Z., Sturm, R., & Ebinghaus, R. (2012). Per- and polyfluoroalkyl substances in snow, lake, surface runoff water and coastal seawater in Fildes Peninsula, King George Island, Antarctica. *Journal of Hazardous Materials*, *209–210*, 335–342. https://doi.org/https://doi.org/10.1016/j.jhazmat.2012.01.030

Emílsson, I. (1961). The shelf and coastal waters off southern Brazil . In *Boletim do Instituto Oceanográfico* (Vol. 11, pp. 101–112). scielo .

Ferreira, M. L. de C., & Kerr, R. (2017). Source water distribution and quantification of North Atlantic Deep Water and Antarctic Bottom Water in the Atlantic Ocean. *Progress in Oceanography*, *153*, 66–83. https://doi.org/https://doi.org/10.1016/j.pocean.2017.04.003

González-Gaya, B., Dachs, J., Roscales, J. L., Caballero, G., & Jiménez, B. (2014). Perfluoroalkylated Substances in the Global Tropical and Subtropical Surface Oceans. *Environmental Science & Technology*, *48*(22), 13076–13084. https://doi.org/10.1021/es503490z

Liu, M., & Tanhua, T. (2019). Characteristics of Water Masses in the Atlantic Ocean based on GLODAPv2 data. *Ocean Science Discussions*, *2019*, 1–43. https://doi.org/10.5194/os-2018-139

Miranda, L. B. de. (1985). Forma da correlação T-S de massas de água das regiões costeira e oceânica entre o Cabo de São Tomé (RJ) e a Ilha de São Sebastião (SP), Brasil . In *Boletim do Instituto Oceanográfico* (Vol. 33, pp. 105–119). scielo .

Nascimento, R. A., Nunoo, D. B. O., Bizkarguenaga, E., Schultes, L., Zabaleta, I., Benskin, J. P., Spanó, S., & Leonel, J. (2018). Sulfluramid use in Brazilian

agriculture: A source of per- and polyfluoroalkyl substances (PFASs) to the environment. *Environmental Pollution*, *242*, 1436–1443. https://doi.org/10.1016/J.ENVPOL.2018.07.122

Silveira, I. C. A. da, Schmidt, A. C. K., Campos, E. J. D., Godoi, S. S. de, & Ikeda, Y. (2000). A corrente do Brasil ao largo da costa leste brasileira . In *Revista Brasileira de Oceanografia* (Vol. 48, pp. 171–183). scielo .

Stramma, L., & England, M. (1999). On the water masses and mean circulation of the South Atlantic Ocean. *Journal of Geophysical Research*, *104*(C9), 863–883.

Sverdup, H, U., Fleming, M. W., H., J., & Richard. (1944). The Oceans: Their Physics, Chemistry, and General Biology. *Quarterly Journal of the Royal Meteorological Society*, *70*(304), 159–160. https://doi.org/10.1002/qj.49707030418

Talley, L. D. (2013). Closure of the global overturning circulation through the Indian, Pacific, and Southern Oceans: Schematics and transports. *Oceanography*, *26*(1), 80–97.

Wei, S., Chen, L. Q., Taniyasu, S., So, M. K., Murphy, M. B., Yamashita, N., Yeung, L. W. Y., & Lam, P. K. S. (2007). Distribution of perfluorinated compounds in surface seawaters between Asia and Antarctica. *Marine Pollution Bulletin*, *54*(11), 1813–1818. https://doi.org/https://doi.org/10.1016/j.marpolbul.2007.08.002

Yamashita, N., Taniyasu, S., Petrick, G., Wei, S., Gamo, T., Lam, P. K. S., & Kannan, K. (2008). Perfluorinated acids as novel chemical tracers of global circulation of ocean waters. *Chemosphere*, *70*(7), 1247–1255. https://doi.org/https://doi.org/10.1016/j.chemosphere.2007.07.079

Yeung, L. W. Y., Dassuncao, C., Mabury, S., Sunderland, E. M., Zhang, X., & Lohmann, R. (2017). Vertical Profiles, Sources, and Transport of PFASs in the Arctic Ocean. *ENVIRONMENTAL SCIENCE & TECHNOLOGY*, *51*(12), 6735–6744. https://doi.org/10.1021/acs.est.7b00788

Zhao, Z., Xie, Z., Möller, A., Sturm, R., Tang, J., Zhang, G., & Ebinghaus, R. (2012). Distribution and long-range transport of polyfluoroalkyl substances in the Arctic, Atlantic Ocean and Antarctic coast. *Environmental Pollution*, *170*, 71–77. https://doi.org/https://doi.org/10.1016/j.envpol.2012.06.004

Capítulo 5: ***Bioaccumulation of Per- and polyfluoroalkyl substances (PFASs) in a tropical estuarine food web***

Artigo publicado no periódico *Science of the Total Environment*

Science of the Total Environment 754 (2021) 142146

Contents lists available at ScienceDirect

Science of the Total Environment

journal homepage: www.elsevier.com/locate/scitotenv

Bioaccumulation of Per- and polyfluoroalkyl substances (PFASs) in a tropical estuarine food web

Daniele A. Miranda [a,b,*], Jonathan P. Benskin [b], Raed Awad [b,c], Gilles Lepoint [d], Juliana Leonel [e], Vanessa Hatje [a]

[a] Centro Interdisciplinar de Energia e Ambiente (CIEnAm) and Inst. de Química, Universidade Federal da Bahia, 41170-115 Salvador, BA, Brazil
[b] Department of Environmental Science, Stockholm University, Stockholm, Sweden
[c] Swedish Environmental Research Institute (IVL), Stockholm, Sweden
[d] Freshwater and Oceanic sciences Unit of reSearch (FOCUS – Oceanology), University of Liege, 4000 Liege, Belgium
[e] Departamento de Oceanografia, Universidade Federal de Santa Catarina, 88040-900 Florianópolis, SC, Brazil

HIGHLIGHTS

- Perfluoroalkyl substances (PFAS) were investigated in a tropical estuarine food web.
- Leaves, bivalves, polychaeta, crustaceans, and fish presented PFAS residues.
- PFOS, PFTrDA, and FOSA were the compounds most frequently detected in Subaé biota.
- The PFOS precursors FOSA and EtFOSA were also detected in Subaé estuarine biota.
- PFOS, PFNA and a C_8 PFOS precursor were observed to biomagnify in the food chain.

GRAPHICAL ABSTRACT

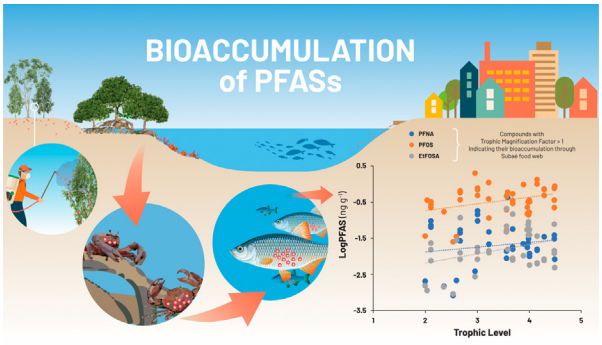

ARTICLE INFO

Article history:
Received 8 June 2020
Received in revised form 30 August 2020
Accepted 31 August 2020
Available online 2 September 2020

Editor: Daniel Wunderlin

Keywords:
POPs
PFOS precursors
Tropical food web
Biomagnification
Todos os Santos Bay

ABSTRACT

The biomagnification of per- and polyfluoroalkyl substances (PFASs) was investigated in a tropical mangrove food web from an estuary in Bahia, Brazil. Samples of 44 organisms (21 taxa), along with biofilm, leaves, sediment and suspended particulate matter were analyzed. Sum ($\sum$) PFAS concentrations in biota samples were dominated by perfluorooctane sulfonate (PFOS, 93% detection frequency in tissues; 0.05 to 1.97 ng g^{-1} ww whole-body (wb)), followed by perfluorotridecanoate (PFTrDA, 57%; 0.01 to 0.28 ng g^{-1} ww wb). PFOS precursors such as perfluorooctane sulfonamide (FOSA, 54%; 0.01 to 0.32 ng g^{-1} ww wb) and N-ethyl perfluorooctane sulfonamide (EtFOSA; 30%; 0.01 to 0.21 ng g^{-1} ww wb) were also detected. PFAS accumulation profiles revealed different routes of exposure among bivalve, crustacean and fish groups. Statistics for left-censored data were used in order to minimize bias on trophic magnification factors (TMFs) calculations. TMFs >1 were observed for PFOS (linear + branched isomers), EtFOSA (linear + branched isomers), and perfluorononanoate (PFNA), and in all cases, dissimilar accumulation patterns were observed among different trophic positions. The apparent biodilution of some long-chain PFCAs through the food chain (TMF < 1) may be due to exposure from multiple PFAS sources. This is the first study investigating bioaccumulation of PFASs in a tropical food web and provides new insight on the behavior of this ubiquitous class of contaminants.

© 2020 The Authors. Published by Elsevier B.V. This is an open access article under the CC BY license (http://creativecommons.org/licenses/by/4.0/).

* Corresponding author at: Universidade Federal da Bahia, CIEnAm I, Campus Ondina, CEP: 41170-115 Salvador, Bahia, Brazil.
E-mail addresses: daniele.miranda@aces.su.se, anielemirandaba@hotmail.com (D.A. Miranda).

https://doi.org/10.1016/j.scitotenv.2020.142146
0048-9697/© 2020 The Authors. Published by Elsevier B.V. This is an open access article under the CC BY license (http://creativecommons.org/licenses/by/4.0/).

1. Introduction

Per- and polyfluoroalkyl substances (PFASs) represent a diverse class of fluorinated anthropogenic chemicals with unique physical-chemical properties including combined hydrophobicity/lipophilicity (Buck et al., 2011), which make them desirable for a wide range of industrial processes and products. Notable applications of PFASs include firefighting foams (Dauchy et al., 2019), fluoropolymer manufacturing (Song et al., 2018), textiles (Wang et al., 2017), food packaging (Schaider et al., 2018; Schultes et al., 2019a), cosmetics (Schultes et al., 2018), and pesticides (Nascimento et al., 2018).

Since the early 2000s, there has been considerable concern over the widespread occurrence of PFASs, in particular the long-chain perfluoroalkyl acids (PFAAs), which display high persistence and have been found in the blood of humans (Giesy and Kannan, 2001; Lau et al., 2007; Wang et al., 2018) and biota (Dorneles et al., 2008; Giesy and Kannan, 2001; Hong et al., 2015; Houde et al., 2006b, 2011; Leonel et al., 2008; Quinete et al., 2009; Routti et al., 2017; Sanganyado et al., 2018). In 2009, one of the most widespread PFAAs, perfluorooctane sulfonate (PFOS), along with its salts and synthetic precursor perfluorooctane sulfonyl fluoride (POSF), were added to Annex B of the Stockholm Convention on Persistent Organic Pollutants (UNSCPOPs, 2009). Despite these regulatory initiatives, production of PFOS and other long-chain PFAAs continues in some parts of the world under regulatory exemptions.

In Brazil, manufacture and use exemptions have been obtained to continue producing and using Sulfluramid, which contains the active ingredient N-ethyl perfluorooctane sulfonamide (EtFOSA), a PFOS-precursor (Avendaño and Liu, 2015; Zabaleta et al., 2018). Sulfluramid is a formicide extensively introduced as a substitute for the organochlorine pesticide Mirex (Nagamoto et al., 2004), which is mostly used in eucalyptus and pine plantations to combat leaf-cutting ants (*Atta* sp. and *Acromyrmex* spp.). Brazil is among the largest consumers of Sulfluramid in the world (MMA, 2015a, 2015b). In the past five years, around 280 t $year^{-1}$ of Sulfluramid (0.3% EtFOSA) was imported, but there are considerable uncertainties with this estimate since the quantities of Sulfluramid precursor (i.e. POSF) imported into Brazil are not available (MDIC, 2019). Based on increasing production of eucalyptus and pine-derived cellulose (Rossato et al., 2018), it is expected that the demand for Sulfluramid will continue in the next years. A recent study suggested an elevated contributions from a PFOS precursor (e.g. Sulfluramid) in Subaé river waters in the Northeast of Brazil (Gilljam et al., 2016), indicated by the presence of PFOS precursors (PreFOS) compounds in the region (i.e. perfluorooctane sulfonamide - FOSA/PFOS ratio above 5:1).

While there are few data available on PFAS-based products beyond Sulfluramid in Brazil (MDIC, 2019), a recent ecotoxicological study suggested that PFAS-based aqueous film-forming foams (AFFFs) continue to be used (da Silva et al., 2019) while the National Implementation Plan for the Stockholm Convention in Brazil (MMA, 2015a, 2015b) highlights several PFAS-based consumer products which are permitted. Also, PFASs contamination in tropical areas has been associated with the AFFF use (Munoz et al., 2017b). Together with the use of Sulfluramid in forestry, PFAS-containing AFFF and consumer products (e.g., food packaging, cosmetics, etc.) may be important PFAS sources to the local environment.

The process of biomagnification is an important mechanism for micronutrient transfer through food chains (Barclay et al., 1994; Gribble et al., 2016), but it is also a mechanism that promotes accumulation of anthropogenic toxic compounds (Borga et al., 2012; Mackay and Boethling, 2000). Unlike the well-known lipophilic bioaccumulation mechanism of most of the POPs, the PFASs enter the food chain due to their proteinophilic characteristics (Goeritz et al., 2013). Despite studies reporting the occurrence of PFASs in organisms globally (Becker et al., 2010; Hong et al., 2015; Houde et al., 2006b, 2011; Martin et al., 2003; Munoz et al., 2017a; Sanganyado et al., 2018), few data are available for South American ecosystems (Dorneles et al., 2008; Leonel et al., 2008; Olivero-Verbel et al., 2006; Quinete et al., 2009), and there is a lack of PFAS bioaccumulation data for tropical ecosystems. Coastal tropical environments concentrate the greatest extent of biodiversity and productivity (Brown, 2014). Additionally, numerous freshwater and marine species use these ecosystems (e.g., mangroves and estuaries) as a nursery, shelter and feeding area, highlighting the importance of those environments as providers of a myriad of ecosystem services.

Despite its ecological importance, the Subaé estuary, located in northeastern Brazil (Fig. 1), has been subject to a high load of domestic and industrial effluents for many years (Hatje et al., 2006; Hatje and Barros, 2012; Krull et al., 2014; Tavares et al., 1999). Seafood harvested in the Subaé estuary is still the main protein consumed by the local people and may also represent a source of contaminant exposure for the locals (Souza et al., 2011, 2014). Moreover, the consumption of contaminated fish and seafood may be a significant pathway of exposure for humans in several countries, including Brazil (Pérez et al., 2014).

The present study addresses the paucity of data on PFAS accumulation in tropical environments by examining the transfer of these compounds through an estuarine food web. Samples were obtained from the Subaé estuary, Brazil, and included several species of bivalves, crustaceans, polychaeta, and fish, along with Suspended Particulate Matter (SPM), sediment, leave of mangrove trees, and algal biofilm. To the best of our knowledge, this is the first study investigating the bioaccumulation of PFAS in a tropical food web.

2. Methodology

2.1. Standards and reagents

Authentic standards of 3 (N-alkyl substituted) perfluorooctane sulfonamides (*N*-methylperfluoro-1-octanesulfonamide (MeFOSA), EtFOSA, and FOSA), 3 perfluoroctane sulfonamidoacetates (*N*-methylperfluoro-1-octanesulfonamidoacetic acid (MeFOSAA), Perfluoro-1-octanesulfonamidoacetic acid (FOSAA), and N-ethylperfluoro-1-octanesulfonamidoacetic acid (EtFOSAA)), 9 perfluoroalkyl carboxylates (C_5-C_{14} PFCAs: Perfluoropentanoic acid (PFPeA), Perfluoroheptanoic acid (PFHpA), Perfluorooctanoic acid (PFOA), Perfluorononanoic acid (PFNA), Perfluorodecanoic acid (PFDA), Perfluoroundecanoic acid (PFUnDA), Perfluorododecanoic acid (PFDoDA), Perfluorotridecanoic acid (PFTrDA), Perfluorotetradecanoic acid (PFTeDA), and 4 perfluoroalkyl sulfonates (PFSAs; Perfluorobutanesulfonic (PFBS), perfluorohexanesulfonic (PFHxS), PFOS, and Perfluorodecanesulfonic (PFDS)), as well as the isotopically-labelled standards $^{13}C_4$-PFHpA, $^{13}C_4$-PFOA, $^{13}C_5$-PFNA, $^{13}C_2$-PFDA, $^{13}C_2$-PFUnDA, $^{13}C_2$-PFDoDA, $^{18}O_2$-PFHxS, $^{13}C_4$-PFOS, $^{13}C_8$-FOSA, D_5-EtFOSA, D_3-MeFOSAA, D_5-EtFOSAA, and the recovery standards used to monitor internal standards performance $^{13}C_8$-PFOA and $^{13}C_8$-PFOS were purchased from Wellington Laboratories (Guelph, ON, Canada). Perfluoropentadecanoic acid (PFPeDA) was included in the target method as a qualitative analyte. A complete list of chemicals (Table S1) and reagents used for sample preparation is provided in the supporting information (SI).

2.2. Study area

The Todos os Santos Bay (BTS) (12°35′30″-13°07′30″S and 038°29′00″- 038°48′00″W) is characterized by a tropical humid climate, with an annual mean temperature around 25 °C and precipitation of 2100 mm, with mesotidal semidiurnal tides that control the currents inside the bay (Cirano and Lessa, 2007). The bay has three major tributaries: Paraguaçu River (56,300 km^2), Jaguaripe River (2200 km^2), and Subaé River (600 km^2). While Subaé is the smallest of the three rivers and has a low mean monthly discharge (9 m^3 s^{-1}), it is known to be a contamination hotspot, due to historically high anthropogenic pressure, especially regarding the introduction of trace elements to the estuarine

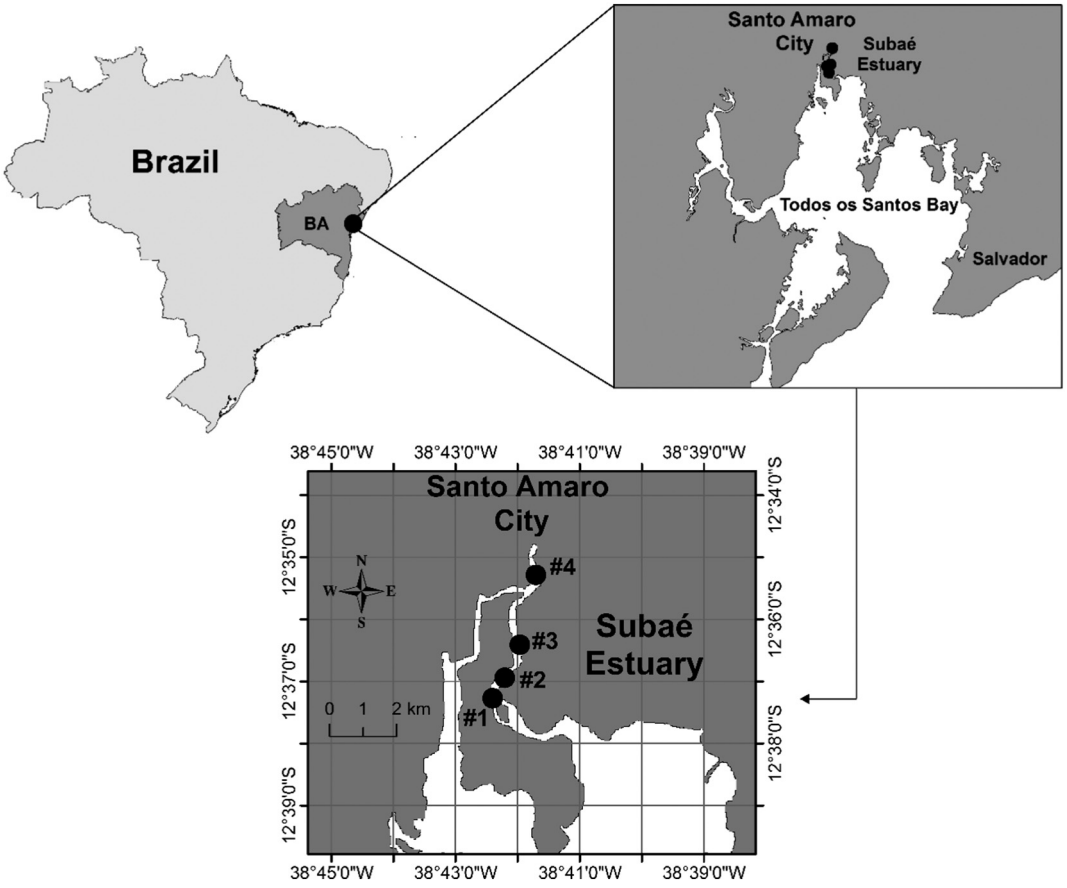

Fig. 1. Sediment and bivalve sampling stations of the Subaé, Todos os Santos Bay, BA, Brazil. Suspended particulate matter (SPM) was collected between sediment sampling stations (SPM#1 between #1 and #2, SPM#2 between #2 and #3, and SPM#3 between #3 and #4). Crustaceans and fishes were sampled between #1 and #4 sampling stations. Sampling point #1 is the closest station to the lower estuary area, while #4 (12° 35,451′S, 38° 41,672′ W) is the closest sampling point to Santo Amaro city.

system (Hatje et al., 2006; Krull et al., 2014). The anthropogenic activities over the last decade around Subaé river represent a risk to the biodiversity and ecological services in the estuary (Almeida et al., 2018; Gilljam et al., 2016; Hatje and Barros, 2012; Ribeiro et al., 2016). The literature regarding biocenosis in the BTS is scarce and is focused mostly on benthic assemblages (e.g. Alves et al., 2020; Magalhães and Barros, 2011; Silvany and Senna, 2019; Barros et al., 2012) and fish (e.g. Dias et al., 2011; Reis-Filho et al., 2019). Those studies show that estuaries of BTS are diverse (Alves et al., 2020; Loureiro et al., 2016; Reis-Filho et al., 2019), and present large variations in the distribution and abundance of assemblages among habitats and salinity gradients (Mariano and Barros, 2015). The presence of a diverse range of deposit feeder polychaeta connecting trophic levels is a remarkable characteristic of BTS food webs (Magalhães and Barros, 2011). Furthermore, the nesting activity of migratory high trophic level piscivorous birds was previously reported through the bay (Lunardi et al., 2012).

2.3. Sample collection

Twenty-one species of estuarine organisms were collected, including mangrove cupped oyster (*Crassostrea rhizophorae,* $n = 14$), mangrove shellfish (*Mytella guyanensis,* $n = 63$), blue crab (*Callinectes sapidus*, $n = 61$), clam (*Anomalocardia brasiliana*, $n = 5$), polychaeta (pooled), mangrove oyster (*Crassostrea brasiliana*, $n = 5$), stout tagelus (*Tagelus plebeius*, $n = 60$), crab (*Ucides cordatus*, $n = 6$), shrimp (*Litopenaeus* sp., $n = 18$), mangrove tree crab (*Goniopsis cruentata*, $n = 12$), mullet (*Mugil* sp., $n = 3$), torroto grunt (*Genyatremus luteus*, $n = 3$), mojarra (*Diapterus* sp., $n = 9$), silver jenny (*Eucinostomus* sp., $n = 1$), madamango sea catfish (*Cathorops spixii*, $n = 5$), fat snook (*Centropomus parallelus*, $n = 3$), drum (*Stellifer* sp., $n = 6$), trevally (*Caranx* sp., $n = 5$), catfish (*Aspistor luniscutis*, $n = 3$), common snook (*Centropomus undecimalis*, $n = 3$), and barbel drum (*Ctenosciaena gracilicirrhus*, $n = 1$). Biofilm, mangrove tree leaves, bivalves, crabs, and polychaeta were manually collected, while shrimp, and fish were sampled using a fixed gill net (authorization SISBIO n. 61269–3/28885–4). Almost all sampled species (i.e. bivalves, crabs, shrimp, and fish) are marketed locally by fishermen (Soares et al., 2011), and none of them are listed on the IUCN red list as being in danger of extinction. Samples were collected along a transect and pooled (i.e. sample points from #1 to #4; Fig. 1). Composite samples of mangrove tree leaves (*Rhizophora mangle*, *Laguncularia racemosa*, and *Avicenia* sp.), biofilm (pool of species), and sediments ($n = 4$) were collected with a clean spoon at the same location as the benthic organisms (i.e. from site #1 to #4) during the low tide, when sediment was exposed. The SPM was sampled during the flood tide at three points ($n = 3$) between the location of the sediment sampling sites (SPM#1: between #1 and #2; SPM#2 between #2 and #3; and SPM#3 between #3 and #4) (Fig. 1). For each organism, biometry information was recorded (Table S2). Samples of muscle, liver/hepatopancreas, for fish and crustaceans, soft tissues for bivalves, and whole body for polychaeta were collected. After dissection, tissue wet weight was recorded and thereafter the samples were freeze-dried. More details on sampling and pre-treatment are provided in the Supplementary Information (SI).

2.4. Targeted PFAS analysis

Samples were processed using the method previously described in Zabaleta et al. (2018). Further details are provided in the SI. Briefly,

isotopically labelled internal standards (2 ng) were added to 0.5 g of freeze-dried sample (biota or sediment), which were extracted with acetonitrile (ACN) aided by sonication. The method was repeated for SPM samples, but with methanol as the extraction solvent. All extracts were stored in the freezer prior to instrumental analysis.

Instrumental analysis was carried out by ultra-performance liquid chromatography-tandem mass spectrometry (UPLC-MS/MS; Waters) operated in negative electrospray ionization mode. Further details on target PFASs analysis and the mobile phase gradient profile can be found in the Table S3. Two precursor/product ion transitions, one for quantification and the other for qualification, were monitored per analyte (Table S4). Either isotope dilution or an internal standard approach using a linear calibration curve with 1/x weighting was used for the quantitative determination of target compounds. Branched isomers were determined semi-quantitatively using the calibration curve for the linear isomer.

2.5. Organic carbon (TOC), total nitrogen (TN) and their stable isotope analysis

Total organic carbon (TOC), total nitrogen (TN), and stable isotopic composition of N and C ($\delta^{15}N$ and $\delta^{13}C$) were analyzed in sediment, muscle of fish and crustaceans, whole body of polychaeta, and soft tissues of bivalves. Samples were treated with 0.1 M HCl for removing carbonates prior to TOC and $\delta^{13}C$ analysis. Stable isotope ratios were measured using an isotope ratio mass spectrometer (IsoPrime100, Isoprime, Cheadle, UK) coupled in continuous flow to an elemental analyser (vario MICRO cube, Elementar Analysensysteme GmbH, Hanau, Germany). Carbon and nitrogen isotope ratios were expressed as δ values (‰) relative to the Vienna PeeDee Belemnite (vPDB) standard and to atmospheric N_2, respectively. We used International Atomic Energy Agency (IAEA, Vienna, Austria) certified reference materials sucrose (IAEA-C6, $\delta^{13}C = -10.8 \pm 0.5$‰; mean ± SD), and ammonium sulfate as primary standards (IAEA-N2, $\delta^{15}N = 20.3 \pm 0.2$‰; mean ± SD), and sulphanilic acid as secondary analytical standard ($\delta^{13}C = -25.6 \pm 0.4$‰; $\delta^{15}N = -0.1 \pm 0.5$‰; mean ± SD in each case).

2.6. Quality control

Each batch of 16 samples included blanks ($n = 2$), duplicates ($n = 1$), and spiked samples ($n = 3$; 2 ng of individual PFAS per replicate). Limits of detection (LODs) were estimated based on a signal-to-noise ratio (S/N) of 3 (Table S5). LODs ranged between 0.02 and 1.11 ng mL^{-1}, depending on the tissue and organism analyzed. Calibration curves (1/x weighting) were constructed using concentrations from LOD to 150 ng mL^{-1} and determination coefficients (R^2) were always in the range of 0.994–0.998. Solvent blanks were run between calibration curve points in order to monitor carryovers.

PFAS concentrations in blanks were below LOD in all instances. Spike/recovery experiments showed generally good results, with most compounds displaying recoveries from 80 to 115%. For a few target compounds (e.g. PFPeA, PFTrDA, PFTeDA, and EtFOSA), recoveries were below 60% or above 120% in specific batches. PFPeA was infrequently detected (i.e. < 30% of organisms) and was not subject to TMF determination. Concentrations of PFHpA, PFTrDA, PFTeDA, and L-EtFOSA, data were used as-is, but these concentrations should be considered underreported for some species (see Table S6), due to low spike recoveries for these compounds. In addition, L-EtFOSA was not reported in polychaeta and SPM due to elevated recoveries for these matrices. Perfluorohexanoic acid (PFHxA) was excluded from the set of data due to interferences with the main transition ion monitored.

2.7. Data handling and statistical analyses

$\delta^{13}C$ and $\delta^{15}N$ values were used to determine the trophic web structure and the trophic position (TP) of the organisms analyzed. The following equation (Eq. (1)) was subsequently used to estimate the trophic position (TP):

$$TP_{consumer} = 2 + \frac{\delta^{15}N_{consumer} - \delta^{15}N_{bivalve}}{2.3‰} \quad (1)$$

where 2.3‰ is assumed to be the $\delta^{15}N$ trophic fractionation factor, according to McCutchan Jr et al. (2003). TP of the organisms was achieved by subtracting $\delta^{15}N$ of bivalves which displayed the lowest $\delta^{15}N$ values among animal species (*C. rhizophorae*; $\delta^{15}N = 8.05$, secondary consumer) and are assumed to have a trophic position of 2 (i.e. first consumer level). $\delta^{13}C$ values without lipid correction were used to predict organic matter sources.

The Trophic Magnification Factor (TMF) was obtained as 10^{slope} by plotting the logarithm-transformed concentration of a given PFAS against the TP. TMF calculations were carried out using soft tissue PFAS concentrations for bivalves, polychaeta and shrimp, and estimated whole-body PFAS concentrations (C_{wb}) for fish and crab according to the follow equation:

$$C_{wb} = \sum_{n=1} C_{tissue_{PFAS}} \times f_{tissue_{PFAS}} \quad (2)$$

where C_{tissue_PFAS} is the concentration of a given PFAS in a specific tissue and f_{tissue_PFAS} is the mass fraction of this tissue in the whole body. A separate calculation was performed for each individual organism based on specific tissue concentration. When the liver concentration was not available, it was estimated that the concentrations in liver were a factor of 10 higher than those of muscle for each compound based on the findings of Nania et al. (2009) (further details are provided in the SI).

Concentrations below the LOD (i.e. non-detected data) were imputed as follows: after ln-transformation, the data were fit to a cumulative normal distribution using a Generalized Reduced Gradient algorithm in the Solver add-in feature of Microsoft Excel. Thereafter, the cumulative normal distribution curve was used to estimate the missing data at the tail of the distribution as previously described by Schultes et al. (2019a, 2019b). The imputation of missing data was previously suggested as a good practice in order to avoid bias introduced in environmental analyses (Helsel, 2006) arising from the use of either raw data or one-half LOD (Borga et al., 2012). However, there is no established threshold for the percentage of left-censored data that could be used without causing a negative effect (i.e. inflation) of TMFs. Detection frequencies of 20 (Munoz et al., 2017a) to 40% (Simmonet-Laprade et al., 2019) have been used in bioaccumulation studies. In the present study, a moderate threshold (30%) was chosen in order to include compounds previously detected in the present study area (Gilljam et al., 2016).

To compare the effect of imputation versus substitution on calculated TMFs, a linear regression of TL versus PFAS concentration was carried out, using the most frequently detected compounds (i.e. L-PFOS, 93% detection frequency [df]), a compound with a moderate detection frequency (PFDoDA, 46% df) and the compound with lowest detection frequency (L-EtFOSA, 30% df) (Fig. S1). In all cases (i.e. regardless of detection frequency), substitution using one-half LOD produced lower TMF estimates compared to imputation (1.19 and 1.53 for L-PFOS, respectively; 0.55 and 0.94 for PFDoDA, and 1.05 and 1.80 for EtFOSA). This is probably due to insertion of fixed values into the data set (i.e. one-half LOD), which tends to decrease the slope of the linear regression (Borga et al., 2012; Helsel, 2006). While we conclude that substitution will produce lower TMFs than imputation, overall, the differences were minimal and did not affect neither the observed biodilution (i.e. TMF < 1) nor bioaccumulation (i.e. TMF >1) for any compound.

BioEstat 5.0 (Informer Technologies, Inc.), and R statistical software (R version 3.5.2, 2018-12-20) were used for statistical analyses, with a critical level of significance of the tests set at ($\alpha = 0.05$). All PFAS concentrations in tissues were log-transformed in order to fit the assumptions of the statistical analyses. Significant relationships between TMF

and PFAS concentrations were determined with nonparametric Kendall's τ_b correlations (Munoz et al., 2017a). Kendall's τ_b correlations was used due to the slightly better fit of this method to outliers when compared to the other nonparametric option (i.e. Spearman correlation), besides their smaller gross error sensitivity (GES) and a smaller asymptotic variance (AV) (Croux and Dehon, 2010; Khamis, 2008). Non-detects and Data Analysis (NADA) and Linear Mixed-Effects Models with Censored Responses (LMEC) R-packages were used to perform the analyses (Helsel, 2005; Munoz et al., 2017a).

3. Results and discussion

3.1. Subaé estuary food web dynamics

Using the bi-plots of $\delta^{15}N$ versus $\delta^{13}C$, and the feeding habits of each species (obtained from the literature (Barletta et al., 2019; Ferreira et al., 2019; Lira et al., 2018; Matich et al., 2017; Souza et al., 2018; Wellens et al., 2015)), we projected the energy flow across the food web. $\delta^{15}N$ values increased from mangrove tree leaves to omnivore fish, ranging from 1.06 to 13.8‰ (Fig. 2) and all species connect to each other within the isotopic mixing space. As expected, $\delta^{13}C$ in mangroves was typical (−29.3 to −26.6‰) of terrestrial plants which the first product of photosynthesis is a 3-carbon molecule (C_3 plants) (Minihan, 1983). A similar $\delta^{13}C$ composition was observed in sediment and SPM (−25.4 and − 26.9‰, respectively) indicating an influence of mangrove material in these matrices. $\delta^{13}C$ varied from −25.9‰ in bivalve (*C. rhizophorae)* to −17.4‰ in fish (*Caranx* sp.). Most bivalves displayed a close relationship with SPM (i.e. an average of 1.11‰ in $\delta^{13}C$ enrichment compared to SPM), except for *M. guyanensis* with an enrichment of 3.19‰, suggesting an additional source of carbon, probably from sediment (1.67‰ enrichment). Among crustaceans, *U. cordatus* displayed lower $\delta^{13}C$ values (−24.8‰) than other crustaceans, which agrees with their restricted leaf-feeder habit (Wellens et al., 2015), and sediment intake associated with leaves (average of 3.14‰ and 0.58‰, for carbon enrichment of leaves and sediment, respectively).

Litopenaeus sp. and *G. cruentata* displayed similar carbon isotopes ratios. These species display generalist feeding habits, but they are found in different locations within the mangrove forest. *G. cruentata* develop an important function in mangroves, recycling carbon in sediments in non-flooded areas (Wellens et al., 2015), while *Litopenaeus* sp. is an important link organism in this tropical food web (Lira et al., 2018; Vinagre et al., 2018), being the prey of several sampled fish in this study. Among fish, *C. undecimalis* showed distinctive low values of $\delta^{13}C$ (−23.8‰), even for a carnivore species showing a link to mangrove basal resource. In general, fish had $\delta^{15}N$ and $\delta^{13}C$ average values of 12.6 ± 0.84‰ and − 20.7 ± 1.91‰ (average ± SD), respectively. Polychaeta and shrimp represent the main food source for these fish species (Lira et al., 2018; Loureiro et al., 2016; Martins et al., 2017; Souza et al., 2018), which is aligned with C and N isotope results (Fig. 2). However, the large carbon variation between fish species may indicate an alternative source of food not considered in the present study and the fact they are not resident all the time in the studied region.

Bivalves represented the lowest TP of the food chain (TP = 2.0, *C. rhizophorae*; to TP = 2.6, *T. plebeius*), followed by crustaceans (TP = 2.1, *C. sapidus* to TP = 3.0, *G. cruentata*), polychaeta (TP = 3.6, pool of species) and fish (TP = 3.2, *Mugil* sp. to TP = 4.5, *C. gracilicirrhus*).

3.2. PFAS concentrations in biota

Sum ($\sum$) $_{22}$PFAS concentrations (and their isomers) above LOD in biota ranged from 0.28 ng g^{-1} ww wb (*C. rhizophorae*) to 3.72 ng g^{-1} ww wb (*Litopenaeus* sp.) (Fig. 3, Table S7) which is lower than the ranges reported for biota in subtropical ($\sum_{21}$PFASs; 0.50 to 17.5 ng g^{-1} ww wb) (Loi et al., 2011), temperate ($\sum_{23}$PFASs; 0.66 to 45.0 ng g^{-1} ww wb) (Munoz et al., 2017a) and polar areas ($\sum_{5}$PFASs 2.00 to 43.0 ng g^{-1} ww wb) (Tomy et al., 2009). PFOS was the most abundant PFAS among all species, with the exception of 3 bivalve samples (which were dominated by FOSA) and 1 fish (in which EtFOSA was dominant). Beyond the consistent observation of PFOS, the PFAS profile among individual species varied considerably. For example, most crustacean, polychaeta and bivalve samples contained relatively high levels of PFCAs compared to fish (Fig. 3). Also notable was that PFNA was the dominant PFCA among most crustacean, fish and polychaeta samples, but was generally not detected in bivalve. Differences in feed behavior, niche and protein contents of each group of organisms can help to explain this dissimilarity. Furthermore, more than one source of contaminants for those organisms could also play an important role in

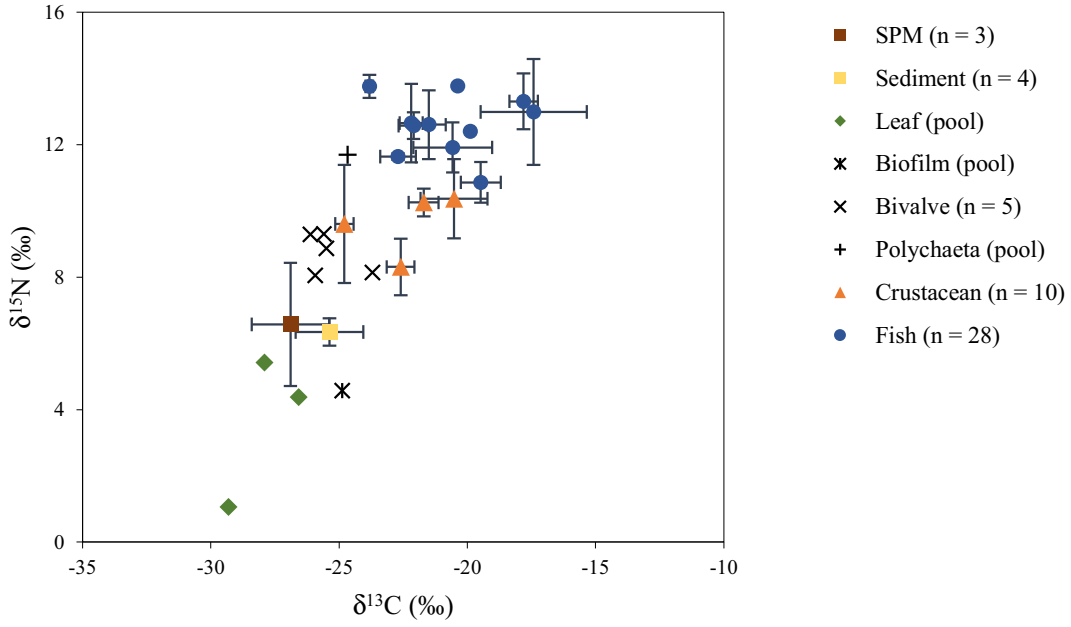

Fig. 2. Distribution of $\delta^{13}C$ and $\delta^{15}N$ in biotic and abiotic samples from the Subaé estuary, NE Brazil. Where SPM represents the suspended particulate matter and n the number of replicates analyzed.

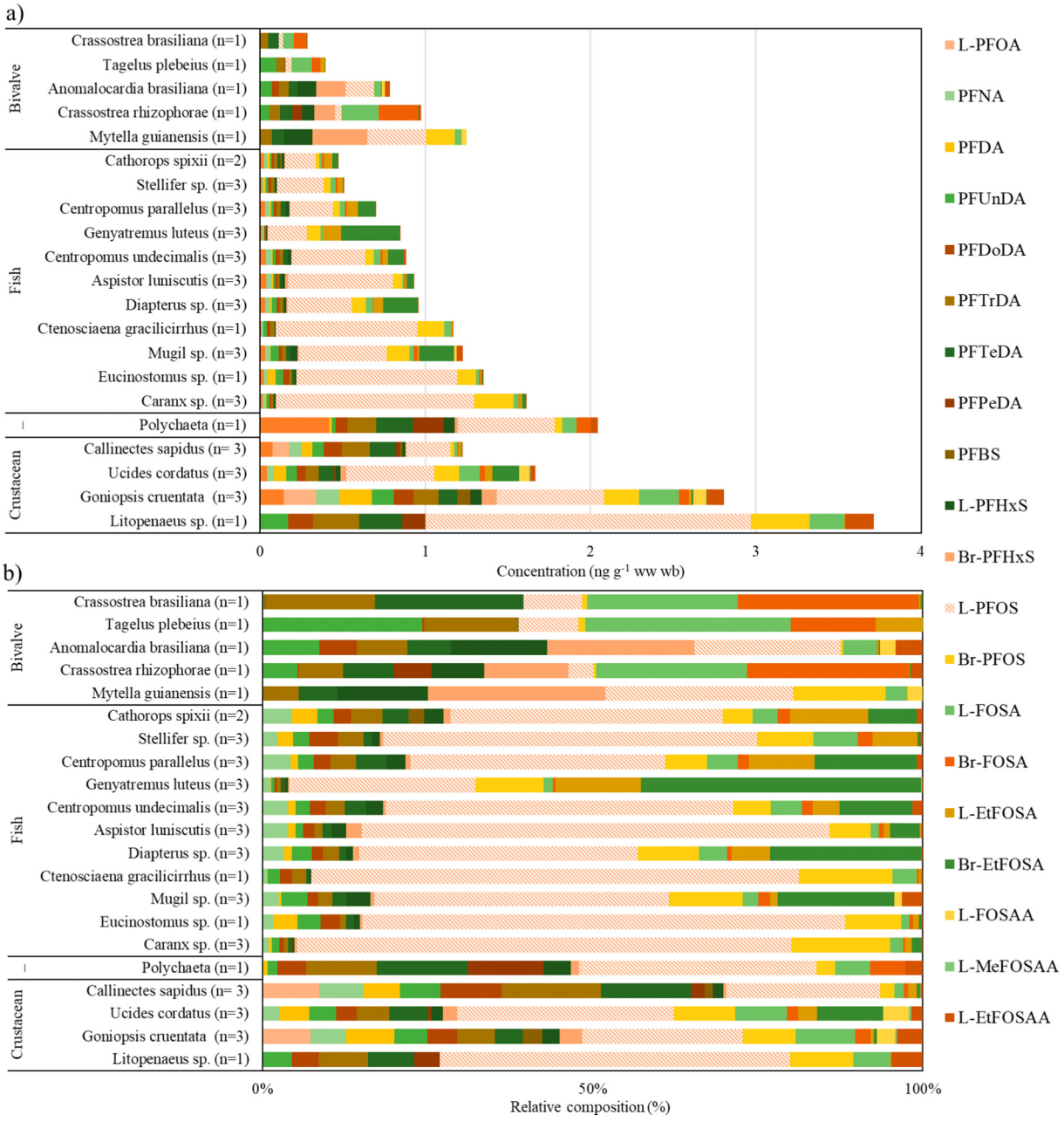

Fig. 3. Sum PFAS concentrations (ng g^{-1} wet weight (ww) for the whole body) measured in different organisms from the Subaé estuary (a); and relative PFAS profiles (normalized to 100%) (b). Number of organisms analyzed is shown in parentheses. EtFOSA was not reported for polychaeta. Br-PFOA, L-PFDS, Br-PFDS, L-MeFOSAA, Br-MeFOSAA, Br-FOSAA, MeFOSAA, and Me-EtFOSAA were not added to the figure due to either detection <LOD or low concentrations.

elucidating the PFASs accumulation patterns. While parts of the river can be under direct effect of sewage (consequently more exposed to AFFF and consumer products), other portions may be more affected by the leaching of forestry carrying Sulfluramid straight in the course of the river. Inputs of metals and nutrients have already been observed for different segments of the Subaé estuarine system (i.e. upper and lower estuary) (da Silva et al., 2017; Motta et al., 2018), but these data are unknown for PFASs. While most of the sampled specimens (i.e. bivalve, crustacean, and polychaeta) show either sessile behavior or limited mobility, fish can be exposed to a higher range of PFAS sources by swimming along the river and outside the estuary. Overall, the fish analyzed in the present study contained lower concentrations of the major PFCAs (PFNA, PFUnDA, PFDoDA, PFTrDA, PFTeDA) than other sampled organisms (Fig. 3). The reason for this is unclear but may indicate different exposure routes and/or PFAS accumulation in fish. Even though most PFCAs were correlated with one another ($p < 0.05$; Table S8), correlations between PFCAs and PFOS were rare, suggesting a different source of contaminants for these organisms.

In *Laguncularia racemosa* (white mangrove) and *Rhizophora mangle* (red mangrove) leaves, only FOSAA was observed (0.16 and 0.07 ng g^{-1} ww, respectively) (Table S9). The PFASs were not detected in the biofilm sample (i.e. concentrations < LOD). The elevated concentrations of PFAS, and in particular L-PFOS in shrimps (1.97 ng g^{-1} ww wb) when compared to other organisms are consistent with the results of Carlsson et al. (2016), who proposed that the higher protein content in shrimp, compared to fish, may lead to higher PFAS concentrations in the former species. The detritivore habit of shrimp may also help to explain the observed profile, since the SPM showed detectable PFAS concentrations, and together with sediment it is an important route of uptake of organic compounds for aquatic epibenthic organisms (Liu

et al., 2018). For fish, L-PFOS concentrations were an order of magnitude lower than those reported for fish from a subtropical region (Loi et al., 2011), but similar to those reported for several species of fish from the Arctic (Butt et al., 2010; Tomy et al., 2004) and temperate (Munoz et al., 2018) zones. Fish and bivalve from the present work also contained lower ΣPFAS when compared with two highly industrialized areas in Rio de Janeiro (Σ_8PFAS, Guanabara Bay and Paraíba do Sul River) (Quinete et al., 2009). While PFAS profiles were similar among the sampled areas, the EtFOSA transformation product FOSA was absent in samples from the tributaries and coastal water from Rio de Janeiro, as well as bivalves and fish muscles, whereas it was present only in the liver of a few fish samples. This is perhaps unsurprising considering that sales of Sulfluramid in Rio de Janeiro were ~ 100 times lower than in Bahia state (i.e. between 2014 and 2017) (IBAMA, 2017) and there are no known records of Eucalyptus and Pine plantations in the area. These previous studies together with the present work may suggest that, although Sulfluramid is not the only source of PFASs for the Subaé River, the use of this pesticide in the region might contribute to greater detection of FOSA in different environmental matrices.

3.3. PFAS concentrations in abiotic samples

In SPM ($n = 3$), 16 PFASs were detected, including 11 linear and 5 branched isomers. Sum PFAS concentrations ranged from 1.85 ng g^{-1} dw (SPM#1) to 7.25 ng g^{-1} dw (SPM#2) (Fig. 4, Table S10). PFNA was the predominant PFAS in samples closer to the lower estuary (Fig. 1), while PFUnDA was the prevalent compound in the upper estuary. In comparison, 5 linear PFAS isomers were detected in sediments ($n = 4$), with sum PFAS concentrations in the range of 0.10 ng g^{-1} dw (#2) to 0.33 ng g^{-1} dw (#1) (Table S11). L-PFOS and L-PFOA were detected in all sediment samples at very low concentrations (L-PFOS: 0.07–0.34 ng g^{-1} ww and L-PFOA: 0.35–0.79 ng g^{-1} ww), while PFOS was detected in all SPM samples ranging from 0.48 to 1.56 ng g^{-1} dw. The presence of L-EtFOSA in sediments and its degradation products (e.g. L-FOSA) in SPM suggest that, even though the overall concentrations in Subaé estuary are low, there may be a source of Sulfluramid in the region. The use of Sulfluramid in this area was previous suggested based on the high FOSA:PFOS detected in the Subaé river (Gilljam et al., 2016). The formicide can be mobilized from plantations to rivers and estuaries due to the leaching of contaminated soils. Stahl et al. (2013) and Zabaleta et al. (2018) suggested that leaching of soils caused by rainwater can promote the transport of EtFOSA and its degradation products to groundwater, rivers, and coastal zones. Sources other than Sulfluramid may also be important. For example, EtFOSAA, which was observed in SPM and sediment samples, does not form from EtFOSA, but rather from *N*-ethyl perfluorooctane sulfonamidoethanol (*N*-EtFOSE) a substance used widely in consumer products (e.g., food packaging) until 2002 (Benskin et al., 2013; Mejia Avendaño and Liu, 2015; USEPA, 2002).

Previous work indicated that sediments and soils can act as a sink for long chain PFASs, due to their sediment-water partitioning coefficient (Nascimento et al., 2018). Several species investigated in the present study display either benthic or demersal habits, which indicates that sediment exposure may represent a secondary source of PFASs for those organisms (Munoz et al., 2017a), in addition to bioaccumulation through the food chain. Nonetheless, estuarine areas are naturally dynamic and dilution of organic matter (and consequently PFASs) may occur at the site, thereby lowering observed concentrations in abiotic matrices.

3.4. Bioaccumulation of PFASs in the food chain

Bioaccumulation of PFASs in the present food web was evaluated for L- and Br-PFOS, PFTrDA, L-FOSA, PFUnDA, PFDoDA, PFTeDA, PFNA, and L- and Br-EtFOSA. TMFs and biomagnification factors (BMFs) greater than 1.0 are both considered reliable indicators of bioaccumulation (Borga et al., 2012). However, TMF is considered the most consistent way to characterize biomagnification of organic compounds over an entire food web (Franklin, 2016). TMFs were greater than 1 for L- and Br-PFOS, L- and Br-EtFOSA, and PFNA, indicating biomagnification across trophic levels. The concentration of four PFASs were significantly correlated with trophic level ($p < 0.05$; Table 1, Kendell's rank correlation;

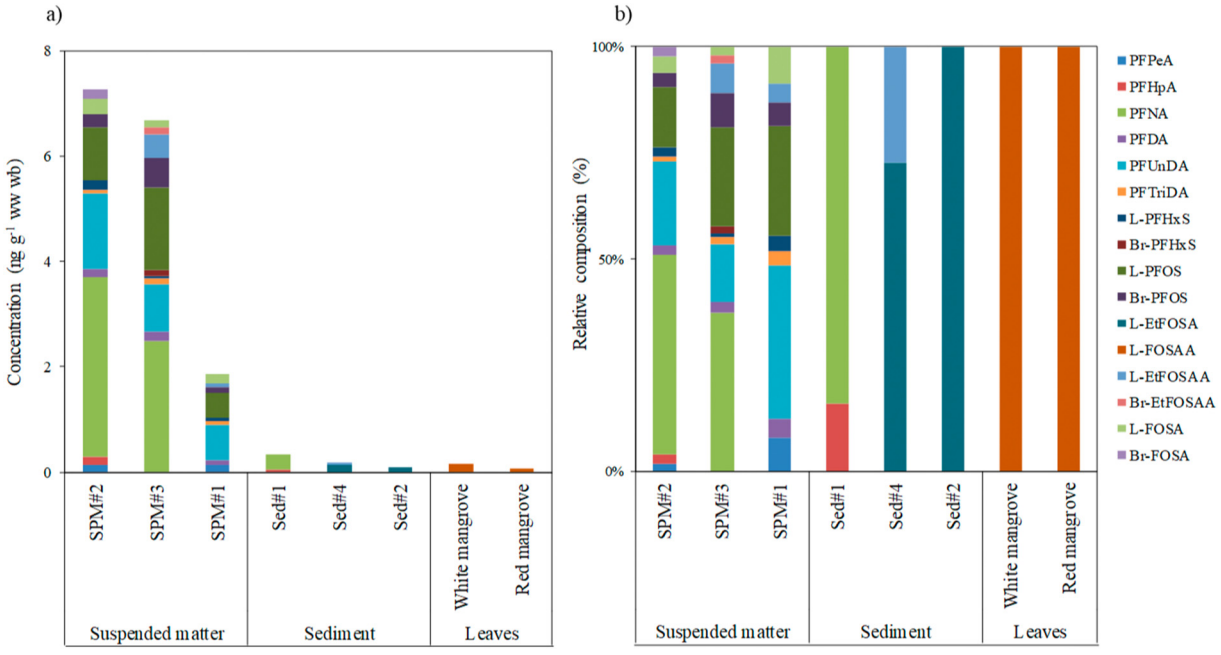

Fig. 4. Sum of PFAS concentrations in different samples from the Subaé estuary. (a) Concentrations are expressed in ng g^{-1} dry weight (dw) for sediment and SPM, and ng g^{-1} wet weight (ww) for leave and (b) corresponding composition profiles (relative abundance in % of Σ PFAS). Sed#3, Black mangrove and biofilm were excluded from this figure due no detected PFASs above LOD.

Table 1
Regressions of Log Concentration (concentrations expressed in ng g^{-1} ww whole body, min-max) vs TP (trophic position) in the whole food web, obtained with the NADA R-package [a], including the *p*-value of the regression, and Kendall's τ correlation coefficient (Helsel, 2005; Munoz et al., 2017a), compounds detection frequency[a], minimum and maximum whole-body wet weight concentrations, and Kendall's τ correlation coefficient[b]. EtFOSA was not reported for polychaeta.

Compound	Detection frequency (%)	Concentration average (min-max)	τ	TMF_{FW} (min–max)
L-PFOS	93	0.49 (0.05–1.97)	0.215	**1.53** (1.49–1.57)
Br-PFOS	73	0.09 (0.01–0.35)	0.052	1.53 (1.45–1.61)
PFTrDA	57	0.06 (0.01–0.28)	−0.386	**0.39** (0.38–0.40)
L-FOSA	54	0.06 (0.01–0.32)	−0.177	0.64 (0.62–0.66)
Br-FOSA	27	0.02 (0.01–0.24)	−0.119	0.83 (0.78–0.88)
PFUnDA	48	0.04 (0.01–0.17)	−0.226	**0.41** (0.39–0.43)
PFDoDA	46	0.03 (0.01–0.15)	−0.075	0.94 (0.88–1.00)
PFTeDA	46	0.05 (0.01–0.26)	−0.329	**0.62** (0.48–0.80)
PFNA	41	0.03 (0.01–0.42)	0.029	1.34 (1.27–1.42)
L-EtFOSA	30	0.03 (0.01–0.21)	0.112	1.80 (1.72–1.89)
Br-EtFOSA	30	0.09 (0.01–0.58)	−0.021	1.60 (1.38–1.86)

[a] Note that for detection frequency percentage of individual tissue (muscle, liver, hepatopancreas and soft tissue of bivalves and shrimp, $n = 56$) was used;
[b] It was obtained with the NADA R-package, including Kendall's τ correlation coefficient, the resulting trophic magnification factor ($TMF = 10^{slope}$) with the confidence interval of 95% (min – max). Bold numbers indicate significant regressions ($p < 0.05$).

Figs. S2 and S3), showing bioaccumulation of L-PFOS ($n = 44$; $\tau = 0.215$, $p = 0.043$) and biodilution of PFUnDA (n = 44; $\tau = -0.226$, $p = 0.034$), PFTrDA (n = 44; $\tau = -0.386$, $p \leq 0.001$), PFTeDA (n = 44; $\tau = -0.329$, $p = 0.002$). These data further highlight the potential of PFOS to be biomagnified through the tropical food web, which is consistent with prior studies in temperate and subtropical zones (Liu et al., 2018; Loi et al., 2011; Munoz et al., 2017a).

The absence of TMFs greater than 1 for most PFCAs was initially surprising, since bioaccumulation of C_9-C_{12} PFCAs has been reported elsewhere (Houde et al., 2006a; Munoz et al., 2017a). However, biodilution has also been reported for C_{13}-C_{14} PFCAs (Munoz et al., 2017a), which may be associated with the limitation of PFCAs with >10 fluorinated carbons to penetrate cell membranes due to their large molecular size (Conder et al., 2008; Hong et al., 2015). Alternatively, different sources of PFCAs for (1) bivalve, crustacean, and polychaeta, and (2) fish may also lead to an apparent lack of bioaccumulation. The low detection frequency of those compounds in organisms (i.e. from 41% (PFNA) to 57% (PFTrDA)) should also be considered.

The TMF determined here for PFOS was lower than previously reported for polar food webs, but similar to those in subtropical regions (Table S12) (Boisvert et al., 2019; Loi et al., 2011; Munoz et al., 2017a; Tomy et al., 2004). Variations in PFAS sources and/or proximity to sources may play a role in explaining these differences. For example, biota from the Northern Hemisphere tends to contain higher PFAS concentrations due to its proximity to point sources (Benskin et al., 2012). On the other hand, the ongoing use of EtFOSA in South America is unique, and exposure to this compound may cause PFOS accumulation in the Subaé estuarine wildlife due to its biotransformation (Gilljam et al., 2016; Nascimento et al., 2018). In addition, the upper trophic levels of polar food webs is occupied by top predator mammals, which means higher energy flow compared to tropical environments (Hobson et al., 2002). The lower TMFs in tropical aquatic ecosystems possibly reflects not only the lower input of PFASs, but also the structure of food webs that generally larger number of organisms, which may dilute the energy flows (and by extension, contaminants) among them (Borga et al., 2012). Also, variances in protein content in the blood and tissues of distinct species can result in variability in the accumulation of proteinophilic contaminants (Goeritz et al., 2013). Finally, climatic factors cannot be excluded (e.g. water temperature) and water chemistry, which may also have an impact on PFAS accumulation at different trophic levels (Vidal et al., 2019; Xu et al., 2014).

Surprisingly, the TMF for L-EtFOSA was above 1 (1.80), suggesting that this compound is bioaccumulating in the Subaé estuarine food chain. However, since EtFOSA was rarely detected throughout the food chain and also in low concentrations (0.01 to 0.21 ng g^{-1} ww wb, 30% detection frequency), TMFs should be interpreted cautiously, and further studies are warranted to corroborate these results. To the best of our knowledge, TMFs for EtFOSA have not been previously reported, but Tomy et al. (2004) showed Trophic Position-adjusted BMFs above 1 for species from the Arctic web food and suggested that organisms from different TP will metabolize/accumulate EtFOSA in different proportions. It is well-known that EtFOSA is readily biotransformed into FOSA in a few types of soil under aerobic conditions (Avendaño and Liu, 2015; Yin et al., 2018; Zabaleta et al., 2018), and also in earthworms (Zhao et al., 2018) but no studies have been carried out in estuarine environments. The presence of PreFOS (i.e. L-EtFOSA, L-EtFOSAA, and FOSA) in the Subaé biota may contribute indirectly to the occurrence of PFOS in top-level organisms via biotransformation, which may in turn contribute to increasing the TMF of PFOS (Simonnet-Laprade et al., 2019). This is supported by the observed biodilution of FOSA through the food web. Nonetheless, an in-depth evaluation of a larger range of PreFOS (and long-chain PFCAs precursors) will be necessary to confirm if TMF inflation is occurring due to PFAS precursors biotransformation.

Interestingly, when EtFOSA TMFs were re-calculated after splitting the organisms into 2 groups based on their trophic level (i.e. group 1: $n = 18$, TP 2.00 to 3.22; and group 2: $n = 26$, TP 3.56 to 4.49), a much higher TMF was observed for group 1 (2.65) compared to group 2 (0.22), suggesting that dilution of this compound is occurring in top organisms (Table S13). Besides the differences related to habitats and trophic level between the aforementioned groups, the first group (TP 2.00 to 3.22) is composed mainly by filter-feeding organisms, while the second group (TP 3.56 to 4.49) comprises mostly omnivorous organisms. The different feeding habits of those organisms can imply dissimilar contaminant exposure and hence uptake. Higher TMFs for bottom species were previously reported for other PFASs (Munoz et al., 2017a), and may point to greater efficiency in metabolizing and/or excreting xenobiotics in higher trophic level organisms. This metabolic difference in the accumulation/depuration of PFAA precursors between fish and invertebrates has been previously reported (Langberg et al., 2019).

The divergence in TMFs observed for EtFOSA upon splitting the food web into two groups was not observed for PFNA, L-PFOS, or Br-PFOS (Table S13). These substances all displayed TMFs >1 regardless of whether the food web was split into two groups or considered together, suggesting a linear trend in bioaccumulation among the sampled organisms. However, this was not the case for L-FOSA and C_{11}-C_{14} PFCAs. These substances all displayed apparent biodilution (i.e. TMF < 1) when the entire food web was considered but upon splitting the food web into two groups, L-FOSA, PFUnDA, and PFDoDA displayed bioaccumulation (i.e. TMFs>1) for both groups, while PFTrDA and PFTeDA displayed biodilution (i.e. TMF < 1) in the first group and bioaccumulation (i.e. TMF > 1) in the second group, which was the opposite of what was observed for EtFOSA. The factors controlling these phenomena are currently unclear and warrant further investigation, once the metabolization of PFASs by different organisms can help to explain the bioaccumulation pattern of these compounds through the food chain.

4. Conclusions

The bioaccumulation of PFASs was accessed in a tropical estuary in northeastern Brazil. PFASs were detected in all organisms analyzed, alongside with abiotic matrices (SPM and sediment). Unique accumulation profiles and low levels of PFASs were generally found in biotic and abiotic matrices when compared to subtropical, temperate and polar environments. Different patterns of bioaccumulation were observed through the sampled group of organisms (i.e. bivalve, crustacean, polychaeta, and fish), suggesting a set of factors (physical, chemical, biological and spatial) must be influencing on the PFAS assimilation. Moreover, PFOS, PFNA and EtFOSA were found to be bioaccumulating in this food chain, even though the bioaccumulation of the latter compound should be considered cautiously due to the low detection of EtFOSA in organisms. Nonetheless, the occurrence of PFASs in coastal marine biota is particularly concerning due to the potential for human exposure via consumption of these organisms. Further investigations into the sources of PFASs to Subaé estuary are warranted.

CRediT authorship contribution statement

Daniele A. de Miranda: Conceptualization, Investigation, Writing - original draft, Writing - review & editing. **Jonathan P. Benskin:** Writing - review & editing, Visualization, Resources. **Raed Awad:** Investigation, Writing - review & editing. **Gilles Lepoint:** Formal analysis. **Juliana Leonel:** Writing - review & editing, Visualization. **Vanessa Hatje:** Conceptualization, Writing - review & editing, Resources, Visualization, Supervision.

Declaration of competing interest

There are no conflicts of interest to declare.

Acknowledgments

This work was supported by Fundação de Amparo à Pesquisa do Estado da Bahia, Brazil (FAPESB) (PET0034/2012), CNPQ (441829/2014-7), and The Rufford Foundation (n° 2992-1). The authors were supported by FAPESB (D. Miranda, n° BOL0122/2017), Coordenação de Aperfeiçoamento de Pessoal de Nível Superior, Brazil (Ph.D. Sandwich, D. Miranda, n° 88881.188589/2018-01), and CNPq (V. Hatje - 304823/2018-0). J. Leonel were sponsored by CNPq (401443/2016-7 and 310786/2018-5). G. Lepoint is supported by the F.R.S.-FNRS. Thanks to Krishna Das for the collaboration with the Isotope Data. Thanks to Taiana A. Guimarães for the sample collection and sample preparation for the isotopic analyses.

Appendix A. Supplementary data

Supplementary data to this article can be found online at https://doi.org/10.1016/j.scitotenv.2020.142146.

References

Almeida, M., Nascimento, D.V., Mafalda, P.O., Patire, V.F., Albergaria-Barbosa, A.C.R., 2018. Distribution and sources of polycyclic aromatic hydrocarbons (PAHs) in surface sediments of a Tropical Bay influenced by anthropogenic activities (Todos os Santos Bay, BA, Brazil). Mar. Pollut. Bull. 137, 399–407. https://doi.org/10.1016/j.marpolbul.2018.10.040.

Alves, A.T., Petsch, D.K., Barros, F., 2020. Drivers of benthic metacommunity structure along tropical estuaries. Sci. Rep. 10, 1739. https://doi.org/10.1038/s41598-020-58631-1.

Avendaño, S., Liu, J., 2015. Production of PFOS from aerobic soil biotransformation of two perfluoroalkyl sulfonamide derivatives. Chemosphere 119, 1084–1090. https://doi.org/10.1016/j.chemosphere.2014.09.059.

Barclay, W.R., Meager, K.M., Abril, J.R., 1994. Heterotrophic production of long chain omega-3 fatty acids utilizing algae and algae-like microorganisms. J. Appl. Phycol. 6, 123–129. https://doi.org/10.1007/BF02186066.

Barletta, M., Lima, A.R.A., Costa, M.F., 2019. Distribution, sources and consequences of nutrients, persistent organic pollutants, metals and microplastics in South American estuaries. Sci. Total Environ. 651, 1199–1218. https://doi.org/10.1016/j.scitotenv.2018.09.276.

Barros, F., de Carvalho, G.C., Costa, Y., Hatje, V., 2012. Subtidal benthic macroinfaunal assemblages in tropical estuaries: generality amongst highly variable gradients. Mar. Environ. Res. 81, 43–52. https://doi.org/10.1016/j.marenvres.2012.08.006.

Becker, A.M., Gerstmann, S., Frank, H., 2010. Perfluorooctanoic acid and perfluorooctane sulfonate in two fish species collected from the Roter Main River, Bayreuth, Germany. Bull. Environ. Contam. Toxicol. 84, 132–135. https://doi.org/10.1007/s00128-009-9896-0.

Benskin, J.P., Muir, D.C.G., Scott, B.F., Spencer, C., De Silva, A.O., Kylin, H., Martin, J.W., Morris, A., Lohmann, R., Tomy, G., Rosenberg, B., Taniyasu, S., Yamashita, N., 2012. Perfluoroalkyl acids in the Atlantic and Canadian Arctic oceans. Environ. Sci. Technol. 46, 5815–5823. https://doi.org/10.1021/es300578x.

Benskin, J.P., Ikonomou, M.G., Gobas, F.A.P.C., Begley, T.H., Woudneh, M.B., Cosgrove, J.R., 2013. Biodegradation of N-ethyl perfluorooctane sulfonamido ethanol (EtFOSE) and EtFOSE-based phosphate diester (SAmPAP Diester) in marine sediments. Environ. Sci. Technol. 47, 1381–1389. https://doi.org/10.1021/es304336r.

Boisvert, G., Sonne, C., Rigét, F.F., Dietz, R., Letcher, R.J., 2019. Bioaccumulation and biomagnification of perfluoroalkyl acids and precursors in East Greenland polar bears and their ringed seal prey. Environ. Pollut. 252, 1335–1343. https://doi.org/10.1016/j.envpol.2019.06.035.

Borga, K., Kidd, K.A., Muir, D.C.G., Berglund, O., Conder, J.M., Gobas, F.A.P.C., Kucklick, J., Malm, O., Powell, D.E., 2012. Trophic magnification factors: considerations of ecology, ecosystems, and study design. Integr. Environ. Assess. Manag. 8, 64–84. https://doi.org/10.1002/ieam.244.

Brown, J.H., 2014. Why are there so many species in the tropics? J. Biogeogr. 41, 8–22. https://doi.org/10.1111/jbi.12228.

Buck, R.C., Franklin, J., Berger, U., Conder, J.M., Cousins, I.T., de Voogt, P., Jensen, A.A., Kannan, K., Mabury, S.A., van Leeuwen, S.P.J., 2011. Perfluoroalkyl and polyfluoroalkyl substances in the environment: terminology, classification, and origins. Integr. Environ. Assess. Manag. 7, 513–541. https://doi.org/10.1002/ieam.258.

Butt, C.M., Berger, U., Bossi, R., Tomy, G.T., 2010. Levels and trends of poly- and perfluorinated compounds in the arctic environment. Sci. Total Environ. 408, 2936–2965. https://doi.org/10.1016/j.scitotenv.2010.03.015.

Carlsson, P., Crosse, J.D., Halsall, C., Evenset, A., Heimstad, E.S., Harju, M., 2016. Perfluoroalkylated substances (PFASs) and legacy persistent organic pollutants (POPs) in halibut and shrimp from coastal areas in the far north of Norway: small survey of important dietary foodstuffs for coastal communities. Mar. Pollut. Bull. 105, 81–87. https://doi.org/10.1016/j.marpolbul.2016.02.053.

Cirano, M., Lessa, G.C., 2007. Oceanographic characteristics of BaÃ\-a de Todos os Santos, Brazil. Rev. Bras. GeofÃ\-sica 25, 363–387.

Conder, J.M., Hoke, R.A., Wolf, W. de, Russell, M.H., Buck, R.C., 2008. Are PFCAs bioaccumulative? A critical review and comparison with regulatory criteria and persistent lipophilic compounds. Environ. Sci. Technol. 42, 995–1003. https://doi.org/10.1021/es070895g.

Croux, C., Dehon, C., 2010. Influence functions of the Spearman and Kendall correlation measures. Stat. Methods Appt. 19, 497–515. https://doi.org/10.1007/s10260-010-0142-z.

da Silva, G.S., Gloaguen, T.V., Couto, C.F., Motta, P.N.S.D., 2017. Persistence and mobility of metals in an estuarine environment 25 years after closure of a lead smelter, Bahia State, Brazil. Environ. Earth Sci. 76, 548. https://doi.org/10.1007/s12665-017-6886-0.

da Silva, S.C., Pusceddu, F.H., dosSantos Barbosa Ortega, A., de Souza Abessa, D.M., Pereira, C.D.S., Maranho, L.A., 2019. Aqueous film-forming foams (AFFFs) are very toxic to aquatic microcrustaceans. Water Air Soil Pollut. 230, 260. doi:https://doi.org/10.1007/s11270-019-4291-x.

Dauchy, X., Boiteux, V., Colin, A., Bach, C., Rosin, C., Munoz, J.-F., 2019. Poly- and perfluoroalkyl substances in runoff water and wastewater sampled at a firefighter training area. Arch. Environ. Contam. Toxicol. 76, 206–215. https://doi.org/10.1007/s00244-018-0585-z.

Dias, J.F., Gonçalves, A.M., Fernandez, W.S., Silbiger, H.L.N., Fiadi, C.B., Schmidt, T.C. dos S., 2011. Ichthyofauna in an estuary of the Mataripe area, Todos os Santos Bay, Bahia, Brazil. Braz. J. Oceanogr. 59 (1). https://doi.org/10.1590/S1679-87592011000100006.

Dorneles, P.R., Lailson-Brito, J., Azevedo, A.F., Meyer, J., Vidal, L.G., Fragoso, A.B., Torres, J.P., Malm, O., Blust, R., Das, K., 2008. High accumulation of perfluorooctane sulfonate (PFOS) in marine tucuxi dolphins (Sotalia guianensis) from the Brazilian coast. Environ. Sci. Technol. 42, 5368–5373. https://doi.org/10.1021/es800702k.

Ferreira, G.V.B., Barletta, M., Lima, A.R.A., Morley, S.A., Costa, M.F., 2019. Dynamics of marine debris ingestion by profitable fishes along the estuarine Ecocline. Sci. Rep. 9, 13514. https://doi.org/10.1038/s41598-019-49992-3.

Franklin, J., 2016. How reliable are field-derived biomagnification factors and trophic magnification factors as indicators of bioaccumulation potential? Conclusions from a case study on per- and polyfluoroalkyl substances. Integr. Environ. Assess. Manag. 12, 6–20. https://doi.org/10.1002/ieam.1642.

Giesy, J.P., Kannan, K., 2001. Global distribution of perfluorooctane sulfonate in wildlife. Environ. Sci. Technol. 35, 1339–1342. https://doi.org/10.1021/es001834k.

Gilljam, J.L., Leonel, J., Cousins, I.T., Benskin, J.P., 2016. Is ongoing Sulfluramid use in South America a significant source of perfluorooctanesulfonate (PFOS)? Production inventories, environmental fate, and local occurrence. Environ. Sci. Technol. 50, 653–659. https://doi.org/10.1021/acs.est5b04544.

Goeritz, I., Falk, S., Stahl, T., Schaefers, C., Schlechtriem, C., 2013. Biomagnification and tissue distribution of perfluoroalkyl substances (PFASs) in market-size rainbow trout (Oncorhynchus mykiss). Environ. Toxicol. Chem. 32, 2078–2088. https://doi.org/10.1002/etc.2279.

Gribble, M.O., Karimi, R., Feingold, B.J., Nyland, J.F., O'Hara, T.M., Gladyshev, M.I., Chen, C.Y., 2016. Mercury, selenium and fish oils in marine food webs and implications for

human health. J. Mar. Biol. Assoc. 96, 43–59. https://doi.org/10.1017/S0025315415001356 UNITED KINGDOM.
Hatje, V., Barros, F., 2012. Overview of the 20th century impact of trace metal contamination in the estuaries of Todos os Santos Bay: past, present and future scenarios. Mar. Pollut. Bull. 64, 2603–2614. https://doi.org/10.1016/j.marpolbul.2012.07.009.
Hatje, V., Barros, F., Figueiredo, D.G., Santos, V.L.C.S., Peso-Aguiar, M.C., 2006. Trace metal contamination and benthic assemblages in Subaé estuarine system, Brazil. Mar. Pollut. Bull. 52, 982–987. https://doi.org/10.1016/j.marpolbul.2006.04.016.
Helsel, D.R., 2005. Nondectects and Data Analysis; Statistics for Censored Environmental Data. John Wiley and Sons.
Helsel, D.R., 2006. Fabricating data: how substituting values for nondetects can ruin results, and what can be done about it. Chemosphere 65, 2434–2439. https://doi.org/10.1016/j.chemosphere.2006.04.051.
Hobson, K.A., Fisk, A., Karnovsky, N., Holst, M., Gagnon, J.-M., Fortier, M., 2002. A stable isotope (δ13C, δ15N) model for the North Water food web: implications for evaluating trophodynamics and the flow of energy and contaminants. Deep Sea Res. Part II Top. Stud. Oceanogr. 49, 5131–5150. https://doi.org/10.1016/S0967-0645(02)00182-0.
Hong, S., Khim, J.S., Wang, T., Naile, J.E., Park, J., Kwon, B.-O., Song, S.J., Ryu, J., Codling, G., Jones, P.D., Lu, Y., Giesy, J.P., 2015. Bioaccumulation characteristics of perfluoroalkyl acids (PFAAs) in coastal organisms from the west coast of South Korea. Chemosphere 129, 157–163. https://doi.org/10.1016/j.chemosphere.2014.06.023.
Houde, M., Bujas, T.A.D., Small, J., Wells, R.S., Fair, P.A., Bossart, G.D., Solomon, K.R., Muir, D.C.G., 2006a. Biomagnification of perfluoroalkyl compounds in the bottlenose dolphin (Tursiops truncatus) food web. Environ. Sci. Technol. 40, 4138–4144. https://doi.org/10.1021/es060233b.
Houde, M., Martin, J.W., Letcher, R.J., Solomon, K.R., Muir, D.C.G., 2006b. Biological monitoring of polyfluoroalkyl substances: a review. Environ. Sci. Technol. 40, 3463–3473. https://doi.org/10.1021/es052580b.
Houde, M., De Silva, A.O., Muir, D.C.G., Letcher, R.J., 2011. Monitoring of perfluorinated compounds in aquatic biota: an updated review. Environ. Sci. Technol. 45, 7962–7973. https://doi.org/10.1021/es104326w.
IBAMA, Institute of Environment and Natural Resources, 2017. Sales of Active Ingredientsby State Brasília.
Khamis, H., 2008. Measures of association: how to choose? J. Diagnostic Med. Sonogr. 24, 155–162. https://doi.org/10.1177/8756479308317006.
Krull, M., Abessa, D.M.S., Hatje, V., Barros, F., 2014. Integrated assessment of metal contamination in sediments from two tropical estuaries. Ecotoxicol. Environ. Saf. 106, 195–203. https://doi.org/10.1016/j.ecoenv.2014.04.038.
Langberg, H.A., Breedveld, G.D., Grønning, H.M., Kvennås, M., Jenssen, B.M., Hale, S.E., 2019. Bioaccumulation of fluorotelomer sulfonates and perfluoroalkyl acids in marine organisms living in aqueous film-forming foam impacted waters. Environ. Sci. Technol. 53, 10951–10960. https://doi.org/10.1021/acs.est.9b00927.
Lau, C., Anitole, K., Hodes, C., Lai, D., Pfahles-Hutchens, A., Seed, J., 2007. Perfluoroalkyl acids: a review of monitoring and toxicological findings. Toxicol. Sci. 99, 366–394.
Leonel, J., Kannan, K., Tao, L., Fillmann, G., Montone, R.C., 2008. A baseline study of perfluorochemicals in Franciscana dolphin and Subantarctic fur seal from coastal waters of Southern Brazil. Mar. Pollut. Bull. 56, 778–781. https://doi.org/10.1016/j.marpolbul.2008.01.012.
Lira, A., Angelini, R., Le Loc'h, F., Menard, F., Lacerda, C., Fredou, T., Fredou, F.L., 2018. Trophic flow structure of a neotropical estuary in northeastern Brazil and the comparison of ecosystem model indicators of estuaries. J. Mar. Syst. 182, 31–45. https://doi.org/10.1016/j.jmarsys.2018.02.007.
Liu, W., He, W., Wu, J., Qin, N., He, Q., Xu, F., 2018. Residues, bioaccumulations and biomagnification of perfluoroalkyl acids (PFAAs) in aquatic animals from Lake Chaohu, China. Environ. Pollut. 240, 607–614. https://doi.org/10.1016/j.envpol.2018.05.001.
Loi, E., Zhao, S., Wang, B., Zhu, L., Liang, T., Chen, M., Yang, L., Lv, J., Liu, L., 2011. Trophic magnification of poly- and perfluorinated compounds in a subtropical food web. Environ. Sci. Technol. 45, 598–678. https://doi.org/10.1080/10643389.2011.627016.
Loureiro, S.N., Reis-Filho, J.A., Giarrizzo, T., 2016. Evidence for habitat-driven segregation of an estuarine fish assemblage. J. Fish Biol. 89, 804–820. https://doi.org/10.1111/jfb.13017.
Lunardi, V.O., Macedo, R.H., Granadeiro, J.P., Palmeirim, J.M., 2012. Migratory flows and foraging habitat selection by shorebirds along the northeastern coast of Brazil: the case of Baía de Todos os Santos. Estuar. Coast. Shelf Sci. 96, 179–187. https://doi.org/10.1016/j.ecss.2011.11.001.
Mackay, D., Boethling, R.S., 2000. Bioconcentration and biomagnification in the aquatic environment. Handbook of Property Estimation Methods for Chemicals. CRC Press, pp. 211–254.
Magalhães, W.F., Barros, F., 2011. Structural and functional approaches to describe polychaete assemblages: ecological implications for estuarine ecosystems. Mar. Freshw. Res. 62, 918–926.
Mariano, D.L.S., Barros, F., 2015. Intertidal benthic macrofaunal assemblages: changes in structure along entire tropical estuarine salinity gradients. J. Mar. Biol. Assoc. United Kingdom 95, 5–15. https://doi.org/10.1017/S002531541400126X.
Martin, J.W., Mabury, S.A., Solomon, K.R., Muir, D.C.G., 2003. Bioconcentration and tissue distribution of perfluorinated acids in rainbow trout (Oncorhynchus mykiss). Environ. Toxicol. Chem. 22, 196–204.
Martins, M.M., Mendonça, H.S., Rodrigues, S.S., Araújo, F.G., 2017. Trophic ecology of two syntopic sciaenid species (Micropogonias furnieri (Desmarest, 1823) and Ctenosciaena gracilicirrhus) (Metzelaar, 1919) in a tropical bay in south-eastern Brazil. J. Appl. Ichthyol. 33, 740–745. https://doi.org/10.1111/jai.13360.
Matich, P., Ault, J.S., Boucek, R.E., Bryan, D.R., Gastrich, K.R., Harvey, C.L., Heithaus, M.R., Kiszka, J.J., Paz, V., Rehage, J.S., Rosenblatt, A.E., 2017. Ecological niche partitioning within a large predator guild in a nutrient-limited estuary. Limnol. Oceanogr. 62, 934–953. https://doi.org/10.1002/lno.10477.
McCutchan Jr., J.H., Lewis Jr., W.M., Kendall, C., McGrath, C.C., 2003. Variation in trophic shift for stable isotope ratios of carbon, nitrogen, and sulfur. Oikos 102, 378–390. https://doi.org/10.1034/j.1600-0706.2003.12098.x.
MDIC, 2019. Bureau of Foreign Trade [WWW document]. URL. http://comexstat.mdic.gov.br/pt/geral.
Minihan, S., 1983. Principles of biochemistry by Albert L Lehninger. pp 1011. 11. Worth Publishers, New York, pp. 41–42. https://doi.org/10.1016/0307-4412(83)90020-1 1982. £13. ISBN 0-87901-136-X. Biochem. Educ.
(Ministério do Meio Ambiente) MMA, 2015a. Inventário Nacional de Novos Poluentes Orgânicos Persistentes (Novos POPs) de uso industrial - Convenção de Estocolmo. vol 166. Ministério do Meio Ambiente, Brasília.
(Ministério do Meio Ambiente) MMA, 2015b. Plano Nacional de Implementação da Convenção de Estocolmo no Brasil. Ministério do Meio Ambiente.
Motta, P.N.D.S., Gloaguen, T.V., Couto, C.F., Merdy, P., Lucas, Y., 2018. Hydrogeochemistry of the Subaé River Impacted by Lead Smelting Activities, Bahia State, Brazil: Geochemical Characterization and Fluxes of Metals. https://doi.org/10.1007/s11270-018-4032-6.
Munoz, G., Budzinski, H., Babut, M., Drouineau, H., Lauzent, M., Menach, K. Le, Lobry, J., Selleslagh, J., Simonnet-Laprade, C., Labadie, P., 2017a. Evidence for the trophic transfer of perfluoroalkylated substances in a temperate macrotidal estuary. Environ. Sci. Technol. 51, 8450–8459. https://doi.org/10.1021/acs.est.7b02399.
Munoz, G., Labadie, P., Botta, F., Lestremau, F., Lopez, B., Geneste, E., Pardon, P., Dévier, M.-H., Budzinski, H., 2017b. Occurrence survey and spatial distribution of perfluoroalkyl and polyfluoroalkyl surfactants in groundwater, surface water, and sediments from tropical environments. Sci. Total Environ. 607–608, 243–252. https://doi.org/10.1016/j.scitotenv.2017.06.146.
Munoz, G., Fechner, L.C., Geneste, E., Pardon, P., Budzinski, H., Labadie, P., 2018. Spatio-temporal dynamics of per and polyfluoroalkyl substances (PFASs) and transfer to periphytic biofilm in an urban river: case-study on the River Seine. Environ. Sci. Pollut. Res. 25, 23574–23582. https://doi.org/10.1007/s11356-016-8051-9.
Nagamoto, N.S., Forti, L.C., Andrade, A.P.P., Boaretto, M.A.C., Wilcken, C.F., 2004. Method for the evaluation of insecticidal activity over time in Atta sexdens rubropilosa workers (Hymenoptera: Formicidae). SOCIOBIOLOGY 44, 413–431.
Nania, V., Pellegrini, G.E., Fabrizi, L., Sesta, G., De Sanctis, P., Lucchetti, D., Di Pasquale, M., Coni, E., 2009. Monitoring of perfluorinated compounds in edible fish from the Mediterranean Sea. Food Chem. 115, 951–957. https://doi.org/10.1016/j.foodchem.2009.01.016.
Nascimento, R.A., Nunoo, D.B.O., Bizkarguenaga, E., Schultes, L., Zabaleta, I., Benskin, J.P., Spanó, S., Leonel, J., 2018. Sulfluramid use in Brazilian agriculture: a source of per- and polyfluoroalkyl substances (PFASs) to the environment. Environ. Pollut. 242, 1436–1443. https://doi.org/10.1016/J.ENVPOL.2018.07.122.
Olivero-Verbel, J., Tao, L., Johnston-Restrepo, B., Guette-Fernandez, J., Baldiris-Avila, R., O'byrne-Hoyos, I., Kannan, K., 2006. Perfluorooctanesulfonate and related fluorochemicals in biological samples from the north coast of Colombia. Environ. Pollut. 142, 367–372. https://doi.org/10.1016/j.envpol.2005.09.022.
Pérez, F., Llorca, M., Köck-Schulmeyer, M., Škrbić, B., Oliveira, L.S., da Boit Martinello, K., Al-Dhabi, N.A., Antić, I., Farré, M., Barceló, D., 2014. Assessment of perfluoroalkyl substances in food items at global scale. Environ. Res. 135, 181–189. https://doi.org/10.1016/j.envres.2014.08.004.
Quinete, N., Wu, Q., Zhang, T., Yun, S.H., Moreira, I., Kannan, K., 2009. Specific profiles of perfluorinated compounds in surface and drinking waters and accumulation in mussels, fish, and dolphins from southeastern Brazil. Chemosphere 77, 863–869. https://doi.org/10.1016/j.chemosphere.2009.07.079.
Reis-Filho, J.A., Schmid, K., Harvey, E.S., Giarrizzo, T., 2019. Coastal fish assemblages reflect marine habitat connectivity and ontogenetic shifts in an estuary-bay-continental shelf gradient. Mar. Environ. Res. 148, 57–66. https://doi.org/10.1016/j.marenvres.2019.05.004.
Ribeiro, L.F., Eça, G.F., Barros, F., Hatje, V., 2016. Impacts of shrimp farming cultivation cycles on macrobenthic assemblages and chemistry of sediments. Environ. Pollut. 211, 307–315. https://doi.org/10.1016/j.envpol.2015.12.031.
Rossato, F.G.F.S., Susaeta, A., Adams, D.C., Hidalgo, I.G., de Araujo, T.D., de Queiroz, A., 2018. Comparison of revealed comparative advantage indexes with application to trade tendencies of cellulose production from planted forests in Brazil, Canada, China, Sweden, Finland and the United States. For. Policy Econ. 97, 59–66. https://doi.org/10.1016/j.forpol.2018.09.007.
Routti, H., Aars, J., Fuglei, E., Hanssen, L., Lone, K., Polder, A., Pedersen, A.O., Tartu, S., Welker, J.M., Yoccoz, N.G., 2017. Emission changes dwarf the influence of feeding habits on temporal trends of per- and polyfluoroalkyl substances in two Arctic top predators. Environ. Sci. Technol. 51, 11996–12006. https://doi.org/10.1021/acs.est.7b03585.
Sanganyado, E., Rajput, I.R., Liu, W., 2018. Bioaccumulation of organic pollutants in Indo-Pacific humpback dolphin: a review on current knowledge and future prospects. Environ. Pollut. 237, 111–125. https://doi.org/10.1016/j.envpol.2018.01.055.
Schaider, L., Balan, S., Blum, A., Andrews, D., Strynar, M., Dickinson, M., Lunderberg, D., Lang, J., Peaslee, G., 2018. Fluorinated compounds in U.S. fast food packaging. Environ. Sci. Technol. 4, 105–111. https://doi.org/10.1002/etc.3500.Molecular.
Schultes, L., Vestergren, R., Volkova, K., Westberg, E., Jacobson, T., Benskin, J.P., 2018. Per- and polyfluoroalkyl substances and fluorine mass balance in cosmetic products from the Swedish market: implications for environmental emissions and human exposure. Environ Sci Process Impacts 20, 1680–1690. https://doi.org/10.1039/c8em00368h.
Schultes, L., Benskin, J.P., Majumdar, A., Peaslee, G.F., Brockman, J.D., McGuinness, S.R., Ngwenyama, R.A., Wilkinson, J.T., Sandblom, O., 2019a. Total fluorine measurements in food packaging: how do current methods perform? Environ. Sci. Technol. Lett. 6, 73–78. https://doi.org/10.1021/acs.estlett.8b00700.

Schultes, L., Sandblom, O., Broeg, K., Bignert, A., Benskin, J., 2019b. Temporal trends (1981–2013) of per- and polyfluoroalkyl substances and total fluorine in Baltic cod (Gadus morhua). Environ. Toxicol. Chem. 39 (2), 300–309. https://doi.org/10.1002/etc.4615.

Silvany, L., Senna, A.R., 2019. Three new species of Colomastix Grube, 1861 (Amphipoda: Colomastigidea) from Todos-os-Santos Bay, northeastern Brazilian coast, with identification keys to Atlantic Ocean species. Zootaxa 4629 (4). https://doi.org/10.11646/zootaxa.4629.4.3 9 Jul. 2019.

Simmonet-Laprade, C., Budzinski, H., Babut, M., Le Menach, K., Munoz, G., Lauzent, M., Ferrari, B.J.D., Labadie, P., 2019. Investigation of the spatial variability of poly- and perfluoroalkyl substance trophic magnification in selected riverine ecosystems. Sci. Total Environ. 686, 393–401. https://doi.org/10.1016/j.scitotenv.2019.05.461.

Simonnet-Laprade, C., Budzinski, H., Maciejewski, K., Le Menach, K., Santos, R., Alliot, F., Goutte, A., Labadie, P., 2019. Biomagnification of perfluoroalkyl acids (PFAAs) in the food web of an urban river: assessment of the trophic transfer of targeted and unknown precursors and implications. Environ Sci Process Impacts https://doi.org/10.1039/C9EM00322C.

Soares, L.S.H., Lopez, J.P., Muto, E.Y., 2011. Giannini. Capture fishery in northern Todos os Santos Bay, tropical southwestern Atlantic, Brazil. Brazilian J. Oceanogr, R.

Song, X., Vestergren, R., Shi, Y., Huang, J., Cai, Y., 2018. Emissions, transport, and fate of emerging per- and polyfluoroalkyl substances from one of the major fluoropolymer manufacturing facilities in China. Environ. Sci. Technol. https://doi.org/10.1021/acs.est.7b06657.

Souza, M.M., Windmöller, C.C., Hatje, V., 2011. Shellfish from Todos os Santos Bay, Bahia, Brazil: treat or threat? Mar. Pollut. Bull. 62, 2254–2263. https://doi.org/10.1016/j.marpolbul.2011.07.010.

Souza, M.M., Windmöller, C.C., Hatje, V., 2014. Corrigendum to “shellfish from Todos os Santos Bay, Bahia, Brazil: treat or threat?” [mar. Pollut. Bull. 62 (2011) 2254–2263]. Mar. Pollut. Bull. 88, 401. https://doi.org/10.1016/j.marpolbul.2014.07.027.

Souza, I. da C., Arrivabene, H.P., Craig, C.A., Midwood, A.J., Thornton, B., Matsumoto, S.T., Elliott, M., Wunderlin, D.A., Monferrán, M.V., Fernandes, M.N., 2018. Interrogating pollution sources in a mangrove food web using multiple stable isotopes. Sci. Total Environ. 640–641, 501–511. https://doi.org/10.1016/j.scitotenv.2018.05.302.

Stahl, T., Riebe, R.A., Falk, S., Failing, K., Brunn, H., 2013. Long-term lysimeter experiment to investigate the leaching of perfluoroalkyl substances (PFASs) and the carry-over from soil to plants: results of a pilot study. J. Agric. Food Chem. 61, 1784–1793. https://doi.org/10.1021/jf305003h.

Tavares, T.M., Beretta, M., Costa, M.C., 1999. Ratio of DDT/DDE in the all saints bay, Brazil and its use in environmental management. Chemosphere 38, 1445–1452. https://doi.org/10.1016/S0045-6535(98)00546-3.

Tomy, G.T., Budakowski, W., Halldorson, T., Helm, P.A., Stern, G.A., Friesen, K., Pepper, K., Tittlemier, S.A., Fisk, A.T., 2004. Fluorinated organic compounds in an eastern arctic marine food web. Environ. Sci. Technol. 38, 6475–6481. https://doi.org/10.1021/es049620g.

Tomy, G.T., Pleskach, K., Ferguson, S.H., Hare, J., Stern, G., MacInnis, G., Marvin, C.H., Loseto, L., 2009. Trophodynamics of some PFCs and BFRs in a Western Canadian Arctic marine food web. Environ. Sci. Technol. 43, 4076–4081. https://doi.org/10.1021/es900162n.

UNSCPOPs, 2009. No Title [WWW Document]. Stock. Conv. Persistent Org. Pollut URL. http://chm.pops.int/.

USEPA, 2002. Perfluoroalkyl Sulfonates; Significant New Use Rule (SNUR) (Washington, DC).

Vidal, A., Lafay, F., Daniele, G., Vulliet, E., Rochard, E., Garric, J., Babut, M., 2019. Does water temperature influence the distribution and elimination of perfluorinated substances in rainbow trout (Oncorhynchus mykiss)? Environ. Sci. Pollut. Res. 26, 16355–16365. https://doi.org/10.1007/s11356-019-05029-w.

Vinagre, C., Mendonça, V., Flores, A.A.V., Baeta, A., Marques, J.C., 2018. Complex food webs of tropical intertidal rocky shores (SE Brazil) – an isotopic perspective. Ecol. Indic. 95, 485–491. https://doi.org/10.1016/j.ecolind.2018.07.065.

Wang, Z., Dewitt, J.C., Higgins, C.P., Cousins, I.T., 2017. A never-ending story of per- and polyfluoroalkyl substances (PFASs)? Environ. Sci. Technol. 51, 2508–2518. https://doi.org/10.1021/acs.est.6b04806.

Wang, Y., Zhong, Y., Li, J., Zhang, J., Lyu, B., Zhao, Y., Wu, Y., 2018. Occurrence of perfluoroalkyl substances in matched human serum, urine, hair and nail. J. Environ. Sci. 67, 191–197. https://doi.org/10.1016/j.jes.2017.08.017.

Wellens, S., Sandrini-Neto, L., González-Wangüemert, M., Lana, P., 2015. Do the crabs Goniopsis cruentata and Ucides cordatus compete for mangrove propagules? A field-based experimental approach. Hydrobiologia 757, 117–128. https://doi.org/10.1007/s10750-015-2245-x.

Xu, J., Guo, C.-S., Zhang, Y., Meng, W., 2014. Bioaccumulation and trophic transfer of perfluorinated compounds in a eutrophic freshwater food web. Environ. Pollut. 184, 254–261. https://doi.org/10.1016/j.envpol.2013.09.011.

Yin, T., Te, S.H., Reinhard, M., Yang, Y., Chen, H., He, Y., Gin, K.Y.-H., 2018. Biotransformation of Sulfluramid (N-ethyl perfluorooctane sulfonamide) and dynamics of associated rhizospheric microbial community in microcosms of wetland plants. Chemosphere 211, 379–389. https://doi.org/10.1016/j.chemosphere.2018.07.157.

Zabaleta, I., Bizkarguenaga, E., Nunoo, D.B.O., Schultes, L., Leonel, J., Prieto, A., Zuloaga, O., Benskin, J.P., 2018. Biodegradation and uptake of the pesticide sulfluramid in a soil-carrot Mesocosm. Environ. Sci. Technol. 52, 2603–2611. https://doi.org/10.1021/acs.est.7b03876.

Zhao, S., Zhou, T., Zhu, L., Wang, B., Li, Z., Yang, L., Liu, L., 2018. Uptake, translocation and biotransformation of N-ethyl perfluorooctanesulfonamide (N-EtFOSA) by hydroponically grown plants. Environ. Pollut. 235, 404–410. https://doi.org/10.1016/j.envpol.2017.12.053.

Supplementary Information

Bioaccumulation of Per- and Polyfluoroalkyl substances (PFASs) in a Tropical Estuarine Food Web

Daniele de A. Miranda[a,b]*, Jonathan P. Benskin[b], Raed Awad[b,c], Gilles Lepoint[d], Juliana Leonel[e], Vanessa Hatje[a]

[a]Centro Interdisciplinar de Energia e Ambiente (CIEnAm) and Inst. de Química, Universidade Federal da Bahia, 41170-115, Salvador, BA, Brazil;

[b]Department of Environmental Science, Stockholm University, Stockholm, Sweden;

[c]Swedish Environmental Research Institute (IVL), Stockholm, Sweden;

[d]Freshwater and Oceanic Sciences Unit of Research (FOCUS – Oceanology) University of Liege, 4000 Liege, Belgium;

[e]Departamento de Oceanografia, Universidade Federal de Santa Catarina, 88040-900, Florianópolis, SC, Brazil.

*Corresponding author: Daniele Miranda (danielealmeida@ufba.br / Daniele.Miranda@aces.su.se)

R-Scripts for Kendal correlation and individual PFASs Trophic Magnification Factors (TMF).

Adapted from Munoz et al. (2017)

```
#kendall correlation
library(NADA)
cor.test(foodweb$TL,foodweb$PFNA, method="kendall")
library("ggpubr")
ggscatter(foodweb, x = "TL", y = "PFNA",
          add = "reg.line", conf.int = TRUE,
cor.coef = TRUE, cor.method = "kendall",
xlab = "TL", ylab = "PFNA")

#Lmec (Linear Mixed-Effects Models with Censored Responses)
cens = foodweb$L_EtFOSA
yL = foodweb$L_EtFOSA
X = cbind(rep(1, length(yL)), foodweb$TL)
cluster = as.numeric(foodweb$ID)
Z = matrix(rep(1, length(yL)), ncol = 1)
fit <- lmec(yL, cens, X, Z, cluster, method = "ML", maxstep = 40)
res <- cbind.data.frame(lowerbound = fit$beta - 1.96*diag(fit$varFix), estimate=fit$beta,
upperbound=fit$beta+1.96*diag(fit$varFix))
TMF = 10^res[2,]
TMF
nbparam = length(fit$beta) + length(fit$bi) + 2
AICmod = -2*fit$loglik + 2*(nbparam)
AICcens_mod = AICmod + 2*(nbparam)*(nbparam+1)/(length(yL)-nbparam-1)
AICcens_mod
```

Standards and reagents

Methanol MeOH (HPLC grade) was purchased from J.T. Baker (Atlantic Labo, Bruges, France). Acetonitrile was purchased from Honeywell (Steinheim, Germany). Formic acid and acetic acid were purchased from Merck (Darmstadt, Germany). Ammonium formate salts was purchased from FLUKA analytical (Buchs, Switzerland). Ammonium hydroxide salts was purchased from Mallinckrodt chemicals (Dublin, Ireland). All standards were purchased from Wellington Laboratories (Guelph, ON, Canada). Lastly, water was purified with a Millipore water purification system (Millipore, Bedford, MA, USA) and had a resistance of 18,2 MΩ cm^{-1}.

Cleaning of materials

Polypropylene bottles, tubes and spoons were used to handle sediment samples. These materials were kept in a detergent Extran® bath (10%) for at least 24h and then washed with water and rinsed with Milli-Q® water. The materials were dried at environment temperature and then cleaned three times with 1% of NaOH in methanol. Glass materials were calcined at 450 °C for 4 hours and rinsed three times with 1% of NaOH in methanol.

Suspended matter and sediment samples

Samples of suspended particulate matter (n = 3) were manually collected using 4-liter glass bottles. In the laboratory, the samples were filtered on a glass fiber filter (25 µm) and the samples were then kept frozen until the time of analysis. Dissolved PFASs in surface water could not be analyzed due to the small sample size in the light of all parameters to be analyzed by our project. Composed sediment samples (n = 4) were collected in the same places where the benthic organisms were sampled. The samples were collected with the aid of a stainless-steel spoon and then kept frozen until the analysis.

Extraction of sediments and suspended matter

Sediment samples were extracted using previously published method by Zabaleta et al. (2018). First of all, 500 mg of sediment were weighted in a 50 mL polypropylene tube, and then 2 ng of isotopically-labelled standards and 8 mL of ACN were added. The mixture was sonicated for 20 min. The tubes were shaken for 40 minutes and then centrifuged by 2900 rpm for 20 minutes. The supernatant was removed and an 8 mL of ACN with 25mM NaOH (7.2 mL ACN + 0.6 mL deionized water + 0.2 mL NaOH 1M) was added and the proceeding (ultrasonic, shaken and centrifuged) were repeated. The supernatant was put together with the first extract. The final extract was dried until dryness by a gently nitrogen (analytical grade, 5.0) flux. The extract was resuspended with 400 µL of methanol (MeOH):Milli-Q water (1:1, v/v) with 20 mM formic acid and 20 mM ammonium formate. The suspended matter followed the same methodology, but the solvent used was pure methanol. Extracts were transferred to an ampoule and sealed.

Extraction of biotic samples

Biotic samples were extracted using previously published method by Zabaleta et al. (2018) (Zabaleta et al., 2017). First of all, 500 mg of samples were weighted in a 50 mL polypropylene tube, and then 2 ng of isotopically-labelled standards and 8 mL of ACN were added. The mixture was sonicated for 20 min. The tubes were shaken for 40 minutes and then centrifuged by 2900 rpm for 20 minutes. The supernatant was removed and an 8 mL of ACN with 25mM NaOH (7.2 mL CAN + 0.6 mL deionized water + 0.2 mL NaOH 1M) was added and the proceeding (ultrasonic,

shaken and centrifuged) were repeated. The supernatant was put together with the first one. The final extract was dried until 200 µL by a gently nitrogen flux (analytical grade, 5.0), which was mixed with 200 µL of Milli-Q water containing 20 mM formic acid and 20 mM ammonium formate. Extracts were transferred to an ampoule and sealed.

Targeted PFAS analysis

Instrumental analysis was carried out by ultra-performance liquid chromatography-tandem mass spectrometry (UPLC-MS/MS) using a Waters Acquity UPLC coupled to a Waters Xevo TQ-S triple quadrupole mass spectrometer, operated in negative ion electrospray ionization, selected reaction monitoring mode. Five microliters of the extracts were chromatographed on a BEH C18 analytical column (2.1×50mm, 1.7 µm particle size, Waters) operated at a flow rate of 0.4 mL/min, using a mobile phase composition of 90% water/10% acetonitrile containing 2 mM ammonium acetate (solvent A) and 100% acetonitrile containing 2 mM ammonium acetate (solvent B).

Conversion of whole fish contaminant concentration

In an attempt to avoid bias in the TMF calculations of PFAS compounds, some authors have pointed out a concern about the PFASs whole-body (wb) burden in larger species (Houde et al., 2006; Müller et al., 2011). When whole-body concentrations are not available, an alternative is to predict them through the concentration and masses of tissues available for analysis. Goeritz et al. (2013) suggested the concentrations of different PFASs found in muscle resemble those found in most fish tissues, except for liver and blood which accumulate higher PFAS concentrations due to higher protein content. Based on these assumptions the wb concentration was calculated for most of the PFASs following the equation below:

$$wbc = \frac{(mus\ g \times [\,]\ mus\ ng\ g^{-1}) \ldots + (carc\ g \times [\,]\ mus\ ng\ g^{-1}) \ldots + (liv\ g \times [\,]\ liv\ ng\ g^{-1})}{Total\ weight}$$

where wbc is the whole body concentration in ng g^{-1} (wet weight, ww), mus g represents the mass measurement of muscle in grams, mus ng g^{-1} represents the concentration of each PFASs in muscle in ng g^{-1}ww, total weight represents the entire organism weight in grams. When the biometric information of the organism was not available, literature was accessed to achieve the representative percentage of each organ in the whole organism, either in the same species or in the most similar existing. Since gonadal tissue has a higher lipid and protein content as liver, when this first PFASs concentration data was not available, the tissue mass was assumed as similar to liver tissue.

Nania et al. (2009) suggested the concentrations of PFOS in the liver is approximately 10 times the one found in muscle. Based on that assumption and in the lack of information, the PFASs concentration of muscle was multiplied by 10 when the liver concentrations were not available. And then the whole-body concentration was estimated.

Table S1: Perfluoroalkyl substances (PFASs) analyzed in the present study. Perfluorohexanoic acid (PFHxA) was removed from the scope of this study due to analytical issues.

Acronym	Name	Formula	CAS#
	Perfluoroalkyl carboxylic acids (PFCAs)		
PFPeA	Perfluoropentanoic acid	C_4F_9COOH	2706-90-3
PFHpA	Perfluoroheptanoic acid	$C_6F_{13}COOH$	375-85-9
PFOA*	Perfluorooctanoic acid	$C_7F_{15}COOH$	335-67-1
PFNA	Perfluorononanoic acid	$C_8F_{17}COOH$	375-95-1
PFDA	Perfluorodecanoic acid	$C_9F_{19}COOH$	335-76-2
PFUnDA	Perfluoroundecanoic acid	$C_{10}F_{21}COOH$	2058-94-8
PFDoDA	Perfluorododecanoic acid	$C_{11}F_{23}COOH$	307-55-1
PFTrDA	Perfluorotridecanoic acid	$C_{12}F_{25}COOH$	72629-94-8
PFTeDA	Perfluorotetradecanoic acid	$C_{13}F_{27}COOH$	376-06-7
PFPeDA	Perfluoropentadecanoic acid	$C_{14}F_{29}COOH$	1214264-29-5
	Perfluoroalkyl sulfonic acids (PFSAs)		
PFBS	Perfluorobutanesulfonic acid	$C_4F_9SO_3H$	375-73-5
PFHxS*	Perfluorohexanesulfonic acid	$C_6F_{13}SO_3H$	355-46-4
PFOS*	Perfluorooctanesulfonic acid	$C_8F_{17}SO_3H$	1763-23-1
PFDS*	Perfluorodecanesulfonic acid	$C_{10}F_{21}SO_3H$	355-77-3
	Perfluoroalkyl sulfonamido acetic derivatives (FASAAs)		
FOSAA*	Perfluoro-1-octanesulfonamidoacetic acid	$C_8F_{17}SO_2NHCH_2COOH$	2806-24-8
MeFOSAA	N-methylperfluoro-1-octanesulfonamidoacetic acid	$C_{11}H_3D_3F_{17}NO_4S$	1400690-70-1
EtFOSAA*	N-ethylperfluoro-1-octanesulfonamidoacetic acid	$C_8F_{17}SO_2NH(C_2H_5)CH_2COOH$	2991-50-6
	Perfluoroalkyl sulfonamide derivatives (FASAs)		
MeFOSA	N-methylperfluoro-1-octanesulfonamide	$C_{11}H_8F_{17}NO_3S$	24448-09-7
FOSA*	Perfluorooctanesulfonamide	$C_8F_{17}SO_2NH_2$	754-91-6
EtFOSA*	N-Ethyl perfluorooctanesulfonamide	$C_8F_{17}SO_2NH(C_2H_5)$	4151-50-2

*Compounds analyzed for both linear (L-) and branched (Br-) isomers.

Table S2: Biometric information and food habit of organisms sampled at Subaé estuary. Species are presented with common and scientific names. N = number of species measured.

Group	Species	N	TL (cm)	TW (g)	Mus (g)	Hepat/Liv (g)	Food Habit
Mollusk	Mangrove cupped oyster	14	6.16	41.8	3.96		Filter-feeder
	(*Crassostrea rhizophorae*)		(3.85-12.0)	(6.56-585)	(1.13-55.4)		
	Mangrove shellfish	63	3.59	2.41	0.51		Filter-feeder
	(*Mytella guyanensis*)		(2.13-5.50)	(0.74-6.45)	(0.12-1.7)		
	Clam	61	2.78	6.88	1.05		Filter-feeder
	(*Anomalocardia brasiliana*)		(0.74-5.76)	(3.09-10.2)	(0.36-1.54)		
	Mangrove oyster	5	9.98	155	17.3		Filter-feeder
	(*Crassostrea brasiliana*)		(8.20-13.2)	(68.6-255)	(11.6-26.5)		
	Stout tagelus	60	3.84	2.62	1.39		Filter-feeder
	(Tagelus plebeius)		(3.14-4.87)	(1.17-4.09)	(0.65-2.26)		
Annelida	Polychaeta			5.28			Detritivore
Crustacean	Blue crab	4	8.17		34.4	14.3	Zoobenthivore
	(*Callinectes sapidus*)		(5.11-10.3)		(25.3-44.0)	(12.2-17.3)	
	Ucides	6	4.22	109	18.	9.53	Herbivore
	(*Ucides cordatus*)		(3.86-4.52)	(76.8-137)	1(11.5-27.4)	(7.84-11.1)	
	Whiteleg shrimp	18	9.82	7.89			Detritivore
	(*Litopenaeus* sp.)		(8.5-11.3)	(4.13-10.3)			
	Mangrove tree crab	12	3.19	24.9	8.30	2.73	Carnivore
	(*Goniopsis cruentata*)		(2.53-4.18)	(12.7-44.1)	(3.49-18.7)	(1.41-5.38)	
Fish	Mullet (*Mugil* sp.)	3		196			Detritivore
				(77.1-405)			
	Torroto grunt	3	23.7	276	72.1	4.08	Zoobenthivore
	(*Genyatremus luteus*)		(22.5-24.9)	(230-327)	(56.4-85.8)	(2.68-6.73)	
	Mojarra (*Diapterus* sp.)	9	10.3	15.3	4.08		Omnivore
			(9.30-12.0)	(10.5-26.9)	(2.66-8.47)		
	Silverjenny (*Eucinostomus* sp.)	1		19.8	9.26		Zoobenthivore
	Madamango sea catfish	5	17.0	46.2	9.55	4.47	Zoobenthivore
	(*Cathorops spixii*)		(14.3-19.8)	(35.7-64.2)	(6.04-12.5)	(2.97-5.70)	
	Fat snook	3		236	78.2	1.27	Carnivore
	(*Centropomus parallelus*)			(27.4-500)	(9.17-174)	(0.07-2.83)	
	Drum	6	14.7	40.9	11.0	0.25	Zoobenthivore
	(*Stellifer* sp.)		(13.6-17.0)	(30.2-62.2)	(8.00-17.4)	(0.10-0.46)	
	Trevally	5	18.4	108	35.4	1.03	Piscivore
	(*Caranx* sp.)		(13.6-23.5)	(30.4-214)	(8.85-70.6)	(0.26-1.98)	
	Catfish	3	37.4	204	34.8	2.11	Omnivore
	(*Aspistor luniscutis*)		(26.8-61.1)	(174-237)	(28.7-42.2)	(1.57-2.58)	
	Common snook	3		102	37.5	0.73	Carnivore
	(*Centropomus undecimalis*)			(38.4-136)	(10.7-54.7)	(0.16-1.08)	
	Barbel drum	1	25.08	12.7		0.02	Zoobenthivore
	(*Ctenosciaena gracilicirrhus*)						

Where: TL: total length, TW: Total weight, Mus: Muscle, Hepat: Hepatopancreas (crab). Liver was sampled for fish.

Table S3: Mobile phase gradient profile used in LC-MS/MS.

	LC Gradient Program		**LC Flow Rate**
Time (min)	Mobile phase A (%)[1]	Mobile Phase B (%)[2]	(mL/min)
0.0	90	10	0.40
0.3	90	10	0.40
4.5	20	80	0.40
4.6	0	100	0.40
7.5	0	100	0.55
9.5	90	10	0.40

[1] Mobile phase A: 90 % water and 10 % acetonitrile containing 2 mM ammonium acetate.
[2] Mobile phase B: 100 % acetonitrile containing 2 mM ammonium acetate.

Table S4: List of retention times, and monitored ions for each compound analyzed in the present study. Perfluorohexanoic acid (PFHxA) was removed from the scope of this study due to detected interferences in the main transition ion.

Target	Retention Time (min)	Quant. Ion (m/z)	Qual Ion (m/z)	Standard	Internal Standard	IS Ion	Data quality
L-PFPeA	0.99	263/219	263/169	L-PFPeA	^{13}C-PFPeA	266/222	Quantitative
L-PFHpA	2.18	363/319	363/169	L-PFHpA	^{13}C-PFHpA	367/322	Quantitative
L-PFOA	2.49	413/369	413/169	L-PFOA	^{13}C-PFOA	417/372	Quantitative
Br-PFOA	~2.49	413/369	413/169	L-PFOA	^{13}C-PFOA	417/372	Semi-quantitative
L-PFNA	2.76	463/419	463/219	L-PFNA	^{13}C-PFNA	468/423	Quantitative
L-PFDA	3.02	513/469	513/269	L-PFDA	^{13}C-PFDA	515/470	Quantitative
L-PFUnDA	3.27	563/519	563/269	L-PFUnDA	^{13}C-PFUnDA	565/520	Quantitative
L-PFDoDA	3.52	613/569	613/169	L-PFDoDA	^{13}C-PFDoA	615/570	Quantitative
L-PFTrDA	3.74	663/619	663/169	L-PFTrDA	^{13}C-PFDoA	615/570	Quantitative
L-PFTeDA	3.97	713/669	713/169	L-PFTeDA	^{13}C-PFDoA	615/570	Quantitative
L-PFPeDA	4.20	763/719	763/169	L-PFTeDA	^{13}C-PFDoA	615/570	Qualitative
L-PFBS	1.69	298.9/80	298.9/99	L-PFBS	^{18}O-PFHxS	403/84	Quantitative
L-PFHxS	2.92	399/80	399/99	L-PFHxS	^{18}O-PFHxS	403/84	Quantitative
Br-PFHxS	2.50	399/80	399/99	L-PFHxS	^{18}O-PFHxS	403/84	Semi-quantitative
L-PFOS	3.07	498.9/80	498.9/99	L-PFOS	^{13}C-PFOS	503/80	Quantitative
Br-PFOS	~2.95	498.9/80	498.9/99	L-PFOS	^{13}C--PFOS	503/80	Semi-quantitative
L-PFDS	3.57	598.9/80	599/99	L-PFDS	^{13}C-PFOS	503/80	Quantitative
Br-PFDS	~3.47	599/80	599/99	L-PFDS	^{13}C-PFOS	503/80	Semi-quantitative
L-FOSA	4.17	498/78	498/169	L-FOSA	^{13}C-FOSA	506/78	Quantitative
Br-FOSA	4.05	498/78	498/169	L-FOSA	^{13}C-FOSA	506/78	Semi-quantitative
L-MeFOSA	3.07	512/169	512/219	L-CH_3FOSA	D^3-MeFOSAA	515/169	Quantitative
Br- MeFOSA	~3.07	512/169	512/219	L-CH_3FOSA	D^3-MeFOSAA	515/169	Semi-quantitative
L-EtFOSA	4.91	526/169	526/219	L-EtFOSA	D_5-EtFOSA	531/219	Quantitative
Br-EtFOSA	~4.91	526/169	526/219	L-EtFOSA	D^5-EtFOSA	531/219	Semi-quantitative
L-FOSAA	3.07	556/419	556/483	L-MeFOSAA	D^3-MeFOSAA	573/419	Quantitative
Br-EtFOSA	~3.07	556/419	556/483	L-MeFOSAA	D^3-MeFOSAA	573/419	Semi-quantitative
L-MeFOSAA	3.10	570/419	570/483	L- MeFOSAA	D^3- CH3FOSAA	573/419	Quantitative
Br- MeFOSAA	3.00	570/419	570/483	L- MeFOSAA	D^3- CH3FOSAA	573/419	Semi-quantitative
L-EtFOSAA	3.23	584/419	584/526	L-EtFOSAA	D^5-EtFOSAA	589/419	Quantitative
Br-EtFOSAA	3.13	584/419	584/526	L-EtFOSAA	D^5-EtFOSAA	589/419	Semi-quantitative

Recovery standards

Target	Retention Time (min)	Quant. Ion (m/z)
$^{13}C_8$-PFOA	2.49	421/376
$^{13}C_8$-PFOS	3.07	506.9/80

149 **Table S5:** Individual LOD for tissues types (l - liver; h - hepatopancreas; m - muscle; and whole body (wb) of organisms.
150 n.r. – non-reported.

Description	PFPeA	PFHpA	L-PFOA	Br-PFOA	PFNA	PFDA	PFUnDA	PFDoDA	PFTriDA	PFTeDA	PFPeDA	PFBS	L-PFHxS	Br-PFHxS
Crassostrea brasiliana (wb)	1.06	0.04	0.46	0.02	0.28	0.21	0.07	0.03	0.04	0.04	0.04	0.02	0.07	0.07
Mytella guyanensis (wb)	1.06	0.04	0.46	0.02	0.28	0.21	0.07	0.03	0.04	0.04	0.04	0.02	0.07	0.07
Anomalocardia brasiliana (wb)	1.06	0.04	0.46	0.02	0.28	0.21	0.07	0.03	0.04	0.04	0.04	0.02	0.07	0.07
Tagelus plebeius (wb)	1.06	0.04	0.46	0.02	0.28	0.21	0.07	0.03	0.04	0.04	0.04	0.02	0.07	0.07
Crassostrea rhizophorae (wb)	1.06	0.04	0.46	0.02	0.28	0.21	0.07	0.03	0.04	0.04	0.04	0.02	0.07	0.07
Litopenaeus sp. (wb)	1.06	0.04	0.46	0.02	0.28	0.21	0.07	0.03	0.04	0.04	0.04	0.02	0.07	0.07
Goniopsis cruentata (m)	0.19	0.11	0.38	0.02	0.04	0.04	0.04	0.04	0.08	0.08	0.08	0.04	0.08	0.08
Goniopsis cruentata (h)	0.19	0.11	0.38	0.02	0.04	0.04	0.04	0.04	0.08	0.08	0.08	0.04	0.08	0.08
Callinectes sapidu (m)	0.19	0.11	0.38	0.02	0.04	0.04	0.04	0.04	0.08	0.08	0.08	0.04	0.08	0.08
Callinectes sapidus (h)	0.19	0.11	0.38	0.02	0.04	0.04	0.04	0.04	0.08	0.08	0.08	0.04	0.08	0.08
Ucides cordatus (m)	0.25	0.11	0.55	0.04	0.03	0.35	0.02	0.02	0.02	0.02	0.02	0.11	0.25	0.25
Ucides cordatus (h)	0.25	0.11	0.55	0.04	0.03	0.35	0.02	0.02	0.02	0.02	0.02	0.11	0.25	0.25
Genyatremus luteus (m)	0.25	0.11	0.55	0.04	0.03	0.35	0.02	0.02	0.02	0.02	0.02	0.11	0.25	0.25
*Caranx*sp. (m)	0.23	0.14	0.66	0.05	0.05	0.02	0.02	0.02	0.02	0.02	0.02	0.14	0.23	0.23
*Caranx*sp. (l)	0.23	0.14	0.66	0.05	0.05	0.02	0.02	0.02	0.02	0.02	0.02	0.14	0.23	0.23
Ctenosciaena gracilicirrhus (m)	0.23	0.14	0.66	0.05	0.05	0.02	0.02	0.02	0.02	0.02	0.02	0.14	0.23	0.23
*Stellifer*sp.	0.23	0.14	0.66	0.05	0.05	0.02	0.02	0.02	0.02	0.02	0.02	0.14	0.23	0.23
Diapterus sp. (m)	0.23	0.14	0.66	0.05	0.05	0.02	0.02	0.02	0.02	0.02	0.02	0.14	0.23	0.23
Eucinostomus sp. (m)	0.46	0.46	0.60	0.04	0.03	0.02	0.02	0.02	0.02	0.02	0.02	0.02	0.05	0.05
Mugil sp. (m)	0.46	0.46	0.60	0.04	0.03	0.02	0.02	0.02	0.02	0.02	0.02	0.02	0.05	0.05
Mugil sp. (l)	0.46	0.46	0.60	0.04	0.03	0.02	0.02	0.02	0.02	0.02	0.02	0.02	0.05	0.05
Aspistor luniscutis (m)	0.46	0.46	0.60	0.04	0.03	0.02	0.02	0.02	0.02	0.02	0.02	0.02	0.05	0.05
Aspistor luniscutis (l)	0.48	0.24	0.60	0.04	0.02	0.02	0.02	0.02	0.02	0.02	0.02	0.02	0.05	0.05
Cathorops spixii (m)	0.48	0.24	0.60	0.04	0.02	0.02	0.02	0.02	0.02	0.02	0.02	0.02	0.05	0.05
Centropomus parallelus (m)	0.48	0.24	0.60	0.04	0.02	0.02	0.02	0.02	0.02	0.02	0.02	0.02	0.05	0.05
Centropomus undecimalis (m)	0.48	0.24	0.60	0.04	0.02	0.02	0.02	0.02	0.02	0.02	0.02	0.02	0.05	0.05
Polychaeta (wb)	0.06	0.07	0.50	0.03	1.11	0.04	0.37	0.15	0.03	0.06	0.03	0.03	0.03	0.03
Genyatremus luteus (l)	0.06	0.07	0.50	0.03	1.11	0.04	0.37	0.15	0.03	0.06	0.03	0.03	0.03	0.03

151

152 *continue...*

Description	L-PFOS	Br-PFOS	L-PFDS	Br-PFDS	L-FOSA	Br-FOSA	L-CH_3FOSA	Br-CH_3FOSA	L-EtFOSA	Br-EtFOSA	L-FOSAA	Br-FOSAA	L-CH_3FOSAA	Br-CH_3FOSAA	L-EtFOSAA	Br-EtFOSAA
Crassostrea brasiliana (wb)	0.08	0.00	0.02	0.02	0.02	0.02	0.02	0.02	0.02	0.02	0.02	0.02	0.02	0.02	0.02	0.02
Mytella guyanensis (wb)	0.08	0.00	0.02	0.02	0.02	0.02	0.02	0.02	0.02	0.02	0.02	0.02	0.02	0.02	0.02	0.02
Anomalocardia brasiliana (wb)	0.08	0.00	0.02	0.02	0.02	0.02	0.02	0.02	0.02	0.02	0.02	0.02	0.02	0.02	0.02	0.02
Tagelus plebeius (wb)	0.08	0.00	0.02	0.02	0.02	0.02	0.02	0.02	0.02	0.02	0.02	0.02	0.02	0.02	0.02	0.02
Crassostrea rhizophorae (wb)	0.08	0.00	0.02	0.02	0.02	0.02	0.02	0.02	0.02	0.02	0.02	0.02	0.02	0.02	0.02	0.02
Litopenaeus sp. (wb)	0.08	0.00	0.02	0.02	0.02	0.02	0.02	0.02	0.02	0.02	0.02	0.02	0.02	0.02	0.02	0.02
Goniopsis cruentata (m)	0.08	0.04	0.04	0.04	0.11	0.04	0.02	0.02	0.02	0.02	0.02	0.02	0.02	0.02	0.02	0.02
Goniopsis cruentata (h)	0.08	0.04	0.04	0.04	0.11	0.04	0.02	0.02	0.02	0.02	0.02	0.02	0.02	0.02	0.02	0.02
Callinectes sapidu (m)	0.08	0.04	0.04	0.04	0.11	0.04	0.02	0.02	0.02	0.02	0.02	0.02	0.02	0.02	0.02	0.02
Callinectes sapidus (h)	0.08	0.04	0.04	0.04	0.11	0.04	0.02	0.02	0.02	0.02	0.02	0.02	0.02	0.02	0.02	0.02
Ucides cordatus (m)	0.02	0.02	0.04	0.04	0.02	0.02	0.02	0.02	0.04	0.04	0.02	0.02	0.02	0.02	0.02	0.02
Ucides cordatus (h)	0.02	0.02	0.04	0.04	0.02	0.02	0.02	0.02	0.04	0.04	0.02	0.02	0.02	0.02	0.02	0.02
Genyatremus luteus (m)	0.02	0.02	0.04	0.04	0.02	0.02	0.02	0.02	0.04	0.04	0.02	0.02	0.02	0.02	0.02	0.02
*Caranx*sp. (m)	0.02	0.02	0.05	0.05	0.02	0.02	0.02	0.02	0.02	0.02	0.02	0.02	0.02	0.02	0.02	0.02
*Caranx*sp. (l)	0.02	0.02	0.05	0.05	0.02	0.02	0.02	0.02	0.02	0.02	0.02	0.02	0.02	0.02	0.02	0.02
Ctenosciaena gracilicirrhus (m)	0.02	0.02	0.05	0.05	0.02	0.02	0.02	0.02	0.02	0.02	0.02	0.02	0.02	0.02	0.02	0.02
*Stellifer*sp.	0.02	0.02	0.05	0.05	0.02	0.02	0.02	0.02	0.02	0.02	0.02	0.02	0.02	0.02	0.02	0.02
Diapterus sp. (m)	0.02	0.02	0.05	0.05	0.02	0.02	0.02	0.02	0.02	0.02	0.02	0.02	0.02	0.02	0.02	0.02
Eucinostomus sp. (m)	0.02	0.02	0.02	0.02	0.02	0.02	0.02	0.02	0.09	0.03	0.02	0.02	0.02	0.02	0.02	0.02
Mugil sp. (m)	0.02	0.02	0.02	0.02	0.02	0.02	0.02	0.02	0.09	0.03	0.02	0.02	0.02	0.02	0.02	0.02
Mugil sp. (l)	0.02	0.02	0.02	0.02	0.02	0.02	0.02	0.02	0.09	0.03	0.02	0.02	0.02	0.02	0.02	0.02
Aspistor luniscutis (m)	0.02	0.02	0.02	0.02	0.02	0.02	0.02	0.02	0.09	0.03	0.02	0.02	0.02	0.02	0.02	0.02
Aspistor luniscutis (l)	0.02	0.02	0.02	0.02	0.02	0.02	0.02	0.02	0.02	0.02	0.02	0.02	0.02	0.02	0.02	0.02
Cathorops spixii (m)	0.02	0.02	0.02	0.02	0.02	0.02	0.02	0.02	0.02	0.02	0.02	0.02	0.02	0.02	0.02	0.02
Centropomus parallelus (m)	0.02	0.02	0.02	0.02	0.02	0.02	0.02	0.02	0.02	0.02	0.02	0.02	0.02	0.02	0.02	0.02
Centropomus undecimalis (m)	0.02	0.02	0.02	0.02	0.02	0.02	0.02	0.02	0.02	0.02	0.02	0.02	0.02	0.02	0.02	0.02
Polychaeta (wb)	0.05	0.03	0.03	0.03	0.07	0.03	0.03	0.03	n.r.	n.r.	0.03	0.03	0.03	0.03	0.03	0.03
Genyatremus luteus (l)	0.05	0.03	0.03	0.03	0.07	0.03	0.03	0.03	0.00	0.00	0.03	0.03	0.03	0.03	0.03	0.03

153

Table S6: Results of triplicate spike/recovery for leaf, muscle of fish and crab, and sediment samples. Branched compounds are assumed to be associated with their respective linear compound. (n.r.: not-reported).

Compound	Batch 1 (Leaf, *Avicennia* sp.)		Batch 2 (*C. sapidus*)		Batch 3 (*G. luteus*)		Batch 4 (*G. luteus*)		Batch 5 (*Mugil* sp.)		Batch 6 (*C. parallelus*)		Batch 7 (Sediment)		Batch 8 (Sediment)	
	Recovery	RSD	Recovery	RSD	Recovery	RSD	Recovery	RSD	Recovery	RSD	Recovery	RSD	Recovery	RSD	Recovery	RSD
PFPeA	59	18	74	14	91	12	63	6	113	42	59	13	85	11	*180	3
PFHpA	85	13	90	9	91	17	107	7	88	7	93	9	82	14	*28	8
L-PFOA	81	29	91	12	98	9	93	6	99	7	88	7	88	12	89	8
PFNA	84	23	91	9	94	9	95	4	97	10	89	7	86	7	83	7
PFDA	84	18	90	10	91	6	96	4	103	13	89	3	88	5	84	9
PFUnDA	85	21	92	15	99	7	96	1	100	8	88	11	94	7	89	8
PFDoDA	86	13	88	10	97	11	95	3	98	6	90	7	90	10	86	8
PFTrDA	*41	10	109	15	120	10	123	6	119	7	102	17	*32	10	*25	55
PFTeDA	*14	32	93	25	114	9	124	8	109	7	103	11	*4	3	*4	47
PFPeDA***	-	-	-	-	-	-	-	-	-	-	-	-	-	-	-	-
PFBS	52	24	70	10	83	12	81	12	88	10	81	4	77	11	69	11
L-PFHxS	87	22	82	12	94	14	94	4	101	12	86	2	87	6	89	12
L-PFOS	76	19	76	9	111	6	102	1	110	18	101	10	87	6	88	20
L-PFDS	64	17	74	16	96	10	97	2	111	15	88	12	61	11	49	43
L-FOSA	93	14	83	9	83	13	88	7	93	6	79	6	89	14	109	49
L-CH_3FOSA	72	14	75	14	75	33	96	0	100	10	85	11	*102	43	68	51
L-EtFOSA	76	21	77	12	63	21	68	1	*32	11	73	3	78	10	nr**	nr**
L-FOSAA	104	26	75	9	100	8	108	4	87	13	86	11	92	11	105	16
L-CH_3FOSAA	109	27	102	5	109	2	105	3	111	1	93	12	96	12	92	11
L-EtFOSAA	77	47	87	15	99	15	96	14	105	7	84	6	80	10	71	23

**Either low recovery or high relative standard deviation;*
***Data were not reported for this compound for this specific batch*
*** There was no data for PFPeDA recovery since there is an absence of native standard. In this case, the data quality was semi-quantitative based on another long-chain carboxylated compounds.

Table S7: Concentrations of PFASs in biota samples from the Subaé estuary, expressed in ng g^{-1}ww whole body (wb) showed as either average (min-max) when more than 3 samples or measured concentration for single sample (n.d. = non-detected, n.r. = not-reported). Only compounds above LOD were computed in the ∑PFAS.

Variable	*Crassostrea rhizophorae*	*Mytella guyanensis*	*Anomalocardia brasiliana*	*Crassostrea brasiliana*	*Tagelus plebeius*	*Callinectes sapidus*	*Ucides cordatus*	*Litopenaeus* sp.	*Goniopsis cruentata*
Class	Bivalve	Bivalve	Bivalve	Bivalve	Bivalve	Crustacean	Crustacean	Crustacean	Crustacean
N	14 (pool)	63 (pool)	61 (pool)	5 (pool)	60 (pool)	4	6	18 (pool)	12
Trophic Level	2.00	2.04	2.11	2.36	2.54	2.60	2.68	2.96	3.01
Carbon	-25.93	-23.71	-25.50	-26.11	-25.61	-22.10	-24.79	-21.70	-19.97
PFPeA	n.d.	n.d.	n.d.	n.d.	n.d.	n.d.	n.d.	n.d.	n.d.
PFHpA	n.d.	n.d.	n.d.	n.d.	n.d.	0.08 ± 0.03	0.27 ± 0.38	n.d.	n.d.
L-PFOA	n.d.	n.d.	n.d.	n.d.	n.d.	0.10 ± 0.08	n.d.	n.d.	0.20 ± 0.15
Br-PFOA	n.d	n.d.	n.d	n.d.	n.d	n.d.	n.d.	n.d.	n.d.
PFNA	n.d.	n.d.	n.d.	n.d.	n.d.	0.08 ± 0.01	0.04 ± 0.01	n.d.	0.14 ± 0.04
PFDA	n.d.	n.d.	n.d.	n.d.	n.d.	0.06 ± 0.02	0.07 ± 0.06	n.d.	0.20 ± 0.05
PFUnDA	n.d.	n.d.	n.d.	n.d.	0.09	0.07 ± 0.01	0.07 ± 0.05	0.17	0.13 ± 0.03
PFDoDA	n.d.	n.d.	0.04	n.d.	n.d.	0.11 ± 0.002	0.05 ± 0.04	0.15	0.12 ± 0.02
PFTrDA	0.07	0.07	0.06	0.05	0.06	0.17 ± 0.01	0.08 ± 0.05	0.28	0.15 ± 0.04
PFTeDA	0.07	0.07	0.05	0.06	n.d.	0.16 ± 0.02	0.10 ± 0.08	0.26	0.11 ± 0.07
PFPeDA	0.06	n.d.	n.d.	n.d.	n.d.	0.02 ± 0.01	0.01 ± 0.001	0.14	n.d.
PFBS	n.d.	n.d.	n.d.	n.d.	n.d.	0.01 ± 0.02	n.d.	n.d.	0.08 ± 0.11
L-PFHxS	0.08	0.17	0.11	n.d.	n.d.	0.02 ± 0.01	0.03 ± 0.02	n.d.	0.07 ± 0.06
Br-PFHxS	0.12	0.33	0.17	n.d.	n.d.	0.01 ± 0.01	0.04 ± 0.004	n.d.	0.09 ± 0.04
L-PFOS	n.d.	0.36	0.17	n.d.	n.d.	0.27 ± 0.04	0.53 ± 0.12	1.97	0.65 ± 0.12
Br-PFOS	n.d.	0.17	n.d.	n.d.	n.d.	0.02 ± 0.01	0.15 ± 0.06	0.35	0.21 ± 0.08
L-PFDS	n.d.	n.d.	n.d.	n.d.	n.d.	n.d.	n.d.	n.d.	n.d.
Br-PFDS	n.d.	n.d.	n.d.	n.d.	n.d.	n.d.	n.d.	n.d.	n.d.
L-FOSA	0.22	0.04	0.04	0.06	0.12	0.02 ± 0.01	0.13 ± 0.14	0.21	0.24 ± 0.04
Br-FOSA	0.24	n.d.	n.d.	0.08	0.05	0.01 ± 0.002	0.03 ± 0.01	n.d.	0.06 ± 0.06
L-CH_3FOSA	n.d.	n.d.	n.d.	n.d.	n.d.	n.d.	n.d.	n.d.	n.d.
Br-CH_3FOSA	n.d.	n.d.	n.d.	n.d.	n.d.	n.d.	n.d.	n.d.	n.d.
L-EtFOSA	n.d.	n.d.	n.d.	n.d.	0.03	0.02 ± 0.01	0.05 ± 0.05	n.d.	0.01 ± 0.004
Br-EtFOSA	n.d.	n.d.	n.d.	n.d.	n.d.	n.d.	0.16 ± 0.22	n.d.	0.01 ± 0.004
L-FOSAA	n.d.	0.03	0.02	n.d.	n.d.	n.d.	0.06 ± 0.07	n.d.	0.08 ± 0.05
Br-FOSAA	n.d.	n.d.	n.d.	n.d.	n.d.	n.d.	n.d.	n.d.	n.d.
L-CH_3FOSAA	n.d.	n.d.	n.d.	n.d.	n.d.	n.d.	0.01 ± 0.01	n.d.	0.01 ± 0.01
Br-CH3FOSAA	n.d.	n.d.	n.d.	n.d.	n.d.	n.d.	n.d.	n.d.	n.d.
L-EtFOSAA	0.02	n.d.	0.03	n.d.	n.d.	n.d.	0.03 ± 0.02	0.18	0.10 ± 0.05
Br-EtFOSAA	n.d.	n.d.	n.d.	n.d.	n.d.	n.d.	n.d.	n.d.	n.d.
∑PFASs	0.88	1.25	0.71	0.35	0.35	1.24 ± 0.05	1.89 ± 0.85	3.71	2.67 ± 0.66

163 Continue…

Variable	*Polychaeta*	*Mugil sp.*	*Genyatremus luteus*	*Diapterus* sp.	*Eucinostomus* sp.	*Cathorops spixii*	*Centropomus parallelus*	*Stellifer* sp.	*Caranx* sp.	*Aspistor luniscutis*	*Centropomus undecimalis*	*Ctenosciaena gracilicirrhus*
Class	Annelida	Fish	Fish	Fish	Fish	Fish	Fish	Fish	Fish	Fish	Fish	Fish
N	(pool)	3	3	9	1	5	3	6	5	3	3	1
Trophic Level	3.22	3.56	3.59	3.68	3.89	3.97	3.98	4.00	4.15	4.29	4.48	4.49
Carbon	-24.67	-20.25	-23.68	-21.85	-19.89	-21.83	-20.77	-22.49	-17.42	-18.09	-23.82	-20.38
PFPeA	n.d.	n.d.	n.d.	n.d.	n.d.	n.d.	n.d.	n.d.	n.d.	0.12 ± 0.01	n.d.	n.d.
PFHpA	n.d.	0.52 ± 0.69	0.01 ± 0.002	n.d.	n.d.	n.d.	n.d.	0.11 ± 0.08	0.15 ± 0.16	n.d.	n.d.	n.d.
L-PFOA	n.d.	n.d.	n.d.	n.d.	n.d.	n.d.	n.d.	n.d.	n.d.	n.d.	n.d.	n.d.
Br-PFOA	n.d.	n.d.	n.d.	n.d.	n.d.	n.d.	n.d.	n.d.	n.d.	n.d.	n.d.	n.d.
PFNA	0.42	0.03 ± 0.01	0.01 ± 0.002	0.03 ± 0.02	0.02 ± 0.02	0.02 ± 0.002	0.03 ± 0.003	0.01 ± 0.001	0.02 ± 0.0005	0.04 ± 0.001	0.03 ± 0.003	0.01
PFDA	0.08	n.d.	n.d.	0.01 ± 0.01	0.05	0.03 ± 0.02	0.01 ± 0.001	0.01 ± 0.01	0.01 ± 0.001	0.01 ± 0.001	0.01 ± 0.001	n.d.
PFUnDA	n.d.	0.05 ± 0.03	n.d.	0.03 ± 0.01	0.05	0.02 ± 0.02	0.02 ± 0.002	0.01 ± 0.01	0.02 ± 0.01	0.01 ± 0.001	0.02 ± 0.002	0.02
PFDoDA	n.d.	0.02 ± 0.01	n.d.	0.02 ± 0.01	0.04	0.02 ± 0.01	0.02 ± 0.002	0.02 ± 0.01	0.01 ± 0.0004	0.02 ± 0.01	0.02 ± 0.002	0.02
PFTrDA	0.17	0.03 ± 0.02	n.d.	0.02 ± 0.02	0.01	0.02 ± 0.01	0.03 ± 0.01	0.02 ± 0.01	0.01 ± 0.0005	0.01 ± 0.0005	0.02 ± 0.004	0.03
PFTeDA	0.22	0.02 ± 0.01	n.d.	0.01 ± 0.001	0.01	0.02 ± 0.002	0.03 ± 0.01	0.01 ± 0.001	0.01 ± 0.004	0.01 ± 0.001	0.03 ± 0.002	n.d.
PFPeDA	0.19	n.d.	n.d.	n.d.	n.d.	n.d.	n.d.	n.d.	n.d.	n.d.	n.d.	n.d.
PFBS	n.d.	n.d.	n.d.	n.d.	n.d.	0.01 ± 0.01	n.d.	n.d.	n.d.	n.d.	n.d.	n.d.
L-PFHxS	0.07	0.04 ± 0.02	n.d.	0.01 ± 0.001	0.01	0.01 ± 0.001	0.02 ± 0.002	0.01 ± 0.001	0.01 ± 0.0003	0.02 ± 0.001	0.02 ± 0.002	n.d.
Br-PFHxS	0.02	0.01 ± 0.01	n.d.	0.01 ± 0.01	0.01	0.01 ± 0.0004	0.01 ± 0.01	n.d.	0.01 ± 0.002	0.02 ± 0.003	n.d.	n.d.
L-PFOS	0.59	0.53 ± 0.42	0.24 ± 0.17	0.39 ± 0.10	0.97	0.45 ± 0.37	0.26 ± 0.08	0.28 ± 0.08	1.20 ± 0.15	0.63 ± 0.11	0.45 ± 0.23	0.86
Br-PFOS	0.05	0.13 ± 0.09	0.09 ± 0.07	0.09 ± 0.04	0.11	0.05 ± 0.04	0.04 ± 0.02	0.04 ± 0.01	0.24 ± 0.03	0.06 ± 0.03	0.05 ± 0.02	0.16
L-PFDS	n.d.	n.d.	n.d.	n.d.	n.d.	n.d.	n.d.	n.d.	n.d.	n.d.	n.d.	n.d.
Br-PFDS	n.d.	n.d.	n.d.	n.d.	n.d.	n.d.	n.d.	n.d.	n.d.	n.d.	n.d.	n.d.
L-FOSA	0.09	0.03 ± 0.02	0.01 ± 0.01	0.04 ± 0.04	0.02	0.02 ± 0.002	0.03 ± 0.005	0.03 ± 0.02	0.03 ± 0.02	0.01 ± 0.0005	0.04 ± 0.02	0.04
Br-FOSA	0.09	0.02 ± 0.01	n.d.	0.01 ± 0.001	0.01	0.01 ± 0.001	0.01 ± 0.001	0.01 ± 0.01	n.d.	0.01 ± 0.0002	0.01 ± 0.001	n.d.
L-CH_3FOSA	n.d.	n.d.	n.d.	n.d.	n.d.	n.d.	n.d.	n.d.	n.d.	n.d.	n.d.	n.d.
Br-CH_3FOSA	n.d.	n.d.	n.d.	n.d.	n.d.	n.d.	n.d.	n.d.	n.d.	n.d.	n.d.	n.d.
L-EtFOSA	n.r.	0.01 ± 0.0004	0.11 ± 0.07	0.05 ± 0.07	0.01	0.04 ± 0.02	0.07 ± 0.02	0.03 ± 0.02	0.02 ± 0.01	0.01 ± 0.0003	0.03 ± 0.03	n.d.
Br-EtFOSA	n.r.	0.21 ± 0.26	0.35 ± 0.19	0.21 ± 0.19	n.d.	0.02 ± 0.03	0.10 ± 0.08	n.d.	0.02 ± 0.03	0.04 ± 0.05	0.09 ± 0.12	n.d.
L-FOSAA	n.d.	0.01 ± 0.02	n.d.	n.d.	n.d.	n.d.	n.d.	n.d.	n.d.	n.d.	n.d.	n.d.
Br-FOSAA	n.d.	n.d.	n.d.	n.d.	n.d.	n.d.	n.d.	n.d.	n.d.	n.d.	n.d.	n.d.
L-CH_3FOSAA	n.d.	n.d.	n.d.	n.d.	n.d.	n.d.	n.d.	n.d.	n.d.	n.d.	n.d.	n.d.
Br-CH_3FOSAA	n.d.	n.d.	n.d.	n.d.	n.d.	n.d.	n.d.	n.d.	n.d.	n.d.	n.d.	n.d.
L-EtFOSAA	0.04	0.04 ± 0.03	n.d.	n.d.	n.d.	n.d.	0.01 ± 0.01	n.d.	n.d.	n.d.	0.01 ± 0.01	n.d.
Br-EtFOSAA	n.d.	n.d.	n.d.	n.d.	n.d.	n.d.	n.d.	n.d.	n.d.	n.d.	n.d.	n.d.
∑PFASs	2.05	1.71 ± 1.17	0.85 ± 0.10	0.93 ±0.30	1.30	0.45 ±0.10	0.67 ± 0.22	0.60 ± 0.19	1.75 ± 0.30	1.02 ± 0.15	0.85 ± 0.27	1.14

Table S8: Pearson correlation and significance of the most found PFCAs compounds in fish samples (n = 28) and PFOS.

Variable	p	r (Pearson)
PFNA x PFUnDA	0.0202	0.4362
PFNA x PFDoDA	0.1564	0.2751
PFNA x PFTrDA	0.1275	0.2949
PFNA x PFTeDA	< 0.0001	0.7229
PFUnDA x PFDoDA	< 0.0001	0.7413
PFUnDA x PFTrDA	< 0.0001	0.6772
PFUnDA x PFTeDA	0.0026	0.547
PFDoDA x PFTrDA	< 0.0001	0.8451
PFDoDA x PFTeDA	0.0029	0.5407
PFTrDA x PFTeDA	< 0.0001	0.6756
PFNA x L-PFOS	0.8601	0.0349
PFUnDA x L-PFOS	0.0707	0.3466
PFDoDA x L-PFOS	0.0275	0.4162
PFTrDA x L-PFOS	0.3022	0.2021
PFTeDA x L-PFOS	0.5631	0.1141

Table S9: Concentrations in ng g^{-1}ww found in mangrove leaves and biofilm sampled at Subaé estuary.

Compound	White mangrove	Black mangrove	Red mangrove	Biofilm
		Perfluoroalkyl carboxylic acids (PFCAs)		
PFPeA	< 1.06	< 1.06	< 1.06	< 1.06
PFHpA	< 0.04	< 0.04	< 0.04	< 0.04
L-PFOA	< 0.46	< 0.46	< 0.46	< 0.46
Br-PFOA	< 0.02	< 0.02	< 0.02	< 0.02
PFNA	< 0.28	< 0.28	< 0.28	< 0.28
PFDA	< 0.21	< 0.21	< 0.21	< 0.21
PFUnDA	< 0.07	< 0.07	< 0.07	< 0.07
PFDoDA	< 0.03	< 0.03	< 0.03	< 0.03
PFTrDA	< 0.04	< 0.04	< 0.04	< 0.04
PFTeDA	< 0.04	< 0.04	< 0.04	< 0.04
PFPeDA	< 0.04	< 0.04	< 0.04	< 0.04
		Perfluoroalkyl sulfonic acids (PFSAs)		
PFBS	< 0.02	< 0.02	< 0.02	< 0.02
L-PFHxS	< 0.07	< 0.07	< 0.07	< 0.07
Br-PFHxS	< 0.07	< 0.07	< 0.07	< 0.07
L-PFHpS	< 0.02	< 0.02	< 0.02	< 0.02
L-PFOS	< 0.08	< 0.08	< 0.08	< 0.08
Br-PFOS	< 0.08	< 0.08	< 0.08	< 0.08
L-PFNS	< 0.02	< 0.02	< 0.02	< 0.02
Br-PFNS	< 0.02	< 0.02	< 0.02	< 0.02
L-PFDS	< 0.02	< 0.02	< 0.02	< 0.02
Br-PFDS	< 0.02	< 0.02	< 0.02	< 0.02
PFUnDS	< 0.02	< 0.02	< 0.02	< 0.02
		Perfluoroalkyl sulfonamido acetic derivatives (FASAAs)		
L-FOSAA	0.16	< 0.02	0.07	< 0.02
Br-FOSAA	< 0.02	< 0.02	< 0.02	< 0.02
L-CH_3FOSAA	< 0.02	< 0.02	< 0.02	< 0.02
Br-CH_3FOSAA	< 0.02	< 0.02	< 0.02	< 0.02
L-EtFOSAA	< 0.02	< 0.02	< 0.02	< 0.02
Br-EtFOSAA	< 0.02	< 0.02	< 0.02	< 0.02
		Perfluoroalkyl sulfonamide derivatives (FASAs)		
L-CH_3FOSA	< 0.02	< 0.02	< 0.02	< 0.02
Br-CH_3FOSA	< 0.02	< 0.02	< 0.02	< 0.02
L-FOSA	< 0.02	< 0.02	< 0.02	< 0.02
Br-FOSA	< 0.02	< 0.02	< 0.02	< 0.02
L-EtFOSA	< 0.02	< 0.02	< 0.02	< 0.02
Br-EtFOSA	< 0.02	< 0.02	< 0.02	< 0.02

Table S10: Concentrations in ng g^{-1} dw found in mangrove suspended particulate matter (SPM) sampled at Subaé estuary (n.r. = not-reported).

Compound	SPM#1	SPM#2	SPM#3
Perfluoroalkyl carboxylic acids (PFCAs)			
PFPeA	0.15	0.13	< 0.10
PFHpA	< 0.13	0.15	< 0.13
L-PFOA	< 0.88	< 0.88	< 0.88
Br-PFOA	< 0.05	< 0.05	< 0.05
PFNA	< 1.97	3.41	2.49
PFDA	0.08	0.15	0.18
PFUnDA	0.67	1.43	0.90
PFDoDA	< 0.26	< 0.26	< 0.26
PFTrDA	0.06	0.08	0.11
PFTeDA	< 0.10	< 0.10	< 0.10
PFPeDA	< 0.05	< 0.05	< 0.05
Perfluoroalkyl sulfonic acids (PFSAs)			
PFBS	< 0.05	< 0.05	< 0.05
L-PFHxS	0.07	0.16	0.06
Br-PFHxS	< 0.05	< 0.05	0.11
L-PFOS	0.480	1.02	1.56
Br-PFOS	0.10	0.25	0.55
L-PFDS	< 0.05	< 0.05	< 0.05
Br-PFDS	< 0.05	< 0.05	< 0.05
Perfluoroalkyl sulfonamido acetic derivatives (FASAAs)			
L-FOSAA	< 0.05	< 0.05	< 0.05
Br-FOSAA	< 0.05	< 0.05	< 0.05
L-CH_3FOSAA	< 0.05	< 0.05	< 0.05
Br-CH_3FOSAA	< 0.05	< 0.05	< 0.05
L-EtFOSAA	0.08	< 0.05	0.45
Br-EtFOSAA	< 0.05	< 0.05	0.14
Perfluoroalkyl sulfonamide derivatives (FASAs)			
L-CH_3FOSA	< 0.05	< 0.05	< 0.05
Br-CH_3FOSA	< 0.05	< 0.05	< 0.05
L-FOSA	0.16	0.28	0.14
Br-FOSA	< 0.05	0.18	< 0.05
L-EtFOSA	n.r.	n.r.	n.r.
Br-EtFOSA	n.r.	n.r.	n.r.

Table S11: Concentrations in ng g^{-1} w found in mangrove sediment sampled at Subaé estuary in four different sites.

Compound	#1	#2	#3	#4
		Perfluoroalkyl carboxylic acids (PFCAs)		
PFPeA	< 0.08	< 0.08	< 0.08	< 0.08
PFHpA	0.045	< 0.04	< 0.04	< 0.04
L-PFOA	< 0.92	< 0.92	< 0.92	< 0.92
Br-PFOA	< 0.05	< 0.05	< 0.05	< 0.05
PFNA	0.278	< 0.21	< 0.21	< 0.21
PFDA	< 0.04	< 0.04	< 0.04	< 0.04
PFUnDA	< 0.17	< 0.17	< 0.17	< 0.17
PFDoDA	< 0.04	< 0.04	< 0.04	< 0.04
PFTrDA	< 0.05	< 0.05	< 0.05	< 0.05
PFTeDA	< 0.06	< 0.06	< 0.06	< 0.06
PFPeDA	< 0.04	< 0.04	< 0.04	< 0.04
		Perfluoroalkyl sulfonic acids (PFSAs)		
PFBS	< 0.04	< 0.04	< 0.04	< 0.04
L-PFHxS	< 0.06	< 0.06	< 0.06	< 0.06
Br-PFHxS	< 0.04	< 0.04	< 0.04	< 0.04
L-PFOS	< 0.37	< 0.37	< 0.37	< 0.37
Br-PFOS	< 0.11	< 0.11	< 0.11	< 0.11
L-PFDS	< 0.04	< 0.04	< 0.04	< 0.04
Br-PFDS	< 0.04	< 0.04	< 0.04	< 0.04
		Perfluoroalkyl sulfonamido acetic derivatives (FASAAs)		
L-FOSAA	< 0.04	< 0.04	< 0.04	< 0.04
Br-FOSAA	< 0.04	< 0.04	< 0.04	< 0.04
L-CH_3FOSAA	< 0.04	< 0.04	< 0.04	< 0.04
Br-CH_3FOSAA	< 0.04	< 0.04	< 0.04	< 0.04
L-EtFOSAA	< 0.04	< 0.04	< 0.04	0.05
Br-EtFOSAA	< 0.04	< 0.04	< 0.04	< 0.04
		Perfluoroalkyl sulfonamide derivatives (FASAs)		
L-CH_3FOSA	< 0.04	< 0.04	< 0.04	< 0.04
Br-CH_3FOSA	< 0.04	< 0.04	< 0.04	< 0.04
L-FOSA	< 0.04	< 0.04	< 0.04	< 0.04
Br-FOSA	< 0.04	< 0.04	< 0.04	< 0.04
L-EtFOSA	< 0.04	0.10	< 0.04	0.14
Br-EtFOSA	< 0.04	< 0.04	< 0.04	< 0.04

Table S12: Comparison of PFASs Trophic Magnification Factors (TMF) and Nitrogen isotope values (‰) found in biota from different studies worldwide.

PFNA	PFUnDA	PFTrDA	PFTeDA	L-PFOS	Br-PFOS	L-FOSA	$\delta^{15}N$	Local	Ref.
–	–	–	–	4.6	–	–	8.1-18.3	Lake Ontario (Canada)	(Zhao et al., 2018)
–	–	–	–	3.1	–	–	–	Arctic	(Tomy et al., 2004)
–	–	–	–	6.3	–	–	9.3 - 15.6	Arctic	(Tomy et al., 2009)
–	1.74	–	1.12	1.3	–	–	9.7 - 22.9	China	(Loi et al., 2011)
1.5	1.1	1.1	0.79	1.5	2.2	1.9	5.1 - 15.4	France	(Munoz et al., 2017)
1.34	0.41	0.39	0.62	1.53	1.53	0.64	8.05 - 13.78	Brazil	This study
1.66	1.53	1.41	1.41	1.43	–	–	–	Lake Chaohu (China)	(Liu et al., 2018)

Table S13: Details on regressions of Log Concentrations (expressed in ng g^{-1} ww whole body) vs TP (trophic position) in group 1 (n = 18; trophic positions from 2.00 to 3.22) and group 2 (n = 26; trophic levels from 3.56 to 4.49), obtained with the NADA R-package [a], including the p-value of the regression, and Kendall's τ correlation coefficient (Helsel, 2005; Munoz et al., 2017). EtFOSA was not reported for polychaeta.

Compound	τ	$TMF_{Group\ 1}$	$TMF_{Group\ 1}$ Range
PFNA	0.219	3.95	(1.88 – 8.31)
PFUnDA	0.233	2.37	(1.34 - 4.16)
PFDoDA	0.131	3.15	(1.29 – 7.68)
PFTrDA	-0.234	0.53	(0.45 – 0.62)
PFTeDA	-0.225	0.44	(0.27 -0.74)
L-PFOS	0.374	**3.22**	(2.40 – 4.33)
Br-PFOS	0.369	**8.82**	(5.18 – 15.0)
L-FOSA	0.959	1.84	(1.33 – 2.54)
L-EtFOSA	0.226	2.65	(1.85 – 3.78)
Br-EtFOSA	0.273	5.16	(1.40 - 18.9)

Compound	τ	$TMF_{Group\ 2}$	$TMF_{Group\ 2}$ Range
PFNA	0.176	0.99	(0.79 - 1.24)
PFUnDA	1.787	1.82	(1.53 – 2.15)
PFDoDA	0.221	2.04	(1.71 – 2.44)
PFTrDA	0.215	1.5	(1.20 – 1.87)
PFTeDA	0.192	1.42	(1.07 – 1.88)
L-PFOS	0.294	**2.64**	(2.21– 3.16)
Br-PFOS	0.074	1.31	(1.01 – 1.71)
L-FOSA	0.179	1.54	(1.26 – 1.88)
L-EtFOSA	-0.313	0.22	(0.15 - 0.32)
Br-EtFOSA	-0.306	0.08	(0.02 - 0.24)

[a]It was obtained with the NADA R-package, including Kendall's τ correlation coefficient, and the resulting trophic magnification factor ($TMF = 10^{slope}$) with the confidence interval (min – max). Bold numbers indicate significant regressions ($p < 0.05$).

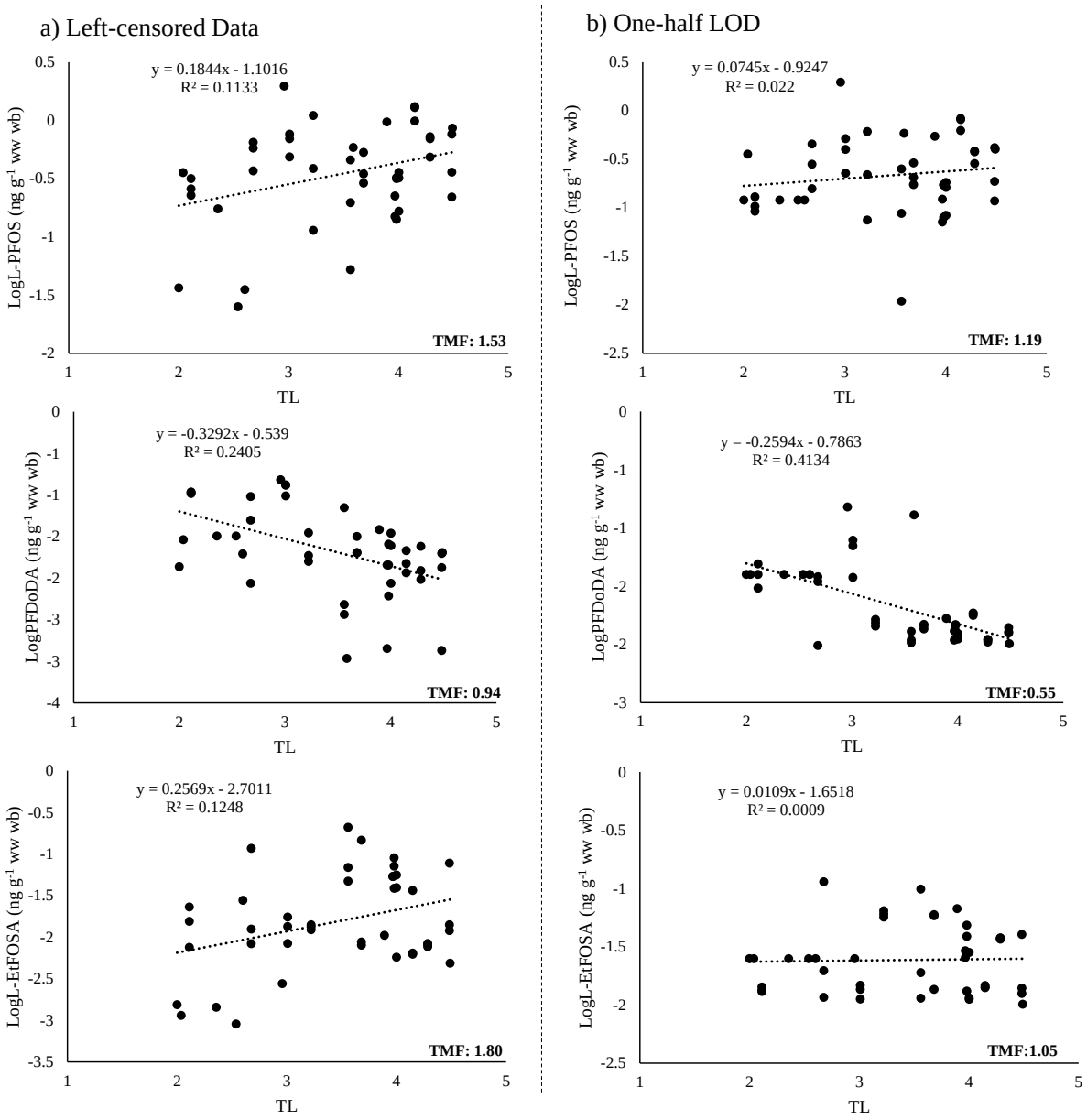

Figure S1: Linear regression comparison between log PFASs concentrations (L-PFOS, 93% detection frequency; PFDoDA, 46%; and L-EtFOSA, 30%) and Trophic Level (TL) with different approaches to access the influence of nondetected data substitution approaches (i.e. (a) left-censored and (b) one-half LOD) in Subaé estuarine food chain. TMF: Trophic Magnification Factor was calculated by Kendall correlation for all compounds.

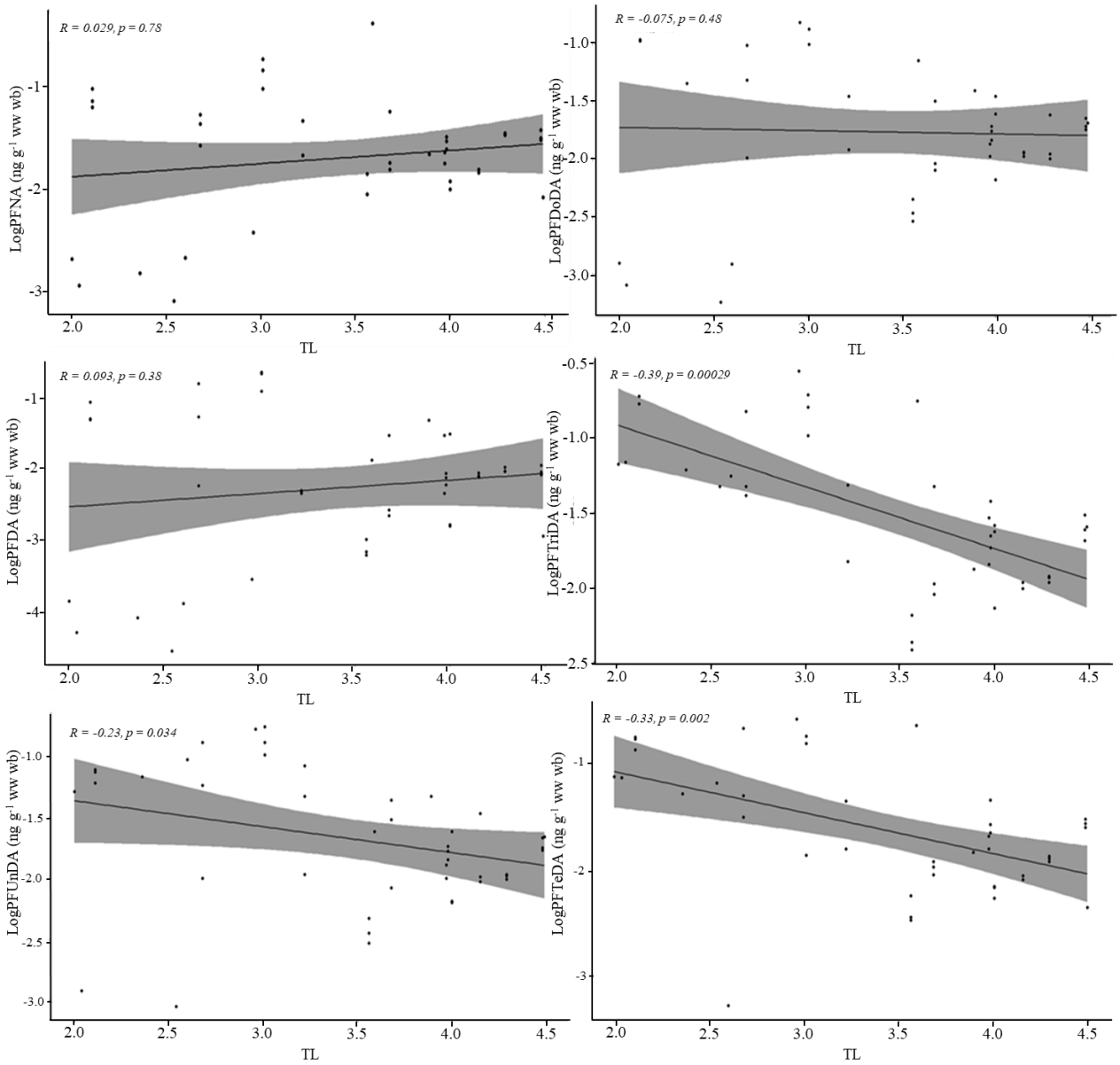

205

206 **Figure S2:** Kendall correlation of log transformed perfluoroalkyl carboxylic acids (PFCAs) and trophic position (TL)
207 organisms sampled (n = 44) at Subaé estuary. Grey area represents 95% confidence interval.

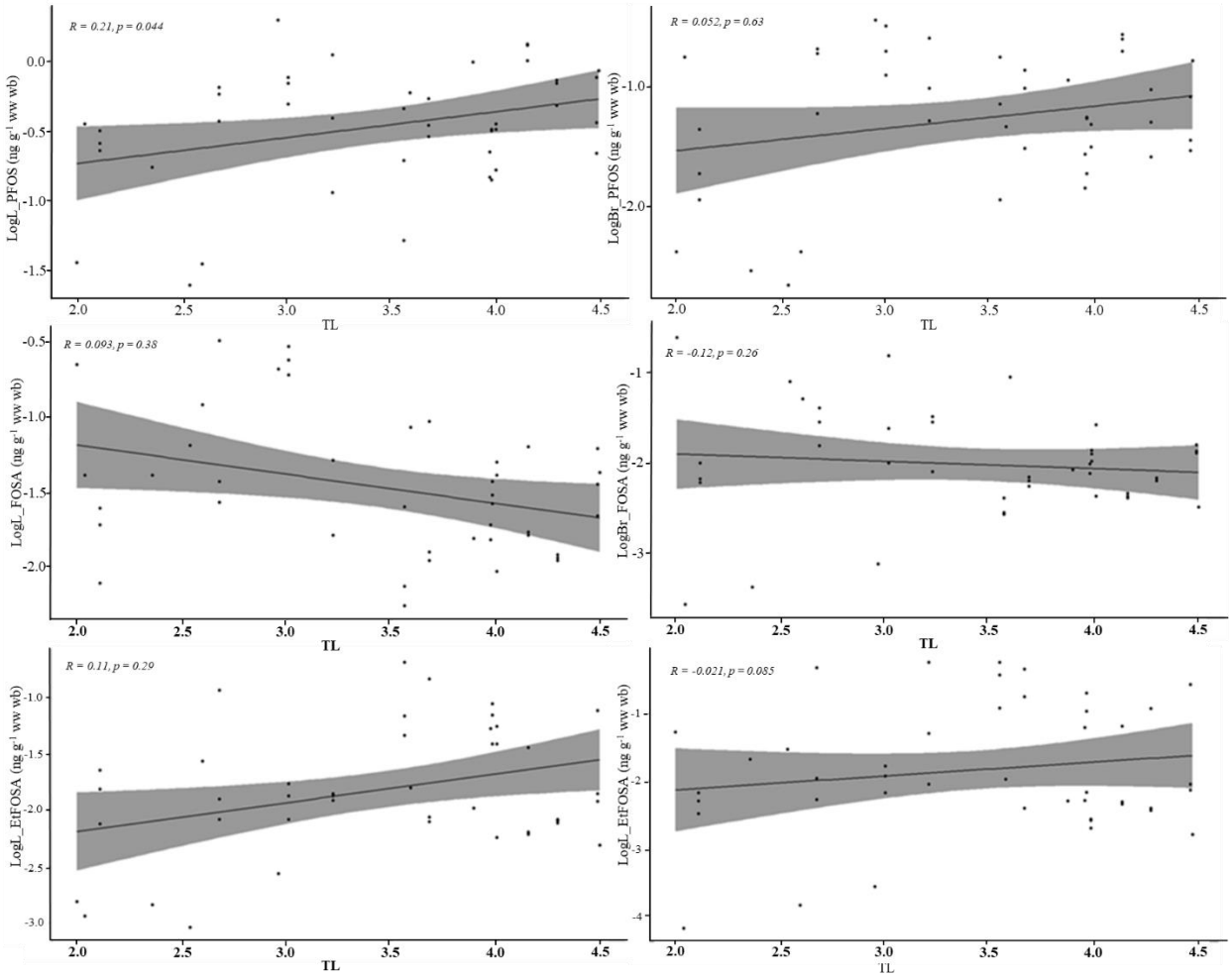

Figure S3: Kendall correlation of log transformed perfluoroalkyl sulfonamide derivatives (FASAs) and perfluoroalkyl sulfonic acids (PFSAs), and trophic position (TL) organisms sampled (n = 44) at Subaé estuary. EtFOSA was not reported for polychaeta. Grey area represents 95% confidence interval.

212 **References**

213 Goeritz, I., Falk, S., Stahl, T., Schaefers, C., Schlechtriem, C., 2013. Biomagnification
214 and tissue distribution of perfluoroalkyl substances (PFASs) in market-size rainbow
215 trout (Oncorhynchus mykiss). Environ. Toxicol. Chem. 32, 2078–2088.
216 https://doi.org/10.1002/etc.2279

217 Helsel, D.R., 2005. Nondectects and Data Analysis; Statistics for censored environmental
218 data, John Wiley and Sons.

219 Houde, M., Martin, J.W., Letcher, R.J., Solomon, K.R., Muir, D.C.G., 2006. Biological
220 monitoring of polyfluoroalkyl substances: A review. Environ. Sci. Technol. 40,
221 3463–3473. https://doi.org/10.1021/es052580b

222 Liu, W., He, W., Wu, J., Qin, N., He, Q., Xu, F., 2018. Residues, bioaccumulations and
223 biomagnification of perfluoroalkyl acids (PFAAs) in aquatic animals from Lake
224 Chaohu, China. Environ. Pollut. 240, 607–614.
225 https://doi.org/10.1016/j.envpol.2018.05.001

226 Loi, E.I.H., Yeung, L.W.Y., Taniyasu, S., Lam, P.K.S., Kannan, K., Yamashita, N., 2011.
227 Trophic Magnification of Poly- and Perfluorinated Compounds in a Subtropical
228 Food Web. Environ. Sci. Technol. 45, 5506–5513.
229 https://doi.org/10.1021/es200432n

230 Müller, C.E., De Silva, A.O., Small, J., Williamson, M., Wang, X., Morris, A., Katz, S.,
231 Gamberg, M., Muir, D.C.G., 2011. Biomagnification of perfluorinated compounds
232 in a remote terrestrial food chain: Lichen-Caribou-Wolf. Environ. Sci. Technol. 45,
233 8665–8673. https://doi.org/10.1021/es201353v

234 Munoz, G., Budzinski, H., Babut, M., Drouineau, H., Lauzent, M., Menach, K. Le, Lobry,
235 J., Selleslagh, J., Simonnet-Laprade, C., Labadie, P., 2017. Evidence for the Trophic
236 Transfer of Perfluoroalkylated Substances in a Temperate Macrotidal Estuary.
237 Environ. Sci. Technol. 51, 8450–8459. https://doi.org/10.1021/acs.est.7b02399

238 Nania, V., Pellegrini, G.E., Fabrizi, L., Sesta, G., De Sanctis, P., Lucchetti, D., Di
239 Pasquale, M., Coni, E., 2009. Monitoring of perfluorinated compounds in edible fish
240 from the Mediterranean Sea. FOOD Chem. 115, 951–957.
241 https://doi.org/10.1016/j.foodchem.2009.01.016

Tomy, G.T., Budakowski, W., Halldorson, T., Helm, P.A., Stern, G.A., Friesen, K., Pepper, K., Tittlemier, S.A., Fisk, A.T., 2004. Fluorinated organic compounds in an Eastern arctic marine food web. Environ. Sci. Technol. 38, 6475–6481. https://doi.org/10.1021/es049620g

Tomy, G.T., Pleskach, K., Ferguson, S.H., Hare, J., Stern, G., Macinnis, G., Marvin, C.H., Loseto, L., 2009. Trophodynamics of some PFCs and BFRs in a western Canadian Arctic marine food web. Environ. Sci. Technol. 43, 4076–4081. https://doi.org/10.1021/es900162n

Zabaleta, I., Bizkarguenaga, E., Izagirre, U., Negreira, N., Covaci, A., Benskin, J.P., Prieto, A., Zuloaga, O., 2017. Biotransformation of 8:2 polyfluoroalkyl phosphate diester in gilthead bream (Sparus aurata). Sci. Total Environ. 609, 1085–1092. https://doi.org/https://doi.org/10.1016/j.scitotenv.2017.07.241

Zabaleta, I., Bizkarguenaga, E., Nunoo, D.B.O., Schultes, L., Leonel, J., Prieto, A., Zuloaga, O., Benskin, J.P., 2018. Biodegradation and Uptake of the Pesticide Sulfluramid in a Soil-Carrot Mesocosm. Environ. Sci. Technol. 52, 2603–2611. https://doi.org/10.1021/acs.est.7b03876

Zhao, S., Liang, T., Zhou, T., Li, D., Wang, B., Zhan, J., Liu, L., 2018. Biotransformation and responses of antioxidant enzymes in hydroponically cultured soybean and pumpkin exposed to perfluorooctane sulfonamide (FOSA). Ecotoxicol. Environ. Saf. 161, 669–675. https://doi.org/10.1016/j.ecoenv.2018.06.048

Capítulo 6: Conclusões

O objetivo desta tese foi contribuir para o entendimento do destino, distribuição e comportamento de PFASs em diferentes compartimentos ambientais. Este objetivo foi alcançado através de estudos empíricos, que mostraram como processos ambientais determinam a ocorrência e o espalhamento de PFASs em ambientes tropicais.

O estudo de degradação mostrou que a velocidade de degradação da Sulfluramida em sedimentos de manguezais foi significativamente menor do que em estudos semelhantes realizados em laboratório. A lenta degradação da Sulfluramida em solos de mangue foi associada às características anóxicas do ambiente estudado, diferente das condições favoráveis a rápida degradação para esse composto (i.e., ambiente rico em oxigênio). Dentro das condições avaliadas, as maiores taxas de degradação de Sulfluramida foram observadas nas áreas de mangue com raízes quando comparada a áreas de mangue sem raízes, devido a maior lixiviação nessas últimas áreas. Contudo, a degradação da Sulfluramida em solos de mangue não foi identificada como uma fonte de PFOS para o ambiente ao longo dos 192 dias monitorados. No entanto, a utilização da Sulfluramida em áreas adjacentes a manguezais pode favorecer o aumento do estoque do formicida e de seus produtos de degradação nesses ecossistemas. Uma vez que os manguezais são áreas de transição, as diferentes condições físico-químicas das áreas em conexão com o mangue podem favorecer a maior atividade de degradação dos PFASs, portanto, distribuindo os produtos de degradação do formicida para estuários e zonas costeiras, representando um risco para a vida selvagem.

A presença de PFASs observada em organismos estuarinos, no sedimento e em MPS reforça o risco da utilização desses compostos em áreas próximas a estuários, sendo essas áreas consideradas como berçário da vida marinha e importantes para diversos serviços ecossistêmicos. A bioacumulação de PFASs em organismos estuarinos do rio Subaé deve ser avaliada com atenção, pois o consumo de organismos/mariscos contaminados é uma via importante de exposição a saúde humana. Além disso, ainda que os efeitos adversos da exposição a PFASs estejam sendo estudados, pouco se sabe sobre os riscos da interação desses compostos com outros contaminantes, como metais, que podem causar efeitos sinérgicos deletérios na biota e saúde humana. Sendo assim, ainda que as concentrações de PFASs no estuário do rio Subaé tenham sido baixas, a presença

desses contaminantes nesse estuário já contaminando por outros poluentes pode representar um risco ainda maior do que a sua ação isolada.

Não apenas no ambiente costeiro, próximo as fontes, a presença de PFASs foi encontrada. Ainda que em baixas concentrações, esses compostos foram observados em áreas oceânicas remotas, reforçando a sua característica de baixa degradabilidade e de dispersão em longas distâncias. No oeste do oceano Atlântico Tropical (TAO), a ocorrência destes compostos foi associada a entrada de contaminantes através das correntes equatoriais superficiais e do deslocamento das massas d'água oriundas de diferentes regiões do Atlântico como o mar de Labrador, do Mediterrâneo e intrusão da corrente das Agulhas. A ressurgência costeira que ocorre na costa do Rio de Janeiro também atuou no espalhamento dos PFASs não só em profundidade, mas também trazendo compostos de massas d'agua intermediárias para a superfície. Além disso, a baixa frequência com que PFOS foi encontrado ao norte do Atlântico Tropical reflete restrições na utilização/produção desses compostos adotadas pela Europa e Estados Unidos. Em contraponto, o uso de Sulfluramida no Brasil pode ter contribuído para a presença de FOSA e PFOS no Atlântico Sul, particularmente, na costa do Rio de Janeiro. Ainda, a presença de PFCAs em diferentes amostras superficiais e na coluna d'agua por todo o TAO deve ser ressaltada, pois esses compostos foram observados aqui e em estudos anteriores bioacumulando na cadeia alimentar.

A ampla presença de PFASs em diferentes compartimentos ambientais em áreas tropicais reflete o uso contínuo desses compostos na região como, por exemplo, a utilização da Sulfluramida na silvicultura, enquanto para o oceano essas fontes são difusas, envolvendo diferentes locais de produção e uso. A variedade de PFASs encontrada nas matrizes ambientais no presente estudo demonstra que as fontes de exposição a esses compostos são múltiplas e estão associadas a entradas históricas e recentes no ambiente. Futuros estudos devem abordar as fontes desses compostos para o ambiente, visando a implementação de medidas regulatórias para o uso e manejo desses compostos.